AD-A134 441 INTERNATIONEL CONFERENCE ON LIQUID AND AMORPHOUS MET2L (5TH) HELD AT LOS.. (U) CALIFORNIA UNIV LOS ANGELES DEPT OF MATERIALS SCIENCE AND ENG.. 19 AUG 83 1/1

UNCLASSIFIED F/G 11/6 NL

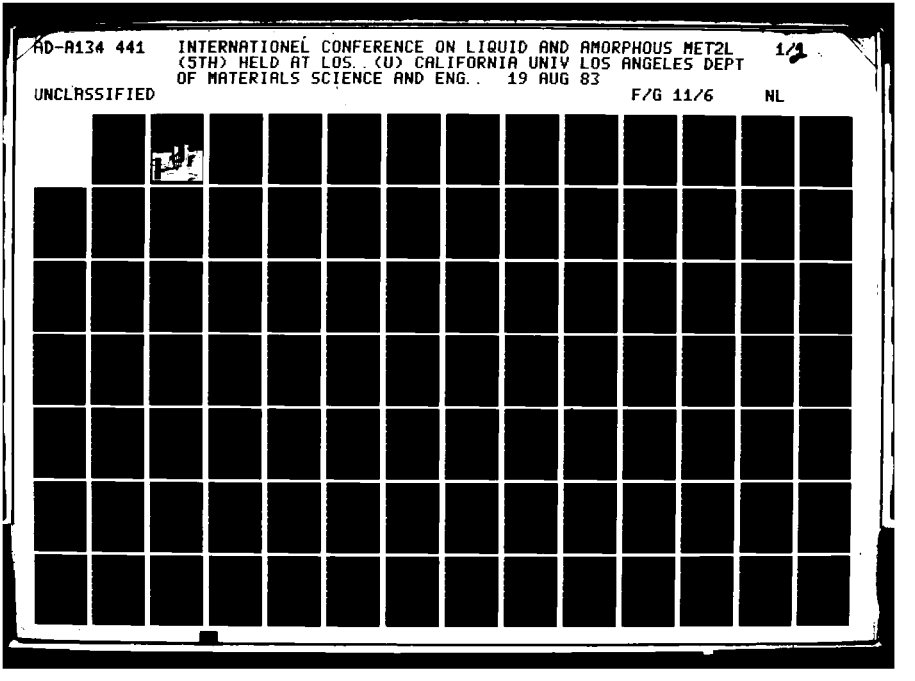

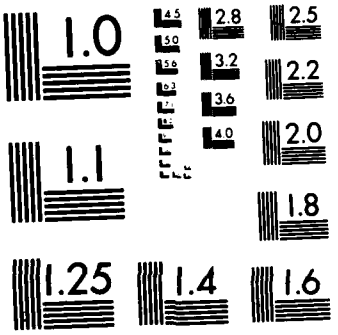

AD-A134 441

LAM5

Fifth International Conference on Liquid and Amorphous Metals

August 15-19, 1983

University of California
Los Angeles, California, USA

ABSTRACT

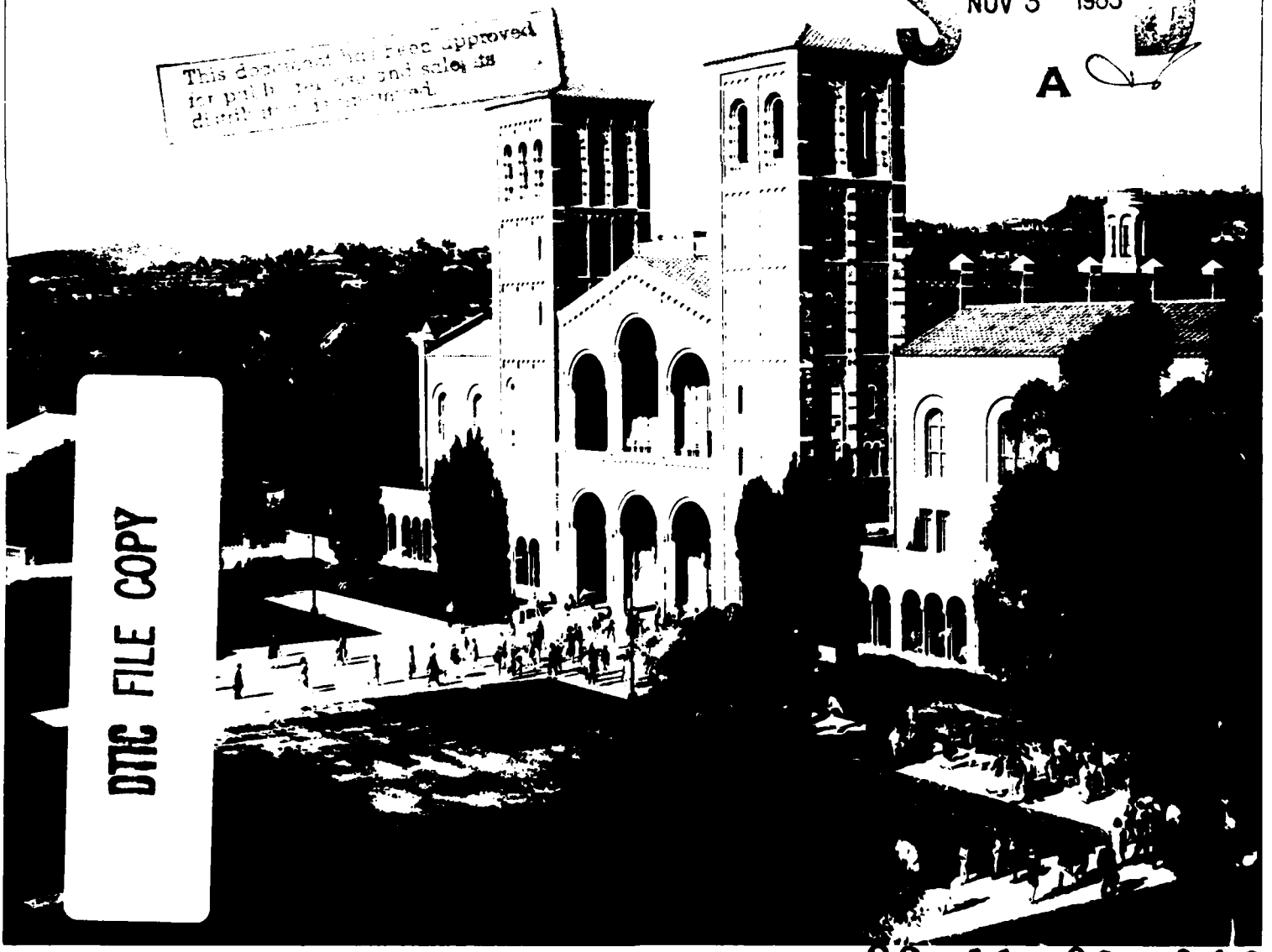

83 11 03 040

DEDICATION

To honor their valuable contributions which they have made to the field of liquid and amorphous metals, the Fifth International Conference has been dedicated to:

Professor A.B. Bhatia

Professor Pol Duwez

Professor N.F. Mott

Professor David Turnbull

SPONSORS

The financial support of the following agencies and companies is gratefully acknowledged:

National Science Foundation

Office of Naval Research

Allied Corporation

Exxon Research and Engineering Company

General Electric Company

Hughes Aircraft Company

International Business Machines Corporation

Lockheed Corporation

Minnesota Mining and Manufacturing Company

Xerox Corporation

University of California, Los Angeles

LAM5

FIFTH INTERNATIONAL CONFERENCE ON LIQUID AND AMORPHOUS METALS

August 15-19, 1983 at University of California
Los Angeles, California USA

SCOPE

The Fifth International Conference on Liquid and Amorphous Metals, to be held in Los Angeles during 15-19 August 1983, is the successor to the Grenoble conference held in 1980. It will cover all aspects of the physics and chemistry of liquid and amorphous metals and alloys.

CONFERENCE SITE

The conference will be held on the campus of the University of California in Los Angeles. The oral presentations will be given in the lecture halls (Rooms 2250 and 2276) of Young Hall (Chemistry Building) and the poster sessions will take place in the Grand Ballroom of Ackerman Union (see attached map).

The conference administrative center (consisting of a registration desk, information desk, and travel assistance) will be located in front of the lecture halls in Young Hall. It will be open during the week of the conference from 8 am to 6 pm. For those arriving Sunday, 14 August, a registration and information desk will be available from 4-10 pm in Rieber Hall (one of the Students' Residence Halls) where the reception will take place.

REGISTRATION

The registration fee (including conference proceedings) for participants is $185. Students will be charged a fee of $80, which does not include the proceedings. The price of a separate copy of the proceedings is $45. The registration fee for accompanying persons is $20 per person.

Payments should accompany FORM A and be made by check or money order, payable to Regents of UC, LAM5.

PROCEEDINGS

The conference proceedings will be published as a special issue of the Journal of Non-Crystalline Solids. They will contain only papers presented at the conference and accepted for publication after refereeing. Typing instructions have been sent to all first authors.

CONFERENCE CHAIRMEN

- C.N.J. Wagner, Materials Science and Engineering Department, University of California, Los Angeles, California USA

- W.L. Johnson, W.M. Keck Laboratory, California Institute of Technology, Pasadena, California USA

INTERNATIONAL ADVISORY BOARD

- G.S. Cargill, III (Yorktown Heights, New York, USA)
- N.E. Cusack (Norwich, United Kingdom)
- F. Cyrot-Lackmann (Grenoble, France)
- H.A. Davies (Sheffield, United Kingdom)
- P. Desre (Grenoble, France)
- J. Durand (Nancy, France)
- T. Egami (Philadelphia, Pennsylvania, USA)
- P.A. Egelstaff (Guelph, Canada)
- H. Endo (Kyoto, Japan)
- R. Evans (Bristol, United Kingdom)
- U. Gonser (Saarbrucken, Federal Republic of Germany)
- H.J. Guntherodt (Easel, Switzerland)
- J. Hafner (Vienna, Austria)
- F. Hensel (Marburg, Federal Republic of Germany)
- F.E. Luborsky (Schenectady, New York, USA)
- N. March (Oxford, United Kingdom)
- D. Quitmann (Berlin, Federal Republic of Germany)
- J.F. Sadoc (Orsay, France)
- M. Shimoji (Sapporo, Japan)
- S. Steeb (Stuttgart, Federal Republic of Germany)
- K. Suzuki (Sendai, Japan)
- J.C. Thompson (Austin, Texas, USA)
- W. van der Lugt (Groningen, The Netherlands)
- W.W. Warren (Murray Hill, New Jersey, USA)
- F. Yonezawa (Yokohama, Japan)

NATIONAL SCIENTIFIC COMMITTEE

- A. Bienenstock (Stanford University)
- C. Cline (Lawrence Livermore National Laboratory)
- G.S. Cargill, III (IBM Research Laboratory)
- M. Cutler (Oregon State University)
- M.H. Cohen (Exxon Research and Engineering Company)
- T. Egami (University of Pennsylvania)
- B.C. Giessen (Northeastern University)
- R. Hasegawa (Allied Corporation)
- N.C. Halder (University of South Florida)
- C.J. Kleppa (University of Chicago)
- F.E. Luborsky (General Electric Company)
- D. Polk (Office of Naval Research)
- R.J. Reynik (National Science Foundation)
- F. Spaepen (Harvard University)
- J.C. Thompson (University of Texas)
- W.W. Warren (Bell Telephone Laboratory)

LOCAL ORGANIZING COMMITTEE

- I. Aksay (Materials Science and Engineering Department, UCLA)
- A.J. Ardell (Materials Science and Engineering Department, UCLA)
- R. Braunstein (Physics Department, UCLA)
- W.G. Clark (Physics Department, UCLA)
- R. Kikuchi (Hughes Research Laboratory)
- J.D. Mackenzie (Materials Science and Engineering Department, UCLA)
- H. Reiss (Chemistry Department, UCLA)
- L.E. Tanner (Lawrence Livermore National Laboratory)
- A. Williams (Los Alamos National Laboratory)

Correspondence should be addressed to:

C.N.J. Wagner
Materials Science and Engineering Department
6531 Boelter Hall
University of California
Los Angeles, California 90024 USA
Telephone (213) 825-6265

ACCOMMODATIONS

Housing for the conference participants is available in the residential suites and residence halls on campus, or in hotels and motels in close proximity to UCLA.

1. RESIDENTIAL SUITES
Each suite consists of TWO BEDROOMS, EACH WITH TWO SINGLE BEDS, A LIVING ROOM, AND A BATHROOM. The cost depends on the number of people occupying the suite. The price for one person covers the room charge, daily maid service, breakfast and dinner, and admittance to the Sunset Recreation Center (with two Olympic-size swimming pools and tennis courts). Participants may request a box dinner to be used for lunch, or a meal ticket redeemable toward the cost of lunch at any campus food facility. The rates for the week of the conference (Sunday night to Saturday morning) are as follows:

1 person/suite:	$456/week
2 persons/suite:	$306/week/ person
3 persons/suite:	$222/week/ person
4 persons/suite:	$186/week/ person

There will be no reduction for a stay of less than five nights.

For children, age 4-12 years, the rates are reduced by $27, and children 3 years and under are free if they do not require a bed.

The residential suites are within walking distance (10 minutes) to the conference center, but a shuttle bus will operate between the two sites during the conference week.

2. RESIDENCE HALLS (Hershey Hall)
(Rooms are no longer available in Hershey Hall, located next to the conference center.)
EACH ROOM HAS TWO SINGLE BEDS, AND A BATHROOM IS LOCATED ON EACH FLOOR. Linen and bath towel are provided, but no maid service or meals are included in the price of the room. The rates are as follows:

1 person/room:	$28/day
2 persons/room:	$14/day/ person

Maid service is available at an additional $3/person/day.

3. HOTELS AND MOTELS
There are several hotels and motels in close proximity to UCLA. It is planned to run a shuttle bus between the conference center and the hotels in areas (a) and (b) below:

(a) One-Half Mile from Campus (On Wilshire Boulevard in Westwood)

Holiday Inn--Westwood
10740 Wilshire Boulevard
Los Angeles, CA 90024
(213) 475-8711
Single: $67
Double: $77

Del Capri Hotel--Westwood
10587 Wilshire Boulevard
Los Angeles, CA 90024
(213) 474-3511
Single: $59
Double: $69
Price includes continental breakfast

3. HOTELS AND MOTELS (cont.)

Holiday Inn--Brentwood
170 North Church Lane
Los Angeles, CA 90049
(213) 476-6411
Room price $46 allowing 1-2-3-4 persons per room
This hotel is in close proximity to the San Diego Freeway. Consequently, some rooms may be prone to freeway noise.

Bel Air Sands Hotel
11461 Sunset Boulevard
Los Angeles, CA 90049
(213) 476-6571
Single: $70
Double: $80

Brentwood Motor Inn
600 Beverly Park Drive
Los Angeles, CA 90049
(213) 476-6255
Room price $53 independent of number of occupants
This motel is in close proximity to the San Diego Freeway. Consequently, some rooms may be prone to freeway noise.

Please contact the hotel of your choice directly, indicating that you will be attending the LAMS Conference at UCLA.

TRANSPORTATION

Participants arriving at Los Angeles International Airport (LAX) can take the express bus (Fly-Away Service) to West Los Angeles (WLA) Terminal. The fare is $3.25/person. The bus runs every 30 minutes from all airline terminals. For example, the bus stop for passengers arriving at the International Terminal is in front of Baggage Area A which is to the left when you exit the "bubble" housing the baggage area for international arrivals.

A shuttle bus will take the participants from the WLA Terminal to the Residential Suites, the Residence Halls, and the local hotels on the afternoon of Sunday, 14 August.

Participants who travel by car can reach UCLA by taking the San Diego Freeway (I-405) north from the airport to Wilshire Boulevard--East Exit. Go one-half mile east on Wilshire Boulevard, turn left (north) at Westwood Boulevard. Take Westwood Boulevard for one mile into the UCLA campus. Inquire at the information kiosk for parking and directions to the Residential Suites, Residence Halls, and/or conference site. The parking fee is $2 per entry.

SOCIAL PROGRAM

Sunday, 14 August
Reception at Residential Suites (Rieber Hall) from 6-10 pm.

Monday, 15 August
Barbeque at the Residential Suites, 7 pm. The price for the chicken barbeque is $15 per person.

Tuesday, 16 August
Banquet at UCLA Faculty Center, 7 pm. The price for the banquet is $25 per person.

Thursday, 18 August
Hollywood Bowl Concert and Picnic. The price for the picnic, concert, and transportation is $30 per person.

Friday, 19 August
Farewell Party

SIGHTSEEING PROGRAM DURING CONFERENCE WEEK

The following excursions have been scheduled during the week of LAM5. In order to reserve special buses for the conference participants and guests, confirmation and payment for the selected tours is required before 1 August 1983.

Monday, 15 August:	Hollywood and Los Angeles (6 hours) Fare: Adult $15 / Child (3-11 yrs) $7.50
Tuesday, 16 August:	Coastal Tour and Getty Museum (6 hours) Fare: Adult $15 / Child (3-11 yrs) $7.50
Wednesday, 17 August:	Disneyland (9-1/2 hours) Fare: Adult $25 / Child (3-11 yrs) $16
Thursday, 18 August:	Universal Studios (6 hours) Fare: Adult $22 / Child (3-11 yrs) $15

If there is sufficient demand, another tour to Disneyland can be arranged on Saturday, 20 August. The fare is identical to the Wednesday tour.

Please confirm your tours on the enclosed form.

Separate all-day tours are also possible. Examples are:
(1) Tijuana, Mexico
(2) San Diego Zoo
(3) Sea World in San Diego

Reservations for these tours can be made at the conference registration desk two days in advance of departure.

POST- AND PRE-CONFERENCE TOURS (Las Vegas)

The demand for post- and pre-conference tours was very light, and only one tour to Las Vegas will be organized. This tour will leave Sunday morning, 21 August*, thus permitting participants of LAM5 to visit Disneyland or other sights in Los Angeles on Saturday. It is proposed to take the trip to Las Vegas by an air-conditioned bus so that the Mojave Desert can be seen by day.

The price of the tour will be $220 for single occupancy in a hotel room in Las Vegas, and $150 for double occupancy. The tour will consist of two nights in Las Vegas and will return to Los Angeles on Tuesday, 23 August 1983.

There is the possibility for a one-day excursion by plane from Las Vegas to the Grand Canyon at an extra charge of $159.

---

* Arrangements must be made for a stay in a hotel or the Residence Hall (Hershey Hall) for the night of Saturday, 20 August. No rooms can be made available in the Residential Suites for that night, but occupants can move to Hershey Hall.

NOTES FOR ORAL PRESENTATIONS

Projectors for 35 mm slides (5 cm x 5 cm or 2" x 2") and overhead projectors for transparent sheets (25 cm x 25 cm or 10" x 10") will be available. Authors wishing to use other projectors should contact the Conference Chairman as soon as possible so that arrangements can be made. No projector for 3-1/2" x 4-1/4" slides will be made available.

When preparing slides or transparencies, please remember the following:

1. Be realistic. One slide per minute is probably too much.

2. Make the lettering large, otherwise the slide will be unreadable. No lettering in any slide should be less than 5% of the height of the slides.

3. Avoid non-contrasting colors if possible (e.g. blue and green are often hard to distinguish, and red is hard to see for some people).

INSTRUCTIONS FOR POSTER PRESENTATION

Each poster will be exhibited in the Grand Ballroom of Ackerman Union during the period of Monday, 15 August to Thursday, 18 August. The posters are grouped into sessions, and are numbered and listed in the attached program.

The posters should be prepared in advance and mounted on the poster boards from 8-9 am on Monday, 15 August.

The authors must be present at least 1-1/2 hours for discussion of their poster during the specific poster session, as indicated in the final program.

Each poster will be assigned to a 180 cm (6') wide and 140 cm (4') high board. At the upper left corner of the board, a section 30 cm (12") wide and 20 cm (8") high will be reserved for the number of the poster presentation (to be prepared by the conference). The remainder of the board can be used for the title of the paper, the authors' names and affiliations, and the text and figures.

It is suggested that the posters be prepared in such a way that they can be understood even in the absence of the authors. The following recommendations should be considered:

1. Use large print, readable from a distance of 2 meters (6'-7'). Shade block letters where possible.

2. Keep text and figure legends brief.

3. Simple use of color can help emphasize a point.

SCIENTIFIC PROGRAM

Sunday, 14 August 1983

4:00 pm — Registration in Rieber Hall
7:00 pm — Reception

Monday, 15 August

8:00 am — Registration in Young Hall (Chemistry Building)
9:00 am — Welcome and Opening Remarks (Room 2250, Young Hall)

SESSION A: Expanded Metals (Room 2250, Young Hall)

Chairmen: F. Hensel and W.W. Warren

9:35 am — A1 — H. Endo: METAL-NONMETAL TRANSITIONS IN LIQUIDS UNDER PRESSURE (Invited)

10:10 am — A2 — L. Turkevich and M.H. Cohen: THE NATURE OF PHASE TRANSITIONS IN FLUID MERCURY (Invited)

10:45 am — Break

SESSION B: Thermodynamics (Room 2250, Young Hall)

Chairmen: A.B. Bhatia and M. Shimoji

11:00 am — B1 — O. Kleppa: SYSTEMATIC ASPECTS OF THE THERMODYNAMICS OF LIQUID ALLOYS OF TRANSITION METALS WITH NOBLE METALS (Invited)

11:35 am — B2 — J.H. Perepezko and J.S. Paik: THERMODYNAMIC PROPERTIES OF UNDERCOOLED LIQUID METALS

11:50 am — B3 — D.A. Young and Marvin Ross: THEORETICAL HIGH-PRESSURE EQUATIONS OF STATE AND PHASE DIAGRAMS OF THE ALKALI METALS

12:05 pm — B4 — M. Cyrot: FEASABILITY AND STABILITY OF AMORPHOUS MATERIALS AS A FUNCTION OF THE ENTHALPY OF FUSION

12:20 pm — B5 — R.B. Schwarz, W.L. Johnson, and P.M. Clemens: AMORPHOUS La-Au ALLOYS FORMED BY SOLID-STATE REACTION OF THE ELEMENTAL CRYSTALLINE METALS

12:40 pm — Lunch

2:00 pm — POSTER SESSIONS in the Grand Ballroom of Ackerman Union

Poster Session PA — Thermodynamics
Chairmen: M. Cyrot and J.H. Perepezko

Poster Session PB — Structure I
Chairmen: G. Etherington and P. Lamparter

Poster Session PC — Atomic Transport and Structural Relaxation I
Chairmen: J.R. Cost and M.R.J. Gibbs

Poster Session PD — Electronic Properties I
Chairmen: S.J. Poon and S. Tamaki

SESSION C: Thermodynamics and Expanded Metals (Room 2250 Young Hall)
Chairmen: N.E. Cusack and J.C. Thompson

4:00 pm C1 M. Shimoji, T. Itami, and S. Takahashi: HIGHER-ORDER CORRELATION EFFECTS ON THERMODYNAMIC AND ELECTRONIC PROPERTIES OF LIQUID ALLOYS

4:15 am C2 W.W. Warren, Jr., U. El-Hanany, and G.F. Brennert: NMR STUDIES OF EXPANDED LIQUID CESIUM

4:30 pm C3 S. Takeda, S. Matsunaga, and S. Tamaki: MAGNETIC SUSCEPTIBILITY OF LIQUID Na-IVb ALLOYS

4:45 pm C4 K. Ichikawa: SPECIFIC HEAT AND TIME-OF-FLIGHT NEUTRON DIFFRACTION MEASUREMENTS IN LIQUID Bi-BiI(3) MIXTURES

5:00 pm C5 J.R. Franz: METAL-NONMETAL TRANSITION IN CHARGE TRANSFER ALLOYS AND METAL-MOLTEN SALT SOLUTIONS

5:15 pm C6 M.L. Saboungi: STRUCTURAL IMPLICATIONS OF THERMODYNAMIC MEASUREMENTS IN LIQUID ALLOYS

5:30 pm C7 R. Fainchstein, U. Evan, and J.C. Thompson: OPTICAL REFLECTIVITY OF MOLTEN Cs(x)CsCl(1-x) ALLOYS

5:45 pm C8 J. Dupuy, J.F. Jal, J. Chabrier, and P. Chieux: STRUCTURE AND MODEL OF METAL-MOLTEN SALT SOLUTIONS IN METALLIC TRANSPORT REGIME

SESSION D: Electronic Properties I (Room 2276, Young Hall)
Chairmen: R.W. Cochrane and P. Oelhafen

4:00 pm D1 R. Harris and A.B. Kaiser: ELECTRON-PHONON ENHANCEMENT AND THE THERMOPOWER OF Ni-Zr METALLIC GLASSES

4:15 pm D2 E. Luscher, J. Willer, and G. Fritsch: TRANSPORT-PROPERTIES OF METALLIC GLASSES AT HIGH PRESSURES

4:30 pm D3 W.B. Muir, Z. Altounian, J.O. Strom-Olsen, and R.W. Cochrane: THE THERMOPOWER OF SUPERCONDUCTING AND MAGNETIC Fe-Zr GLASSES

4:45 pm D4 C.L. Chien and S.H. Liou: TEMPERATURE DEPENDENCE OF RESISTIVITY OF AMORPHOUS METAL-METAL SYSTEMS WITH WIDE COMPOSITION RANGES

5:00 pm D5 A.K. Bhatnagar, B. Bhanu-Prasad, K.V. Rao, and K. Fukamichi: THERMOPOWER OF RAPIDLY QUENCHED Fe-RICH Fe-Zr AMORPHOUS ALLOYS

5:15 pm D6 L.K. Varga, A. Lova, J. Toth, and S. Arajs: ELECTRIC PROPERTIES OF Ni(100-x)B(x) and Ni(81.5)B(18.5-y)P(y) METALLIC GLASSES

7:00 pm Barbeque-Picnic at Residential Suites

Tuesday, 16 August

SESSION E: Structure I (Room 2250, Young Hall)
Chairmen: P.A. Egelstaff and K. Suzuki

9:00 am E1 S. Steeb: DIFFRACTION STUDIES OF LIQUID AND AMORPHOUS ALLOYS (Invited)

9:35 am E2 D. Quitmann: MICROSCOPIC STUDIES OF DYNAMICS IN LIQUID AND AMORPHOUS ALLOYS (Invited)

10:10 am E3 G.S. Cargill, III: CAPABILITIES AND LIMITATIONS OF EXAFS FOR AMORPHOUS MATERIALS (Invited)

10:45 am Break

SESSION F: Glass Transition (Room 2250, Young Hall)
Chairmen: C.F. Cline and H.A. Davies

11:00 am F1 M.H. Cohen and G.S. Grest: THE NATURE OF THE GLAS TRANSITION (Invited)

11:35 am F2 F. Yonezawa and M. Kimura: COMPUTER GLASS TRANSIT.

11:50 am F3 F. Spaepen, C.L. Lin, and D. Turnbull: PICOSECOND PULSED LASER-INDUCED MELTING AND GLASS FORMATION IN METALS

12:05 pm F4 R.C. O'Handley, B.W. Corb, and N.J. Grant: REVERSIBLE TRANSFORMATIONS OF SHORT-RANGE ORDER IN COBALT-BASE AMORPHOUS ALLOYS

12:20 pm F5 J. Hillairet, E. Balanzat, N.E. Derradji, and A. Chamberod: REVERSIBLE AND NON-REVERSIBLE EFFECTS IN RELATION TO SHORT-RANGE ORDERING--A KINETIC ANALYSIS OF Ni(24)Zr(76)

12:40 pm Lunch

2:00 pm POSTER SESSIONS in the Grand Ballroom of Ackerman Union

Poster Session PE Metal-Nonmetal Transitions
Chairmen: H. Hoshino and J. Franz

Poster Session PF Structure II
Chairmen: N. Cowlam and H. Rudin

Poster Session PG Atomic Transport and Structural Relaxation II
Chairmen: R.B. Schwarz and D. Pavuna

Poster Session PH Electronic Properties II
Chairmen: P.J. Cote and L.V. Meisel

SESSION G: Structure II (Room 2250, Young Hall)
Chairmen: U. Gonser and T. Mizoguchi

4:00 pm G1 T. Fukunaga, N. Watanabe, and K. Suzuki: EXPERIMENTAL DETERMINATION OF PARTIAL STRUCTURES IN Ni(40)Ti(60) GLASS

4:15 pm	G2	A. Lee, G. Etherington, and C.N.J. Wagner: PARTIAL STRUCTURE FACTORS AND DISTRIBUTION FUNCTIONS OF Ni(35)Zr(65) METALLIC GLASS
4:30 pm	G3	A. Naudon and A.M. Flank: RELATIONSHIP BETWEEN SPACE-CORRELATED FLUCTUATIONS AND INITIAL ALLOY COMPOSITION IN SOME METALLIC GLASSES
4:45 pm	G4	H. Rudin, S. Jost, and H.J. Guntherodt: X-RAY DIFFRACTION FROM LIQUID AND AMORPHOUS Mg(70)Zn(30) ALLOYS
5:00 pm	G5	A. Sadoc: EXAFS STUDY OF AMORPHOUS Cu(33)Zr(66) ALLOY
5:15 pm	G7	M. Silbert: X-RAY SCATTERING, ELECTRON CORRELATIONS, AND THE SMALL k-BEHAVIOUR OF THE STRUCTURE FACTOR OF SIMPLE LIQUID METALS
5:30 pm	G8	W. Glaeser and Ch. Morkel: SELF-DIFFUSION IN SIMPLE LIQUID METALS
7:00		Banquet at the Faculty Center Speaker: Provost Ray Orbach, UCLA

Wednesday, 17 August

SESSION H: Theory (Room 2250, Young Hall)
Chairmen: G.J. Morgan and F. Yonezawa

9:00 am H1 D.R. Nelson: ORIENTATIONAL ORDERING IN 2- AND 3-DIMENSIONAL SYSTEMS (Invited)

9:35 am H2 J. Hafner: THE ELECTRONIC THEORY OF THE STRUCTURAL THERMOCHEMISTRY OF METALS AND ALLOYS (Invited)

10:10 am H3 W. van der Lugt and W. Geertsma: LIQUID ALLOYS WITH STRONG CHEMICAL INTERACTIONS (Invited)

10:45 am Break

SESSION I: Modeling and Structure (Room 2250, Young Hall)
Chairmen: D.E. Polk and V. Vitek

11:00 am I1 J.F. Sadoc and R. Mosseri: MODELING OF THE STRUCTURE OF GLASSES (Invited)

11:35 am I2 J. Kortright and A. Bienenstock: STRUCTURAL STUDY OF AMORPHOUS METALLIC Mo-Ge ALLOYS

11:50 am I3 P. Lamparter, W. Martin, S. Steeb, and W. Freyland: NEUTRON DIFFRACTION STUDY OF THE STRUCTURE OF LIQUID Cs-Sb ALLOYS

12:05 am I4 T. Mizoguchi, H. Narumi, N. Akutsu, N. Watanabe, N. Shiotani, M. Ito, and H. Iwasaki: STRUCTURE RELAXATION OF AN AMORPHOUS Mg(7)Zn(3) ALLOY

12:20 pm I5 J.B. Suck, H. Rudin, H.J. Guntherodt, and H. Beck: INFLUENCE OF STRUCTURAL RELAXATION ON THE ATOMIC DYNAMICS OF THE METALLIC GLASS Mg(7)Zn(3)

12:40 pm Lunch

2:00 pm POSTER SESSIONS in the Grand Ballroom of Ackerman Union

Poster Session PI Surfaces and Hydrides
Chairmen: M.L. Rosinberg and A. Williams

Poster Session PJ Modeling
Chairmen: R. Kikuchi and A. Naudon

Poster Session PK Electronic Properties III
Chairmen: W.H. Hines and S. Ishio

Poster Session PL Atomic Transport and Structural Relaxation III
Chairmen: M. Mehra and H.G. Wagner

SESSION J: Structure, Surfaces, Crystallization (Room 2250, Young Hall)
Chairmen: W. Geertsma and H.S. Chen

4:00 pm J1 A.P. Copestake, R. Evans, H. Ruppersberg, and W. Schirmacher: A MODEL FOR THE STRUCTURE OF LIQUID Li(4)Pb

4:15 pm J2 M.L. Rosinberg, V. Russier, and J.P. Badiali: THEORETICAL CALCULATIONS ON METALLIC SURFACES--THE OCP REFERENCE SYSTEM

4:30 pm J3 M. Grimson and D. Stroud: DENSITY FUNCTIONAL CALCULATIONS OF THE SURFACE TENSION OF LIQUID METALS AND ALLOYS

4:45 pm J4 H.G. Wagner, M. Ackermann, and U. Gonser: CRYSTALLIZATION OF AMORPHOUS METAL-METALLOID ALLOYS

5:00 pm J5 K.V. Rao, K.A. Bertness, R. Aidun, S. Arajs, and H.H. Liebermann: CRYSTALLIZATION PROCESSES IN NITROGEN-BEARING Fe-V-B-Si AMORPHOUS ALLOYS--MAGNETIC, THERMAL, AND TRANSPORT PROPERTY STUDIES

5:30 pm J6 M. Mehra, R. Schulz, and W.L. Johnson: STRUCTURAL RELAXATION AND CRYSTALLIZATION BEHAVIOR OF Mo(0.6)Ru(0.4)(1-x) B(x) GLASSES

5:45 pm J7 P.H. Kes and C.C. Tsuei: COLLECTIVE FLUX PINNING, A PROBE OF DEFECTS IN AMORPHOUS SUPERCONDUCTING FILMS

SESSION K: Hydrides (Room 2276, Young Hall)
Chairmen: B.C. Giessen and U. Koster

4:00 pm K1 K. Samwer and W.L. Johnson: GLASS FORMATION BY SOLID-STATE REACTION OF CRYSTALLINE Zr-X PHASES WITH HYDROGEN, AND STRUCTURE OF GLASSY HYDRIDES

4:15 pm K2 K. Suzuki, N. Hayashi, Y. Tomizuka, T. Fukunaga, K. Kai, and N. Watanabe: HYDROGEN ATOM ENVIRONMENTS IN HYDROGENATED ZrNi GLASS

4:30 pm K3 A. Williams, J. Eckert, X.L. Yeh, M. Atzmon, and K. Samwer: INELASTIC NEUTRON SCATTERING FROM A HYDRIDE OF THE METALLIC GLASS Zr(2)Pd

4:45 pm K4 R.C. Bowman, D.E. Etter, A. Attala, B.D. Craft, J.S. Cantrell, J.E. Wagner, and W.L. Johnson: DIFFUSION PROPERTIES AND PHASE TRANSITIONS OF THE METALLIC GLASS a-Zr(2)PdH(x)

5:00 pm K6 D.J. Sellmyer, M.J. O'Shea, and C.G. Robbins: MAGNETISM AND HYDROGEN ABSORPTION IN RARE-EARTH GLASSES

5:15 pm K7 R.S. Finocchiaro, C.L. Tsai, and B.C. Giessen: HYDROGEN SOLUBILITY AND YOUNG'S MODULUS IN Pd-Si METALLIC GLASSES

Thursday, 18 August

SESSION L: Atomic Transport and Structural Relaxation (Room 2250, Young Hall)
Chairman: F. Spaepen and D.J. Sellmyer

9:00 am L1 A.L. Greer: ATOMIC TRANSPORT AND STRUCTURAL RELAXATION IN METALLIC GLASSES (Invited)

9:35 am L2 T. Egami and V. Vitek: LOCAL STRUCTURAL FLUCTUATIONS AND DEFECTS IN METALLIC GLASSES (Invited)

10:10 am L3 J.A. Leake, M.R.J. Gibbs, S. Vryenhoef, and J.E. Evetts: ACTIVATION ENERGY SPECTRA IN RELAXATION--CROSSOVER AND REVERSIBILITY

10:25 am L4 F. Sommer, H. Haas, and B. Predel: MICROCALORIMETRIC INVESTIGATIONS OF STRUCTURAL RELAXATION PHENOMENA IN GLASSY BINARY TRANSITION-METAL ALLOYS

10:40 am Break

SESSION M: Application of Metallic Glasses (Room 2250, Young Hall)
Chairmen: F.E. Luborsky and L. Davis

11:00 am M1 R. Hasegawa: METALLIC GLASSES IN DEVICES FOR ENERGY CONVERSION AND CONSERVATION (Invited)

11:35 am M2 R.B. Diegle: CHEMICAL PROPERTIES OF METALLIC GLASSES (Invited)

12:10 am M3 R. Wang: CORROSION RESISTANCE OF AMORPHOUS AND CRYSTALLIZED Fe-Ni-Cr-W ALLOYS

12:25 am M4 A. Yokoyama, H. Komiyama, H. Inoue, T. Masumoto, and H.M. Kimura: AN ACTIVE METHANATION CATALYST PREPARED FROM Pd-Zr ALLOYS

12:40 pm Lunch

SESSION N: Atomic Transport (Room 2250, Young Hall)
Chairmen: A. Chamberod and J.A. Leake

2:00 pm N1 J.R. Cost and J.T. Stanley: KINETICS OF STRUCTURAL RELAXATION IN METALLIC GLASSES

2:15 pm N2 H.S. Chen and A. Inoue: SUB-Tg ENTHALPY RELAXATION IN PdNi ALLOY GLASSES

2:30 pm N3 A.I. Taub and J.L. Walter: SCALING THE COMPOSITION DEPENDENCE OF ATOMIC TRANSPORT AND STRUCTURAL RELAXATION IN AMORPHOUS ALLOYS

2:45 pm N4 B.M. Clemens, W.L. Johnson, and R.B. Schwarz: THERMODYNAMICS AND KINETICS OF FORMATION OF AMORPHOUS Zr-Ni ALLOYS FORMED BY SOLID-STATE REACTION OF THE PURE METALS

3:00 pm N5 H.A. Davies and G.P. Gregan: INFLUENCE OF COMPOSITION AND THERMAL HISTORY ON THE RELAXATION BEHAVIOR OF SOME METAL-METALLOID GLASSES

3:15 pm N6 H. Kimura and T. Masumoto: PARTICLE-DISPERSION HARDENING OF AN AMORPHOUS Ni(78)Si(10)B(12) COMPOSITE

3:30 pm Break

3:45 pm N7 F. Luborsky: CRYSTALLIZATION KINETICS OF AMORPHOUS Co-Gd RIBBONS AND FILMS

4:00 pm N8 U. Koster: DIFFUSION IN Fe-Zr-B METALLIC GLASSES

4:15 pm N9 S.H. Whang: PREDICTION OF GLASS-FORMING ABILITY FOR SOME BINARY AND TERNARY ALLOY SYSTEMS IN RELATION TO EQUILIBRIUM PHASE DIAGRAM

SESSION O: Electronic Properties II (Room 2276, Young Hall)
Chairmen: E. Luscher and J. van Zytveld

2:00 pm O1 D.G. Onn, L.Q. Wang, Y. Obi, and K. Fukamichi: LOW-TEMPERATURE SPECIFIC HEAT OF Fe-Zr AND Ni-Zr AMORPHOUS ALLOYS

2:15 pm O2 S.J. Poon: FLUX FLOW RESISTIVITY AND CRITICAL FIELDS IN AMORPHOUS SUPERCONDUCTORS

2:30 pm O3 U. Krey, R. Jeschek, and W. Fembacher: ON THE ELECTRONIC STRUCTURE AND ELECTRICAL RESISTIVITY OF GLASSY METALS

2:45 pm O4 P.J. Cote and L.V. Meisel: APPLICATION OF DIFFRACTION MODEL TO AMORPHOUS MgZn

3:00 pm O5 D. Nicholson, A. Chowdary, and L. Schwartz: PAIR DISTRIBUTION FUNCTIONS AND THE ELECTRONIC PROPERTIES OF LIQUID AND AMORPHOUS METALS

3:15 pm O6 D.M. Kroeger, C.C. Koch, J.O. Scarbrough, and C.G. McKamey: STABILITY AND ELECTRONIC PROPERTIES OF Zr-Ni GLASSES

3:30 pm Break

3:45 pm O7 M. Takahashi, F. Sato, and S. Ishio: MAGNETIC PROPERTY OF LIQUID STATE IN AMORPHOUS (Fe, Co, Ni)-B ALLOYS

5:30 pm Hollywood Bowl Concert and Picnic

Friday, 19 August

SESSION P: Electronic Properties III (Room 2250, Young Hall)
Chairmen: P. Duwez and N.F. Mott

9:00 am P1 F. Cyrot-Lackmann: ELECTRONIC STRUCTURE AND PROPERTIES OF LIQUID AND AMORPHOUS ALLOYS (Invited)

9:35 am P2 T. Fujiwara: ELECTRONIC STRUCTURE CALCULATIONS FOR AMORPHOUS ALLOYS (Invited)

10:10 am P3 M.A. Tenhover: PHOTOEMISSION AND NUCLEAR RESONANCE SPECTROSCOPY (Invited)

10:45 am Break

SESSION Q: Electronic Properties IV (Room 2250, Young Hall)
Chairmen: J. Durand and K.V. Rao

11:00 am Q1 G.A.N. Connell, J.W. Allen, and R. Allen: THE ELECTRONIC DENSITY OF STATES OF AMORPHOUS YTTRIUM-IRON AND TERBIUM-IRON BASED ALLOYS

11:15 am Q2 P. Oelhafen, U.M. Gubler, G. Indlekofer, R. Lapka, H.J. Guntherodt, C.F. Hague, V.L. Moruzzi, and A.R. Williams: THE ELECTRONIC STRUCTURE OF METALLIC GLASSES

11:30 am Q3 W. Schirmacher and D. Belitz: THEORY OF PHONON-CONTROLLED CONDUCTIVITY IN HIGH-RESISTIVITY METALS

11:45 am Q4 Y. Kita and Z. Morita: THE ELECTRICAL RESISTIVITY OF LIQUID Fe-Ni, Fe-Co, and Ni-Co ALLOYS

12:00 pm Q5 J.B. van Zytveld: ELECTRICAL RESISTIVITY OF LIQUID CHROMIUM

12:15 pm Q6 A. Tschumi, T. Laubscher, R. Jeker, H.U. Kunzi, and H.J. Guntherodt: ELECTRICAL RESISTIVITY AND HALL COEFFICIENT OF GLASSY AND LIQUID ALLOYS

12:30 pm Q7 M. Cutler and H. Rasolondramanitra: ACCEPTOR BAND TRANSPORT IN Se-Te LIQUID SEMICONDUCTOR ALLOYS

12:45 pm Lunch

SESSION R: Electronic Properties V (Room 2250, Young Hall)
Chairmen: G.A.N. Connell and M. Cutler

2:00 pm R1 G.J. Morgan, G.F. Weir, and M.A. Howson: THE HALL EFFECT IN AMORPHOUS METALS

2:15 pm R2 D. Malterre, J. Durand, and G. Marchal: VALENCE CONFIGURATION OF CERIUM IN AMORPHOUS Ce(1-x)Si(y) ALLOYS

2:45 pm R3 J. Rivory, J.M. Frigerio, L. Nevot, and Tran Minh Duc: CHARACTERIZATION OF THIN FILMS OF AMORPHOUS Cu(x)Zr(1-x) USING OPTICAL AND ELECTRON SPECTROSCOPY

3:00 pm Break

3:15 pm Round-Table Discussion: (Room 2250, Young Hall)
The Future of Metallic Glasses: Research and Development
U. Gonser, F.E. Luborsky, and Y. Makino (Invited)

4:30 pm Closing Session (Room 2250, Young Hall)

Reception: Courtyard of Young Hall

SESSION A: EXPANDED METALS

A1 METAL-NONMETAL TRANSITIONS IN LIQUIDS UNDER PRESSURE. H. Endo, Kyoto University, Kyoto 606, Japan.

The study on liquids over ranges of temperature and pressure sufficiently wide to include the liquid-gas critical point and the supercritical fluid is especially interesting since there must occur significant modifications of the atomic and electronic structures under these conditions.

A brief review is presented on the thermodynamic and electronic properties of the expanded Hg and Se. When metallic Hg is transformed to a semiconducting state in the density range near 9 g/cc, the thermal pressure coefficient, which is deduced from the data for equation-of-state, exhibit anomalies in the volume variations. The addition of a small amount of the elements with high-valency such as Bi and Pb into expanded liquid Hg bring about substantial volume contraction and large increase in conductivity, which can be attributed to the change in the character of cohesion due to the injection of excess electrons. Near the critical isochore (5.4 g/cc), the abrupt changes in the thermoelectric power and infrared absorption coefficients of expanded Hg are observed, which suggest that there appears inhomogeneous fluid state containing negatively charged clusters across the critical isochore line.

Liquid Se near the critical point transforms from semiconducting to metallic state by a slight application of pressure, accompanied by a substantial volume contraction. A useful structural model for the metallic Se is provided by liquid Te near the melting point. The large fluctuations of dihedral angle in Se chain and increase in the number of dangling bond at high temperature result in the collapse of chain structure and the delocalized threefold corrdinated site similar to liquid Te.

A2 THE NATURE OF THE PHASE TRANSITIONS IN FLUID MERCURY. Leonid A. Turkevich and Morrel H. Cohen, Exxon Research and Engineering Company, Linden, NJ 07036 USA

We review the experimental situation for expanded fluid mercury and find current theoretical interpretations deficient. The vanishing of the Knight shift [1] at ρ = 8.9 g/cm^3 and the concomitant appearance of a gap in the reflectivity [2] unambiguously rule out the Mott pseudogap and compel an assignment of a true band gap for the insulating liquid (ρ<8.9 g/cm^3). On the vapour side, the dielectric anomaly at ρ~3g/cm^3 suggests the formation of clusters [3]; above the "Marburg line" (ρ>3g/cm^3) a corroborating infrared tail appears [4] in the optical absorption. The absence of an accompanying increase in the d.c. conductivity suggests that this clustering is due not to Lifshitz nucleation [5] (as posited in [3]) but rather to excimer condensation. As the density is increased (ρ_c~5.8g/cm^3) the excimers merge into an excitonic insulating liquid. The inhomogeneous nature of this excitonic insulator is guaranteed by its high compressibility for ρ<8.9g/cm^3 [6]. The metal-nonmetal transition occurs when the (primarily) 6p conduction band overlaps sufficiently with the (primarily) 6s valence band, so that normal metallic correlation of the electrons and holes competes effectively with excitonic binding.

[1] U. El-Hanany, W. W. Warren, Jr., Phys. Rev. Lett. 34, 1276 (1975); W. W. Warren, Jr., F. Hensel, Phys. Rev. B 26, 5980 (1982).

[2] H. Ikezi, K. Schwarzenegger, A. L. Simons, A. L. Passner, S. L. McCall, Phys. Rev. B 18 2494 (1978).

[3] W. Hefner, F. Hensel, Phys. Rev. Lett. 48, 1026 (1982).

[4] F. Hensel, Ber. Bunsenges. 75, 847 (1971), H. Uchtmann, F. Hensel, Physics Letters 53A, 239 (1975); H. Uchtmann, F. Hensel, H. Overhof, Phil. Mag. B 42 583 (1980).

[5] I. M. Lifshitz, Sov. Phys.-JETP 26, 462 (1968); I. M. Lifshitz, S. A. Gredeskul, Sov. Phys.-JETP 30, 1197 (1970).

[6] G. Schönnherr, R. W. Schmutzler, F. Hensel, Phil Mag. 40, 411 (1979).

B1 SYSTEMATIC ASPECTS OF THE THERMODYNAMICS OF LIQUID ALLOYS OF TRANSITION METALS WITH NOBLE METALS. O. J. Kleppa, The James Franck Institute, University of Chicago, Chicago, IL, 60637 U.S.A.

Although there has in the past decade been greatly increased interest in the systematic aspects of alloy thermodynamics, experimental information relating to this field still is very limited. This is true in particular for alloys of the early transition metals, which are often highly reactive or very refractory or both. We have attempted to fill part of this gap through systematic investigations of the thermochemistry of alloys of transition metals with the noble metals. A review will be given of the thermodynamic properties of solutions of first row transition metals in liquid copper and in liquid gold.

B2 THERMODYNAMIC PROPERTIES OF UNDERCOOLED LIQUID METALS J. H. Perepezko and J. S. Paik, University of Wisconsin-Madison, Department of Metallurgical and Mineral Engineering, 1509 University Avenue, Madison, Wisconsin 53706 USA.

In the form of a droplet emulsion, fine dispersions of a number of liquid metals and alloys have been undercooled by substantial amounts (0.3-0.4 T_m) before the intervention of crystallization. For example, pure Hg, In, Sn and Bi can be undercooled by 90°C, 110°C, 187°C and 227°C respectively. Liquid droplets can be *maintained* in the metastable undercooled state for extended time periods without significant crystallization. Under these conditions differential scanning calorimetry has been applied to determine the heat capacity difference, ΔCp, between the undercooled liquid and crystalline solid and also the liquid heat capacity, C_p^ℓ. As a liquid droplet sample is cooled below the melting point into the undercooled regime, no discontinuity appears in the C_p^ℓ trend. With increasing undercooling both ΔCp and C_p^ℓ increase by an amount which is greater than that given by a simple extrapolation of the equilibrium data. A similar behavior is observed in an undercooled liquid eutectic Pb-Bi alloy. The trend of increasing C_p^ℓ with decreasing temperature implies a reduction in configurational entropy of the liquid which may be related to a model based on a redistribution of free volume. In addition the heat capacity measurements allow for an accurate determination of the free energy and the onset of the hypercooled regime which are useful in the evaluation of the crystallization kinetics.

The support of the NSF(DMR-79-15802) is gratefully acknowledged.

B3 THEORETICAL HIGH-PRESSURE EQUATIONS OF STATE AND PHASE DIAGRAMS OF THE ALKALI METALS*. David A. Young, Lawrence Livermore National Laboratory, Livermore, CA [illegible] USA

A two-parameter Heine-Abarenkov [illegible] pseudopotential together with [illegible] lattice dynamics model is used to fit experimental room temperature isotherms of lithium, sodium, and potassium to [illegible] kilobar. A one component plasma (OCP) fluid variational theory is then used with the pseudopotential to compute the thermodynamic properties of the liquid phase. The predicted equations of state of the liquids are in good agreement with experiment to [illegible] kbar, as are the predicted pressure-temperature melting curves to [illegible] kbar. The OCP liquid theory is clearly superior to the hard sphere variational theory for the alkalis. A melting temperature maximum is predicted for potassium. Discrepancies between theoretically calculated and experimentally determined shock Hugoniot pressures to 1 megabar probably arise from the local pseudopotential approximation. Rubidium and cesium have more complex phase diagrams due to the influence of d-electrons. A semi-empirical modification of the pseudopotential can account qualitatively for the phase behavior of these metals.

*Work performed under the auspices of the U.S. Department of Energy by LLNL under contract #W-7405-Eng-48

B4 FEASIBILITY AND STABILITY OF AMORPHOUS MATERIALS AS A FUNCTION OF THE ENTHALPY OF FUSION
M. Cyrot, Laboratoire Louis Néel, associé à l'U.S.M.G., C.N.R.S., B.P. 166X, 38042 Grenoble Cédex, France.

The feasibility and the stability of amorphous materials are related to thermodynamical and dynamical properties. The viscosity of the liquid state is an important factor but in this paper we focused on thermodynamical properties which favor the amorphous state. We first emphasize that a small enthalpy of fusion is needed in order to facilitate the amorphous state. This implies, as amorphous materials are generally made of more than one compound that local order is important in the liquid state. This makes the change of entropy when quenching smaller as part of the entropy of configuration has already disappears in the liquid state. Also implied by this consideration is that the free energy between crystalline and amorphous phase are very close. Nucleation of the crystalline phase into the amorphous one is thus difficult. We show that the depression of the fusion temperature near an entectic is due to such properties of the liquid state and thus favor the feasibility of an amorphous state.

B5 AMORPHOUS La-Au ALLOYS FORMED BY SOLID STATE REACTION OF THE ELEMENTAL CRYSTALLINE METALS. R. B. Schwarz* and W. L. Johnson, California Institute of Technology, Pasadena, CA 91125 USA, and B. M. Clemens, General Motors Research Laboratories, Warrensville, MI 48090-9055 USA

Thin films of amorphous $La_{1-x}Au_x$ alloys have been synthesized by a novel solid state reaction of the parent metals in polycrystalline form. The reaction is carried out under isothermal conditions below the crystallization temperature of the amorphous product. An alternating sequence of Au and La layers with thicknesses 100 - 1000 Å are prepared vapor deposition on glass substrates kept at 0°C. The multilayers are subsequently annealed in vacuum for several hours at 80°C. With increasing average La content, the end product of the reaction is: a) Au plus amorphous LaAu, b) single phase amorphous LaAu, and c) La plus amorphous LaAu. The average molar concentrations in the multilayers which separate these regimes are predicted by a proposed metastable free energy diagram model. The kinetics which underlie the amorphous phase formation will be discussed

*On leave from MST Division, Argonne National Laboratory, Argonne, IL 60439

SESSION C: THERMODYNAMICS AND EXPANDED METALS

C1 HIGHER-ORDER CORRELATION EFFECTS ON THERMODYNAMIC AND ELECTRONIC PROPERTIES OF LIQUID ALLOYS. M. Shimoji, T. Itami and S. Takahashi. Department of Chemistry, Faculty of Science, Hokkaido University, Sapporo 060, JAPAN.

The structure of liquid metals and alloys can be interpreted microscopically in terms of the concept of pair correlation functions for the ionic configuration. The electron theory coupled with this formalism has made marked successes in understanding the properties of simple liquid metals and alloys, for which the nearly free electron approximation holds. However, there are still some exceptional results which are unable to be understood from this well established point of view; examples can be seen in anomalous results of the thermoelectric power of liquid mercury-alkali metal alloys. It has been pointed out in an earlier paper [1] that such anomalous electronic properties of liquid mercury-alkali alloys can be related closely to the higher-order correlation effects in the ionic configuration, which reflect in characteristic temperature variations of transport coefficients or thermodynamic functions. Experimental results for the thermoelectric power of liquid Hg-Li alloys are briefly reported here, and are compared with earlier data for other mercury-alkali alloy systems.

It is also emphasized that the mercury alloy systems showing such electronic anomalies can be characterized thermodynamically as a group by examining the data of excess thermodynamic functions, in particular heats of mixing. The higher order correlation effect would arise from local structural features caused by energetic interactions between the component atoms or charge transfer.

[1] Itami T, Wada T and Shimoji M 1982 J. Phys. F: Met. Phys. 12 1959

C2 NMR STUDIES OF EXPANDED LIQUID CESIUM. W.W.Warren, Jr., A.El-Hanany*, and G.F.Brennert, Bell Laboratories, Murray Hill, NJ 07974 USA

We have applied high temperature-high pressure nuclear magnetic resonance (NMR) techniques to investigate the static and dynamic magnetic properties of expanded liquid cesium. Our measurements of the Knight shifts and nuclear spin relaxation rates extend to 1400°C at 1.0 kbars and cover the density range $1.3 < \rho < 1.9$ g cm^{-3}. At lower temperatures, pressure dependences up to 5.0 kbar were measured.

For the high density liquid near the melting point, the isobaric temperature dependence of the Knight shift is negative while the isothermal pressure dependence is positive. Below about 1.5 g cm^{-3}, however, both these dependences change sign. The increasing shift at low density correlates with the enhanced total magnetic susceptibility reported by Freyland.[1] The results show that the enhancement is due predominantly to the effects of volume expansion on the conduction electron spin susceptibility.

Comparison of the variation of the Knight shift with that of the magnetic susceptibility yields the first indication of the volume dependence of the conduction electron density of the states of an expanded metal. We find that $\rho(\epsilon_F)^{-2}\chi$ is nearly constant at about 1.0 the atomic value for $\rho > 1.4$ g m^{-3}. Below this density, however, $\rho(\epsilon_F)^{-2}\chi$ increases rapidly, varying roughly as ρ^{-4}.

The Korringa constant relating the Knight shift and relaxation rate changes substantially in the low density range. This implies the occurrence of changes in the $\vec{q}$-dependence of dynamic susceptibility $\chi''(\vec{q},\omega)$. The inferred form of $\chi''(\vec{q},\omega)$ suggests development of spin fluctuations of antiferromagnetic character.[2]

* Permanent address: Soreq Nuclear Research Center, Yavne, Israel.

[1] W.Freyland, Phys. Rev. B20, 5104 (1979).
[2] A.El-Hanany, G.F.Brennert, and W.W.Warren, Jr., Phys. Rev. Lett. 50, 540 (1983).

C3 MAGNETIC SUSCEPTIBILITY OF LIQUID Na-IVb ALLOYS. S. Takeda, S. Matsunaga and S. Tamaki, Niigata University, Niigata 950-21, JAPAN

The magnetic susceptibility of liquid Na-IVb alloys has been measured as a function of temperature and concentration. The susceptibility isotherm of liquid Na-Sn alloys has a deep minimum at the composition of Na_4Sn_3 in the temperature range near the liquidus point, and its minimum gradually moves toward the equiatomic composition, NaSn, with increasing temperature. This suggests that there has a dissociation process, $Na_4Sn_3 \longrightarrow (4 - c')Na + (3 - c')Sn + c'NaSn$, with increasing temperature. Liquid Na-Sn system has also another compound-formation near the composition of Na_3Sn, which is confirmed by thermodynamic measurements (Tamaki et al, 1982).

On the other hand, the susceptibility isotherm of liquid Na-Pb alloys deviates somewhat from a linearly interpolated curve and its largest deviation appears near the composition of Na_4Pb.

From these, it is inferred that the chemical bonding nature in liquid Na-Sn alloys is considerably different to that in liquid Na-Pb alloys.

Tamaki S, Ishiguro T and Takeda S, 1982, J. Phys. F: Metal Phys., 12, 1613

C4 SPECIFIC HEAT AND TOF NEUTRON DIFFRACTION MEASUREMENTS IN MOLTEN Bi-BiI_3 MIXTURES. K. Ichikawa, Department of Chemistry, University of Hokkaido, Sapporo 060, Japan

Current interest in molten metal-salt solutions has brought about the study of microscopic properties and the metal-nonmetal (MNM) transition, using the techniques of neutron scattering and NMR. The heat-capacity measurement may be of considerable value in connecting the thermodynamics with the structural or chemical bonding property. This paper focuses on the C_p and TOF neutron-scattering measurements in the molten Bi(x_m)-BiI_3 mixtures (or liquid Bi_xI_{1-x} alloys).

Measurements of the high-temperature heat capacity C_p have been made with an adiabatic calorimeter. Calorimeter operation was tested by measuring C_p of standard synthetic saphire (99.99 weight % purity) between 50°C and 500°C. Our results of synthetic saphire agree with the selected values within an experimental uncertainty of ±1.0%. This agreement is sufficient for our present purpose. The samples were sealed under vacuum in quartz cell with a dead space of less than ca.1.5×10^{-6} m^3. The total structure factor S(Q), for the nine compositions in the liquid state, was measured with pulsed neutron scattering method using the Hokkaido University Electron Linac. The observed C_p shows a maximum value at ca.55 mol% BiI_3 (or 42.5 at% Bi), just above the concentration of which the abrupt increase of the Bi-Bi distance takes place, and below the consolute composition (i.e., 62.5 at% Bi) the curve of S(Q) shows a tendency towards small-angle scattering produced by the microscopic inhomogeneity in the molten mixtures. The peak observed in C_p vs x_m (or x) results from the appearance of the bismuth homopolyatomic ions because of their vibrational and rotational contributions. The clusters composed of the Bi species give rise to the continuous metal-nonmetal transition between 40 and 60 at% Bi, associated with the change of the structural and bonding pattern in the polybismuth clusters.

C5 METAL-NONMETAL TRANSITION IN CHARGE TRANSFER ALLOYS AND METAL-MOLTEN SALT SOLUTIONS. Judy R. Franz, Indiana University, Bloomington, IN 47405, USA.

A theoretical model, first developed to explain the metal-nonmetal transition in dilute alkali systems, has been applied to liquid and amorphous charge-transfer alloys and metal-molten salt solutions. The model is based on the quantum percolation Hamiltonian, $H = \sum t_{ij} c_i c_j$, where t_{ij} is a hopping parameter which varies randomly from site to site. The model thus emphasizes the disorder in the system and, in particular, the disorder in the coordination number. A sharp metal-nonmetal transition is predicted for all systems with a high degree of charge transfer. Density of states and conductivity calculations for model systems will be presented and compared to previous results[1,2] obtained using the cluster-Bethe lattice technique. Similarities and differences between the charge transfer alloys and the dilute alkali systems will also be discussed.

[1]J.R. Franz, F. Brouers, and C. Holzhey, J. Phys. F: Metal Phys. 10, 235 (1980).
[2]C. Holzhey, F. Brouers, and J.R. Franz, J. Phys. F: Metal Phys. 11, 1047 (1981).

C7 OPTICAL REFLECTIVITY OF MOLTEN $Cs_x(CsCl)_{1-x}$ ALLOYS.* R. Fainchtein, U. Even**, and J.C. Thompson, University of Texas at Austin, Austin, Texas 78712 USA

Normal reflectance of 11 $Cs_x(CsCl)_{1-x}$ alloys were obtained. The measurements were performed 25°C above the liquidus curve over a 0.65 to 5.5 eV range. A large drop in the reflectivity was observed over a small range of concentration: from a metallic regime for $x \geq 0.98$ to an apparent insulating state for $x \leq 0.85$. Reflectivities of less than 0.10 were obtained for photon energies above 1 eV for $x \leq 0.85$. The metal-nonmetal transition is sharp and well marked in the optical data. However, reported measurements of conductivity for similar alloys[1] $[K_x(KBr)_{1-x}]$ vary only from 17×10^3 to 7×10^3 $ohm^{-1}cm^{-1}$ on the $0.90 \leq x \leq 1.00$ range.

*Supported in part by the US NSF under grant DMR 78-21744 and by the R.A. Welch Foundation.
**Present address: Tel-Aviv University.
[1]H.R. Bronstein, A.S. Dworkin and M.A. Bredig, J. Chem. Phys., 37 677 (1962).

C6 **STRUCTURAL IMPLICATIONS OF THERMODYNAMIC MEASUREMENTS IN LIQUID ALLOYS.** **Marie-Louise Saboungi, Chemical Technology Division, Argonne National Laboratory, Argonne, Illinois 60439 USA**

A tendency for a metal to nonmetal transition has been known to occur in some liquid alloys at a composition corresponding roughly to the ratios of the chemical valencies of the constituent atoms. The behavior of dilute solutions was examined to determine the influence of the ordering known to accompany the MNM transition. In dilute solutions, the magnitude and temperature dependence of the slope of the activity coefficient of the solute are related to statistical mechanical correlation functions and to the relative attractions or repulsions existing between the solute atoms. Thermodynamic properties of liquid sodium and lithium containing alloys have been measured . Analysis of the activity coefficient of either sodium, or lithium in dilute solutions has been conducted within the framework of a statistical mechanical theory developed by Kirkwood and Buff.[1] The first derivative of the logarithm of the activity coefficient of the solute is related to integrals of the pair radial distribution function of the species present in solution. In all the systems that we have studied it is shown that (i) the sign of the *limiting* slope is positive and (ii) its magnitude is relatively small. The positive sign indicates a relative repulsion between the solute atoms and an attraction between the unlike atoms. The fact that even for systems such as Na-Bi,[2] and Na-Pb,[3] the limiting slope is smaller than a coordination number of a molten salt, e.g., 6 could be explained by screening which decreases the effective range of the coulomb repulsions between charged alkali atoms. Electronic shielding appears to be an important factor which, to a certain extent decreases the tendency toward unlike atoms to pair and like atoms to repel.

References

1. J. G. Kirkwood and F. P. Buff J. Chem. Phys 19, (1951), 774
2. M. L. Saboungi and T. P. Corbin Submittted for publication
3. M. L. Saboungi and S. Herron (in preparation)

Acknowledgement

This work was performed under the auspices of the Division of Materials Science, Office of Basic Energy Sciences of the United States Department of Energy.

C8 STRUCTURE AND MODEL OF METAL -MOLTEN SALTS SOLUTIONS IN METALLIC TRANSPORT REGIME

J DUPUY*, J.F. JAL*, J. CHABRIER* , P. CHIEUX**,

The structure of an alkali metal is strongly perturbed by the addition of a molten salt as already shown in LAM 4. *Neutron diffraction* experiments give a direct access to the short range or the medium range order in these systems. In particular the use of a pair of atoms with identical coherent scattering lengths gives the density-density correlations. This is verified for the systems Cs-CsI, Rb-RbBr and K-KCl[37] which we have investigated at concentrations of about 90 % and 80 % in metal fraction, i.e. in the metallic conduction regime. We have also investigated the isotoped K-KCl systems at 80 % in metal fraction.

As compared to the pure metal one observes that the first interference maximum in $S_{NN}(q)$ and the first interference maximum in $S_{Metal-Metal}(q)$ are strongly reduced and becomes out of the phases with the second maximum. The ionic short M^+X^- distance characteristic of the salt is obtained at quite lowsalt content. This indirectly increases the free volume accessible to the metallic atoms. The medium range order as detected from the strong small angle scattering observed on the $S_{NN}(q)$ curves is attributed to a strong coupling between the density and the concentration fluctuations.

We present and discuss a multicomponent plasma model and give first very promising results deduced by M.S.A. and H.N.C. methods. The approach by plasma model based on statistic methods is more powerful than the one deduced from solid state description.

* Département de Physique des Matériaux, L.A. 172
Université Claude Bernard - Lyon Villeurbanne (France)
** Institut Laue Langevin - Grenoble (France)

SESSION D: ELECTRONIC PROPERTIES I

D1 ELECTRON-PHONON ENHANCEMENT AND THE THERMOPOWER OF NiZr METALLIC GLASSES. R. Harris, Physics Department, McGill University, 3600 University Street, Montreal, Quebec, Canada H3A 2T8. and A.B. Kaiser, Physics Department, Victoria University of Wellington, New Zealand.

We show that the thermopower of several NiZr metallic glasses measured by Altounian et al. (1) is consistent with the hypothesis that the low-temperature thermopower is enhanced by the electron-phonon interaction and by spin fluctuation effects. The temperature dependence of the electron phonon enhancement appears as the well known "knee" in the thermopower (1,2,3), but the temperature dependence due to spin fluctuations would appear only well above room temperature. The analysis suggests that the electron-phonon enhancement is largely independent of concentration.

(1) Z. Altounian, C.L. Foiles, W.B. Muir and J.O. Strom-Olsen, Phys. Rev. B27, 1955, 1983.
(2) B.L. Gallagher, J. Phys. F11, L207, 1981.
(3) A.B. Kaiser, J. Phys. F12, L223, 1982.

D2 TRANSPORT-PROPERTIES OF METALLIC GLASSES AT HIGH PRESSURES. E. Lüscher, J. Willer, TU München, Garching, Germany, and G. Fritsch, HSBw München, Neubiberg, Germany

We report on the pressure and temperature dependence of the electrical resistivity of several amorphous alloys. The pressure range covered extends from zero to 130 kbar. The temperature is varied simultaneously betwee 1,3 and 300 K. Data for metal-metal, metal-transitionmetal, transition-metal-transitionmetal, as well as transitionmetal-nonmetal alloys will be presented.

Whereas the temperature dependence of the alloys, belonging to the first three groups is negative, the transitionmetal-nonmetal-alloys examined show a positive temperature coefficient at high temperatures and a negative one at low temperatures. The pressure dependence of the metal-metal alloy turns out to be positive contrary to the behaviour of the metal-transitionmetal or transitionmetal-transitionmetal alloys which exhibit a negative pressure dependence. Finally, the transitionmetal-nonmetal group possesses a pressure dependence, varying from almost zero to negative values.

The behaviour of all these groups will be discussed within existing theories.

D3 THE THERMOPOWER OF SUPERCONDUCTING AND MAGNETIC Fe-Zr GLASSES. W.B. Muir, Z. Altounian, J.O. Strom-Olsen, McGill University, Physics Department, 3600 University Street, Montreal, Quebec, Canada H3A 2T8 and R.W. Cochrane, Universite de Montreal, Montreal, Quebec, Canada.

Thermopower has been measured from 4K to 600K in a wide range of Fe-Zr glasses. At the Zr rich end where the glasses are superconducting the thermopower is approximately linear in temperature with small deviations caused by electron mass enhancement effects similar to those seen in Ni-Zr(1).As the Fe concentration increases the alloys become magnetic rather than superconducting and the thermopower becomes very non linear changing sign with temperature in some cases. The behavior through the Curie temperature suggests that these non linearities are not caused directly by the magnetism but probably reflect the strong enhancement of the density of states.

(1) Z. Altounian, C.L. Foiles, W.B. Muir and J.O. Strom-Olsen, Phys. Rev. B27, 1955 (1983).

D4 TEMPERATURE DEPENDENCE OF RESISTIVITY OF AMORPHOUS METAL-METAL SYSTEMS WITH WIDE COMPOSITION RANGES* C. L. Chien and S. H. Liou, The Johns Hopkins University, Baltimore, MD 21218 USA

We have studied a number of binary, amorphous transition metal-metal solids made by a sputtering technique over a wide range in composition. These include Fe-Zr, Fe-Nb, Fe-Ti, Fe-Mo, Ni-Nb, etc. These samples may be magnetic, non-magnetic or superconducting. By varying the composition, the temperature dependence of the resistivity changes systematically, thus allowing the various contributions to the resistivity to be elucidated. Within the temperature range of 2 K < x < 300 K, the temperature coefficient of resistance (TCR) of most samples changes sign. This indicates contributions with opposing temperature dependences. For the non-magnetic samples, a term proportional to T, attributed to electron-phonon scattering, and a term with a negative TCR give rise to a resistance maximum. For the magnetic samples, a resistance minimum and a -lnT term at low temperatures are observed. The -lnT term, attributable to the Kondo mechanism, is not however responsible for the resistance minimum occuring at high temperatures. Various models for negative TCR terms are discussed and compared quantitatively by fitting the experimental data.

*Work supported by the NSF Grant No. DMR82-05135.

DE THERMO-POWER OF RAPIDLY QUENCHED Fe-RICH Fe-Zr AMORPHOUS ALLOYS. A.K. Sharma, S. Shamasundar, University of Hyderabad, Hyderabad, India, A.V. Narlikar, 3M Laboratories, St. Paul, MN 55144, and K. Fukamichi, Tohoku University, Sendai, Japan.

The magnetic and transport properties of amorphous Fe-rich Fe-Zr alloys are unusual: The Ferromagnetic transition temperature, T_C, plotted as a function of Zr concentration exhibits a broad maximum around 20 at .% Zr with a T_C ≈280K; for the Fe-rich alloys T_C decreases rather sharply indicating a possible non-magnetic state for pure amorphous Fe; at temperatures below T_C, a spin-glass-like behaviour has been reported[1] for alloys with 8-12 at .% Zr; the electrical resistance increases below around T_C, and has a negative temperature coefficient down to helium temperatures. In addition, thermal expansion curves for these Fe-rich alloys have been found to show typical invar characteristics[2] below T_C. In order to understand these properties in detail we have measured the thermo-power, in the temperature range 80 - 400 K, of rapidly quenched $Fe_{90}Zr_{10}$, and $Fe_{91}Zr_9$ amorphous alloys obtained from the same batch of samples that were used in the above mentioned studies. The thermopower for both the alloys is found to be negative (in the range -2 to -4μV/K), and has a negative temperature coefficient indicating a contribution of magnetic origin. In the $Fe_{90}Zr_{10}$ alloy a small change in slope is observed below T_C, with the thermopower increasing at lower temperatures. In both the alloys the observed S(T) behaviour between 120K and 250 K is found to be similar to that reported for amorphous $Fe_{80}B_{20}$ alloy which is also known to exhibit invar characteristics.[3] These results can be explained in the frame work of the Coherent-exchange scattering model, and are consistent with recent electrical and magneto-resistance studies on the same samples.

1 H.Hiroyoshi, and K. Fukamichi, J. App. Phys. 53(3), 2226 (1982)
2 K. Shirakawa et al IEEE trans. MAG-16, 910 (1980)
3 M.N. Baibich et al, Phys Letters 73A, 328 (1979).

DC ELECTRIC PROPERTIES OF $Ni_{100-x}B_x$ and $Ni_{81.5}B_{18.5-y}Py$ METALLIC GLASSES.
L.K. Varga, A. Lova, J. Tóth, Central Research Institute for Physics, 1525 Budapest P.O. B.49 Hungary, and S. Arajs, Clarkson College, Potsdam, New York 13676

Measurements of the electrical resistivity, ρ, from 4.2 K to room temperatures and the temperature coefficient of the resisitivity, TCR, and the thermoelectric power, TP, at room temperatures are reported for nonmagnetic Ni-base metallic glasses, $Ni_{100-x}B_x$ and $Ni_{81.5}B_{18.5-y}Py$, for values of x between 18.5 and 40.0 and y between 0 and 18.5. It is found to be difficult to prepare the Ni-B system free of remanent crystals.

The TCR decreases and the TP increases almost linearly with the P content in the Ni-B-P system similarly to the behavior found in the Ni-P system (1,2).

The ρ minimum in the Ni-B-P system is an order of magnitude smaller than in alloys containing magnetic impurities. The minimum is displaced systemically with increasing P/B ratio.

The above metallic glasses satisfy the Mooij correlation between the TCR and ρ.

References

1. L.K. Varga, K. Tompa, T. Schmidt, phys. stat. sol. 68, 603 (1981).
2. L.K. Varga and T. Schmidt, phys. stat. sol. (a) 74, 279 (1982).

SESSION E: STRUCTURE I

E1 DIFFRACTION STUDIES OF LIQUID AND AMORPHOUS ALLOYS.

S. Steeb
Max-Planck-Institute for Metal Research, Institute for Materials Science, Seestraße 92, 7000 Stuttgart-1, Germany.

From n, x, e diffraction experiments with molten alloys total structure factors S as function of momentum transfer Q can be evaluated, which themselves yield important features:

i) A rise of S(Q) versus small Q's, i.e. small angle scattering, indicates segregation tendency.
ii) A premaximum indicates compound forming tendency.
iii) A splitting up of the second maximum of S(Q), which was up to now observed with the Fe-B, Ni-B, and Mn-Si systems, indicates that the corresponding melt rather probably forms amorphous substances during rapid solidification.

Detailed structural information is obtained by the so called partial structure factors which yield the following items:

i) Quantitative information concerning the chemical short range order.
ii) The possibility to calculate various physical properties.
iii) The possibility to check models.

The author will give a review on the progress which was done in the field of diffraction experiments with liquids and amorphous materials since LAM 4 in 1980.

E2 MICROSCOPIC STUDIES OF DYNAMICS IN LIQUID AND AMORPHOUS ALLOYS

D. Quitmann, Institut für Atom- und Festkörperphysik Freie Universität Berlin, D1000 Berlin 33, Fed. Rep. Germany.

The report shall be concerned with experimental information about dynamics of the matrix atoms in binary liquid or amorphous alloys. The techniques applicable are inelastic (quasielastic) neutron scattering and nuclear spin relaxation. The interconnection and differences are pointed out. Three examples from the literature will be discussed which represent collective motion in a metallic glass, and single particle as well as correlated motion in liquid alloys with chemical short range order. Emphasis will be on the liquid systems (Li_4Pb, InSb etc). The close relation between structure and dynamics, i.e. excitations, is stressed. Existing model calculations compare favourably with experiment. From the results for the examples emerges a picture for the dynamics in the stable amorphous, and in the liquid state, the general features of which may be expected to apply to many disordered metallic systems.

Of the existing literature we can quote here only a few papers to which reference will be made:

J.B. Suck, H. Rudin, H.J. Güntherodt and H. Beck: Phys. Rev. Lett. 50 (3) 49; J.B. Suck and H. Rudin, in the press.
J. Hafner: Phys. Rev. B27 (83) 678, and J. Phys. C in print
M. Soltwisch, D. Quitmann, H. Ruppersberg and J.B. Suck: Phys. Lett 86A (81) 241, and in the press
M. Elwenspoek, R. Brinkmann, P. Maxim, C. Paulick and D. Quitmann: Ber. Bunsenges. 1983

E3 CAPABILITIES AND LIMITATIONS OF EXAFS FOR AMORPHOUS MATERIALS. G. S. Cargill III, IBM T. J. Watson Research Center, Yorktown Heights, NY 10598, USA

This paper provides a critical overview of the role of EXAFS in determining the structures of amorphous materials, particularly amorphous metallic alloys. Both measurement techniques and analysis procedures are described. The importance of peak asymmetry and of thermal vibrations in complicating interpretation of experimental EXAFS data is discussed. The use of crystalline model systems in evaluating EXAFS experiments on amorphous alloys and in testing the reliability of usual EXAFS analysis procedures is reviewed. EXAFS results for amorphous alloys are compared with structural data obtained by other techniques. Competing and complimentary aspects of EXAFS, x-ray scattering, and neutron scattering for structural characterization of amorphous alloys are assessed.

SESSION F: GLASS TRANSITION

F1 THE NATURE OF THE GLASS TRANSITION. Morrel H. Cohen and Gary S. Grest, Exxon Research and Engineering Company, Linden, NJ 07036 USA

In this paper, we review the recent progress that has been made towards developing the free-volume model into a unified theory of dense liquids, glasses and the glass transition. We present results on nonequilibrium phenomena and on the origin of the dispersion of relaxation times observed in dense liquids and glasses near the glass transition temperature. We propose an explanation of the low temperature tunnelling centers observed on glasses which agrees with observations of the dependence of the density of states on glass transition temperature and annealing temperature. We also discuss generalization of the model appropriate to wider classes of materials than is the free volume model itself.

F2 COMPUTER GLASS TRANSITION
F. Yonezawa, Keio University, Yokohama 223 Japan and M. Kimura, Tokyo Institute of Technology, Tokyo 152 Japan

By means of the molecular dynamics technique, we have prepared *computer glasses* and studied the structural, thermodynamic, transport and dynamical properties of the obtained glasses in comparison with those for corresponding liquids and crystals. The computer glasses have been produced by quenching *under constant pressures* several model liquids characterized by various interatomic interactions.

The physical properties we have observed of our computer glasses include:

[I] Structural properties
1) g(r):Pair distribution function
2) S(q):Structure factor

[II] Thermodynamic properties
1) PVT :Equation-of-state data(isobars in v-T plane)
2) α_p :Isobaric thermal expansion coefficient
3) H :Enthalpy
4) c_p :Specific heat at constant pressure
5) c_v :Specific heat at constant volume
6) κ_T :Isothermal compressibility

[III] Dynamical properties
1) $\psi(t)$:Velocity autocorrelation function (VAF)
2) $f(\omega)$:Power spectrum

[IV] Transport properties
1) D :Diffusion constant(from VAF and from mean square displacement)
2) η :Shear viscosity(from stress autocorrelation function)

[V] Microscopic information of the atomic distributions
1) $\overline{g(r)}$:Pair distribution function of time-averaged atomic positions
2) Voronoi analyses

We have examined these physical properties in detail to elucidate the mechanism of the glass transition. In this context, we discuss the free volume concept and the cage-structure idea. Potential dependence of the glass transition and glassy structures is also investigated.

F3 PICOSECOND PULSED LASER-INDUCED MELTING AND GLASS FORMATION IN METALS. Frans Spaepen, Chien-lung Lin and David Turnbull, Division of Applied Sciences, Harvard University, Cambridge, Massachusetts 02138, U.S.A.

Irradiation of a metal surface with a picosecond laser pulse can produce heating and cooling rates as high as 10^{13}K/second [1], which is an entirely new regime for the study of melting, crystal regrowth and glass formation in metals. The thermodynamics and kinetics of these transformations, together with the atomic transport in the short-lived molten state, will be discussed [2].

The high cooling rates in this process have led to the formation of new metallic glasses [3]. The experimental technique for obtaining and characterizing these glasses, a survey of the results, and the criteria for glass formation under these conditions will be reviewed.

[1] N. Bloembergen, in "Laser-Solid Interactions and Laser Processing," ed. by S.D. Ferris, H.T. Leamy and J.M. Poate, AIP Conf. Proc. 50, (1979), p. 1.

[2] F. Spaepen and D. Turnbull, "Laser annealing of semiconductors," ed. by J.M. Poate and J.W. Mayer, Academic, New York, (1982), p. 15.

[3] C.J. Lin and F. Spaepen, Appl. Phys. Lett., 41, 721 (1982).

Work supported by the Office of Naval Research, Contract N00014-83-K-0030.

F4 REVERSIBLE TRANSFORMATIONS OF SHORT-RANGE ORDER IN COBALT-BASE AMORPHOUS METALS. R. C. O'Handley, B. W. Corb and N. J. Grant, Massachusetts Institute of Technology, Cambridge, MA 02139 USA

Co-Nb-B glasses show a reversible change in magnetic anisotropy (with no change in saturation magnetization) upon thermal cycling about a transformation temperature T_o. In amorphous $Co_{80}Nb_{14}B_6$ $T_o = 108^oC$ and the kinetics of transformation from the higher anisotropy state ($T < T_o$) to the lower anisotropy state ($T > T_o$), or vice versa, become more rapid with increasing $|T - T_o|$ above or below T_o. The temperature dependence of the activation energy is well described by the linear relation $Q(T) = Q_o - Q_1|T - T_o|$, where Q_o = 0.15 eV and Q_1 = 1.5 meV/K. We model the transforamation by considering the short-range orders in the glass to be similar to those in clusters of icosahedral, trigonal and octahedral symmetry (the latter two by analogy with hcp and fcc Co-base alloys). Assuming the transformation to consist of a change in local symmetry from trigonal-like ($T < T_o$) to octahedral-like ($T > T_o$), and using the change in entropy for the hcp (trigonal) - fcc (octahedral) transformation in crystalline cobalt, ΔS = 0.15 cal/mole, we can estimate that a critical cluster for our transformation contains approximately 200 atoms (a sphere 17 A in diameter). DSC results indicate a latent heat for the transformation of approximately 5 cal/mole. This is 10% of the value expected if the entire sample transforms from hcp-like to fcc-like short-range order. Group theoretical arguments support the greater anisotropy of trigonal clusters relative to octahedral clusters, consistent with the higher anisotropy we observe in the $T < T_o$ phase.

This work was supported in part by U. S. Army Research Office Contract No. DAAG-29-80-K-0088.

F5 REVERSIBLE AND NON-REVERSIBLE EFFECTS IN RELATION TO SHORT RANGE ORDERING : A KINETIC ANALYSIS IN $Ni_{24}Zr_{76}$.

J. Hillairet, E. Balanzat, N.E. Derradji, A. Chamberod, Centre d'Etudes Nucléaires de Grenoble, Département de Recherche Fondamentale, Section de Physique du Solide, 85 X, 38041 Grenoble Cedex, France.

The detection and analysis of the evolution of local order by use of resistivity methods combined with heat and quench cycles is discussed. Application to $Ni_{24}Zr_{76}$ alloys prepared by melt-spinning and sputtering is presented. In both cases, a reversible variation of the electrical resistance with anneal temperature could clearly be separated from a non reversible resistance decrease. Comparison with elastic modulus measurements conducted in the same materials, for which a reversible effect has been evidenced also, leads to consider that this reversibility is reflection of the thermodynamical variations of the (metastable) equilibrium degree of compositional short range order, while the non-reversible term arises from a distinct ordering process, mostly topological in character. Length measurements of the dimensional variation which takes place during structural relaxation have brought further indications about the ordering processes being operative.

The kinetics of the reversible effect has been analyzed in some detail, according to a scheme already proposed [1]. Just like for $Cu_{50}Ti_{50}$ and $Ni_{35}Ti_{65}$, one is led to conclude to the existence of ordering domains, in $Ni_{24}Zr_{76}$, each characterized by a specific relaxation rate and evolution degree of compositional short range order. Atomic jump rates have been derived also. Finally, the influence of the amorphisation process on the initial structural state will be considered.

[1] E. Balanzat, J. Hillairet - J. Phys. F, 12, 2907, 1982.

SESSION G: STRUCTURE II

G1 EXPERIMENTAL DETERMINATION OF PARTIAL STRUCTURES IN $Ni_{40}Ti_{60}$ GLASS

T.Fukunaga, N.Watanabe* and K.Suzuki
The Research Institute for Iron, Steel and Other Metals,
Tohoku University, Sendai 980, Japan
*National Laboratory for High Energy Physics,
Oho-machi, Tsukuba-gun, Ibaraki-ken, 305, Japan

The partial structures of $Ni_{40}Ti_{60}$ glass in terms of the atomic species-atomic species correlations and the dens ty-concentration correlations were experiemtally derived from the combination of X-ray and neutron diffraction experiments. The $S_{cc}(Q)$ was first observed by neutron diffraction from a neutron zero-scattering $Ni_{40}Ti_{60}$ glass substituted partially with ^{60}Ni-isotope. The $S_{NN}(Q)$ and $S_{NC}(Q)$ were separated from neutron and X-ray S(Q) of $^{nat}Ni_{40}Ti_{60}$ glass using the $S_{cc}(Q)$ obtained above. Finally, the $S_{NN}(Q)$, $S_{NC}(Q)$ and $S_{cc}(Q)$ were transformed into the $S_{NiNi}(Q)$, $S_{NiTi}(Q)$ and $S_{TiTi}(Q)$ as shown below. A drastic feature existing in the partial structures of $Ni_{40}Ti_{60}$ glass is a large peak situated at Q-1.9 A^{-1} in $S_{NiNi}(Q)$, which has never been observed in metal-metal alloy glasses so far.

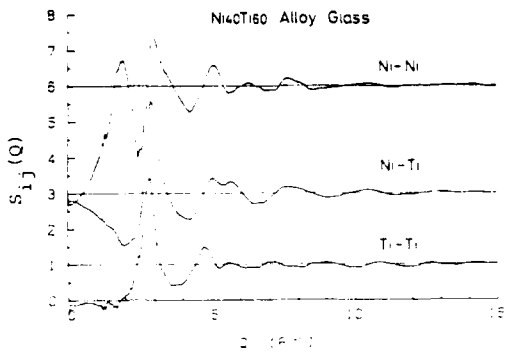

G2 STRUCTURE OF AMORPHOUS $Ni_{35}Zr_{65}$. Alfred Lee, George Etherington and C.N.J. Wagner, Department of Materials Science and Engineering, University of California, Los Angeles, California 90024.

The structure of amorphous $Ni_{35}Zr_{65}$ has been determined using X-ray and neutron diffraction techniques. The variable 2^{θ} method was used with X-rays and the variable λ method with neutrons. X-ray and nuetron structure factors I(K) were measured from a $Ni_{35}Zr_{65}$ sample, and in addition an X-ray structure factor was measured from a sample of the structurally isomorphous alloy $Ni_{35}Zr_{35}Hf_{30}$. The three experimentally measured structure factors were used to determine the partial structure factors $I_{ij}(K)$ using the method of ridge analysis [1]. Fourier transformation of the $I_{ij}(K)$ yielded the partial atomic distribution functions $\rho_{ij}(r)$. The partial reduced atomic distribution functions $G_{ij}(r)$ show that the nearest neighbor interatomic distances for Ni-Ni, Ni-Zr and Zr-Zr pairs are 2.67 A, 2.67 A and 3.16 A, respectively. A comparison of the Ni-Zr separation with the sum of the atomic radii in the pure metals suggests chemical ordering in amorphous $Ni_{35}Zr_{65}$.

[1] A. Hoerl, Chem. Eng. Progr. 58 (1962) 54

*Supported by NSF contract DMR80-07935

G3 RELATIONSHIP BETWEEN SPACE CORRELATED FLUCTUATIONS AND INITIAL ALLOY COMPOSITION IN SOME METALLIC GLASSES.

A. Naudon and A.M. Flank, Laboratoire de Metallurgie Physique 86022 Poitiers, FRANCE.

It is now well established that many amorphous alloys reveal a small-angle scattering intensity which is linked with heterogeneities in these samples. However the genuine nature of these heterogeneities is not easy to determine by a direct interpretation of an experimental result. Furthermore, depending upon the alloy preparation, obvious differences between observed small-angle scattering patterns appear. There are in fact some variables associated with these techniques which may influence the state of quench and hence the structure of the glass, at least in a medium range scale. For X-rays the heterogeneities are variations in electron density which can be due to fluctuations of the chemical composition. Insights concerning these chemical fluctuations can be obtained when measuring the chemical short range order parameters or by determining the nature of the crystallized phases.

Small-angle scattering experiments have been carried out on an absolute scale in order to quantify the amplitude of the fluctuations which appear when the alloy is heated. The more often a maximum appears in the low angle region. It is linked with space correlated fluctuations, the amplitude of which increases with temperature. Examples are given for different systems as Cu-Ti, Ni-Y or Cu-Y in a wide range of compositions. The alloys which have the same initial composition as the crystalline phase one do not exhibit small-angle scattered intensity. On the contrary, in the case of a different composition, a scattering is observed. Measurement of the integrated intensity leads to a value which can reach 15 % for the amplitude of the fluctuations just before crystallization.

G4 X-RAY DIFFRACTION FROM LIQUID AND AMORPHOUS $Mg_{70}Zn_{30}$ ALLOYS. H. Rudin, S. Jost and H.-J. Güntherodt, Institut für Physik, Universität Basel, CH-4056 Basel, Switzerland

The total interference function S(q) of the system $Mg_{70}Zn_{30}$ has been determined in the glassy state at R.T. and in the liquid state at 670 K using the method of energy dispersive X-ray diffraction in connection with a transmission geometry. The liquid sample of 0.5 mm thickness was produced by melting metglass ribbons between two parallel beryllium windows. A pronounced prepeak, characteristic for chemical short range order, and a well split second main maximum of S(q) are the essential features for the metallic glass. In the liquid state the prepeak is still clearly observed but less pronounced, whereas the second main maximum shows a shoulder on the high q side rather than two peaks. After recrystallization of the sample a number of Bragg reflections appear at the position of the former premaximum, suggesting that the local order in the liquid and glassy state corresponds approximately to the crystalline order. The observed results are compared with model calculations.

G5 EXAFS STUDY OF AMORPHOUS $Cu_{33}Zr_{66}$ ALLOY

A. Sadoc, Laboratoire de Physique des solides, bât. 510 et LURE, bât. 209C, Université Paris-Sud, 91405 Orsay, France.

The Exafs spectra of amorphous Cu_xZr_{1-x} alloys (x = 0.33, 0.46, 0.60) have been recorded on both Cu and Zr K absorption edges. We present here the analysis for the alloy which has the higher zirconium content, i.e. $Cu_{33}Zr_{66}$. This amorphous material crystallizes homogeneously to a single $CuZr_2$ phase of known crystal structure (Si_2Mo type). The existence of the $Cu_{33}Zr_{66}$ composition in both crystalline and glassy phases makes it an attractive model system for quantitative Exafs investigation of the local atomic environment in metallic glasses.

The spectra of glassy $Cu_{33}Zr_{66}$ have been reconstructed using a two subshell modelling for the Cu-Cu pairs and for the Zr-Zr ones. The RDF of the Cu-Cu pairs is very different in the glass and in the crystalline alloy. But, it is similar to that found in the two richer copper concentrations (1,2).

(1) A. Sadoc, D. Raoux, P. Lagarde, A. Fontaine, J.N.C.S. 50 (1982) 331.

(2) A. Sadoc, A.M. Flank, D. Raoux, P. Lagarde 5th Int. Conf. The Physics of Non-crystalline Solids, Montpellier (1982).

G7 X-RAY SCATTERING, ELECTRON CORRELATIONS, AND THE SMALL k-BEHAVIOUR OF THE STRUCTURE FACTOR OF SIMPLE LIQUID METALS.

M. Silbert, School of Mathematics and Physics, University of East Anglia, Norwich, NR4 7TJ, UK

Recent X-ray scattering data on the small k-behaviour of the structure factor of liquid metals $S_X(k)$, suggests the presence of a linear term in the small k expansion, ie.

$$S_X(k) - S(0) = a_1k + a_2k^2 + a_3k^3 + \ldots$$

A proper analysis of the X-ray data requires the liquid metal to be described as a binary mixture of ions and conduction electrons. For simple metals, where electron-ion coupling is weak and hence the interaction between electrons and ions can be represented by a pseudopotential, it is shown that the linear term is accounted by the purely electronic Fermi liquid; hence electron correlations dominate the small k-behaviour of $S_X(k)$.

On the other hand, small k neutron scattering data probes the long range part of the effective interionic forces, and it is expected that

$$S_n(k) - S(0) = O(k^2)$$

A large part of this work was carried out while the author was on study leave at the Ben Gurion University of the Negev at Beer Sheva, and he wishes to thank the Chairman of its Physics Department for the hospitality which he received, and the Royal Society for financial support.

G8 SELF-DIFFUSION IN SIMPLE LIQUID METALS

W. Glaeser and Ch. Morkel, Physik-Department, Technische Universität München, D 8046 Garching, FRG

Abstract: In spite of considerable progress in the kinetic theory of simple dense liquids our understanding of single particle motions in such systems is still unsatisfactory.
Inelastic incoherent neutron scattering can provide more detailed information on the diffusion process than classical diffusion measurements. Only a few experimental results have been reported up to now. With the advanced scattering techniques available now we have started a systematic investigation of the self motion in liquid alkali metals.
The paper will report first results on liquid sodium in the temperature range from 400K to 1000K.
Besides the known Lorentzian behaviour of the scattering function in the low momentum transfer region a resonance like transition to Gaussian behaviour is observed at intermediate momentum transfers.
This observation is interpreted as a sudden change from a more "bound" to a more gas like behaviour of the liquid particles.

SESSION H: THEORY

H1 ORIENTATIONAL ORDERING IN 2- AND 3-DIMENSIONAL SYSTEMS. D.R. Nelson, Lyman Laboratory, Harvard University, Cambridge, MA 02138 USA

Two broken symmetries distinguish the crystalline state from an isotropic liquid. Intermediate phases of matter are possible, with long range correlations in the orientations of local cluster axes, but without extended translational order. An example is the hexatic phase, which appears in recent theories of 2d melting, and in bulk smectic liquid crystals. Large six-fold orientational correlation lengths can also occur in nominally "disordered" binary 2d particle arrays,[1] where they show up as a modulation in the structure function $S(\vec{q})$. Correlations in the orientations of *icosahedral* packing units have been observed in recent computer simulations of supercooled liquids in three dimensions.[2] Supercooled liquids and metallic glasses can in fact be viewed as defected states of icosahedral bond orientational order. In two dimensions, surfaces of constant negative curvature in d=2 contains an irreducible density of point disclinations in a hexatic order parameter. Analogous defect lines in an icosahedral order parameter appear in three-dimensional flat space. The Frank-Kasper phases are ordered networks of these lines, which, when disordered, provide an appealing model for structure in metallic glasses.[3]

1. D.R. Nelson, M. Rubinstein, and F. Spaepen, Phil. Mag. A46, 105 (1982).
2. P. Steinhardt, D.R. Nelson, and M. Ronchetti, Phys. Rev. Lett. 47, 1297 (1981); Phys. Rev. B (in press).
3. D.R. Nelson, Phys. Rev. Lett. 50, 982 (1983).

H2 THE ELECTRONIC THEORY OF THE STRUCTURAL THERMOCHEMISTRY OF METALS AND ALLOYS. J.Hafner, Institut für Theoretische Physik, Technische Universität, A 1040 Wien, Austria and Laboratoire de Thermodynamique et Physico-Chimie Métallurgiques, E.N.S.E.E.G., F 38402 Saint Martin d'Hères, France

The purpose of this paper is to review recent advances in the electronic theory of the structural and the thermodynamic properties of liquid and amorphous metals and alloys.

The combined application of electronic and thermodynamic perturbation methods has led to a microscopic understanding of the properties of liquid normal metals and alloys; as was reviewed by Shimoji in the Grenoble conference. Recent work has concentrated on the study of the influence of attractive interactions on density-fluctuations in expanded liquid metals and on concentration-fluctuations in liquid alloys with strong chemical interactions.

The application of tight-binding methods and of simple bandschemes has greatly contributed to deepen our insight into the physical mechanism of chemical bonding in inter-transition metal and transition metal - normal metal alloys. On this basis, reliable calculations of the enthalpy and of the entropy of formation can be performed. The first steps have been made towards the derivation of interatomic forces in the transition metals and their alloys. In the near future, this should lead to an improved understanding of their structural properties.

H3 LIQUID ALLOYS WITH STRONG CHEMICAL INTERACTIONS
W. van der Lugt and W. Geertsma, Solid State Physics Laboratory, Materials Science Center, University of Groningen, 1 Melkweg, 9718 EP Groningen, The Netherlands.

Some recent experimental results on alloys of alkali metals and group IV-A elements (Na-Sn, Li-Ge, Rb-Pb) are discussed. Their properties can not be described in terms of a simple metal-to-salt transition with one stoechiometric composition. The appearance of a second compound-forming composition indicates that more complex chemical interactions than ionic bonding only have to be considered.

These results give rise to some comtemplations on the nature of compounds in the liquid state: how are they defined and how can they be recognized? What is the meaning of stoechiometry and what does the phase diagram tell us? How strongly are the physical properties (electronic-structural) in the liquid state related to those in the solid state? What is the relation between liquid structure and electronic properties? It will be shown from recent results that such questions can not be answered unambiguously.

The theoretical procedures for calculating band structure and chemical bonding are not yet sufficiently far developed to include the more complex types of chemical short range order, mentioned above. Indeed, tight-binding models provide a nice qualitative picture. Also one may derive insight from numerical band structure calculations on well-chosen rigid models representing the liquid.

SESSION I: MODELING AND STRUCTURE

I1 MODELLING OF THE STRUCTURE OF GLASSES

J.F. Sadoc
Laboratoire de Physique des Solides
Université Paris-Sud 91405 Orsay

Order and disorder are two main words used in glassy structure description. But their meaning have to be strictly defined. The order concept is needed to define a disorder and also intermediate concept as "local order". In this paper I propose a review of the order concept and in a second step a definition of the disorder. One of the more important point recently studied is the topological nature of the order and disorder. Some examples of this point of view will be presented :

- Penrose tilling in 2-D : the importance of the 5-fold symmetry ; the non-periodic order without distortions.

- space curvature : a way to release the topological constraint.

Disorder will be discussed in terms of defects (disclination lines) appearing in the order. Classical models (C.R.N. packing of prismatic chemical units, D.R.P.H.S., etc...) have to be compared with models derived from the topological point of view. In some simple cases the comparison will be done.

I2 STRUCTURAL STUDY OF AMORPHOUS METALLIC Mo-Ge ALLOYS*

C. Kortright and A. Bienenstock, Dept. of Materials Science and Engineering, Stanford University, Stanford, CA 94305 USA

Results from EXAFS, RDF, differential anomalous scattering (DAS) and x-ray small-angle scattering techniques applied to sputtered amorphous Mo_xGe_{1-x} films in the composition range ($.25 < x < .75$) will be presented and discussed. RDF's indicate metallic first shell coordination numbers over this range and significant structural change with composition. At the Ge-rich end, the RDF's show a broader first shell and less intermediate range order than at the Mo-rich end where the RDF's look much like those of typical melt-quenched metallic glasses. EXAFS indicates strong chemical ordering at the shortest near neighbor distances. DAS differential distribution functions show Mo and Ge to have very different average environments that change with composition. These data and small-angle scattering data are more consistent with models in which the material is not seperated into two phases. Models consistent with structural results will be discussed.

*Supported in part by the NSF through the Metastable Materials Thrust Program of the Center for Materials Research at Stanford and by the Stanford Synchrotron Radiation Laboratory which is supported by the DoE and the NIH.

I3 NEUTRON DIFFRACTION STUDY ON THE STRUCTURE OF LIQUID Cs-Sb ALLOYS

P. Lamparter, [illegible] Martin, S. Steeb, Max-Planck-Institut für Metallforschung, Stuttgart, BRD, and [illegible] Freyland, Fachbereich Physikalische Chemie, Philipps-Universität, Marburg, BRD

[illegible]

I4 STRUCTURE RELAXATION OF AN AMORPHOUS $Mg_{.7}Zn_{.3}$ ALLOY

T. Mizoguchi, H. Narumi and N. Akutsu, Gakushuin University, Mejiro, Tokyo 171, Japan, and
N. Watanabe, KEK Laboratory, Tsukuba, Ibaragi, Japan, and
N. Shiotani, M. Ito and H. Iwasaki, The Institute of Physical and Chemical Research, Wakoshi, Saitama, 351, Japan

An amorphous Mg-Zn alloys of near the eutectic composition crystallized to a single phase of an orthorombic crystal of $Mg_{51}Zn_{20}$. Under isothermal annealing at relatively low temperature(60-90°C), only after certain incubation period the crystalline diffraction peaks become detectable and started to grow without changing much their width. It is quite interesting that what structural change occures in the amorphous phase during the incubation period before the crystallization.

In order to get direct information of structure relaxation, TOF neutron diffraction experiments were done for both as-prepared and annealed amorphous $Mg_{.7}Zn_{.3}$ alloys. The latter had been annealed so as to give the resistivity maximum. No trace of crystalline diffraction peaks were observed for the annealed sample.

The interference function of the annealed sample becomes a little bit sharper than that of the as-prepared one. Height of the first peak increases by about 4% and the splitting of second peak becomes much clear.

The reduced radial distribution function G(r) in real space for the annealed sample shows a little but clear increase of oscillatory peak compared to that for the as-quenched one. The difference between G(r) of the annealed sample and that of the as-prepared sample resembles the atomic distribution function of the cry-$Mg_{51}Zn_{20}$ whose structure is described as an arrangement of icosahedral coordination polyhedra, quite similar to those found in random close packing structure. The first stage of structure relaxation of the amorphous Mg-Zn alloys is to make local ordering of Mg and Zn atoms [illegible] various polyhedral configurations [illegible] the cry-$Mg_{51}Zn_{20}$. These may be regarded as the precursors [illegible] crystallization [illegible]

THE EFFECT OF STRUCTURAL RELAXATION ON THE ATOMIC DYNAMICS OF THE METALLIC GLASS $Mg_{70}Zn_{30}$

J.-B. Suck, Kernforschungszentrum Karlsruhe, Institut für Angewandte Kernphysik-I, P.O.B. 3640, D-7500 Karlsruhe, B. Rudin and H.-J. Güntherodt, Institut für Physik der Universität, Klingelbergstr. 81, CH-4056 Basel and J. Beck, Institut de Physique, Université, rue A.L. Breguet 1, CH-2000 Neuchâtel.

The influence of structural relaxation on the atomic dynamics of a metallic glass was studied for the first time using the cold neutron time-of-flight spectrometer IN6 at the HFR of the Institut Laue-Langevin in Grenoble. The dynamic structure factor and the generalized vibrational density of states were determined before and after isochronal and isothermal annealing at 325K and at 338K, i.e. below the crystallization temperature of approximately 380K. Three different samples were used, freshly made under identical conditions, so that each annealing was done with an as-quenched glass in order to avoid effects from nucleation in pre-annealed samples. Two of the samples were also investigated after crystallization.

Depending on the annealing time and on the annealing temperature we observe a progressive reduction of the low energy modes which are characteristic for the atomic dynamics of (metallic) glasses and, on stronger annealing (12 h at 338K), we find an increase of intensity for energy transfers between 12 and 20 meV. These changes are especially strong at momentum transfers just below Q_p, the momentum transfer corresponding to the first maximum of the static structure factor, while the static structure factor, integrated from the t-o-f spectra, shows little change in this Q-region. Also the collective modes near Q_p are very little affected by the relaxation of the glass, - but strongly after crystallization.

We interpret our results in the framework of two recent theoretical investigations of a computer simulation of an amorphous metal. This enables us to localize on a microscopic scale the possible origin of the low frequency "disorder characteristic" modes.

SESSION J: STRUCTURE, SURFACES, CRYSTALLIZATION

J1 A MODEL FOR THE STRUCTURE OF LIQUID Li_4Pb.
A.P. Copestake*, R. Evans*, H. Ruppersberg**, W. Schirmacher***

We present the results of calculations of the partial structure factors and radial distribution functions of liquid Li_4Pb at different temperatures. Assuming that this alloy is partially ionic, we have modelled the interionic forces by pairwise potentials that are strongly repulsive at small separations r and electronically screened Coulombic at large r. This model was motivated by the fact that a r dependent 'ordering potential' which exhibits approximately screened Coulombic decay for large r, can be extracted from the neutron diffraction data for $S_{CC}(q)$ in Li_4Pb. Our calculations, which are based on the mean-spherical and the hyper-netted-chain approximations, show that the wave number dependence of the measured concentration structure factor $S_{CC}(q)$ can be reasonably well accounted for by our model with effective electron charges of about 0.5 and -2.0 at the Li and Pb sites, respectively, and an inverse screening length of 1.1 $Å^{-1}$. These parameters are consistent with values obtained from the ordering potential extracted from experiment.

In order to explain the observed temperature dependence of $S_{CC}(q)$ it is necessary to assume that the charge transfer between species decreases with increasing temperature.

* H.H. Wills Physics Laboratory, University of Bristol, Bristol, BS8 1TL, UK
** FB Angewandte Physik, Universität des Saarlandes, 6600 Saarbrucken, W.Germany
***Physik-Department, Technische Universität München, 8046 Garching, W.Germany

J2 THEORETICAL CALCULATIONS ON METALLIC SURFACES : THE OCP REFERENCE SYSTEM.

M.L. Rosinberg, V. Russier and J.P. Badiali, Groupe de Recherche n° 4 du CNRS, Physique des Liquides et Electrochimie associé à l'Université Pierre et Marie Curie, Tour 22, 4, place Jussieu - 75230 Paris Cedex 05.

The one-component plasma (OCP) which is a simple coulombic system characterized by the sole parameter Γ is now recognized as a good reference system for liquid alkali metals. For the study of surface properties it may be thought as a more natural reference system than neutral hard spheres. However our understanding of the inhomogeneous OCP still remains very primitive. We present here an ensemble of results concerning the surface structure and the thermodynamics of the OCP. The situation where the fluid is in contact with a hard wall is also considered.

Monte Carlo (MC) computations which give the exact ionic profile and surface energy are compared to several approximated theories. Except in the weak-coupling case, MC profiles are highly structured and for Γ = 30 one can remove the wall without changing the structure. In the hard wall situation, HNC and MSA integral equations yield a surface profile in qualitative agreement with MC results for Γ = 30. The MSA is then used to investigate the influence of an Ashcroft pseudopotential. The main effect is the damping of oscillations in the profile.

For the free surface, the density functional formalism is considered and a relation between the derivative of the surface tension relative to density and the surface profile is given. The square gradient expansion of the functional which has been recently used to calculate the surface tension of liquid alkali metals is tested for Γ = 10. We find that it yields bad results for the structure and the thermodynamics.

MC results for Γ = 30 are also used to test the influence of anisotropy in the two-body correlation function. This effect appears to be very important and must be handled with care in the calculation of the surface tension.

J3 DENSITY FUNCTIONAL CALCULATIONS OF THE SURFACE TENSION OF LIQUID METALS AND ALLOYS*. M. Grimson and D. Stroud, Ohio State University--We have investigated the surface tension of a number of simple liquid metals and alloys using the ionic density functional formalism developed by Wood and Stroud. The theory includes the conduction electrons within the adiabatic approximation. The free energy density of the uniform liquid metal (one of the inputs of the theory) is computed within the structural expansion, and the gradient coefficient (which involves the fourth moment of the direct correlation function) using Weeks-Chandler-Anderson perturbation theory. Agreement between the theoretical and experimental surface tensions is very good for both the alkali metals and for Al; the polyvalent results are much improved over those of Wood and Stroud. Calculations have also been carried out for liquid alloys, and in particular for alloys such as NaCs which phase separate in the liquid state. The results show how surface segregation lowers the surface tension in a phase-separating alloy. The effects of going beyond the gradient approximation are briefly considered, to investigate the possibility raised by Rice and coworkers, that there are density oscillations near the surface of a liquid metal.

*Work supported in part by NASA under grant NASW3601.

J4 CRYSTALLIZATION OF AMORPHOUS METAL-METALLOID ALLOYS.

H.-G. Wagner, M. Ackermann, U. Gonser, Angewandte Physik, Universität des Saarlandes, D-6600 Saarbrücken, Federal Republic of Germany

Mössbauer spectroscopy is used to study the crystallization of amorphous transition metal-metalloid alloys. Simultaneous measurements of γ-transmission spectra and conversion electron emission spectra show that on all samples measured the crystallization starts at the ribbon surface. When the annealing is done in vacuum, first traces of crystalline phases appear on the dull ribbon surface which had been in contact with the quenching roller. If an argon atmosphere is used during the heat treatment the onset of crystallization is first observed on the shiny ribbon surface. The crystallization temperature also depends on the atmosphere used during annealing.

These observations are discussed in detail and conclusions are drawn about the possible crystallization mechanisms.

J5 CRYSTALLIZATION PROCESSES IN NITROGEN-BEARING Fe-V-B-Si AMORPHOUS ALLOYS: MAGNETIC, THERMAL, AND TRANSPORT PROPERTY STUDIES. K.V.Rao, K.A.Bertness*, E & I T Sector Labs/3M, St. Paul MN 55133, R.Arajs, S.Arajs, Clarkson College of Technology, Potsdam, NY 13676, and H.H.Liebermann, Allied Corporation, Parsippany, NJ 17054.

The metstable character of metallic glasses for application mandates an understanding of their crystallization processes. Yet, only a few amorphous systems have been studied in detail. The effects of nitrogen, and vanadium on the thermal stability and the crystallization processes of glassy $Fe_{83}B_{14}Si_3$ alloys have been studied in detail through the temperature dependence of the magnetization [in both low, ~10 Oe, and high, <10 kOe, applied magnetic fields], and electrical resistance of $Fe_{83-x}V_xB_{14}Si_3$ amorphous alloys with $0 < x < 12$ upto 1000 K. The effects of 50 and 2050 ppm nitrogen in solid solution for each vanadium concentration has also been studied. In order to compare the information obtained using different experimental approaches, Differential Scanning Calorimetry (DSC) studies have also been conducted on samples obtained from the same batch of ribbons at heating rates identical to those used above. We find that the glass transition temperature, T_g, and the various stages of crystallization determined from magnetic and resistance measurements show a strong correlation, but differ significantly from those that can be inferred from DSC data. Such discrepencies have also been observed for a number of other Fe and Co based glassy alloys. The emphasis of this presentation will be to demonstrate the sensitivity of electrical and magnetic properties to microscopic changes in magnetic amorphous alloys.

On heating, $Fe_{83}B_{14}Si_3$ amorphous alloy crystallizes in two major stages around $T^s_{x1} \approx 713$ K, and $T_{x2} \approx 781$ K. Substitution of V for Fe, while increasing T_g, suppresses the initial crystallization step T^s_{x1}, and shifts T_{x2} to higher temperatures, thus enhancing the overall thermal stability. In addition, a nitrogen-induced phase, as yet unidentified in detail, is observed. Further details on the kinetics of relaxation processes as studied from low-field thermomagnetic studies will be discussed.

* *Presently at: Dept. of Physics, Stanford University.*
[1] *Samples prepared by H²L while at General Electric.*

J6 STRUCTURAL RELAXATION AND CRYSTALLIZATION BEHAVIOR OF $(Mo_{0.6}Ru_{0.4})_{1-x}B_x$ GLASSES. Madhav Mehra, Robert Schulz and William L. Johnson, California Institute of Technology, Pasadena, CA 91125 USA

Evidence of phase separation in $(Mo_{0.6}Ru_{0.4})_{82}B_{18}$ upon annealing at $T \geq 450$ C has been reported[1]. It was suggested that similarily to the case of $Fe_{40}Ni_{40}B_{20}$[2] this glass could separate into a boron rich phase having one type of short range order and a boron poor phase having a second distinct type of short range order. The present study reports the radial distribution function (RDF) of as quenched and annealed samples for 14, 18 and 22 at.% boron concentration, the change in the electrical resistivity during structural relaxation and crystallization, and an analysis of the crystalline structures obtained from the glass. We also report the effect of structural relaxation on the low temperature specific heat for the same concentrations. Our results are consistent with the suggestions of C. C. Koch et al.

(1) C. C. Koch, W. L. Johnson and A. C. Anderson, Phys. Rev. B 27, 1586 (1983).
(2) J. Piller and P. Haasen, Acta Metall 30, 1 (1982).

J7 COLLECTIVE FLUX PINNING, A PROBE OF DEFECTS IN AMORPHOUS SUPERCONDUCTING FILMS. P.H. Kes, Kamerlingh Onnes Laboratory, 2300 RA Leiden, Netherlands, and C.C. Tsuei, IBM Research Center, Yorktown Heights, NY 10598 USA

Recently two-dimensional collective flux pinning (2-DCP) has been observed in thin amorphous films of sputter deposited Nb_xGe, Nb_xSi, and Mo_xSi[1] ($x \approx 3$). In this contribution it is shown that 2-DCP provides a useful tool for the study of extended defects of the order of $\xi(0)$(5-10nm). The parameter $W(0) = n_v \langle f_p^2 \rangle$ is experimentally determined. Here n_v is the density, f_p the elementary interaction of a defect and a flux line, and the average is taken over a cell of the flux line lattice. Reasonably, to well established theoretical expressions exist for f_p of defects that are most likely to occur in amorphous materials: voids, micro-crystallites, quasi-dislocation loops, and quasi-dislocation(dipoles). These can be distinguished by their different field (and temperature) dependences. Comparison of the theory with experiment provides estimates for the product of n_v and the size of the defects. In all materials studied evidence was found for the existence of quasi-dislocation loops. The thickest (3μm) Nb_3Ge sample of which the broad (170 mK) superconducting transition revealed inhomogeneities, was heat treated for 24 hours at 580°C. The obvious change in pinning vs. field characteristics is explained by the presence of micro-crystallites that could not be detected by X-ray scattering. The Nb_3Si samples demonstrated a somewhat different behavior that was ascribed to some hydrogen uptake during the deposition. This assumption could be justified by studying the 2-DCP of a Nb_3Ge sample chemically loaded with 0.2% hydrogen. The presence of hydrogen enhanced the dislocation loop pinning by almost a factor of 3, while a nearly equally important contribution was detected that exhibits the characteristics of pinning by micro-crystallites and/or voids.

1. P.H. Kes and C.C. Tsuei, Phys. Rev. Letters 47, 1930 (1981), and Phys. Rev. B, to be published.

SESSION K: HYDRIDES

K1 GLASS FORMATION BY A SOLID STATE REACTION OF CRYSTALLINE ZR-X PHASES WITH HYDROGEN AND STRUCTURE OF GLASSY HYDRIDES

K. Samwer* and W.L. Johnson, California Institute of Technology, Pasadena, CA 91125, USA

A new method of synthesizing metallic glasses by a solid state reaction has been developed. Certain crystalline Zr_3Rh intermetallic phases can be transformed into non-crystalline metallic hydrides by hydriding at about 200C. X-ray diffraction pattern confirms the transition from the crystalline to the amorphous state without any rapid quenching technique. Radial distribution functions of the hydrided glassy metal, which was originally crystalline, are compared with liquid quenched unhydrided and hydrided amorphous Zr_3Rh. No significant difference can be seen between the two hydrided samples made by totally different glass formation prozesses. Superconducting properties and density measurements show very similar behavior for both Zr_3Rh hydrides. The transition can be explained in terms of a "chemical frustation" effect due to a large disparity of interatomic diffusion rates. The structure of glassy Zr based metallic hydrides is investigated using hydrogen as a probe. The measured interatomic distances suggest that hydrogen occupies mainly tetrahedral sites defined by four Zr atoms under normal hydriding conditions ($\simeq$ 200C, 1atm.H_2). A statistical model for these sites is in good agreement with the observed absorption capacity for hydrogen. In this model H-H interaction should limit the upper value of hydrogen content in Zr based glasses to 2.5 (H/metal atom).

*Present permanent address: University of Göttingen, Göttingen FRG

K2 HYDROGEN ATOM ENVIRONMENTS IN A HYDROGENATED ZrNi GLASS

K.Suzuki, N.Hayashi, Y.Tomizuka, T.Fukunaga and K.Kai
The Research Institute for Iron, Steel and Other Metals, Tohoku University, Sendai 980, Japan

N.Watanabe
National Laboratory for High Energy Physics, Oho-machi, Tsukuba-gun, Ibaraki-ken, 305, Japan

Hydrogen atoms may be a promising probe to identify the atomic scale structure and dynamics in metal-metal alloy glasses with good hydrogen-absorbing power. In this study, the local confugurations of metallic atoms surrounding a hydrogen atom in a hydrogenated ZrNi glass was observed as a function of hydrogen content by neutron total and inelastic scattering experiments using a spallation pulsed neutron source.

Initially, hydrogen atoms prefer to occupy the four-coordination site consisting only of Zr-atoms up to about 25 at% hydrogen content, where exactly the relation between the hydrogen content and equilibrium hydrogen-gas pressure obeys Sievert's law. With further increase of hydrogen content, hydrogen atoms are gradually located at the four-coordination sites consisting of three Zr-atoms and one Ni-atom on the average. We conclude that the four-coordination sites occupied by hydrogen atoms have the tetrahedral configuration distorted to some extent in ZrNi glass. The geometrical size of the four Zr-atoms tetrahedron present in hydrogenated ZrNi glass does not correspond to that existing in ZrNiH crystalline compound, but is rather close to that found in ZrH_2 crystal. The hydrogen atom environments available in hydrogenated ZrNi glass always consist of the four-coordination sites and there is no five-coordination site containing three Zr-atoms and two Ni-atoms like in $ZrNiH_3$ crystalline compound.

K3 INELASTIC NEUTRON SCATTERING FROM A HYDRIDE OF THE METALLIC GLASS Zr_2Pd.

A. Williams, J. Eckert, Los Alamos National Laboratory, Los Alamos, NM 87545 USA, X. L. Yeh, M. Atzmon, California Institute of Technology, Pasadena, CA 91125 USA, and K. Samwer, University of Göttingen, Göttingen FRG

Inelastic neutron scattering has proven to be a powerful technique for studying the vibrational optic modes of hydrogen in metal hydrides from which information can often be obtained on the hydrogen interstitial sites and their occupancies. Time of flight inelastic neutron scattering data was therefore obtained on hydrided Zr_2Pd metallic glass using the Crystal Analyzer Spectrometer at the Los Alamos pulsed spallation neutron source. Energy transfers from about 40 meV to several hundred meV were obtained with sufficiently good statistics and signal to noise ratio to show the second harmonic, as well as the fundamental optic mode. The inelastic neutron scattering spectrum from amorphous hydrided Zr_2Pd was found to be structureless and reasonably symmetric and could be fit quite well with a Lorentzian centered at 125 meV and with a FWHM of about 51 meV. Possible schemes of hydrogen occupation of various interstitial sites in these metallic glasses is discussed in view of these results.

K4 DIFFUSION PROPERTIES AND PHASE TRANSITIONS OF THE METALLIC GLASS a-Zr_2PdH_x.

R. C. Bowman, Jr., D. E. Etter, A. Attalla, and B. D. Craft, Monsanto Research Corporation-Mound*, Miamisburg, OH 45342 USA, J. S. Cantrell and J. E. Wagner, Miami University, OH 45056 USA, and W. L. Johnson, California Institute of Technology, Pasadena, CA 91125 USA.

Proton NMR spectroscopy has been used to evaluate hydrogen diffusion in several samples of amorphous a-Zr_2PdH_3 that had been prepared by direct reaction between hydrogen gas and the metallic glass a-Zr_2Pd. The diffusion correlation times (τ_c) between 120K and 550K were deduced from the proton rotating-frame relaxation times ($T_{1\rho}$). The τ_c values for a-Zr_2PdH_3 exhibit non-Arrhenius temperature dependence as well as give enhanced proton hopping rates relative to those found in crystalline Zr_2PdH_x with the same nominal stoichiometry. This behavior is very similar to recent measurements[1] on crystalline and amorphous $TiCuH_x$. The roles of local crystal structures and hydrogen site occupancies on the proton diffusion processes will be briefly described.

Differential scanning calorimetry (DSC) measurements indicate that both the initial a-Zr_2Pd alloy and the amorphous hydride phase undergo irreversible transformations at elevated temperatures. Although low energy exothermic transitions that are associated with crystallization phenomena are observed above 800K for the a-Zr_2Pd alloys, the a-Zr_2PdH_3 samples yield highly endothermic transitions in the temperature range 550K to 700K. Powder x-ray diffraction measurements of the annealed samples suggest both crystalline Zr_2PdH_x and ZrH_x are decomposition products that depend upon experimental conditions. The present results will be compared with reported behavior for other metallic glasses and metastable hydrides.

*Operated for U.S. Department of Energy under Contract No. DE-AC04-76-DP00053.

[1]R. C. Bowman, Jr., et al., Phys. Rev. B 26, 6362 (1982).

K6 MAGNETISM AND HYDROGEN ABSORPTION IN RARE-EARTH GLASSES.* D.J. Sellmyer, M.J. O'Shea, and C.G. Robbins, University of Nebraska, Lincoln, NE 68588 USA.

We report on measurements of magnetic properties and phase transitions in rare-earth-rich metallic glasses, and upon the effect of hydrogen absorption on these properties. The glasses have the nominal form $Gd_{72-x}R_xG_{28}$ where R represents either a nonmagnetic rare earth such as La or an anisotropic rare-earth such as Tb, and G represents glass formers such as Ga, B, 3d transition metals or mixtures thereof. The system $Gd_{72-x}La_xGa_{18}B_{10}$ shows evidence for paramagnetic, ferromagnetic-like, and speromagnetic states, with an apparent multicritical point at $x_c \approx 67$. For x slightly larger then x_c, apparent double transitions (para-ferro and ferro-spero) are seen as T is lowered. The effect of H absorption at the level $H/M \approx 2$ on these transitions is to increase the local random anisotropy, decrease the average exchange, and replace the ferromagnetic transition by a speromagnetic one at lower temperatures. In the system $Gd_{72-x}Tb_xGa_{18}Fe_{10}$ an increase of x from zero continuously converts the magnetic state from ferro- to spero- and a change in the character of the H absorption effect on the magnetism is observed.

*Research supported by NSF Grant DMR-8110520.

K7 **HYDROGEN SOLUBILITY AND YOUNG'S MODULUS IN Pd-Si METALLIC GLASSES.** **R.S. Finocchiaro, C.L. Tsai, and B.C. Giessen, Department of Chemistry and Materials Science Division, Institute of Chemical Analysis, Northeastern University, Boston, Massachusetts 02115, U.S.A.**

Hydrogen solubility of the $Pd_{100-x}Si_x$ metallic glasses with $14 \leq x \leq 22$ has been measured in the temperature range of 10 to 90°C and the hydrogen partial pressure range of 0.1 to 100 torr. Hydrogen solubility decreases from ~6 at.%H at 100 torr, 10°C for x = 14 to ~0.05 at.%H for x = 22. Furthermore, for a constant metalloid concentration, hydrogen solubility decreases by a factor 2 from 10°C to 90°C, which indicates that the absorption of hydrogen is an exothermic process. Sieverts' law is not observed. The Young's moduli of the hydrogenated metallic glasses have been measured as a function of hydrogen content at room temperature and show a decrease with increasing hydrogen concentration. The glasses exhibit hysteresis in the modulus values upon absorption and desorption of hydrogen. Both the solubility and elastic data are analyzed according to a two-site model based on a dense random packing of hard spheres (DRPHS) structure.

SESSION L: ATOMIC TRANSPORT AND STRUCTURAL RELAXATION

L1 ATOMIC TRANSPORT AND STRUCTURAL RELAXATION IN METALLIC GLASSES

A. L. Greer
Division of Applied Sciences
Harvard University
Cambridge, Massachusetts 02138, U.S.A.

Along with other properties, atomic transport rates in metallic glasses are affected by the degree of relaxation of the glass. Since transport measurements are made near the glass transition temperature, where structural relaxation can occur, it is essential to take relaxation effects into account in interpreting the experimental results. Diffusion measurements in metallic glasses are reviewed, and a critical comparison is made of the experimental methods. Measurements of viscosity are also reviewed, and the relationship between the atomic transport in diffusion and in viscous flow is considered. The validity of the Stokes-Einstein relation near the glass transition is examined. Possible diffusion mechanisms are discussed, particularly for the metal-metalloid glasses. Studies of structural relaxation, particularly those based on atomic transport measurements, are outlined. Some views on the mechanisms of structural relaxation are presented.

L2 LOCAL STRUCTURAL FLUCTATIONS AND DEFECTS IN METALLIC GLASSES.

T. Egami and V. Vitek, University of Pennsylvania, Philadelphia, PA 19104, U.S.A.

The atomic structure of liquid and amorphous metals has traditionally been analyzed in terms of the pair distribution function (PDF) or the local Voronoi polyhedra (VP). Neither of them, however, are directly helpful in elucidating many phyiscal properties which are, in crystalline solids, usually associated with defects, and generally regarded as structure sensitive. What is need to describe the possible structural defects, or more widely local structural fluctuations, is some local metrical scale of fluctuations rather than the topological scale such as VP. We pointed out earlier that the atomic level stresses are the best measure available to satisfy such a need. In this review, we describe the physical nature of the atomic level stressses and discuss their usefulness in understanding the structural relaxation, glass transition, mechanical properties and glass formability. In particular, it is suggested that the spherically symmetric (ℓ=0) component of the stress tensor, which is the hydrostatic stress p, and the two-fold (ℓ=2) components of the tensor, which are the shear stresses τ, behave quite differently, resulting in two glass transitions and two distinct modes of structural relaxation. The glass transition due to the freezing of pressure fluctuation corresponds to the usual glass transition, while that due to the shear fluctuation corresponds to the orientational (glass) transition first reported by Steinhardt et al. The relaxation of p is irreversible and results in densification, and most likely the reduction in diffusivity, while the reorientational relaxation of τ is reversible, and contributes to anelasticity and various changes in the magnetic properties such as Curie temperature and anisotropy via the changes in the compositonal short range order. Thus, the glassy state can not be described even globally by a single parameter such as the free volume alone, but at least two parameters are needed. The relation of this theory to other theories of structural state and defect structures is discussed.

L3 ACTIVATION ENERGY SPECTRA IN RELAXATION: CROSSOVER AND REVERSIBILITY.

J.A. Leake, M.R.J. Gibbs, S. Vryenhoef and J.E. Evetts, Department of Metallurgy and Materials Science, University of Cambridge, Cambridge, England.

We recently proposed a model for relaxation in metallic glasses based on a spectrum of available activation energies (1). Sub-sets of the observed relaxation behaviour are the "crossover effect" and "reversibility". A definition of these terms is given in (1), along with several predictions which can be tested by experiment. Using differential scanning calorimetry, measurements have been made of changes in Curie temperature, T_c, on annealing $Fe_{80}B_{20}$. The data agree with and extend previous work (2), several key points emerging in line with the model. Firstly, a crossover effect can be observed on annealing at high temperature after any annealing time at low temperature provided the measured value of T_c has not exceeded the final value for annealing at the high temperature. If this annealing time is exceeded, reversible behaviour is observed. It is thus clearly shown that crossover and reversibility arise from the same atomic processes. Secondly, using (1) it is possible to compare the predicted position of the minimum in T_c on the high temperature anneal with experiment. The agreement is excellent. Finally, it has been demonstrated that the shape of the curve beyond this minimum is independent of the low temperature anneal. In (1) we used a simplified formalism for clarity, but in this work the full form of the annealing function has been used, giving close agreement between theory and experiment throughout.

(1) M.R.J. Gibbs, J.E. Evetts and J.A. Leake: J. Mat. Sci. 18 (1983) 278.
(2) A.L. Greer and J.A. Leake: J. Non-Cryst. Sol. 33 (1979) 291.

L4 MICROCALORIMETRIC INVESTIGATIONS OF STRUCTURAL RELAXATION PHENOMENA IN GLASSY BINARY TRANSITION-METAL ALLOYS

F. Sommer, H. Haas and B. Predel, Max-Planck-Institut für Metallforschung, Institut für Werkstoffwissenschaften, Stuttgart and Institut für Metallkunde, Universität Stuttgart, Seestr. 75, D-7000 Stuttgart 1

The changes of the thermic properties caused by structural relaxation processes of glassy alloys have been determined for Cu-Ti, Ni-Ti and Pd-Zr alloys. For this, measurements with a dynamic as well as with an isothermal temperature program have been carried out using a Differential Scanning Calorimeter (DSC-2-Perkin Elmer). Reversible as well as irreversible relaxation processes have been found and the enthalpy changes connected herewith have been determined. Different models for relaxation in glassy alloys are tested in describing the obtained results. The kinetics of the relaxation processes is discussed in detail.

SESSION M: APPLICATION OF METALLIC GLASSES

M1 METALLIC GLASSES IN DEVICES FOR ENERGY CONVERSION AND CONSERVATION. R. Hasegawa, Materials Laboratory, Corp. R & D, Allied Corporation, Morristown, NJ 07960 USA

Combination of various physical properties of metallic glasses leads to the possibility of a number of energy conversion/conservation devices with high efficiencies. Pertinent physical properties include low magnetic loss, high magnetic permeability, high electrical resistivity, superconductivity with a high upper critical field, high corrosion resistance, low radiation damage, high mechanical strength and hardness with high ductility, and hydrogen sorption. Among these, magnetic properties have been receiving the most attention and a number of devices have been considered or actually fabricated. To illustrate the property-device relationship, we select several representative magnetic applications including commercial and high frequency transformers, sensors, transducers and magnetic switches. One of the most significant developments in these areas is the fabrication of energy-saving power transformers using metallic glass which has an ac core loss about 1/5 that of conventional silicon steel. A high B-H loop squareness ratio and high electrical resistivity of some magnetic metallic glasses make them suited for the magnetic cores to generate high-power pulse sources for accelerators and lasers. The wide variety of magnetic applications realized thus far or to be explored arises largely from the fact that the magnetic properties of glassy alloys can be modified widely by post-fabrication treatments. Other energy-related applications of metallic glasses are in superconducting devices and hydrogen storage systems. Some of the recent developments in these areas will also be included in the present talk.

M2 [illegible] OF METALLIC Fe-Ni-Cr-W ALLOYS. [illegible] Kase, Institute for Materials Research, Tohoku University, Sendai 980, Japan

[illegible] behavior of amorphous and crystallized Fe-Ni-Cr-W alloys prepared by co-sputtering of 304 stainless steel and W were studied in chloride solutions by potentiodynamic polarization methods. In both neutral and acidic solutions, the as-prepared amorphous alloys had excellent corrosion resistance, which was similar to that of metal-metalloid amorphous alloys containing Cr and P. This result shows that P is not essential for producing corrosion-resistance in glassy alloys. More significantly, the corrosion resistance of amorphous Fe-Ni-Cr-W alloys was preserved after heat treatment at the crystallization temperature. In neutral solutions, amorphous and crystallized alloys have similar corrosion behavior and resistance. In acidic solutions, these heat-treated alloys showed a slight increase in active dissolution but remained highly passivated at high potentials. The retention of corrosion resistance of the heat-treated alloys was attributed to a two-stage crystallization process wherein fine bcc crystallites were formed in the amorphous matrix. This amorphous matrix protects the alloy from corrosion of the bcc phase.

M3 CHEMICAL PROPERTIES OF METALLIC GLASSES.* R. B. Diegle, Sandia National Laboratories, Albuquerque, NM 87185

Chemical properties of metallic glasses continue to interest certain segments of the scientific community, most notably those studying corrosion and catalysis. This presentation will review both the corrosion and catalytic behavior of metallic glasses, but it will emphasize the former subject because the major portion of chemical properties research has, to date, focused on corrosion.

Concerning corrosion, the single most important phenomenon influencing the corrosion resistance of metals that are not inert for thermodynamic reasons (e.g., Au and Pt) is passivity. Since the introduction of Metglas™ alloys in the early 1970's, corrosion scientists have used metallic glasses as a new tool for probing the influences of alloy structure and composition on such important phenomena as passivity and passivity breakdown. The excellent corrosion resistance exhibited by certain compositions of metallic glasses is due to the formation of stable, protective passive films. Film forming additives, e.g. Cr, Ti, and Mo, play much the same role in metallic glasses as in crystalline alloys, but often the passive films formed on metallic glasses are considerably more resistant to electrochemical breakdown. This enhanced stability is ascribed to the structural and chemical homogeneity of the glassy state. However, in metal-metalloid type glasses the metalloid addition can create a synergistic effect with the film former, giving rise to increased rates of film formation and to relatively large degrees of enrichment of the film forming species in the film. This novel and unanticipated effect has been the subject of studies of repassivation kinetics of metal-metalloid glasses.

Research into the catalytic and electrocatalytic activity of metallic glasses has shown promising behavior for alloys containing such elements as Fe, Ni, Co, and Pd. Results of studies of catalytic behavior applicable to methanol fuel cells, production of chlorine, and hydrogenation of carbon monoxide will be reviewed.

*This work performed at Sandia Natl. Labs., a U.S. Dept. of Energy Facility, supported by Contract No. DE-AC04-76-DP00789.

M4 AN ACTIVE METHANATION CATALYST PREPARED FROM Pd-Zr ALLOYS

A. Yokoyama, H. Komiyama and H. Inoue, Department of Chemical Engineering, Faculty of Engineering, University of Tokyo, Hongo 7-3-1, Bunkyo-ku, Tokyo, Japan and T. Masumoto, H.M Kimura, The Research Institute for Iron Steel and Other Metals, Tohoku University, Katahira Sendai 980, Japan

Highly active catalyst of the reaction of carbon monoxide and hydrogen to produce methane was prepared in situ from an amorphous $Pd_{35}Zr_{65}$ alloy. In the reaction, the catallytic activity remarkably increased with time, showing about [illegible]undred fold enhancement, compared with the initial value, at the steady state attained in 60 h. Its turnover frequency (specific catalytic activity) was greater than those for the most active methanation catalysts as ever known. The activity of the catalyst was compared with those of the crystalline $Pd_{1-x}Zr_x$ (x=0-1) alloys.

The X-ray analysis showed some evidence of the structure change during the reaction, because several broad peaks appeared in the spectrum. The spectrum, however, did not coincide with any spectrum of Pd, Zr, Pd-Zr alloys ($PdZr$, $PdZr_2$, etc.), their oxides or hydrides. The resemblance of the spectrum to that of the specimen which was prepared by heating the amorphous $Pd_{35}Zr_{65}$ alloy in a stream of oxygen at the reaction temperature indicate that an unknown complex oxide was formed during the reaction. PdO catalysts, showing a high initial activity, was easily reduced to the metallic state and deactivated. This result indicates that palladium is active only in its oxidative state, for the present reaction system.

It is concluded that the active species, prepared in situ from amorphous $Pd_{35}Zr_{65}$ alloy, is a complex oxide of Pd and Zr, in which palladium exists in the oxidative state under the highly reducing reaction condition. The amorphous structure is especially suited for the formation of this highly active species.

SESSION N: ATOMIC TRANSPORT

N1 KINETICS OF STRUCTURAL RELAXATION IN METALLIC GLASSES, J. R. Cost, Los Alamos National Laboratory, Los Alamos, NM 88545 USA, and J. T. Stanley, Arizona State University, Tempe, AZ 85281 USA

One of the most difficult problems in characterizing structural relaxation in metallic glasses has been that of determining the spectrum of relaxation times which controls the kinetics of the relaxation process. Recently, detailed investigations of the relaxation kinetics have indicated that the relaxation time spectrum is more complicated than was formerly supposed, being multi-modal for some relaxations. The finding of fine structure in the spectra presents two important challenges. First, we need to determine accurately and without prior assumptions the details of the relaxation time spectra. Second, based on these spectral details, we must re-examine some of our previous concepts concerning mechanisms for atomic mobility in amorphous metals.

The first part of this paper describes a method for direct spectrum analysis (DSA) of relaxation response data. The only assumption made with the method is that of simple first-order kinetics. When applied to computer-generated data derived from a known relaxation time spectrum and with varying amount of random experiment error added, this method is shown to reproducibly yield histograms which are good approximations of the input spectrum. Applications of DSA to experimental results for the reversible structural relaxations occurring in several metallic glasses will be described.

In the second part of this paper relaxation time spectra will be reported and discussed for the amorphous alloys $Pd_{80}Ge_{20}$ and $Fe_{40}Ni_{40}P_{14}B_6$. For the latter alloy, it had been previously reported that the spectra have four relatively distinct peaks; this finding is confirmed by DSA for all sets of data which were analyzed. For the binary Pd-Ge alloy, it is shown that the spectra contain two peaks, both of which are broader than those in the quaternary alloy. The significance of these results will be discussed in terms of possible mechanisms for atomic motion in amorphous metals.

N2 SUB-Tg ENTHALPY RELAXATION IN PdNi ALLOY GLASSES. H.S. Chen, Bell Laboratories, Murray Hill, NJ 07974 USA, and A. Inoue, The Research Institute for Iron, Steel and Other Metals, Tohoku University, Sendai 980 Japan

Sub-Tg enthalpy relaxation processes have been investigated in a series of PdNi alloy glasses. The samples are either in the form of cylinder ~ 0.5mm in diameter, or ribbons 1mm wide x 30μm thick. The as-quenched samples were annealed at temperatures well below the glass transition temperature Tg. Upon heating, the annealed samples show an endothermic peak above the annealing temperature, and the specific heat then falls on that of the as-quenched samples below Tg.

The endothermic reaction processes are found to be strongly composition dependent. A close correlation between the sub-Tg relaxation and other thermal properties, such as Tg, crystallization temperature and the enthalpy of relaxation is seen. Possible mechanisms and implications of the results are discussed.

N3 SCALING THE COMPOSITION DEPENDENCE OF ATOMIC TRANSPORT AND STRUCTURAL RELAXATION IN AMORPHOUS ALLOYS. A.I. Taub and J.L. Walter, General Electric Corporate Research and Development, PO Box 8, Schenectady, NY 12301 USA

The temperature dependence of isoconfigurational flow and the rate of structural relaxation were measured for several amorphous alloys in the series $Fe_{82-x}B_{18}M_x$ (M=Si, Ni, V, Mo: $0 \leq x \leq 12$). Elemental substitutions that produce an increase in the crystallization temperature T_x were found to produce a corresponding increase in the structural relaxation rate. However, the relative magnitudes of the changes in T_x were not in agreement with the observed changes in relaxation rate.

These results will be supported by a compilation of the literature data which shows that the observed variation with composition of both isoconfigurational flow and the viscosity relaxation rate does not scale with the glass transition temperature. Reduced temperature normalization of the form $T_{red} = T-T_g$ and T_g/T is applied to all the available flow data. Both scalings are shown to be only moderately successful at reducing the equilibrium, isoconfigurational and relaxation data to master curves.

N4 THERMODYNAMICS AND KINETICS OF FORMATION OF AMORPHOUS Zr-Ni ALLOYS FORMED BY SOLID STATE REACTION OF THE PURE METALS. B. M. Clemens, General Motors Research Laboratories, Warrensville, MI 48090-9055 USA, and W. L. Johnson and R. B. Schwarz*, California Institute of Technology, Pasadena, CA 91125 USA

A solid state diffusion controlled reaction was used to produce amorphous $Zr_{1-x}Ni_x$ layers by reaction of multilayer films of elemental polycrystalline Zr and Ni. The multilayers are prepared by e-beam evaporation of Ni and Zr layers. Each layer has a thickness of 100-200 Å. The amorphous phase is formed by annealing at 300 C for times ranging up to one week. Auger depth profiling, x-ray diffraction, and electron microscopy were used to study the reaction kinetics. The formation of an amorphous phase is explained in terms of a proposed metastable free energy diagram together with consideration of the nucleation and growth processes involved.

*On leave from MST Division, Argonne National Laboratory, Argonne, IL 60439

N5 INFLUENCE OF COMPOSITION AND THERMAL HISTORY ON THE RELAXATION BEHAVIOUR OF SOME METAL-METALLOID GLASSES. H. A. Davies and G. P. Gregan, Dept. of Metallurgy, University of Sheffield, Sheffield, S1 3JD, U.K.

Structural relaxation in a series of metal-metalloid glasses has been investigated by differential scanning calorimetry using ribbon samples produced by different casting techniques.

The influence of the concentration and species of both metal and metalloid components on the relaxation behaviour has been investigated. The increasing relaxation energies on traversing from nickel-rich to iron-rich glasses and on substitution of boron by silicon are discussed in terms of alloy chemistry and compared with the composition dependence of crystallisation energy investigated earlier.

It is shown that the relaxation behaviour during annealing is dependent also on the thermal history of the glassy alloy. This is determined both by the cooling rate in the formation of the original glass and by other process parameters such as time of contact with the roller substrate and the pressure and composition of the gaseous environment, which influence secondary cooling of the ribbon.

Relaxation in samples produced by chill block melt spinning is compared with that in compositionally identical, but wider, strip samples produced by planar flow casting. In the latter case, the relaxation has been monitored across the width of the strip.

Also, relaxation in metal-boron alloys manifests itself as changes in Curie temperature, as measured with the galvanometric

N6 PARTICLE-DISPERSION HARDENING OF AN AMORPHOUS $Ni_{78}Si_{10}B_{12}$ COMPOSITE

H. Kimura and T. Masumoto, The Research Institute for Iron, Steel and Other Metals, Tohoku University, Sendai 980, JAPAN

The micro-structure and the mechanical properties of an amorphous $Ni_{78}Si_{10}B_{12}$ composite are studied as a function of WC-volume fraction, in order to present an experimental formulation of particle-dispersion hardening in an amorphous structure.

We obtained a ductile-amorphous $Ni_{78}Si_{10}B_{12}$ composite with a three dimensional distribution of second phase particles, up to 20% for the volume fraction of WC, throughout an amorphous matrix. The Young's modulus of an amorphous composite(E) increases as the volume fraction (V_f) of WC increases; and attains, for 18.2% WC-volume fraction, 20130 kg/mm^2; this value is 2.2 times higher than that of a non-dispersed amorphous alloy (Fig. 1). This increase is excellently expressed as a mixture rule (upper bound rule) of two phase materials:

$$E = E_m(1-V_f) + E_pV_f \quad (1)$$

where E_m, and E_p are the Young's modulus of the matrix and the second phase particles respectively. The yield stress for an amorphous $Ni_{78}Si_{10}B_{12}$ composite, as deduced from the measurement (σ_{yc}) of the elastic spring-back in bending, also increases with increasing volume fraction; and the ratio of Young's modulus to yield stress(E/σ_{yc}) is found to be constant within this study's range of the volume fraction of WC; it is about 60, equal to that of the non-dispersed alloy (E_m/σ_y). With these equations, we can derive an upper bound law of the yield stress for an amorphous composite as:

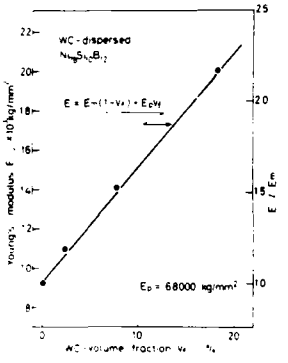

Fig. 1

$$\sigma_{yc} = \sigma_y[1+V_f(E_p/E_m-1)] \quad (2)$$

where σ_y is the yield stress for a non-dispersed amorphous alloy.

N7 **CRYSTALLIZATION KINETICS OF AMORPHOUS Co-Gd RIBBONS AND FILMS.** **F. E. Luborsky, General Electric Corporate Research and Development, Schenectady, NY 12301 USA**

Amorphous films with compositions of approximately $Co_{80}Gd_{20}$ are of particular interest for use in thermomagnetic recording systems. In such systems it is necessary to heat the recording area to ~ 200°C many times for short periods. It is thus necessary to know the ultimate lifetime of the film, defined here as the time-temperature exposure to initiate crystallization. The films were prepared by sputter deposition. The beginning of crystallization was obtained from resistivity, ρ, vs. temperature curves as the temperature at which the ρ started to drop. This measure for the beginning of crystallization was confirmed by x-ray diffraction. In addition ribbons of amorphous Co_xGd_{1-x} have been prepared by melt spinning with compositions from 35 < x < 55. Amorphous ribbons could not be prepared outside this range. Differential scanning calorimetry, DSC, and resistivity, ρ, were both used to study the kinetics of crystallization of these ribbons. The DSC gave single exothermic peaks. The beginning of crystallization from DSC was taken as the beginning of the exothermic peak. The Kissinger method was used to obtain the activation energy, ΔE from both the DSC and ρ using various constant heating rates. On the ribbon samples, where both methods could be used, the two methods gave the same results; the ΔE for the inception of crystallization varied from 4.3 eV for x = 0.35 to 2.8 eV for x = 45 to 4.5 eV for x = 55. For the films using the ρ, for two different thicknesses, ~ 0.1 μm and ~ 2 μm, ΔE was 1.2 eV. The value of the exponent n in the Johnson-Mehl-Avrami equation $X = 1 - \exp(-kt^n)$ was also evaluated where X is the fraction of material crystallized in time t and k is the rate constant. These results are discussed in terms of the possible atomic mechanisms involved in the crystallization and the expected ultimate lifetime of the films.

N8 DIFFUSION IN Fe-Zr-B METALLIC GLASSES

U.Köster, Dept.Chem.Eng., University Dortmund D-4600 Dortmund 50, F.R.Germany

Iron-rich Fe-Zr (intertransition metal) glasses are much softer than Fe-B (metal-metalloid) glasses (HV 700 in $Fe_{88}Zr_{12}$ versus HV 1100 in $Fe_{80}B_{14}$), exhibit larger Fe-Fe distances (0.263 vs. 0.257 nm), but have been found to show a significant higher thermal stability. Therefore it is of some interest to study systematically diffusion in these binary as well as in some ternary Fe-Zr-B glasses. The samples were produced by melt spinning in a helium atmosphere of about 200 mbar.

As shown elsewhere information on diffusivity can be obtained from the kinetics of crystallization (1). Using this method diffusivities estimated in Fe-Zr-B glasses have been found to obey quite reasonable an Arrhenius type relationship with pre-exponential factors of $2 \cdot 10^{-4}$ m^2/s in Fe-B glasses and 20 m^2/s in Fe-Zr glasses as well as activation energies of 180 and 305 kJ/mol, respectively.

At least three diffusion mechanisms should be considered in metallic glasses (2): extended vacancy, cooperative, and interstitial mechanisms. Our results will be discussed on the basis of actual structural models of these glasses (3) taking into account the differences in diameter between Zr- and B-atoms as well as Fe-atoms (0.286 vs. 0.164 nm; Fe: 0.234 nm). In addition, for checking such a geometrical explanation diffusion data from Co-Zr-B glasses will be used, because Co possesses about the same atomic diameter as Fe but exhibits a different electronic structure.

(1) U.Köster, U.Herold, A.Becker, Proc. Int. Conf. on Rapidly Quenched Metals IV (Sendai 1981), p.587

(2) M.Ahmadzadeh, B.Cantor, J.Non-Cryst.Solids 43 (1981), 189

(3) H.S.Chen, K.T.Aust, Y.Waseda, J.Non-Cryst.Solids 46 (1981), 307

N9 PREDICTION OF GLASS FORMING ABILITY FOR SOME BINARY AND TERNARY ALLOY SYSTEMS IN RELATION TO EQUILIBRIUM PHASE DIAGRAM. Sung H. Whang, Institute of Chemical Analysis, Northeastern University, Boston, MA 02115 USA

Despite increasing understanding of glass forming behavior from kinetic and thermodynamic points of view, it has been a difficult task to predict the precise glass forming ability of a given composition.

Recently, some progress has been made in this area due to the use of two parameter maps to predict glass forming property of an alloy composition. One of the approaches is to use two parameters such as reduced liquid temperature and reduced eutectic composition, both of which are derived from equilibrium phase diagram. Following previous investigations of a few binary alloy systems, binary alloys containing Group IB (Cu, Ag, Au) and Group IVA (Ge, Sn, Pb) elements are subjects of the current study. This study also includes ternary alloys, Ti-Zr-Si and Ti-Zr-B.

The following are some of the topics discussed about the suggested model in this paper.

1. Ideal liquidus temperature
2. Linear T_0 model
3. GFA of a metalloid-rich composition
4. Kinetic points of view

Sponsored by the Office of Naval Research

SESSION O: ELECTRONIC PROPERTIES II

01 LOW TEMPERATURE SPECIFIC HEAT OF Fe-Zr and Ni-Zr AMORPHOUS ALLOYS.* David G. Onn and L. Q. Wang, University of Delaware, Newark, DE 19711 USA, and Y. Obi and K. Fukamichi, Research Institute for Iron, Steel and Other Metals, Tohoku University, Sendai-980, Japan

We have determined the specific heat C_p from 0.6 K to 40 K of the amorphous metal alloys $Ni_{100-x}Zr_x$ (x = 35,55, 65,75) and $Fe_{100-x}Zr_x$ (x = 10,60,65,70,75,80). The Ni-based alloys are superconducting for $x > 37\pm2$ and paramagnetic for other compositions. The Fe-based alloys are superconducting for $x > 68\pm2$. At higher Fe concentrations the specific heat and magnetic susceptibility show spin-glass and, for $Fe_{90}Zr_{10}$ ferromagnetic and spin-glass behaviors.

From C_p we obtain the electronic density of states N_0 (E_F) and the Debye temperature $\theta_D(0)$. We find that for the alloys we have studied, and for Cu-Zr alloys, the factor $\eta = N_0(E_F)\langle I^2\rangle$ is composition independent and the same for the three alloy series. In addition $\theta_D(0)$ has an identical trend for all three series. From these results we conclude that T_c of amorphous Zr will be 5.1 K in excellent agreement with the value observed for sputtered amorphous Zr films.

Other results to be discussed include the electronic specific heat for $T<T_c$ and the phonon specific heat for $T>>T_c$. Electrical resistivity and thermopower results for many of these alloys will also be presented.

*Research supported by NSF.

02 FLUX FLOW RESISTIVITY AND CRITICAL FIELDS IN AMORPHOUS SUPERCONDUCTORS. S.J. Poon, University of Virginia, Charlottesville, VA 22901 USA

Flux flow resistivity ρ_f, lower critical field H_{c1}, and upper critical field H_{c2} in extreme type II ($\kappa \simeq 70$-80) amorphous bulk superconductors with minimal flux pinning force have been studied. Results on $H_{c1}(T)$ and $H_{c2}(T)$ are found to depend on sample conditions. The low-field ($H_{c1} < H << H_{c2}$) and high-field ($H \simeq H_{c2}$) flux flow resistivity can only be accounted for if both normal dissipation terms (Bardeen-Stephen, Tinkham), and anomalous terms in the time-dependent microscopic theory (Gor'kov-Kopnin, Thompson, Takayama-Ebisawa) are included. Universal scalings in the viscosity coefficient are also observed. The lower critical fields follow the theoretical predictions of Maki. Combining critical field and specific heat data, a consistent test of the theories of 'dirty' superconductors can be made. The different trends in the critical fields of homogeneous and inhomogeneous samples are presented and discussed.

03 ON THE ELECTRONIC STRUCTURE AND ELECTRICAL RESISTIVITY OF GLASSY METALS. U. Krey, H. Jeschke, and W. Fembacher, Univ. of Regensburg, F.R.G.

The electronic structure and the electrical resistivity of liquid and glassy metals are calculated numerically for large structural models by means of recursive techniques. For the resistivity this implies a direct evaluation of the Kubo formula.

From our studies of the density of states $g(E)$ and of the electronic structure function $E(K,E)$ we find that for s-electrons in the region of $k_f \simeq k_p/2$ ($k_f \approx 1.6$ Å^{-1}, Nagel-Tauc condition) the wavenumber is relatively well defined, whereas for k-values larger than 3 Å^{-1} it is ill-defined. On the other hand, in contrast to a common opinion the conductivity of the s-electrons is not minimal under the Nagle-Tauc condition.

Generally, our numerical values for the resistivity fit quite well to experimental numbers.

Additionally the localization properties of the s-electrons are studied and it is found that not more than roughly ten per cent of the states, with energies near the band edges, are localized.

Also for d-electrons results will be presented.

04 APPLICATION OF DIFFRACTION MODEL TO AMORPHOUS MgZn. P. J. Cote and L. V. Meisel, US Army Armament Research & Development Command, Large Caliber Weapon Systems Laboratory, Benet Weapons Laboratory, Watervliet, NY 12189

The diffraction model for electron transport is expected to be valid when the electron mean free path is substantially greater than the ionic spacing. A proper test of transport theory for metallic glasses (extended Ziman theory) has not been possible due to the generally high resistivity values for these alloys. Matsuda and Mizutani have recently provided extensive data on low resistivity amorphous MgZn alloys where the model is more likely to apply. These alloys are well characterized so that information is available on the parameters needed for computations of resistivity and its temperature dependence. In this paper we present results computed with the diffraction model, using the phase shift expansion for the scattering matrix elements, structure factors appropriate for an amorphous Debye solid and incorporating phonon ineffectiveness effects. Extended Ziman theory results, neglecting phonon ineffectiveness (i.e., for infinite electron mean free path Λ) are in qualitative agreement with experiment. Quantitative agreement is found when phonon ineffectiveness effects (finite Λ) are incorporated. Theoretical and experimental results are given in the table for the position T_M of the resistivity maxima in the ρ vs. T curves, the coefficient A of T^2 in the low temperature region where $\rho = \rho_0 + AT^2$, and the magnitude of the room temperature TCR.

	THEORY		EXPT (Avg)
$q_D\Lambda$	∞	11.7	
T_M(K)	90	45	47
10^6(K^{-2})	1.01	0.48	0.53
10^4 TCR(K^{-1})	-0.97	-1.2	-1.9

05 PAIR DISTRIBUTION FUNCTIONS AND THE ELECTRONIC PROPERTIES OF LIQUID AND AMORPHOUS METALS. D. Nicholson, Oak Ridge National Laboratory, Oak Ridge TN 37830, A. Chowdary, Brandeis University, Waltham MA 02254, and L. Schwartz, Schlumberger-Doll Research, Ridgefield CT 06877.

In a series of recent papers we have shown that a satisfactory description of the electronic properties of strong scattering liquid and amorphous metals can be obtained by applying the effective medium approximation (EMA) to the muffin tin model. In this approach the short range order of the system enters the calculation via the radial distribution function. [In the case of two component systems, we require three functions which describe the AA, AB, and BB correlations.] An essential feature of the theory is the fact that the pair distributions must satisfy physical requirements in both coordinate space and momentum space. For example, g(R) must vanish for R less than some effective hard sphere cutoff while its Fourier transform must be such that the structure function s(k) is non-negative. Experimentally determined g(R), because they are based on uncertain data that extends over only a limited range of momentum space, do not usually satisfy these constraints. To overcome this difficulty, we have developed a Monte Carlo procedure that introduces very small changes in the experimentally derived g(R) and s(k) in such a way as to guarantee consistency with the requirements described above. We use this technique to study the temperature dependence of the electronic spectrum and the electrical resistivity in amorphous metals. In particular we calculate, ab initio, negative temperature coefficients of the resistivity for systems whose Fermi energy lies within the structure induced minimum of the electronic density of states.

06 STABILITY AND ELECTRONIC PROPERTIES OF Zr-Ni GLASSES* D. M. Kroeger, C. C. Koch, J. O. Scarbrough, and C. G. McKamey, Metals and Ceramics Division, Oak Ridge National Laboratory, Oak Ridge, Tennessee 37830 USA

The kinetics of crystallization and the low temperature specific heat of Zr-Ni glasses have been measured as a function of composition in the Zr-rich part of the glass-forming range. The activation energy associated with the first crystallization peak exhibits a strong maximum in the region of the compound Zr_2Ni and the nearby eutectic at 83.5% Zr, and the density of electronic states at the Fermi level exhibits unusual behavior near the eutectic which suggests significant changes in short range order. This apparent correlation between electronic properties and stability of the glass will be discussed in relation to current ideas on stability and glass forming tendency.

*Research sponsored by the Division of Materials Sciences, U. S. Department of Energy, under contract W-7405-eng-26 with the Union Carbide Corporation.

07 MAGNETIC PROPERTY IN LIQUID STATE IN AMORPHOUS Fe-B, Co-B AND Ni-B ALLOYS. M. Takahashi, F. Mori and S. Tsuda, Dept. Appl. Phys., Tohoku University, Sendai 980, JAPAN.

The arrangement of atoms in an amorphous state of rapidly quenched metals and alloys has been thought conceptually similar to that of the liquid state. Therefore, it is of interest to compare the magnetic properties in the amorphous state with those in their liquid state. The present paper describes experimental results on the magnetic susceptibility in the liquidus of $Fe_{100-x}B_x$ ($15 \le x \le 25$), $Co_{100-x}B_x$ ($15 \le x \le 27$) and $Ni_{100-x}B_x$ ($15 \le x \le 37$) alloys.

Measurements of the magnetic susceptibility χ were carried out at temperatures up to 1650 K by using a magnetic balance in fields up to 15 kOe. Figure 1 shows the temperature dependence of $1/\chi$ of Fe-B alloys together with the temperature dependence of magnetization σ_s at 15 kOe. As seen in the figure, χ in the liquidus of Fe-B alloys obeys the Curie Weiss' law. Note here that the paramagnetic Curie temperature $\theta_p(L)$ for 15~21 at%B-Fe is in agreement well with the Curie temperature T_c of amorphous state, while that for 23~25 at%B-Fe is about 100°C lower than T_c.

These results will be discussed in connection with the atomic structure of the liquid and amorphous state.

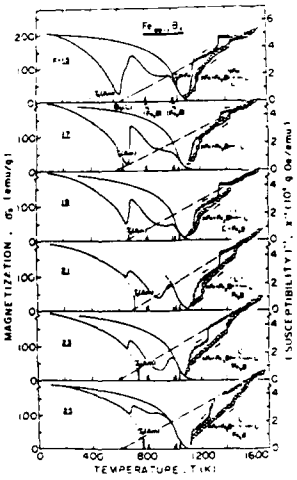

Fig.1. Temperature dependence of the inversed susceptibility $1/\chi$ and magnetization at 15 kOe.

SESSION P: ELECTRONIC PROPERTIES III

P1 ELECTRONIC STRUCTURE AND PROPERTIES OF LIQUID AND AMORPHOUS ALLOYS

F. *Cyrot-Lackmann*
Groupe des Transitions de Phases, C.N.R.S.
B.P. 166, 38042 Grenoble Cedex, France

We described the methods available for calculating the density of states of pure and alloys of liquid and amorphous transition metals with particular emphasis on the tight-binding description of the d band. We show, using various structural models, that the electronic properties are more sensitive to local compacity than to local geometry. For alloys chemical short range order is shown to be the most important parameter for the electronic structure and macroscopic properties in agreement with recent spectroscopical experiments. We applied these calculations to the thermodynamical properties of liquid alloys between transition metal and p-metals (Si, Ge, Al). We calculate the mixing entropy and enthalpy whose strong negative behaviours are shown to be due to the electronic contribution. There is a charge rearrangement of the valence electrons of the p metal with the d band of the transition metal which explains the position of the minimum in these quantities. We finally discuss elastic properties of amorphous materials, explaining the decrease of the shear modulus in the amorphous state compared to the crystalline one.

P2 ELECTRONIC STRUCTURE CALCULATION FOR AMORPHOUS ALLOYS

Takeo Fujiwara[§], Max-Planck-Institut für Festkörperforschung, 7000 Stuttgart 80, Federal Republik of Germany

A review of the electronic structure calculations for amorphous metals and metallic alloys will be given. The most conventional method is the calculation in an idealized fictitious "crystalline" structure. Another conventional way may be the equation of motion (or the moment expansion) method in a constructed model amorphous system, by using the tight-binding parameters determined in the crystalline system.

Here, enphasis will be on the method of the LMTO (linear muffin-tin orbital) directly applied to constructed model amorphous alloys, such as Fe-B, Fe-P and Cu-Zr. The potentail parameters are determined in the muffin-tin potentials of model amorphous alloys and the local densities of states are calculated by the recursion method. The procedure can be pursued in a selfconsistent way under the condition of fixed structural models. The local densities of states show a strong hybridization between d and p states or between f and d states, which is in a good agreement with the experimentally observed XPS, UPS and x-ray emission spectra.

The recent progress for extending the above method will also be reported.

§ Permanent Address; Institute of Materials Science, University of Tsukuba, Ibaraki 305, Japan

P3 PHOTOEMISSION AND NUCLEAR RESONANCE SPECTROSCOPY.

M. Tenhover, Department of Research, The Standard Oil Co. (OHIO), Warrensville Heights, OH 44128, USA

The most informative aspect of the electronic structure of metallic glasses is the electronic density of states function D(E). Direct methods for experimently obtaining D(E) involve photoemission techniques such as Ultraviolet Photoemission Spectroscopy (UPS) and X-ray Photoemission Spectroscopy (XPS). In the first section of this talk, the application of these techniques to the various types of metallic glasses will be reviewed. The remainder of the talk will focus on recent results on early transition metal based glasses such as Zr-3d, Zr-4d, and Y-3d alloys. XPS and UPS measurements have provided a wealth of information on the electronic structure of these glasses. The relationship of the photoemission results to such topics as superconductivity, low temperature heat capacity, localized magnetic moment formation, and trends in electron density deduced from Mossbauer experiments will be discussed. Special emphasis will be placed on the differences between the photoemission spectra of crystalline and glassy alloys.

SESSION Q: ELECTRONIC PROPERTIES IV

Q1 THE ELECTRONIC DENSITY OF STATES OF AMORPHOUS YTTRIUM-IRON AND TERBIUM-IRON BASED ALLOYS. G. A. N. Connell, J. W. Allen, Se-Jung Oh, and R. Allen, Xerox Palo Alto Research Center, Palo Alto, CA 94304 USA.

Amorphous $Y_{0.21}Fe_{0.79}$ and $Tb_{0.21}(Fe_{1-y}M_y)_{0.79}$ alloys with M≡V, Mn, Co and Cu were prepared by rf sputtering in a UHV-system. Photoemission and inverse photoemission measurements were then performed to obtain the magnetic moment of the iron from its 3S-core level splitting[1] and the density of iron d-states within ±10 eV of the Fermi level. In the Tb-based alloys, the locations of the f-levels were also obtained. Assuming a value of 1.8 eV for the exchange splitting of iron, we are able to decompose the measured density of states into majority and minority spin bands and show that this decomposition is consistent with the iron 3S-splitting. The analysis also implies that charge transfer between the rare-earth or (pseudo-rare earth) and iron is rather small or zero and that the majority spin band is almost full.

These results can then be used to discuss the behavior of the iron-moment in amorphous Tb-Fe alloys when iron is replaced by other 3d-transition metals. In this case, the experimental trends are obtained from low-temperature magneto-optical measurements,[2] and the connection between them and the density of states is provided by the Friedel model and the calculations of Malozemoff et al.[3]

In this paper, we will also discuss the extent to which these specific results for amorphous Y-Fe and Tb-Fe alloys carry over to other rare earth-transition metal alloys, and what similarities and differences there appears to be with simple metglasses containing equivalent amounts of iron.

1. S.P. Kowalczyk, F.R. McFeely, L. Ley and D.A. Shirley, Mag. and Magn. Mats. (AIP, NY 1975), p. 207, 1974.
2. G.A.N. Connell and R. Allen, J. Mag. and Mag. Mater., 1983 (in press).
3. A. P. Malozemoff, A. R. Williams, K. Terakura, and V. L. Moruzzi, J. Mag. and Mag. Mater. 35, 1983 (in press).

Q2 THE ELECTRONIC STRUCTURE OF METALLIC GLASSES P. Oelhafen, U.M. Gubler, G. Indlekofer, R. Lapka, H.-J. Güntherodt, Institut für Physik, Universität Basel, CH-4056 Basel, Switzerland, C.F. Hague, Laboratoire de Chimie Physique, Université P. et M. Curie, F-75231 Paris Cedex 05, and V.L. Moruzzi and A.R. Williams, IBM Yorktown Heights, N.Y. 10598

We have studied the electronic structure of a great variety of glassy alloys by electron spectroscopy, X-ray emission spectroscopy and self consistent energy band calculations. The d-bands of the minority constituents in the Zr based transition metal glasses show interesting alloying effects in the various alloys A_xZr_{100-x} (A = V,Cr,Mn,Fe,Co,Ni,Cu, Rh,Pd and Au, with x approximately 25). The measured and calculated state densities are in close agreement and account for the observed trends in the superconducting transition temperatures.

The electronic structure of several actinide glasses (e.g. U-Co, U-Ni and Th-Cu) have been examined experimentally and a distinct dominance of the actinide 5f and 6d electron states near the Fermi level has been found.

The glassy normal metal alloy Mg-Zn has been studied and will be compared with Ca-Al. In contrast to the latter one no valence band band splitting and no structure induced minimum in the state density near the Fermi level has been observed.

Q3 THEORY OF PHONON-CONTROLLED CONDUCTIVITY IN HIGH-RESISTIVITY METALS. W. Schirmacher and D. Belitz, Physik-Department der Technischen Universität München, D 8046 Garching, F. R. G.

We present a theory for the conductivity of disordered metallic systems based on the mode coupling theory of Götze(1978). We use a model in which a zero temperature electron gas is coupled to a phonon system in an environment allowing for random scattering and random tunnelling. The conductivity is expressed in terms of two frequency and temperature dependent memory kernels describing density and current relaxation processes,and selfconsistency equations for these functions are derived.

Solution of these equations in the DC limit shows that phonon-controlled tunnelling processes dominate the conductivity if the electronic mean free path approaches the deBroglie wavelength. The resulting competition between scattering and tunnelling gives rise to anomalies of the temperature-dependent conductivity which are frequently observed in high-resistivity conductors as e. g. liquid and amorphous alloys or A15 compounds.

Q4 THE ELECTRICAL RESISTIVITY OF LIQUID Fe-Ni, Fe-Co AND Ni-Co ALLOYS. Y. Kita and Z. Morita, Department of Metallurgical Engineering, Osaka University, Suita, Osaka 565, Japan

A growing interest has been focused on the electronic transport properties of liquid transition metals and their alloys, both from a physical and a metallurgical viewpoint. In order to perform a direct and precise measurement of the electrical resistivity, ρ, of these liquid metals and alloys at high temperature, the four-probe method has been improved by constructing a newly-designed alumina cell in which the four electrodes were composed of the same material as the specimen.

The results of preliminary experiments on liquid Cu, Sn and Cu-Sn by this method, i.e. "improved four-probe method", were in excellent agreement with those of previous studies by other investigators. Therefore, it was proved that this method was quite suitable for the measurement of the electrical resistivity of liquid metals at high temperature.

By use of this method, the electrical resistivities of liquid Fe-Ni, Fe-Co and Ni-Co alloys have been measured at temperatures from the liquidus to about 1650°C over the whole concentration range.

For all of three systems, i.e. liquid Fe-Ni, Fe-Co and Ni-Co, the experimental results can be summarized as follows:
(1) The electrical resistivity increased slowly and almost linearly with increasing temperature in the studied temperature range.
(2) The electrical resistivity isotherm, showing composition dependence, can be expressed by a smooth curve being convex upward. No anomalous bump was observed.
(3) The temperature coefficient, dρ/dt, hardly changed with composition.

For liquid Ni-Co alloys, our results agreed with those reported by Dupree et al[1].

The experimental results are discussed in relation to extended Faber-Ziman theory.

1) B.C.Dupree, J.E.Enderby, R.J.Newport and J.B.Van Zytveld: Proc.3rd Inter.Conf.on Liquid Metals, Bristol, (1977),337

Q5 **ELECTRICAL RESISTIVITY OF LIQUID CHROMIUM.**
J. B. Van Zytveld,* Physics Dept., Calvin College, Grand Rapids, MI 49506 USA

We have measured the electrical resistivity, ρ, of Cr from room temperature to above its melting point. The resistivity, ρ_L, of liquid Cr is found to be 150 ± 5 μΩ-cm, and $(\rho_L-\rho_S)/\rho_S = 0.27$. We also report a melting temperature for Cr of 1812 ± 10°C. We compare ρ_L with values calculated on the extended Ziman theory, and examine the implications of ρ_S and ρ_L for the density of states for solid and liquid Cr.

Work supported by National Science Foundation Grants DMR77-05213 and DMR 79-09969.

***Temporary address: Solid State Physics Program, Division of Materials Research, National Science Foundation, Washington, DC 20550.**

Q6 ELECTRICAL RESISTIVITY AND HALL COEFFICIENT OF GLASSY AND LIQUID ALLOYS.
A. Tschumi, T. Laubscher, R. Jeker, H.U. Künzi and H.-J. Güntherodt, Institut für Physik, Universität Basel, CH-4056 Basel, Switzerland

The electrical resistivity and the Hall coefficient of a variety of alloys have been studied in the glassy and liquid state as a function of concentration and temperature. The liquid state covers the entire concentration range. The temperature range varies from 4K up to the liquid state. Our main aim is a comparison of the data in the glassy and liquid state. The investigated examples are Ca-Aℓ, U-alloys with Fe, Co and Ni, Zr- and Ti-alloys with Fe, Co, Ni, Rh, Pd, Pt, Au and Cu, $(Fe_xNi_{1-x})_{77}B_{13}Si_{10}$ alloys and Co-alloys across the series of the rare earths $(Co_{35}RE_{65})$. These detailed experimental results provide a clear insight into the systematic variation of the negative temperature coefficient of the electrical resistivity and the positive Hall coefficient which will be discussed in the framework of recent theories of the electrical resistivity and the Hall coefficient.

Q7 ACCEPTOR BAND TRANSPORT IN Se-Te LIQUID SEMICONDUCTOR ALLOYS.
M. Cutler and H. Rasolondramanitra, Oregon State University, Corvallis, OR 97331 USA* It has long been suggested that the increased activation energy of the electrical conductivity σ at high T observed in Se_xTe_{1-x} at compositions x ~ 0.3 to 0.7, is due to acceptor states created by broken bonds. But the absence of a corresponding break in the linear dependence of the thermopower S on 1/T has caused difficulty in this explanation. We have recently found such breaks in S at compositions $0.5 < x < 0.8$ and have made a two-band analysis of S and σ in terms of added transport in a narrow acceptor band. It is possible to deduce from the analysis the total number of states and the fraction of holes in the acceptor band, the average mobility μ_A of the acceptor band states, and the acceptor state energy E_A in relation to the valence band edge. μ_A increases rapidly as the number of states in the band increases, indicating that delocalization of an increasing fraction of the states is a primary factor. Although E_A becomes negative at high T, acceptor band transport is appreciable while the states are still above the valence band edge. It has not yet been possible to quantitatively characterize the acceptor band at high T or at $x < 0.5$, where the transition to a metal takes place. But the persistent pattern of the conductivity curves indicates that when this transition takes place, transport is primarily in the acceptor band, which is no longer narrow.

*Supported by NSF Grant DMR80-23682

SESSION R: ELECTRONIC PROPERTIES V

R1 THE HALL EFFECT IN AMORPHOUS METALS. G.J. Morgan, G.F. Weir, M.A. Howson, Physics Department, The University of Leeds, England.

The Hall effect in many amorphous alloys is positive as indeed it is for many transition metals and transition metal alloys. We have investigated the Hall effect within the random phase model for a hard sphere model of an amorphous or liquid metal. Although we find positive contributions the overall sign of the Hall effect remains negative in this simple approximation. We suggest that the origin of the positive sign lies in hybridisation between s and d electrons.

We have devised a method for simulating the Hall effect by studying the diffusion of electrons in a magnetic field. Results for a 'sample' containing $\sim 10^3$ atoms show that the effect is of the same level as the noise but that the experiment should be possible by increasing the dimensions of the sample within reasonable limits.

R2 VALENCE CONFIGURATION OF CERIUM IN AMORPHOUS $Ce_{1-y}Si_y$ ALLOYS. D. Malterre, J. Durand and G. Marchal, Université de Nancy - I, 54506 Vandoeuvre-les-Nancy (France)

In order to analyse the effects of the structural disorder on the valence configurations of Ce in amorphous alloys, we compare the magnetic properties of amorphous Ce_{1-y} Si_y alloys with those reported for Ce Si_x ($1.55 \leq x \leq 2$) crystalline compounds [1]. Ce_{1-y} Si_y amorphous alloys were produced over a broad concentration range ($0.25 \leq y \leq 1$) by coevaporation onto a liquid-nitrogen cooled substrate. Low-temperature magnetization ($H \leq 50$ kG) and temperature dependence ($2 \leq T \leq 250$ K) of the initial susceptibility were measured on samples of various compositions, with a special attention on alloys whose composition is close to Ce Si_2. In the crystalline state, indeed, two types of magnetic behaviours were observed depending on the concentration ranges. Crystalline Ce Si_x compounds with $1.85 \leq x \leq 2$ exhibit a non-magnetic behaviour at low temperature together with an anomalous high-temperature dependence of the susceptibility, which is attributed to a spin-fluctuation temperature of the order 300 K. Crystalline Ce Si_x compounds with $1.55 \leq x \leq 1.80$ are magnetically ordered below 10 K, but with a very low saturation moment assigned to a dense Kondo effect, while the high temperature susceptibility follows the behaviour expected for Ce^{3+} ions. The magnetic properties of amorphous alloys over both concentration ranges markedly depart from those found in the crystalline counterparts. The amorphous $Ce_{40}Si_{60}$ is not magnetically ordered above 2 K. The susceptibility above 170 K provides the Ce^{3+} ionic Curie-Weiss constant, while crystal-field effects occur at low temperature. On the other hand, on a $Ce_{28}Si_{72}$ amorphous alloy, a depression of the Ce moment is observed at high temperature and at low temperature as well, which suggest an inhomogeneous admixture of valence configurations. These striking effects of structural disorder are discussed in the light of other data concerning the sensitivity of Ce valence states to the atomic environment.

[1] - K. Yoshima and T. Kasuya, *Solid State Comm.*, 41, 723, (1982)

R3 CHARACTERIZATION OF THIN FILMS OF AMORPHOUS Cu_xZr_{1-x} USING OPTICAL AND ELECTRON SPECTROSCOPY. J. Rivory*, J.M. Frigerio, Laboratoire d'Optique des Solides, Université Pierre et Marie Curie, 4 Place Jussieu, 75230 PARIS Cedex 05, France. L. Névot, Institut d'Optique, Service 12, Bât.503, Université Paris-Sud, 91405 Orsay, France. Tran Minh Duc, IN_2P_3 and Université Claude Bernard, 69622 Villeurbanne, France.

Amorphous Cu_xZr_{1-x} ($0.3<x<0.6$) are sputtered from an alloy target onto silica substrates held at room temperature. Reflectance R and transmittance T measurements, performed in air at normal incidence, show modifications of the optical properties as a function of time, important essentially above 4eV, which are related to the oxidation process. Different techniques are used in order to characterize the superficial layer, i.e. Auger electron microanalysis, ESCA, grazing-incidence X-ray reflectivity. All these methods clearly show the existence of a superficial oxide layer (ZrO_2) containing a certain concentration of Cu, the profile of which is given by Auger analysis. Its total thickness is of the order of 30 Å, with a very porous structure at the extreme surface. The interface between the oxide layer and the homogeneous a-CuZr alloy is well defined. X-ray reflectivity also indicates the presence of a transition layer at the interface of the homogeneous material and the substrate, probably due to oxidation at the beginning of the deposition process. This multilayer structure is used in order to obtain more accurate values of the complex dielectric constant deduced from R and T measurements.

POSTER SESSIONS

Monday, 15 August 1983

Poster Session PA: THERMODYNAMICS

PA1 Structural Change in Liquid Iron and its Dilute Alloys
A.-H.K. Abdel-Aziz

PA2 Melting and Adiabats of the Alkali Metals at High Compressions
R. Boehler and D.A. Young

PA3 Self-Consistent Determination of the Structure and Resistivity of Liquid Al and Sn
J.L. Bretonnet and C. Regnaut

PA4 Bonding in Strongly Interacting Liquid Binary Alloys and Nuclear Spin Relaxation
M. Elwenspoek, R. Brinkmann, M.v. Hartrott, M. Kiehl, P. Maxim, C.A. Paulick, F. Willeke, and D. Quitmann

PA5 Iron-Base Liquid Alloy Densities--Measurement and Application to Macrosegregate Formation During Solidification
E.A. Feest, M.G. Nicholas, K.I. Moore, and B. Cantor

PA6 Reversible Temperature Dependence of the Structure Factor of an Fe(81)P(8)C(11) Amorphous Alloy
Ph. Mangin, C. Tete, and G. Marchal

PA7 Estimation of Free Energies of Crystallization of Amorphous Alloys
H. Miura, S. Isa, and K. Omura

PA8 A Thermodynamic Model for Liquid Sodium-Caesium Alloys
F.E. Neale and N.E. Cusack

PA9 Review of the Critical Point Data of the Alkali Metals
R.W. Ohse, J.-F. Babelot, J. Magill, and M. Hoch

PA10 Structure and Thermodynamics of the Liquid Noble Metals
C. Regnaut, E. Fusco, M.L. Rosinberg, and J.P. Badiali

PA11 ^{8}Li Spin-Lattice Relaxation in Liquid Li-Sn and Li-Si Alloys
C. van der Marel, P. Heitjans, H. Ackermann, E. Bader, P. Freilander, G. Kiese, and H.-J. Stockmann

PA12 Core Sizes and Forces as Deduced from Observed Structure Factors
W.H. Young, M. Silbert, and A. Meyer

Poster Session PB: STRUCTURE I

PB1 Mossbauer Study in (InTe)(x) Sn(1-x) Obtained by Splat Cooling
E. Arcondo, G. Quintana, H. Sirkin, and F. Cernuschi

PB2 Local Atomic Structure in Amorphous Mo(50) Ni(50) by Resonance X-Ray Diffraction Using Synchrotron Radiation
S. Aur, D. Kofalt, Y. Waseda, T. Egami, H.S. Chen, B.J. Teo, and R. Wang

PB3 Structural Study of Amorphous Eutectic Mg-Zn Alloy
P. Andonov and P. Chieux

PB4 EXAFS Studies of La(1-x) Ga(x) Metallic Glasses
D.V. Baxter, A. Williams, and W.L. Johnson

PB5 Structural Study of the Liquid Germanium by Means of Thermal Neutron Scattering
M.C. Bellissent-Funel and R. Bellissent

PB6 Ni(64) B(36)--A Transition Metal Metalloid Glass with First Neighbour Metalloid Atoms
N. Cowlam, Wu Guoan, P.P. Gardner, and H.A. Davies

PB7 Atomic Structure of Amorphous Ytterbium-Noble Metal Alloys: A Mossbauer Study
G. Czjzek, D. Weschenfelder, V. Oestreich, H. Schmidt, A. Vaures, and M. Maurer

PB8 EXAFS Study of Amorphous Fe(80)B(20) and Fe(80)P(20)
A. Defrain, L. Bosio, R. Cortes, and P. Gomes Da Costa

PB9 A Structural Investigation of Pd(76) B(24) Glassy Alloy
S. Enzo, G. Cocco, and A. Lucci

PB10 Structural Investigation of Amorphous Cu(9) Y Alloy by EXAFS and X-Ray Scattering
A.M. Frank, D. Raoux, A. Naudon, and J.F. Sadoc

PB11 Formation of Amorphous Fe-Ti-C Surface Layers
D.M. Follstaedt and J.A. Knapp

PB12 TDPAC Study of Liquid and Amorphous Se(x)Te(1-x)
D.K. Gaskill, J.A. Gardner, K.S. Krane, and R.L. Rasera

PB13 Superconductive Assessment of Fine-Scale Structural Homogeneity in Amorphous Alloys
R.R. Hake and M.G. Karkut

PB14 EXAFS Study of Metglas 2605 CC
G.H. Hayes, J.I, Budnick, M. Choi, W.A. Hines, D.M. Pease, D.E. Sayers, and S.M. Heald

PB15 EXAFS Study on Premelting and Supercooling Phenomena of Gallium
M. Hida, H. Maeda, N. Kamijo, K. Tanabe, H. Terauchi, Y. Tsu

PB16 Mossbauer Isomer-Shifts and Quadrupole Splittings in the Amorphous Iron-Boron System
W. Hoving, F. van der Woude, K.H.J. Buschow, and I. Vincze

PB17 Structural Studies on Amorphous Mg(70)Zn(30)
M. Ito, H. Iwasaki, N. Shiotani, H. Narumi, T. Mizoguchi, and T. Kawamura

PB18 Structure, Structural Relaxation and Crystallization of Amorphous Zr(1-x)M(x) Alloys
H.U. Krebs, C. Michaelsen, J. Reichelt, H.A. Wagner, J. Wecker, and H.C. Freyhardt

Poster Session PC: ATOMIC TRANSPORT AND STRUCTURAL RELAXATION I

PC1 Crystallization of Fe(80)B(20) Metallic Glasses
E.E. Alp, M. Saporoschenko, K. Simon, and W.E. Brower, Jr.

PC2 A DSC Study of Structural Relaxation in Metallic Glasses Prepared with Different Quenching Rates
L. Battezzati, G. Riontino, M. Baricco, A. Lucci, and F. Marino

PC3 Effects of Annealing on Curie Temperature in Amorphous Nitrogen-Bearing Fe-V-B-Si Alloys
K.A. Bertness, K.V. Rao, and H.H. Liebermann

PC4 Interdiffusion Studies in Metallic Glasses Using Compositionally Modulated Thin Films
R.C. Cammarata and A.L. Greer

PC5 Carbon Migration in the Amorphous Alloy Fe(81) B(13.5) Si(3.5) C(2) as Studied by Magnetic Anisotropy Measurements
W. Chambron, F. Lancon, and A. Chamberod

PC6 Investigation of the Crystallization of the (Fe, CC, Ni, Cr, Mn) B, Si Amorphous System
A. Cziraki, E. Fogarassy, I. Szabo, E. Albert, and K. Wetzig

PC7 Thermal Stability of Amorphous Metallizations for Semiconductor Devices
E.A. Dobisz, D.E. Aaron, K.J. Guo, J.H. Perepezko, R.F. Thomas, and J.D. Wiley

PC8 Investigation of Thermal Relaxation in Glassy Ni(80-x)Fe(x)P(20)
E. Fogarassy, A. Bohonyei, A. Cziraki, I. Szabo, G. Faigel, T. Kemeny, and I. Vincze

PC9 Anomaly in Young's Modulus of Fe-Zr Amorphous Alloys
K. Fukamichi, M. Kikuchi, and T. Masumoto

PC10 Crystallization Behavior of Binary Metallic Glasses Containing Pt
Y.-Q. Gao and S.H. Whang

PC11 Self-Diffusion in Liquid Metals: A Generalized Stokes-Einstein Equation
T. Gaskell

Poster Session PD: ELECTRONIC STRUCTURE I

PD1 Temperature Dependence of the Frequency Spectrum of the Magnetic Permeability After-Effect in Co-Rich Amorphous Metals
F. Allia and F. Vinai

PD2 Electron-Phonon Coupling and the Temperature Coefficient of Resistivity in Ni-Zr Glasses
Z. Altounian, R. Harris, and J.O. Strom-Olsen

PD3 Magnetic and NMR Studies of Amorphous and Crystalline Ni-P Alloys
I. Bakonyi, P. Panissod, J. Durand, and R. Hasegawa

PD4 Electronic Conduction in s-d Band Liquid Metals
L.E. Ballentine, S.K. Bose, and J.E. Hammerberg

PD5 Magnetic, Electrical and Thermoelectric Studies of Metallic Glass Fe(39)Ni(39)Mo(4)Si(6)P(12)
A.K. Bhatnagar, B.B. Prasad, and N. Muniratnam

PD6 First-Principles Calculation of Electronic Structures of CuxZr(1-x) Glass
W.Y. Ching, L.W. Song, and S.S. Jaswal

PD7 Relation Between Magnetism and Superconductivity in Amorphous Zr(1-x)Fe(x) Alloys
G. Chouteau and O. Bethoux

PD8 Linewidth Asymmetries in the Mossbauer Zeeman Spectrum of Amorphous Iron-Metalloid Alloys
M. Eibschutz, M.E. Lines, and H.S. Chen

PD9 Hall-Effect and Thermopower of Metallic Glasses
G. Fritsch, E. Luscher, J. Willer, and A. Schulte

PD10 The Thermopowers of Amorphous Transition Metal Alloys and Electron-Phonon Enhancement
B.L. Gallagher, A.B. Kaiser, and D. Greig

PD11 Electrical Resistivity of Bismuth, Germanium and Bismuth-Germanium Alloys in the Liquid State
J.G. Gasser, M. Mayoufi, G. Ginter, and R. Kleim

PD12 Forming Ability and Stability of Amorphous Alloys M(x)Sn(1-x) (M=Cr, Mn,Fe,Co,Ni,Cu)
J.F. Geny, D. Malterre, M. Vergnat, M. Piecuch, and G. Marchal

PD13 Transport and Magnetic Properties of a- Ce(X)Al(100-X)
A. Guessous, K. Matho, J. Mazuer, and J. Palleau

PD14 Experimental Evidence for a Structure-Induced Minimum of the Density of States at the Fermi Energy in Amorphous Alloys
P. Haussler, F. Baumann, J. Krieg, G. Indlekofer, P. Oelhafen, and H.-J. Guntherodt

PD15 Atomic and Electronic Structures of the Ca-Al Metallic Class System
W.A. Hines, A. Paoluzi, J.I. Budnick, W.G. Clark, and C.L. Tsai

PD16 The Hall Coefficients of Cu(x)Ti(100-x) Amorphous Metallic Alloys
M.A. Howson, D. Greig, and B.L. Gallagher

PD17 Electrical Resistivity, Magnetic Susceptibility and Thermoelectric Power of Amorphous Niobium-Nickel Alloys Synthesized by Vapour Quenching
Gh. Ilonca

PD18 A Reply to Faber's Question about the Minimum in the Thermoelectric Power of Liquid Mercury Alloys
T. Itami, N. Takahashi, and M. Shimoji

Tuesday, 16 August

Poster Session PE: METAL-NONMETAL TRANSITIONS

PE1 An NMR Comparison of Some Alkali-Antimony Alloys Around the Metal-Nonmetal Transition
R. Dupree, L. Bottyan, and W. Freyland

PE2 Properties of Hot Expanded Liquid Aluminum
G.R. Gathers and M. Ross

PE3 Theory of Strong Scattering in Liquid Compound-Forming Alloys
W. Geertsma and A.E. van Oosten

PE4 Self-Consistent Study of Chemical Short-Range Order and Charge Transfer in Liquid Alloys
Ch. Holzhey, J. Franz, F. Brouers, and W. Schirmacher

PE5 Semiconductor-Metal Transition in Liquid Selenium-Tellurium Mixtures at High Temperatures and Pressures
H. Hoshino, K. Tamura, and H. Endo

PE6 Nonmetal-Metal Transition in Liquid Bi-BiBr(3) Mixtures under Pressure
S. Hosokawa, H. Endo, and H. Hoshino

PE7 The Specific Heat of Mercury at Sub- and Super-Critical Temperatures and Pressures
M. Levin and R.W. Schmutzler

PE8 Low-Angle Structure Factors of Expanded Liquid Rubidium
I.L. McLaughlin and W.H. Young

PE9 Electrical Conductivity of Liquid Cs-CsI Mixtures
S. Sotier, H. Ehm, and F. Maidl

PE10 New Results in Liquid Alkali-Group IV-A Alloys
B.P. Alblas, C. van der Marel, W. Geertsma, J.A. Meijer, A.B. van Oosten, J. Dijkstra, P.C. Stein, and W. van der Lugt

PE11 Thermodynamic Properties of Liquid Na-IVb Alloys
S. Tamaki, S. Matsunaga, T. Ishiguro, and S. Takeda

Poster Session PF: STRUCTURE II

PF1 Structural Relaxation of Fe-B Alloy by X-Ray Diffraction
M. Laridjani, J.F. Sadoc, and R. Krishnan

PF2 Vibrational Dynamics of Liquid Tellurium
R.J. Magana and J.S. Lannin

PF3 Structure of Be 43 Hf(x)Zr(57-x) Metallic Glasses
M. Maret, A. Soper, G. Etherington, and C.N.J. Wagner

PF4 X-Ray Diffraction Studies with Liquid Ni-B and Mn-Si Alloys
E. Nassif, P. Lamparter, and S. Steeb

PF5 Structure and Crystallization of Amorphous Co(76)Mo(16)B(8) Alloy
S. Ning-Fu, I.P. Jones, and J.N. Pratt

PF6 EXAFS Study of Electrodeposited Ni-P Binary Alloys
T. Okamoto and Y. Fukushima

PF7 Crystal-Field Effects in Amorphous Alloys Containing Praseodymium
J.C. Cusset, S. Cantaloup, J. Durand, D. Bertrand, and A.R. Fert

PF8 Structural and Electrochemical Effects Induced in Metallic Glasses by Mechanical Deformation
M. Popescu and C. Mihaila

PF9 Mossbauer and X-Ray Studies of Amorphous Fe(67) Co(18) B(14) Si(1)
E. Bhanu Prasad, A.K. Bhatnager, D. Ganesan, R. Jagannathan, and T.R. Anantharaman

PF10 Structural Homogeneity and Crystallization of Amorphous Fe(81) B(13.5) Si(3.5) C(2)
A. Leimkuhler Rosasco, R.E. Pond, Sr., and R.F. Green, Jr.

PF11 XPS and Mossbauer Study on Amorphous FeBSi Alloys
M. Taniwaki, K. Makiuchi, M. Sugiyama, and M. Maeda

PF12 The Accuracy of Experimental Radial Distribution Functions
E.J. Thijsse and J. Sietsma

PF13 Mossbauer Investigations of Amorphous Metal-Metal Alloys
H.-G. Wagner, M. Ghafari, H.-P. Klein, and U. Gonser

PF14 The Effect of Quenching Temperature on the Structure and Crystallization of Glassy NiZr(2)
J.L. Walter, Z. Altounian, and J.O. Strom-Olsen

PF15 An X-Ray Diffraction Study of Liquid Zinc
G. Etherington and C.N.J. Wagner

Poster Session PG: ATOMIC TRANSPORT AND STRUCTURAL RELAXATION II

PG1 Re-Amorphisation of Crystallized (Fe(40) Ni(40))(10 B(20)) by Neutron Irradiation
R. Gerling, R. Wagner, and F.P. Schimansky

PG2 Log Time Relaxation Kinetics and the Activation Energy Spectrum Model
M.R.J. Gibbs, D.W. Stephens, and J.E. Evetts

PG3 The Dilatometric Estimation of Free Volume in Thermally Treated Ni(38) Zr(62) Samples
E. Girt, K. Novelija, Z. Majstorovic, and T. Mihac

PG4 Calorimetric Evidence of Structural Changes in Thermal-Aged CuZr, NiZr, FeBSi(C) and FeCoBSI Amorphous Alloys
M. Harmelin, Y. Calvayrac, A. Quivy, J. Bigot, P. Burnier, and M. Fayard

PG5 Effects of Quench Rate and Cold Drawing on the Structural Relaxation and Young's Modulus of an Amorphous Pd (77.5)Cu(6)Si(16.5) Wire
A. Inoue, H.S. Chen, J.T. Krause, and T. Masumoto

PG6 Young's Modulus of Fe-Based Amorphous Invar Alloys
S. Ishio, Y. Sato, T. Ikeda, and M. Takahashi

PG7 Shock Wave Consolidation of an Amorphous Alloy
P. Kasiraj, D. Kosta, T. Vreeland, Jr., and T.J. Ahrens

PG8 Diffusion of Gold and Nickel in Metallic Glasses
M. Kijek and D.W. Palmer

PG9 Thermal Stability and Creep Behavior of Fe-Ni Metallic Glasses
A. Kursumovic and B. Toloui

PG10 Thermal Stability, Magnetic and Mechanical Properties of Amorphous Fe(80-x) M(x) B(14)Si(6) with M = Mn,Cr,V,Mo,W
S.T. Lin, H.B. Wu, and W.T. Ku

PG11 Crystallization Behavior in Amorphous Inter-Transition Metal Alloys
A.F. Marshall, R.G. Walmsley, Y.S. Lee, and D.A. Stevenson

Poster Session PH: ELECTRONIC PROPERTIES II

PH1 Theory of Electronic Transport in Liquid Non-Simple Metals
M. Itoh, K. Niizeki, and M. Watabe

PH2 Electronic Structure of Transition Metal Glasses: Zr(x) T(1-x)
S.S. Jaswal and W.Y. Ching

PH3 Electrical Resistivities of Liquid Ag, In, Sn and Sb Solvents with Light Rare Earth Solutes
F. Kakinuma, M. Harada, and S. Ohno

PH4 (Withdrawn)

PH5 High-Frequency Properties in a Participle-Dispersed Amorphous Co(70.5)Fe(4.5)Si(10)B(15) Composite with Zero Magnetostriction
K. Kimura, T. Masumoto, A. Makino, and T. Sasaki

PH6 Thermoelectric Power of the Sn-Se Liquid Alloy
D.H. Kurlat

PH7 Effect of Structural Relaxation on Critical Fields H(c) and H(c2) and Resistivity in Sputtered Amorphous Alloys Zr(76)Cu(24) and Zr(76)Ni(24)
O. Laborde, C. Bethoux, J.C. Lasjaurias, and A. Ravex

PH8 Magnetic Properties of Amorphous Metal-Metalloid Alloys
B.W. Lau, T.K. Kim, and Y.E. Ihm

PH9 Optical Properties of Amorphous Fe(1-x)B(x) Alloys
N. Lustig, L.J. Pilione, K.C. Woo, and J.S. Lannin

PH10 Drude Optical Properties of Amorphous Nickel-Phosphorus Alloys
S.W. McKnight and A. Ibrahim

PH11 Test of Diffraction Model Predictions for Low Resistivity Amorphous Metals
L.V. Meisel and P.J. Cote

PH12 Effect of 2k(f)/K(p) on Electron Transport and Density of States in Hume-Rothery Type Metallic Glasses
U. Mizutani and K. Yoshino

PH13 Calculation of Full Spectral Function for an Amorphous Transition Metal
C.J. Morgan and G.F. Weir

PH14 In-Situ Investigations of the Electronic Properties of Co-Evaporated Amorphous MgZn Alloy Films
V. Nguyen Van, S. Fisson, and M.-L. Theye

PH15 On the Nature of Bonding in Liquid Semiconductor Cs(3)Sb and Some Other Alkali Antimonides
K. Niizeki, H. Tanaka, and K. Shindo

PH16 The Relativistic KKR-EMA Densities of States of Liquid Heavy Polyvalent Metals
A. Nishikawa and K. Niizeki

PH17 On the Stability of an Amorphous Hume-Rothery-Phase
H.J. Nowak

PH18 Magnetic Property of Transition Metal Solutes in Liquid In, Sn, Sb, Te and Se-Te Alloy Solvents
S. Ohno

PH19 D-C Electrical Resistivity in the Amorphous-Crystalline Transition of Cu(60)-Zr(40) Alloy System
M.A. Otooni

Wednesday, 17 August

Poster Session PI: SURFACES AND HYDRIDES

PI1 Thermodynamics of Hydrogen Absorption in Amorphous Zr-Ni Alloys
K. Aoki, M. Kamachi, and T. Masumoto

PI2 Experimental Study of Density Profile in the Liquid-Vapor Interface of Mercury and Gallium
L. Bosio, R. Cortes, A. Defrain, and M. Curezine

PI3 Hydrogen in Amorphous Magnetic Re-TM Alloys: A New Approach
D.W. Forester, P. Lubitz, J.H. Schelleng, and C. Vittoria

PI4 Monte Carlo Simulations of the Liquid-Vapor Interface of Sodium-Cesium Alloys
J. Gryko and S.A Rice

PI5 Theory of Surface Properties of Liquid Metals
M. Hasegawa and M. Watabe

PI6 Distribution of Activation Energies in Zr(2)PdH(x)
L.E. Hazelton

PI7 Hydrogen in Ni-Zr-B Metallic Glasses
U. Koster and H.-W. Schroeder

PI8 Effects of Elemental Additions and Superheat on Melt Surface Tension and Metallic Glass Embrittlement
H.H. Liebermann

PI9 Surface Modes in Spin Wave Resonance in Thin Amorphous Films
L.J. Maksymowicz and D. Sendorek

PI10 Diffusion of Hydrogen in Some Amorphous Alloys
Y. Sakamoto and K. Baba

PI11 Electrochemical Characterization of Amorphous and Microcrystalline Metals
R.G. Walmsley, Y.S. Lee, A.F. Marshall, and D.A. Stevenson

PI12 The Surface Composition of Liquid Fe-Mn and Fe-S Systems
J. Wang, M. Bian, and L. Ma

Poster Session PJ: MODELING

PJ1 Isotropic Variation in $s(\alpha)$ of the Small Angle Scattering Obtained from a Density Model Based on a Random Space Function (Point Geometry). Application to $\alpha = 3$
E. Boucher, P. Chieux, P. Convert, and M. Tournaire

PJ2 Spectrum of Electric Field-Gradient Fluctuations in Liquid Rubidium
J. Bosse and C. Wetzel

PJ3 Disorder Structure of Molten Monatomic Metals, Semi-Metals, and Semiconductors
M. Davidovic, M. Stojic, and Dj. Jovic

PJ4 Collective Excitations in Metallic Glasses
J. Hafner

PJ5 Structure of Multi-Component Hard-Sphere Mixtures--Application to the Liquid Li-Pb Alloys
K. Hoshino

PJ6 The Disclination Model of Non-Homogeneous Deformation in Amorphous Alloys
J. Gui and Z. Wang

PJ7 Nature of Amorphous and Liquid Structures-Computer Simulations and Statistical Geometry
M. Kimura and F. Yonezawa

PJ8 Topological and Chemical Ordering in a Two-Atoms Simulated Amorphous Structure
F. Lancon, L. Billard, and A. Chamberod

PJ9 A Computer-Simulated Structural Model for Fe(80)B(20)
L.J. Lewis and R. Harris

PJ10 A Model for the Kinetics of TSRO and CSRO Structural Relaxation in Metallic Glasses: Comparison with Experimental Results
I. Majewska-Glabus, B.J. Thijsse, and S. Radelaar

PJ11 Geometrical Features of Dense Random-Packed Structure of Spheres
T. Ninomiya

PJ12 Thermal Pressure Coefficients of Liquid Alkali Metals
S. Ono, I. Yokoyama, and T. Satoh

PJ13 Coupling of Two-Level Systems with (91)Zr Nuclei in Zirconium-Based Amorphous Alloys
A. Ravex and J.C. Lasjaunias

PJ14 Radiation-Induced Growth in Amorphous Pd(80) Si(20) and Cu(50) Zr(50)
G. Schumacher, S. Klaumunzer, S. Rentzsch, and G. Vogl

PJ15 Disordered Systems: Determination of Effective Pair Potentials from Experimental Structure Data
W. Schommers

PJ16 Molecular Dynamics Study of Atomic-Level Structural Parameters in Liquid and Amorphous Metals
V. Vitek, S.F. Chen, and T. Egami

PJ17 Flux-Pinning, Defects, and Structural Relaxation in Amorphous Superconducting Mo(5) Ge(3) Films
S. Yoshizumi, W.L. Carter, and T.H. Geballe

PJ18 Phonon Theory of Liquids and Amorphous Metals: Extension to Universal Generalized Disorder via Static Synergetics
E. Siegel

Poster Session PK: ELECTRONIC PROPERTIES III

PK1 Ferromagnetic Resonance Study of Thermal Stability in Fe(40)Ni(40)P(20) Amorphous Alloy
R.S. Parashar, C.S. Sunandana, and A.K. Bhatnagar

PK2 On the Magnitude of Electrical Resistivity of Amorphous, Liquid and Concentrated Crystalline Alloys
D. Pavuna

PK3 On the Local Density of Unoccupied d-States in Transition Metal-Metalloid Metallic Glasses
D.M. Pease, G. Hayes, M.C. Choi, J.I. Budnick, W.A. Hines, and R. Hasegawa

PK4 Resistometric Study of Short-Range Ordering in Metallic Glasses Having Different Free-Volume Content
G. Riontino, P. Allia, and F. Vinai

PK5 Thermal Stability and Magnetic and Electrical Properties in Amorphous Re-Al Alloys
K. Shirakawa, K. Aoki, and T. Masumoto

PK6 Electrical and Magnetic Properties of Amorphous FeZr and FeCd Films
T. Stobiecki, J. Sokulski, K. Kowalski, and F. Stobiecki

PK7 Resistivity and Hall Effect of Amorphous CdCo, CdCoMo and CoMo Films
T. Stobiecki, K. Kowalski, and J. Sokulski

PK8 Muffin-Tin Model Calculation of the Density of States of Liquid Copper
M. St. Peters

PK9 The Thermopower of Fe-B Metallic Glasses
J.C. Strom-Olsen, M. Clivier, and R.W. Cochrane

PK10 Modified C.P.A. Theory for Amorphous and Crystalline Alloys for Constituents of Different Band Structure
B. Szpunar and P. Dawber

PK11 The Magnetic Properties of Liquid Cd-Sb Alloys
P. Terzieff, K.L. Komarek, E. Wachtel, and B. Predel

PK12 Electrical Transport Properties of Metallic Glasses
C.L. Tsai and F.C. Lu

PK13 Composition Dependence of the Effective Hyperfine Field in Amorphous Fe-Early Transition Metal Alloys
K.M. Unruh and C.L. Chien

PK14 New Construction of First-Principles Pseudopotentials and their Applications to Liquid Metals
M. Watabe and M. Hasegawa

PK15 Study of Magnetic Regimes in a-Fe(x)B(100-x) by DC Magnetization Measurements
D.J. Webb, S.M. Bhagat, K. Moorjani, F.C. Satkiewicz, T.C. Poehler, and M.A. Manheimer

Poster Session PL: ATOMIC TRANSPORT AND STRUCTURAL RELAXATION III

PL1 Activation Energies for Crystallization of Amorphous Fe-Ni-P-B Alloys
H. Miura and S. Isa

PL2 Correlation of the Shear Modulus and Internal Friction in the Reversible Structural Relaxation of a Glassy Metal
N. Morito and T. Egami

PL3 On the Kinetics of Structural Relaxation in Amorphous Fe(40) Ni(40) B(20)
A.L. Mulder, S. van der Zwaag, and A. van den Beukel

PL4 Kinetics of Crystallization in the Cu(60)-Zr(40) Alloy System
M.A. Ctooni

PL5 Synthesis and Thermal Relaxation of Metallic Glasses Quenched at Ambient and Elevated Substrate Temperatures
S.J. Poon and S.E. Anderson

PL6 Atomic Diffusion and Structural Relaxation in Amorphous CuAg Films
I.M. Reda, A. Wagendristel, and H. Bangert

PL7 Superconductivity and Thermal Relaxation of Amorphous Be-Nb-Zr Alloys
H. Riesemeier, K. Luders, H.C. Freyhardt, and J. Reichelt

PL8 Evolution of Phase Separation in Cu(0.5) Zr(0.5) Metallic Glasses
R. Schulz, K. Samwer, and W.L. Johnson

PL9 Enthalpy Relaxation of Some Metallic Glasses Near Tg
R.C. Suzuki and P.H. Shingu

PL10 Annealing Effects on Electrical Resistivity, Thermoelectric Power and Crystallization of Iron-Rich Metallic Glasses Containing Molybdenum
S. Venkataraman, K.V. Reddy, Uno N. Virata Swaroop, G. Venugopal Rao, and A.K. Bhatnager

PL11 Formation and Stability of Amorphous and Part-Crystalline Zr(76)Ni(24) Alloys
B. Toloui, G. Gregan, and M.G. Scott

PL12 Ductility and Swelling of Neutron-Irradiated Amorphous Fe(40) Ni(40) B(20)
R. Wagner, R. Gerling, and F.P. Schimansky

PL13 The Crystallization Kinetics of Amorphous Selenium
J.T. Wang, X.L. Wei, E.Z. Din, and S.L. Li

PL14 Crystallization of Amorphous Alloys--Determination of Activation Energies from Electrical Resistivity Measurements
J. Wolny, J. Soltys, L. Smardz, J.M. Dubois, and A. Calka

PL15 Low-Frequency Internal Friction of Metallic Glasses During Structure Relaxation and Crystallization
W. Xia, J. Gui, Z. Wang, and R. Zhou

PL16 Relaxation and Embrittlement of Fe(40) Ni(40) Si(8) B(12) Glass
P.G. Zielinski and D.G. Ast

PL17 Glassy Pd-RE-Si Alloys: Formation, Properties and Devitrification
Y.Q. Gao and B.C. Giessen

PL18 Application of Analytical Techniques to the Predication of Glass Formation
B.C. Giessen and Y.Q. Gao

POSTER SESSION PA: THERMODYNAMICS

PA1 STRUCTURAL CHANGE IN LIQUID IRON AND ITS DILUTE ALLOYS. Abol-Hassan K. Abdel-Aziz, Chem. Eng. Department, Fac. Engineering, University of Alexandria, Egypt.

It was shown in a previous communication* that published property polytherms for liquid iron approve a proposal of a structural change in the melt in the temperature range of 1873-1973 K. Further review of published data confirms this proposal and shows that this structural change is reflected on the temperature dependence of the properties of molten dilute iron alloys. For molten Fe-C alloys of different carbon contents, the observed structural change temperatures permit the attempt to draw phase boundary lines in the liquid region of the Fe-C equilibrium diagram.

* Abol-Hassan K. Abdel-Aziz, "Effect of Temperature on the Structure of Liquid Iron", Arch. Eisenhuttenw., (52) 8, (1981), pp. 317-20.

PA2 MELTING AND ADIABATS OF THE ALKALI METALS AT HIGH COMPRESSIONS. R. Boehler, University of California, Los Angeles, CA 90024 USA, and D.A. Young, University of California, Lawrence Livermore National Laboratory, Livermore, CA 94550 USA

The melting temperatures of Li, Na, K, Rb, and Cs were measured to 32 kbar (3.2 GPa) in a piston cylinder apparatus. Hydrostatic pressure medium and in situ pressure and temperature measurement yield accuracies in pressure of ± 0.4 percent and in temperature of ± 0.25°C. Our results strongly differ from measurements using solid, non hydrostatic pressure media.

The adiabatic pressure derivative of temperature, $(\partial T/\partial P)_S$, was measured in the same pressure cell to 32 kbar and 500°C. We find a systematic linear decrease of ln $(\partial T/\partial P)_S$ versus volume to compressions of over 50 percent. Our experimental results are compared with theoretical calculations of the melting curves and the adiabatic gradients at high pressure.

The pressure and temperature dependence of the Grüneisen parameter γ was calculated from $\gamma = B_S/T\,(\partial T/\partial P)_S$, where B_S is the adiabatic bulk modulus. γ decreases with pressure in the liquid and in the solid state and increases by several percent at the liquid-solid transition. At constant pressure, γ decreases with temperature.

PA3 SELF CONSISTENT DETERMINATION OF THE STRUCTURE AND RESISTIVITY OF LIQUID Al AND Sn. J.L. Bretonnet, Laboratoire de Physique des Milieux Condensés, Université de Metz, 57045 Metz, France and C. Regnaut, GR4 CNRS, Physique des liquides et électrochimie, Tour 22, 4 place Jussieu, 75230 Paris 5, France.

Accurate theoretical determination of the liquid structure factor a(q) may be obtained from the pseudopential theory and the thermodynamical perturbation approaches such as the optimized random phase approximation (ORPA) and the optimized cluster theory (OCT) [1]. Therefore, the resistivity derived from Ziman's relation and a(q) may be self consistently determined from the pseudopotential.

In this work, we focus on two representative polyvalent simple metals : aluminium and tin. The first element's structure factor is hard sphere fluid like, while in the case of tin, the influence of the long range part of the pair potential on the structure may not be neglected [2,3]. Here, we mainly consider the nonlocal model potential of Shaw as input and we use an improved ORPA development to determine a(q) at low q. We analyze the influence of several factors on a(q) and resistivity : i) The way of calculating the exchange and correlation between electrons, considering either the Vashishta-Singwi self consistent results or the recent Ichimaru-Utsumi derivation. ii) The energy dependence of the model potential using the effective masses corrections. iii) The choice of different depletion hole charge distributions. We find that in the model potential theory, these three contributions have to be considered in order to discuss the best agreement with experimental data of a(q), compressibility and resistivity. The optimal results can be used to investigate temperature or density dependence of these properties.

[1] G. Kahl and J. Hafner, Phys. Chem. Liq. 12, 109 (1982)
[2] C. Regnaut, J.P. Badiali and M. Dupont, J. Physique (Paris) 41, C 8-603 (1980)
[3] J.L. Bretonnet, J.G. Gasser, A. Bath and R. Kleim, Phys. Stat. Sol. (b) 114, 243 (1982)

PA4 BONDING IN STRONGLY INTERACTING LIQUID BINARY ALLOYS AND NUCLEAR SPIN RELAXATION
M. Elwenspoek, R. Brinkmann, M. v.Hartrott, M. Kiehl, P. Maxim, C.A. Paulick, F. Willeke, and D. Quitmann, Institut für Atom- u. Festkörperphysik, Freie Universität Berlin, Arnimallee 14, D-1000 Berlin 33, Fed. Rep. Germany

In metallic liquid binary A-B alloys with strongly attractive A-B interactions, the heat of formation, short range order, etc. are often discussed using models of association. There is clear evidence for chemical short range order from scattering, i.e. in q-space. An experimental quantity which samples (charge density fluctuations in) the neighbourhood of a particular atom on a microscopic scale in r-space is nuclear spin relaxation rate caused by electric, i.e. quadrupolar, interaction (R_Q). We have found that drastic enhancements of R_Q occur rather generally in alloys of s-p-metals with compound forming tendency. That they correlate systematically with thermodynamic properties has been pointed out for In-X alloys earlier[1]. By considering number (n) and lifetime of associations, and using a quasiternary solution model, we have established a connection between the concentration and temperature dependence of R_Q in liquid A-B alloys and AA, BB, AB binding energies. The energy parameters are derived from macroscopic data, viz. thermodynamic functions (ΔH, ΔS, ΔCp). For In-Sb and In-Hg as examples, satisfactory agreement is obtained, see fig. 1. Steps required for a systematic and quantitative extraction of information about association from R_Q data, will be discussed.

[1] E. Weihreter et al., Phys. Lett. 76A (1978) 394.

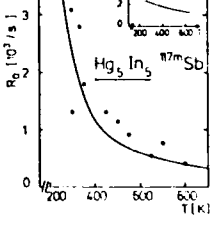

Fig. 1: R_Q in In_5Hg_5, measured on the probe ^{117m}Sb using TDPAD. Full line: associated model, normalized at 650 K.

PA5 IRON BASE LIQUID ALLOY DENSITIES - MEASUREMENT AND APPLICATION TO MACROSEGREGATE FORMATION DURING SOLIDIFICATION

E.A. Feest & M.G. Nicholas (AERE Harwell, UK) and K.I. Moore and B. Cantor (University of Oxford, UK).

A technique for measuring liquid metal alloy densities has been developed based on the photographic measurement of liquid droplet shape on a substrate.

Measurements within the Fe-Si system have shown that the liquid density as a function of composition shows marked deviations from linearity in the region of liquidus depression at ~ 20 wt% Si and these results are related to available thermodynamic data.

Density measurements have also been made on compositions corresponding to interdendritic enriched liquid regions of commercial steels. These results are related to the understanding of macrosegregate formation during solidification.

PA6 REVERSIBLE TEMPERATURE DEPENDENCE OF THE STRUCTURE FACTOR OF AN $Fe_{81}P_8C_{11}$ AMORPHOUS ALLOY. Ph. Mangin, Institut Laue-Langevin, 156X, 38042 Grenoble,France , C. Tete, Ecole des Mines, 54000 Nancy France and G. Marchal, Université Nancy I, C.O. 140, 54037 Nancy Cédex

The temperature dependence of the structure of amorphous alloys has been discussed theoretically by several authors, mainly in terms of the Einstein or Debye models. The crudest approximation predicts an evolution of $S_T(q)$ such as :

$$S_T(q) = 1 + [S_{T=0}(q) - 1]\, e^{-W(q)}$$

where W(q) is the Debye Waller coefficient. As a consequence of this relation, the variation of $S_T(k)$ as a function of the temperature must follow a quadratic law at low temperature and a linear law at high temperature. Moreover, fixed points must occur for q values such $S_{T=0}(q) = 1$.

Up to now,very few accurate results have been published in this area, in particular as concerns the second peak and its splitting and the existence of fixed points.

We present here results obtained by neutron diffraction at the Institut Laue-Langevin on a $Fe_{81}P_8C_{11}$ amorphous alloy for $0.2 < q < 7$ Å^{-1} and $4.2 < T < 500$ K.

With the auxiliary equipment facilities (furnace on cryostat), the use of multidetectors (covering 12° and 80°) and the control of incident flux, a variation of 0.2 % of the scattered intensity could be detected.

We have determined the evolution of maxima and minima (including the second peak and its splitting), we have measured the Debye-Waller coefficient and determined very accurately the positions of the fixed points. These are compared with those for which $S_{T=0}(q) = 0$.

PA7 ESTIMATION OF FREE ENERGIES OF CRYSTALLIZATION OF AMORPHOUS ALLOYS. H. Miura, S. Isa, and K. Omuro, Iron and Steel Technical College, Nishikoya, Amagasaki 661, Japan

In order to estimate the free energy of crystallization of an amorphous alloy, to begin with, the method of estimating the difference between the heat capacities, ΔC_p, of the supercooled liquid and crystalline solid states of the alloy was presented. The data used here were the heat of crystallization, the crystallization temperature, and the melting temperature of the amorphous alloy, which are relatively easy to experimentally obtain, and the other data of the literature for the constituent elements of the alloy such as the entropy of fusion, the heat capacity of the element in liquid and solid states. Here the entropies of fusion of the constituent elements were employed to determine the heat of fusion of the alloy additively from such entropies. The ΔC_p thus obtained for the $Fe_{40}Ni_{40}P_{14}B_6$, $Pd_{82}Si_{18}$, and $Cu_{56}Zr_{44}$ alloys were as follows respectively.

$$\Delta C_p = 22.34 - 0.01146\,T \quad [\,J/K\,mol\,]$$
$$\Delta C_p = 114.52 - 0.1038\,T \quad [\,J/K\,mol\,]$$
$$\Delta C_p = 83.43 - 0.06945\,T \quad [\,J/K\,mol\,]$$

By using these equations, the values of the free energy of crystallization, ΔG_c, of amorphous $Fe_{40}Ni_{40}P_{14}B_6$, $Pd_{82}Si_{18}$, and $Cu_{56}Zr_{44}$ alloys were calculated to be -2.98 kJ/mol, -3.75 kJ/mol, and -2.57 kJ/mol respectively.

It was shown that these calculated values give fairly good estimations for the ΔG_c at least near the crystallization temperature in view of results of statistical analyses of errors included in such calculated values. This method for estimating the ΔG_c value is considered to be more useful especially in case of the application to high-melting-temperature alloys in which the heats of fusion are difficult to obtain experimentally.

PA8 A THERMODYNAMIC MODEL FOR LIQUID SODIUM-CAESIUM ALLOYS. F E Neale and N E Cusack, University of East Anglia, Norwich, NR4 7TJ, UK.

Using a suitably specified interchange energy function $\chi(c,T,p)$ the expression

$$\Delta G = -T\Delta S_{hs} + \chi c(1-c)(V_1^o+V_2^o)/2V + p\Delta V$$

is found to give values of the Gibbs energy, entropy and enthalpy of mixing, activities and concentration fluctuations $S_{cc}(0)$ in excellent agreement with the recently reported data of Neale and Cusack* for liquid sodium-caesium over the entire concentration range. In this semi-empirical expression the second term is written in the usual form for mixtures whose pure component molar volumes $V_1^o(T)$ and $V_2^o(T)$ differ widely, and the observed experimental values are used for the alloy molar volume $V(T)$ and volume of mixing ΔV. Although the hard sphere term ΔS_{hs} is the principal contribution to the entropy of mixing, there is a significant negative contribution, ~ 11%, from the energy term; a small linear dependence of χ on temperature at given c and p is adequate to describe this. At constant T and p the change in χ over the range $0.4 < c < 0.85$ is less than 1%. It has a flat minimum in this region but rises sharply at both ends of the concentration range; this concentration dependence of χ must be incorporated in order to provide an adequate description of all the alloy thermodynamics, particularly the pronounced peak in $S_{cc}(0)$.

* Neale F E and Cusack N E 1982 J Phys F; Met Phys 12 2839

PA9 REVIEW OF THE CRITICAL POINT DATA OF THE ALKALI METALS

R.W.Ohse, J.-F.Babelot, J.Magill

Commission of the European Communities, Joint Research Centre, Karlsruhe Establishment, European Institute for Transuranium Elements, Postfach 2266, D-7500 Karlsruhe, Federal Republic of Germany, Tel. (07247) 84384, Telex 7825 483 EU D

M.Hoch

Department of Materials Sciences and Metallurgical Engineering, University of Cincinnati, Cincinnati, Ohio 45221

An assessment of the measured and estimated critical point data of the alkali metals is presented.

The various models and empirical relationships that have previously been applied to estimate the critical point data of the alkali metals were tested on potassium, rubidium and cesium, where reliable experimental data are available. The applicability of these models and empirical relationships is discussed considering the deviations of the predicted data from the measured data and the physics of the model. The input data used for calculation have been assessed on behalf of the data compilation of an International Collaborative Study Group organized by the IUPAC Commission on High Temperature and Solid State Chemistry.

Based on this analysis a new estimate of the critical point data of lithium is given using the "best" available input data.

PA10 STRUCTURE AND THERMODYNAMICS OF THE LIQUID NOBLE METALS

C. Regnaut, E. Fusco, M.L. Rosinberg, J.P. Badiali, Groupe de Recherche n° 4 du CNRS, Physique des Liquides et Electrochimie associé à l'Université Pierre et Marie Curie, Tour 22, 4 place Jussieu - 75230 Paris Cedex 05.

The OPW and model potential methods have been extended to the noble metals [1][2], and mainly applied to the calculation of the solid state properties. To our knowledge, no investigation of the liquid phase have been done from these two methods. Our first purpose, is to derive structure dependent quantities such as structure factor, entropy and C_v from the invoked theories. This is done by mean of the thermodynamical perturbation method ORPA which has been previously discussed for the simple liquid metals [3]. With this analytic procedure, we find a rather good prediction for liquid copper and silver properties, both from the ab initio OPW calculation of Moriarty [1] and from the parametrized model of Dagens [2]. Uncertainties remain for gold.

We propose a simplified alternative to Moriarty's calculation. We include some degree of parametrization in the characteristical quantities which appear in the OPW expansion. Namely : 1) the hybridization potential between s-d electrons is adjusted in order to reproduce some particular points of the band structure. 2) Setting the hybridization to zero, we define a local pseudo-potential in place of the OPW one. From this model, we determine and discuss liquid properties considering the influence of the pseudo-potential choice, and the local or non local calculation of the hybridization.

The present approach allows a successfull description of solid and liquid properties, and avoids a complete OPW calculation. Extension of our model to the surface properties will appear in a future work.

[1] J.A. Moriarty, Phys. Rev. B, 6, 4, 1239 (1972).
[2] L. Dagens, Phys. Stat. (b), 84, 311 (1977).
[3] C. Regnaut, J.P. Badiali, M. Dupont, J. Physique (Paris), 41, C8-603 (1980).

PA11 ^{8}Li SPIN-LATTICE RELAXATION IN LIQUID Li-Sn AND Li-Si ALLOYS.

C. van der Marel, P. Heitjans, H. Ackermann, B. Bader, P. Freiländer, G. Kiese and H.-J. Stöckmann, Fachbereich Physik, Universität Marburg, Marburg, Germany, and Institut Laue-Langevin, Grenoble, France.

Consecutive to measurements of the ^{8}Li spin-lattice relaxation time, T_1, in liquid Li -Na, -Mg, -Pb and -Bi alloys [1, 2], we have investigated liquid alloys of Li with the group IV elements Sn and Si. Beta-active ^{8}Li nuclei were produced by capture of polarised neutrons ; T_1 was determined from the decay of the β-asymmetry. For both systems, Li-Sn and Li-Si, we measured T_1 on a number of alloys with compositions covering the main part of the concentration range, both as a function of temperature, T, and applied field, B_0. In liquid Li-Sn we observed a concentration dependence of $1/T_1$ similar to that in liquid Li-Pb and Li-Bi [2]. A rather different concentration dependence of $1/T_1$ was observed in liquid Li-Si (resembling the Knight shift in liquid Li-Ge [3]) : two minima occur, one at about 25 at.% Si and a second one at approximately 43 at.% Si. The first minimum is explained in terms of charge transfer from Li to the less electropositive Si (comparable to Li_4Pb). The second minimum is tentatively attributed to the existence of covalently bound Si_4 tetrahedra in the liquid, similar to those postulated in pure liquid Si [4]. Whereas in liquid Li-Pb and Li-Sn no B_0-dependence was observed, it was found that in liquid Li-Si alloys containing about 40 at.% Si T_1 increases as a function of B_0. The origin of this effect is not yet clear.

[1] P. Heitjans, G. Kiese, H. Ackermann, B. Bader, W. Buttler, F. Fujara, H. Grupp, A. Körblein and H.-J. Stockmann, J. de Physique 41 (1980) C8-409
[2] G. Kiese, P. Heitjans, H. Ackermann, B. Bader, W. Buttler, P. Freiländer, C. van der Marel, H. Ruppersberg and H.-J. Stöckmann, Proc. Int. Conf. Ionic Liquids, Berlin 1982, Springer-Verlag (1982) 117
[3] C. van der Marel, A.B. van Oosten, W. Geertsma and W. van der Lugt, J. Phys. F 12 (1982) L-129
[4] J.P. Gabathuler and S. Steeb, Z. Naturforsch. 34a (1979) 1314.

PA12 CORE SIZES AND FORCES AS DEDUCED FROM OBSERVED STRUCTURE FACTORS.

W.H. Young and M. Silbert, University of East Anglia, Norwich, NR4 7TJ, UK, and A. Meyer, Northern Illinois University, Dekalb, ILL 601155, USA.

Observed structure factors which exhibit isotropic metallic bonding (class a in the terminology of Waseda) are analysed using the WCA theory to obtain effective diameters and corresponding effective forces. The results can be checked for internal consistency and the outcome is on the whole satisfactory for simple and noble metals although less clear-cut for transition and rare earth metals. Trends are presented of sizes and hardnesses (as defined by the effective forces) from category to category and within each category.

POSTER SESSION PB: STRUCTURE I

PB1 MÖSSBAUER STUDY IN $(InTe)_xSn_{1-x}$ OBTAINED BY SPLAT COOLING; B. Arcondo, G. Quintana, H. Sirkin, Dpto. de Física, Facultad de Ingeniería, Paseo Colón 850, 1063 Argentina, and F. Cernuschi, CONICET, Rivadavia 1917, Capital Federal, Arg.

Solid samples of $(InTe)_xSn_{1-x}$ have been obtained by means of the splat-cooling technique starting from different temperatures of the liquid state (T_1) and have been analized with electron diffraction and Mössbauer spectroscopy. The alloys were prepared from $In_{1.5}Te_2$ at.with the addition of Tin in different concentrations (from 3 to 20° wt.). The electron diffraction shows two coexisting phases, one amorphous and the other crystalline. The Mössbauer spectra were performed with both source and absorber at room temperature using a SnO_3Ca source. They show in all the cases two single lines, the first with an Isomer Shift around 2.00 mm/sec which is due to the Tin in an amorphous structure of InTe, and the second, with an IS around 3.48 mm/sec, that corresponds to the crystalline structure of SnTe. Samples obtained from the same T_1, present a ratio between the sizes of the first and the second peak that decreases with increasing concentration of Tin. This shows that Tin difficults the formation of the amorphous phase. On the other hand, for a fixed Tin concentration this ratio increases with higher temperature from which the melts were cooled down. This points out greater facility for the formation of the amorphous phase with higher T_1. Both behaviours can be atributed to the fact that the proportion of SnTe compound, which is strongly bounded, grows with increasing Tin concentration and decreasing T_1. In both cases Te is increasingly withdrawed from the InTe alloy taking it apart from the amorphizing concentration zone.

The solids samples were annealed for periods ten hours at different temperatures. The size of the first peak decreases in all the cases with increasing annealing temperature, disappearing at certain temperature.

All the samples obtained by slowly cooling show a single line corresponding to the SnTe crystalline compound.

PB2 LOCAL ATOMIC STRUCTURE IN AMORPHOUS $Mo_{50}Ni_{50}$ BY RESONANCE X-RAY DIFFRACTION USING SYNCHROTRON RADIATION. S. Aur, D. Kofalt, Y. Waseda and T. Egami, University of Pennsylvania, Philadelphia, Pa. 19104 USA, H. S. Chen and B. J. Teo, Bell Laboratories, Murray Hill, N.J. 07974, and R. Wang, Battelle Pacific Northwest Laboratory, Richland, Wash. 99352

The atomic structure of sputter depositied amorphous $Mo_{50}Ni_{50}$ was studied by the resonance (anomalous) X-ray diffraction technique using monochromatic X-ray radiation from the Cornell University synchrotron (CHESS) tuned near the absorption edge of either Mo or Ni. By making use of the energy dependence of the diffraction intensity through anomalous dispersion, f', the local atomic structures around each atomic species were determined. Compared to the earlier effort [1], the statistical accuracy is significantly improved due to the use of the synchrotron radiation which allowed to use the wave length very close to the edge [2]. In detecting the diffracted photons, in order to completely eliminate the fluorescent radiation from the sample, an intrinsic Ge detector was used. The energy resolution of the Ge detector was not high enough to separate K_α radiation from the elastically scattered photons, but was sufficiently high to separate the K_β radiation. The K_α intensity, which is proportional to the intensity of K_α, was then subtracted from the signal during the data reduction process.

We demonstrate that the f' dependence of the scattering intensity can be determined with a sufficiently high accuracy to yield the local structure around Mo atoms and that around Ni atoms with a resolution surpassing the EXAFS method by a very significant amount. The structure of a - MoNi was found to be basically the dense random packed structure. The nearest neighbour peak of the RDF around Ni is nearly symmetric, but that around Mo has a shoulder at the position approximately the 2nd nearest neighbour distance of the b.c.c. structure.

1. e.g. Y. Waseda and S. Tamaki, Phil. Mag., 32, 951 (1975).
2. P. H. Fuoss et al., Phys. Rev. Letter, 46, 1537 (1981).

PB3 STUCTURAL STUDY OF AMORPHOUS EUTECTIC Mg-Zn ALLOY P.ANDONOV, Laboratory of Magnétisme, C.N.R.S., Bellevue, FRANCE P.CHIEUX, Institut Laue-Langevin, Grenoble, FRANCE

The short range order in a simple divalent metal-metal amorphous alloy is studied by the " three radiations technique ".X-ray, neutron and electron scattering measurements were performed on amorphous eutectic $Mg_{1-x}Zn_x$ alloy prepared by the rapid quenching from the [illegible] melt with a single "roller technique ". The resolution control of the three experiments is obtained using the diffraction of a Silicon standard sample.

The experimental partial structure factors are compared with the calculated ones described by the Percus-Yevick hard sphere model and by the Heimendahl cluster relaxed model.

An important prepeak is observed in the $S^N(Q)$ for this alloy using X-rays.This total structure factor is a mixture of two components S_{NN} and S_{CC} arising from density and concentration fluctuations respectively.The scattering lengths for neutron diffraction are nearly similar for the two constituent atoms,so the $S^n(Q)$ relates almost wholly the density fluctuations and [illegible] exhibits only a very small prepeak.

With the Batia-Thornton formalism S_{NN} and S_{CC} are evaluated from X-ray and neutron data.

Then the chemical short range order parameter of the first coordination shell is derived from the Fourier transform of S_{CC}.

PB4 EXAFS STUDIES OF $La_{1-x}Ga_x$ METALLIC GLASSES. D. V. Baxter, A. Williams* and W. L. Johnson, California Institute of Technology, Pasadena, CA 91125 USA

Ga edge EXAFS spectra have been measured on $La_{1-x}Ga_x$ metallic glasses for x = 0.20, 0.24 and 0.28. Comparison is made with previous experiments in which the partial pair correlation functions of these glasses were measured using X-ray diffraction and isostructural substitution of Au and Al for Ga.[1] We use this known structural information to provide a stringent test of the capabilities of the EXAFS technique as applied to metallic glasses. The effect on the results obtained of the model pair distribution used in the curve fitting, is particularly emphasized.

*Permanent Address: Los Alamos National Laboratory, Los Alamos, New Mexico 87545

1.) A. Williams, Sol. St. Comm., 44, 983 (1982).

PB5 STRUCTURAL STUDY OF THE LIQUID GERMANIUM BY MEANS OF THERMAL NEUTRON SCATTERING

M-C. Bellissent-Funel, R. Bellissent, Laboratoire Léon Brillouin, C.E.N. Saclay, 91191 Gif-sur-Yvette Cedex, France.

Various structural investigations of liquid germanium [1][2][3] have been reported up to now. However, all these studies exhibit large discrepancies on the coordination number. Therefore we have performed a very precise measurement of the structure factor of liquid germanium by using a 640-cell position sensitive detector. Moreover, in order to obtain an accurate pair correlation function, we have realized an analytical extension of the structure factor in a self consistent way. Our experiments have been carried out at 1223 K and 1473 K. The coordination number is found to be nearly insensitive to the temperature, on the other hand, the obtained structure factors are compared with those deduced from both quasicrystalline and hard sphere type models in order to explain the strong change of the coordination number of the germanium at the melting point.

(1) ISHERWOOD, S.P., ORTON B.R. and MANAILA, R., J.Non-Cryst. Solids 8 (1972) 691.
(2) WASEDA, Y., SUZUKI, K., Z.Phys.B, 20 (1975) 339.
(3) GABATHULER, J.P. and STEEB , S., Z.Naturforsch.A, 34A (1979) 1314.

PB6 $Ni_{64}B_{36}$ - A TRANSITION METAL METALLOID GLASS WITH FIRST NEIGHBOUR METALLOID ATOMS. N.Cowlam, Wu Guoan**, P.P. Gardner, H.A.Davies*, Department of Physics & *Department of Metallurgy , University of Sheffield, Sheffield, UK

The structures of transition metal-metalloid glasses (TM-Met) may be influenced by the apparently large size difference between the constituents; the usually small fraction of metalloid atoms (for 80/20 compositions); and the tendency for the metalloids to remain apart. The structures of TM-Met glasses may be disordered interstitial-type atomic arrangements, in which the smaller metalloids occupy the largest holes in the Bernal polyhedra of the TM atoms [1].

Re-analysis of sizes of interstices in a DRPHS model [see 2] suggests that these holes are too small to accommodate metalloid atoms at the 20% concentration level in real glasses. Furthermore only TM-Met glasses with boron have extreme values of radius ratio. Those with silicon and phosphorus have values of radius ratio equal to those of TM-TM and simple metal glasses - for which size effects may play a less important role in the structure.

To test the models of TM-Met glass structure more stringently we have used glasses with compositions away from 80/20 and neutron diffraction for improved visibility of the metalloids. We have investigated $Ni_{64}B_{36}$ glass using X-rays and neutrons from reactor and pulsed sources, with both natural and isotopically enriched samples. Good correlation exists between different data sets, and partial structure factors and pair correlation functions obtained. Nearest neighbour distances and coordination numbers, and evidence for first neighbour boron-boron pairs will be presented. The results can be related to simple models of both an interstitial and a substitutional kind.

[1] D.E.Polk, Acta.Met. 20, 485, 1972
[2] P.H.Gaskell, J.Phys.C 12, 4337, 1979

** Home address, Institute for Atomic Reactor Engineering Research & Design, PO Box 291-106, Chengdu, Sichuan, China

PB7 ATOMIC STRUCTURE OF AMORPHOUS YTTERBIUM-NOBLE METAL ALLOYS: A MÖSSBAUER STUDY

G. Czjzek[a], D. Weschenfelder[a], V. Oestreich[a], H. Schmidt[a], A. Vaures[b], and M. Maurer[c]
a) Kernforschungszentrum Karlsruhe, IAK, Posttach 3640, D-7500 Karlsruhe, Federal Republic of Germany
b) Université de Paris-Sud, Lab. de Physique des Solides, F-91405 Orsay, France
c) Centre de Recherches Nucléaires, Chimie Nucléaire, B.P. 20, F-67037 Strasbourg, France

The even-even isotopes of ytterbium are good probes for structural investigations of amorphous materials by Mössbauer spectroscopy. We report on investigations of amorphous ytterbium-noble metal alloys of composition $Yb_{33}X_{67}$ (X=Cu,Ag,Au) by ^{174}Yb Mössbauer spectroscopy. Samples were prepared (a) by sputtering onto a substrate cooled to liquid-nitrogen temperature, (b) by roller-quenching of the melt. The same crystalline alloy ingots were used as starting materials for both types of preparation. The amorphicity of the final samples was checked by X-ray diffraction, the composition by plasma spectroscopy analysis.

Very similar spectra were obtained for the three samples prepared by sputtering whereas for roller-quenched alloys, the average quadrupole splitting is substantially smaller, indicating a different atomic structure compared to sputtered materials.

Starting from the assumptions that the observed field gradients reflect primarily the distributions of the minority component ions X and an Yb-X coordination of 2 to 3, we derive distributions of configurational patterns from the measured distributions of quadrupole splittings.

PB8 EXAFS STUDY OF AMORPHOUS $Fe_{80}B_{20}$ AND $Fe_{80}P_{20}$

A. Defrain, L. Bosio, R. Cortès and P. Gomes Da Costa, G.R.4 du CNRS, Tour 22, 4 Place Jussieu, 75230 PARIS CEDEX 05,France

On account of their practical application, the iron-metalloid glasses are thoroughly studied. However few results are available concerning EXAFS measurements [1,2], even though Fe-B alloys are, at least in principle, suitable for these studies, since the modulation above the Fe K-absorption edge mainly contains Fe-Fe contributions.

A possible explanation of such a disregard for EXAFS spectroscopy may be related to the difficulties inherent in spectra analysis, already found, in the b.c.c. α-Fe : in the real space the first and second shells are not resolved and peaks at larger distances differ appreciably both in amplitude and in position in regard to the expected values. Thus the phase shifts determination from the α-Fe study has to be carefully analysed before transfering them to unknown systems. On the other band, in the metallic glasses the description of the structure by a Gaussian pair distribution leads to inaccurate results on account of the large asymmetry of the first shell ; direct evaluation of EXAFS spectra are impossible without additional data such as X-ray diffraction results.

We have performed experiments and analysed α-Fe spectra. The EXAFS parameters thus determined were tested on the Fe_3B compound obtained after crystallization of the amorphous $Fe_{80}B_{20}$ material. The data reduction of non-crystalline solid spectra were then achieved using the radial distribution function deduced from X-ray diffraction measurements, performed on same samples. In the case of $Fe_{80}P_{20}$-glass the EXAFS spectra were found more easily tractable.

[1] P. Rabe et al. Festkörperproblem (1980), XX, 43.
[2] F. Schmückle et al. Z. Naturforsch (1982), 37a, 572.

PB9 [illegible] ALLOY

[illegible] and M.Sampoli, [illegible]

[illegible] arrangement of amorphous [illegible] experimental [illegible] concentra= [illegible] bond forming regions by conventional Fourier analysis of X-ray [illegible] Patterns. A chemical lo= [illegible] original prismatic units [illegible] distinctive features developed in [illegible] of the hypereutectic glas= [illegible] On the contrary, the overall profile of the experimental [illegible] of an amorphous alloy containing [illegible] at.% boron (i.e. below [illegible] concentration) was satisfactorily reproduced by the pertinent solution of the Percus-Yevick equation for a bi= nary mixture of hard spheres.

[illegible] gain new insights into the structural condition of $Pd_{76}B_{24}$, the PCF was approximated as a sum of analytical expressions, each pertaining to a discrete contribution of distances, a fur= ther term accounting for the structureless range (2). The a= nalysis brought to light the presence of a large spread of pseudo-square distances near to $r\sqrt{2}$ (r, being the nearest neighbour distance), overshadowed, in the experimental PCF, by the slowly rising edge of the second coordination sphere. More over, this feature was supported by the presence of a hump of increasing intensity observed at approximately the same posi= tion in the PCF_S of the specimen submitted to annealing treat= ments to induce more definitive structural conditions. On this basis, the chemical constraints appear to play a significant role also in the $Pd_{76}B_{24}$ in spite of the above possible evalu= ation of its structural condition within the conceptual frame= work of a dense binary mixture of randomly packed hard spheres.

1). G.Cocco, L.Schiffini, M.Sampoli, A.Lucci and G.Riontino. phys. stat. sol. (a), in the press
2). F.Hajdu, phys. stat. sol. (a), 60, 345 (1980).

PB10 STRUCTURAL INVESTIGATION OF AMORPHOUS Cu_9Y ALLOY BY EXAFS AND X RAY SCATTERING

A.M. Flank ★, D. Raoux +, A. Naudon ★, J.F. Sadoc +
★ Laboratoire de Métallurgie Physique, 86022 Poitiers FRANCE
+ Laboratoire de Physique du Solide, Bâtiment 510, 91 ORSAY and LURE, Bâtiment 209 C, U.P.S., 91405 ORSAY Cedex FRANCE

A structural investigation has been performed on an amorphous alloy of low concentration in Yttrium Cu_9Y (which was expected to be a first approximation for an elemental metallic glass), in order to study the topological local order mainly by eliminating chemical effects due to the mixing of two kinds of atoms.

The EXAFS spectrum on the Yttrium K edge can be simulated by the contribution of six Cu neighbors at 2,9 Å, a distance shorter than the sum of the Goldschmidt radii. Such an environment can be found in the Cu_9Y crystalline phase in which each Y atom has also 12 more Cu neighbors at 3,23 Å. This second shell is not observed by EXAFS in the amorphous alloy, probably because of a too great disorder.

On the copper edge an asymmetric distribution of 9 Cu-Cu with a mean distance of 2,55 Å and a closest approach value of 2,4 Å can simulate the EXAFS spectrum.

Complementary X ray diffraction experiments have also been recorded giving the [illegible] radial distribution functions. The amplitude and the shape of the first peak of the R.D.F. gives estimated coordination numbers consistent with EXAFS results.

Such a partial [illegible] number can be interpreted as resulting from a mixture of two sites. The local arrangement at the first site is similar to the one of copper in the crystalline phase Cu_9Y. The second copper site would be similar to the one found in the elemental copper.

A tentative model [illegible] with small angle X ray scattering results. [illegible] the SAXS intensity [illegible] shows a maximum which can be interpreted [illegible]

PB11 FORMATION OF AMORPHOUS Fe-Ti-C SURFACE LAYERS.

D.M. Follstaedt and J.A. Knapp, Sandia National Laboratories*, Albuquerque, NM 87185 USA

Surface alloys (~ 0.1 μm thick) formed by ion implanting Ti into Fe have been characterized by ion beam analysis and TEM. These studies show that C is also incorporated into the alloy at the sample surface from molecules in the vacuum during the Ti implantation. When both Ti and C are present in the Fe at sufficient concentrations (ranging from ~ 3 at.% Ti and ~ 25 at.%C to ~ 20 at.% Ti and ~ 10 at.%C) the surface alloy is found to be amorphous.

Pulsed electron beam melting of surface layers (~ 1 μm deep) and subsequent rapid solidification offer a method for further modifying the microstructure of implanted surface alloys. The rapid cooling rates (10^8 K/s) calculated for the metal just after solidification suggest that the amorphous structure might also be produced by pulsed melting. We therefore have examined the effects of e-beam pulsed melting on Fe alloys implanted with $2x10^{17}$ Ti/cm² at energies of 180-90 keV (which gives ~ 20 at.% Ti) and containing ~ $7x10^{16}$ C/cm² (~ 10 at.% C), alloys which were observed by TEM to be initially amorphous. A 1.85 J/cm², 70 nsec pulse is calculated to produce a melt lasting ~ 200 nsec, with subsequent solid phase cooling rates as high as $3.7x10^9$ K/s.

Ion channeling shows that the alloyed layer is not epitaxial after pulsed melting, while TEM shows that a polycrystalline layer is present instead of the amorphous layer. Electron diffraction patterns consist of rings which index to two phases: bcc Fe and TiC. Dark field imaging shows particle sizes of 20-80 nm for bcc Fe and ~ 3 nm for TiC. Thus our results show that ion implantation is capable of producing amorphous Fe-Ti-C at our concentrations, but melt quenching with ~ 70 nsec electron beam pulses is not.

*This work was performed at Sandia National Laboratories and supported by the U. S. Department of Energy under Contract #DE-AC04-76DP00789.

PB12 "TDPAC Study of Liquid and Amorphous Se_xTe_{1-x} Alloys"*

D. K. Gaskill, J. A. Gardner, K. S. Krane, Oregon State University, Corvallis, OR 97331 USA and R. L. Rasera, University of Maryland, Baltimore County, Catonsville, MD 21118 USA

A time-differential perturbed angular correlation (TDPAC) study on liquid and amorphous splat Se_xTe_{1-x} alloys was performed using dilute ^{111}Cd as the tracer. The liquid spectra exhibited an attenuation factor, λ_{22}, consistent with the motional narrowing approximation. The attenuation factor is proportional to the motional correlation time, τ_c, multiplied by the average square electric quadrupole frequency, ω_q. The ω_q have been characterized by static electric field gradient measurements of the amorphous phase made by quenching the liquid phase. Thus the magnitude of the average quadrupole frequency and the motional correlation time of the liquid alloys are found.

*Supported by the U.S. Office of Naval Research

PB13 SUPERCONDUCTIVE ASSESSMENT OF FINE-SCALE STRUCTURAL HOMOGENEITY IN AMORPHOUS ALLOYS.* R.R. Hake and M.G. Karkut, Indiana University, Bloomington, IN 47405 USA.

Superconducting upper critical field H_{c2} measurements[1] on the melt-spun amorphous Zr-base alloy systems Zr_{1-x} Co_x, Zr_{1-x} Ni_x, $(Zr_{1-x}$ $Ti_x)_{0.78}$ $Ni_{0.22}$, and $(Zr_{1-x}$ $Nb_x)_{0.78}$ $Ni_{0.22}$ show negative curvature of $H_{c2}(T)$ and fair agreement with the standard dirty-limit theory of Werthamer, Helfand, and Hohenberg and of Maki (WHHM). This contrasts sharply with previous reports of anomalous linear (zero-curvature) $H_{c2}(T)$ behavior in amorphous alloys. It has been suggested[2] that such anomalies may be due to inhomogeneity on a scale of the Ginzburg-Landau zero-temperature coherence distance ξ_{GO} ≈ 30-100 A and that $H_{c2}(T)$ may serve as a sensitive probe of fine-scale inhomogeneity. Consistent with an inhomogeneity interpretation, for two exceptional Nb-rich ternary specimens curvature of $H_{c2}(T)$ which (though not zero) is less negative than predicted by WHHM is coupled with other superconductive (but not x ray, density, or normal-state resistivity) evidence for inhomogeneity: relatively broad resistive transitions at T_c and H_{c2}, unusual current-density J dependence of transitions at H_{c2}, and (in one specimen) resistive evidence for J-dependent partial superconductivity at $H >> H_{c2}$ (the "beak effect"). The influence of homogeneity on $H_{c2}(T)$ is also suggested by the fact that those present Zr-base alloys which display $H_{c2}(T)$ in fair agreement with the WHHM theory also display critical flux pinning forces $f_c = J_c H$ lower than reported for most other crystalline and amorphous superconductors.

*Supported by NSF DMR 80-24365 and Indiana UROC 9-20-82-3.

[1]M.G. Karkut and R.R. Hake, Physica 109 and 110B, 2033 (1982) and Phys. Rev., in press.
[2]W.L. Carter, S.J. Poon, G.W. Hull, Jr., and T.H. Geballe, Solid State Commun. 39, 41 (1981).

PB14 EXAFS STUDY OF METGLAS 2605 CO.* G. H. Hayes, J. I. Budnick, M. Choi, W. A. Hines, D. M. Pease, University of Connecticut, Storrs, CT 06268 USA, D. E. Sayers, North Carolina State University, Raleigh, NC 27650 USA, and S. M. Heald, Brookhaven National Laboratory, Upton, LI 11973 USA.

We have undertaken an X-ray absorption study of the Fe and Co K-edges in Metglas 2605 CO (composition $Fe_{67}Co_{18}B_{14}Si_1$), before and after magnetic annealing, in order to investigate the near neighbor atomic environments of the metal atoms and, consequently, the relationship of such environments to the useful magnetoelastic properties of the Metglas. Metglas 2605 CO has a magnetomechanical coupling factor, k_{33}, which is very sensitive to magnetic annealing.[1] k_{33} reaches the relatively large value of 0.71 in a sample which has been annealed for 10 minutes at 369 °C in a magnetic field of 6.1 kOe lying in the plane of the ribbon transverse to its length. We have measured the X-ray absorption coefficients with the X-ray polarization parallel and perpendicular to the length of the ribbon. The extended X-ray absorption fine-structure (EXAFS) data indicate an anisotropy in the as quenched and in the annealed samples. Furthermore, upon comparing data collected at room temperature with that collected at liquid nitrogen temperature, we note an anisotropic behavior in the Debye-Waller type factor, σ. An explanation of the observed anisotropy will be offered and the correlation between the near neighbor atomic environments and the observed magnetoelastic behavior will be discussed.

*Work supported in part by grants from AFOSR (80-0030), NAVAIR (WF 615420), and USDOE Contract (DE-AC02-76CH00016). Absorption measurements carried out at SSRL, which is supported by the National Science Foundation in cooperation with USDOE, and CHESS, which is supported by the National Science Foundation.

[1]C. Modzelewski, H. T. Savage, L. T. Kabacoff, and A. E. Clark, IEEE Trans. on Magnetics, MAG-17, 2837 (1981).

PB15 EXAFS STUDY ON PREMELTING AND SUPERCOOLING PHENOMENA OF GALLIUM

Moritaka Hida and H.Maeda, Okayama Univ. Okayama 700, Japan; N.Kamijo, Government Ind. Res. Inst., Osaka, Ikeda 563, Japan; H.Tanabe and H.Terauchi, Kwansei Gakuin Univ. Nishinomiya 662, Japan; and Y.Tsu, Tohoku Univ. Sendai 980, Japan.

The absence of premelting in gallium has been reported using results obtained by Debye-Waller factor measurements(*), which utilize a conventional X-ray diffraction method. We believe that this method was not sensitive enough to verify local atomic rearrangements and disturbances. We had expected EXAFS to be a more powerful method for detecting local structural changes in pretransformation and metastability, such as premelting, premartensitic, supercooling and/or supersaturating phenomena.

X-ray absorption spectra near the K-edge of gallium were obtained for four states-- 99.9999%Ga crystalline(25.87°C), premelted(29.70°± 3°C/100), melted(32.01°C) and supercooled (28.00°C)-- using an energy dispersion-type apparatus equipped with an asymmetrically-cut flat crystal monochromator in the magnifying mode, and a position-sensitive proportional counter(**). The continuous radiation emitted at an accelerating voltage of 20 kV with a Co tube current of 50 mA was diffracted by a (220) reflection of a Si single crystal.

We found a certain premelted state which differs from a partially melted state, because we observed some differences among the Fourier transform spectra profiles of the above first three states. The second peak of the premelting profile slightly approaches the first peak of the crystal state profile, and it is expected from this proximity that Frenkel or interstitial-type defects will be formed in the premelted state. We also found that the supercooled state is not only s simple contraction of the melted state, but also contains a substructure which is more obvious than the substructure of the melted state. The neighbor distances and coordination numbers obtained from the least square parameter fitting for the above four states will be presented at the meeting.

(*) H.Wenzl et al : Z. Physik., B21(1975), 95.
(**) H.Maeda et al : J.Japan Appl. Phys., 21(1982), 1342.

PB16 MOSSBAUER ISOMER-SHIFTS AND QUADRUPOLE SPLITTINGS IN THE AMORPHOUS IRON-BORON SYSTEM, W. Hoving[1], F. van der Woude[1], K.H.J. Buschow[2], I. Vincze[3]. (1) Solid State Physics Laboratory, University of Groningen, 1 Melkweg, 9718 EP GRONINGEN, The Netherlands, (2) Philips Research Laboratories, EINDHOVEN, The Netherlands, (3) Central Research Institute for Physics, P.O.B. 49, H-1525 BUDAPEST, Hungary.

Several amorphous Fe_xB_{1-x}-alloys (10 a/o ≤ x ≤ 90 a/o) have been made by various quench techniques and on different substrates. Some electronic and magnetic properties were studied with ^{57}Fe Mössbauer spectroscopy in transmission geometry and with CEMS (Conversion-Electron Mössbauer Spectroscopy). Special attention has been paid to the isomer shift and quadrupole splitting as a function of the iron concentration. The isomer shift reflects the charge on the iron-atoms, whereas the quadrupole splitting is determined by the charge distribution on neighboring atoms. Both effects give information about the chemical and topological short-range order in the amorphous Fe_xB_{1-x} system.

The isomer shift as a function of iron concentration can be described with the ΔU^*- and Δn_{WS}-terms of Miedema's empirical model to predict the heat of formation of alloys [1] and a term for the additional elastic contribution [2]. ΔU^* reflects the interatomic charge transfer and Δn_{WS} the intra-atomic charge redistribution on alloying. The elastic contribution is necessary for boron-rich alloys (x < 50 a/o) and of minor importance at the iron-rich side. From this we conclude that the iron-rich samples have a dense-packed and the boron-rich samples have a more open atomic structure.

The quadrupole-splitting gives more insight in the near-neighbor configurations. Computer models for the atomic structure were used to reproduce the quadrupole splitting as a function of the composition.

[1] A.R. Miedema & F. van der Woude, Physica 100B (1980) 145-156.
[2] J.D. Eshelby, Solid State Physics, Edited by F. Seitz and D. Turnbull, vol. 3, p. 79, Academic Press, New York 1956.

PB17 STRUCTURAL STUDIES ON AMORPHOUS $Mg_{70}Zn_{30}$

M.Ito, H.Iwasaki and N.Shiotani, The Institute of Physical and Chemical Research, Wakoshi, Saitama 351, Japan, and
H.Narumi and T.Mizoguchi, Gakushuin University, Mejiro, Tokyo 171, Japan, and
T.Kawamura, Yamanashi University, Kofushi, Yamanashi 400, Japan

Structural studies on as-quenched and isothermally annealed amorphous $Mg_{70}Zn_{30}$ alloy are carried out by EXAFS, X-ray small angle and large angle scattering SAS and LAS, and electrical resistivity measurements. This amorphous alloy is known to crystallize into a single phase of $Mg_{51}Zn_{20}$ under isothermal annealing at about 80C. For the as quenched state, the EXAFS structure function for the nearest neighbor shell, which is Fourier filtered from the EXAFS data, has a single peak. The LAS interference function has a characteristic form for amorphous alloys, with the intense first peak and well developed second peak shoulder. Besides these a definite pre-peak is observed. The SAS intensity curve is in a single Gaussian form. When subjected to isothermal annealing at 76C, the electrical resistivity first increases with annealing time, then starts to decrease. During the increase of the electrical resistivity the height of the first peak and the splitting of the second peak of the LAS interference function become intense, and the SAS intensity curve tends to deviate from a single Gaussian form. After the electrical resistivity starts to decrease, the Bragg peaks corresponding to $Mg_{51}Zn_{20}$ crystalline phase appear and the peak in the EXAFS structure function starts to split. From these experimental results the atomic structure of the as quenched state and development of the short range and medium range ordering will be discussed in relation to the structure of $Mg_{51}Zn_{20}$.

PB18 **STRUCTURE, STRUCTURAL RELAXATION AND CRYSTALLIZATION OF AMORPHOUS $Zr_{1-x}M_x$ ALLOYS.** **H.U. Krebs, C. Michaelsen, J. Reichelt, H.A. Wagner, J. Wecker and H.C. Freyhardt, Institut für Metallphysik, Universität Göttingen, D-3400 Göttingen and SFB 126**

Amorphous, Zr-rich $Zr_{1-x}M_x$ alloys, with M = Fe, Co and Ni, were prepared in a wide composition range by a vacuum-melt-spinning technique. Their physical properties, in particular the electrical resistivity, thermal expansion and superconducting transition temperature, were measured as a function of the concentration of magnetic transition elements M, annealing time and temperature.

A combined analysis of X-ray and small-angle-neutron scattering, TEM, Mössbauer-effect, DSC and SEM investigations allowed the determination of topological and chemical relaxation as well as crystallization processes,which were connected to the property changes observed upon annealing.

Detailed DSC measurements of $Zr_{1-x}Fe_x$ alloys (x = 0.2 - 0.35) revealed a two-step crystallization with a strong exothermal peak at T_I, which enhances from 635 K to 705 K for Fe concentrations varying between 0.2 and 0.35, and a second, distinctly weaker peak at T_{II} exhibiting a pronounced dependence on x (T_{II}: 720 K - 920 K, for x: 0.22 - 0.33). The transition at T_I - with an activation energy between 1.2 and 2.8 eV - is connected with a 5 % increase of the specimen length and resistivity; at T_{II} the resistivity drops. X-ray and Mössbauer-effect structural analyses indicate that the first peak corresponds to the crystallization of a Zr_2Fe (with $NiTi_2$ structure) and α-Zr phase mixture. The second peak is tentatively ascribed to a transformation of the Zr_2Fe. No clear evidences for the occurence of Zr_3Fe - or other phases - are found so far.

POSTER SESSION PC: ATOMIC TRANSPORT AND STRUCTURAL RELAXATION I

PC1 CRYSTALLIZATION IN $Fe_{80}B_{20}$ METALLIC GLASSES*
E.E. Alp, M. Saporoschenko, K. Simon, W.E. Brower, Jr.
Southern Illinois University, Carbondale, IL 62901

The crystallization behaviors of $Fe_{80}B_{20}$ metallic glasses produced by melt-spinning, shock-tube, and hammer and anvil splat cooling techniques have been compared using Moessbauer Spectroscopy and differential scanning calorimetry. The eutectic crystallization theory - simultaneous crystallization of two crystalline phases - is checked against the primary crystallization theory - one of the phases precipitating out first and acting as preferred nucleation sites for subsequent crystallization. For shock tube samples the effect of superheated melt temperature on glass formation and the metastable phases obtained is also studied. Apart from the differences in kinetics, they basically follow the same crystallization pattern in support of the simultaneous formation of α-Fe and Fe_3B. Finally, upon further heating Fe_3B decomposes into α-Fe and Fe_2B. However, the crystallization kinetics are found to be drastically different in in situ DSC crystallization and vacuum annealing, and these differences are evaluated quantitatively by using the transmission integral technique to fit the Moessbauer spectra. The relaxation of the amorphous structure is monitored by following the distribution of the magnetic hyperfine field strength obtained directly from Moessbauer spectra using Window's method.

PC2 A DSC STUDY OF STRUCTURAL RELAXATION IN METALLIC GLASSES PREPARED WITH DIFFERENT QUENCHING RATES.
L. Battezzati, G. Riontino, M. Baricco, A. Lucci, F. Marino.
Istituto di Chimica Generale ed Inorganica, Facoltà di Farmacia, Università di Torino, TORINO (Italy).

Sets of amorphous alloys have been prepared by means of a melt spinning device using different rotation speeds of the wheel from 20 to 50 m/s.
The composition of the alloys are $Fe_{44-x}Ni_{36}Cr_xP_{14}B_6$ ($0 \leq x \leq 14$), crystallizing in a single stage after a manifest T_g and $Fe_{42}Ni_{41.5}Mo_5B_{11.5}$, $Fe_{80}B_{17}C_3$, crystallizing in two stages.
The chemical and topological contributions to the relaxation phenomena (giving rise calorimetrically to endothermal and exothermal responses respectively) have been separated by means of suitable thermal treatments. The quenching rate markedly affects the topological irreversible relaxation which takes place continuously in a wide temperature range from 420÷450 K up to the T_g region (650÷670 K) when a heating rate of 30 K/s is used in the DSC.
The enthalpy of relaxation increases with increasing quenching rate and is very high in the four and five components alloys. The heat release can become more than 50% of the heat of crystallization.
The structural relaxation is governed by a spectrum of activation energies which can be described by the heat evolution at constant heating rate.
The relations among the glass transition temperature, the crystallization temperature and the quenching rate are also discussed.

PC3 EFFECTS OF ANNEALING ON CURIE TEMPERATURE IN AMORPHOUS NITROGEN-BEARING Fe-V-B-Si ALLOYS. *K. A. Bertness*, K. V. Rao, E & I T Sector Laboratories/3M, St. Paul, MN 55133, and H. H. Liebermann, Allied Corporation, Parsippany, NJ 07054.*

The Curie temperature, T_C, of a ferromagnetic material is very sensitive to the nature of the local short range order and therefore corresponds to a particular compositional and topological environment in an amorphous material. The effects of annealing temperature [$250 \leq T_a \leq 500$°C], annealing time [$5 \leq t \leq 5650$ min.], and concentration [$50 \leq N \leq 2080$ ppm] of the metalloid nitrogen on T_C in amorphous nitrogen-bearing $Fe_{83-x}V_xB_{14}Si_3$ alloys[1] with x = 10 and 12, have been studied using a low-field thermomagnetic measurement technique.

An initial *decrease* in T_C with $T_a > 250$°C is observed for a given annealing time. A maximum drop of $\Delta T_C \approx -19$°C is found around $T_a' \approx 387$°C. For temperatures above T_a', ΔT_C decreases and goes through zero at $T_a'' \approx 500$°C. A similar dependence of T_C on T_a has been reported[2] for Fe-Cr-based amorphous alloys. Thus, it appears that ferrous amorphous alloys containing elements to the left of Fe in the periodic table initially show a decrease of T_C on annealing. *Reversibility* of T_C is found on annealing at pre-determined temperatures and for fixed times between T_a' and T_a''. Also, at temperatures below T_a', the lowest value of T_C obtained for long time annealing *does not fall below* that which is observed at T_a'. Such a plateau of T_C below T_a' presumably also occurs in systems where T_C shows a maximum as a function of T_a. The functional form of the data in a ΔT_C Vs T_a plot is found to be identical for alloys with x = 10 and 12 at.%V. However, the addition of N as a metalloid element makes the curve shallow: i.e., ΔT_C at T_a' is reduced. Thus, in the regime above T_a', where T_C is reversible, nitrogen plays an important role. These results suggest that the observed changes in T_C are due to reversible structural changes in the alloy as well, rather than a consequence of variations in the compositional short range order alone.

* *Presently at: Dept. of Physics, Stanford University.*
[1] *These samples were prepared by H²L while at General Electric.*
[2] *T. Kudo et al RQ4 conf. Proc. Sendai, page 1187 (1982).*

PC4 INTERDIFFUSION STUDIES IN METALLIC GLASSES USING COMPOSITIONALLY MODULATED THIN FILMS

R. C. Cammarata and A. L. Greer
Division of Applied Sciences
Harvard University
Cambridge, Massachusetts 02138, U.S.A.

Compositionally modulated, glassy films have been produced by D.C. sputtering alternately from targets of $Pd_{80}Si_{20}$ and $Fe_{80}B_{20}$ compositions. The modulation gives rise to X-ray satellites about the zero order beam, and by monitoring the decay of these satellites on annealing, a Pd-Fe interdiffusivity is obtained. Previous work [1] has shown that this technique is capable of measuring very low interdiffusivities: with this capability, the effects of structural relaxation on atomic diffusion were detected. This work has now been extended, and, taking relaxation effects into account, it has been shown that the measured interdiffusivity is dependent on the wavelength, λ, of the composition modulation. This is the first demonstration of gradient energy effects in an amorphous material. With decreasing λ, the interdiffusivity, D_λ, decreases and goes negative below a critical wavelength of ~20Å. Negative values of D_λ indicate phase separation on a very fine scale, or ordering. This ordering tendency indicates a slight negative heat of mixing for Pd and Fe in the glassy state, in contrast to predictions based on measurements made at high temperature in the liquid state. The potential of the modulated film technique for obtaining thermodynamic information on glassy phases is indicated.

[1] A.L. Greer, C-J. Lin and F. Spaepen, *Proc. 4th Int. Conf. on Rapidly Quenched Metals* (Sendai 1981), p. 567.

PC5 CARBON MIGRATION IN THE AMORPHOUS ALLOY $Fe_{81}B_{13.5}Si_{3.5}C_2$ AS STUDIED BY MAGNETIC ANISOTROPY MEASUREMENTS.

W. Chambron, F. Lançon and A. Chamberod, Centre d'Etudes Nucleaires de Grenoble, Département de Recherche Fondamentale, Section de Physique du Solide, 85 X, 38041, Grenoble Cedex, France.

The magnetic anisotropy induced by a thermomagnetic treatment between 60 and 320°C has been studied in the amorphous alloys $Fe_{81}B_{13.5}Si_{3.5}C_2$ and $Fe_{81.5}B_{14.5}Si_4$, first annealed at 400°C, and in the crystalline alloy $(Fe_{20}Ni_{80})_{1-x}C_x$ where $x = 760.10^{-6}$ at. Comparison of isochronal and isothermal kinetics of anisotropy establishment in both amorphous alloys leads to consider two steps :

a) A first part, corresponding to 42 J/m^3, is the same (magnitude and kinetic) in both amorphous alloys. It sets up with a very broad distribution of time-constants. The apparent activation energy varies form 1.42 eV at 120°C to 2.20 eV at 320°C. This phenomenon is related to rearrangements of the iron, boron and silicon atoms.

b) A second part, corresponding to 15 J/m^3, is peculiar to the alloy $Fe_{81}B_{13.5}Si_{3.5}C_2$. It sets up with a spectrum of time-constants somewhat less broad than the first one. The mean time-constant obeys the Arrhenius law $\tau = \tau_o \exp(E/kT)$. τ_o is found to the equal 2.5×10^{-15} s, and E = 1.36 eV. This phenomenon is considered to be due to the interstitial migration of the carbon atoms.

In the crystalline alloy, in the same temperature range, only the effect due to the migration of carbon interstiti is observed (3 J/m^3, $\tau_o = 1.1 \times 10^{-15}$s, E = 1.54 eV). Thus the carbon mobility in the amorphous alloy is rather close to that observed in the crystalline f.c.c. iron-nickel alloys, and very lower than in b.c.c. iron.

PC6 INVESTIGATION OF THE CRYSTALLIZATION OF THE /Fe,Co,Ni,Cr,Mn/B,Si AMORPHOUS SYSTEM

Á. Cziráki, B. Fogarassy, I. Szabó
Institute for Solid State Physics, Eötvös University, Budapest, Muzeum krt. 6-8. 1088, Hungary
B. Albert, Csepel Metal Works, Budapest, P.O.B. 93, 1751, Hungary
K. Wetzig, Zentralinstitut für Festkörperphysik und Werkstofforschung, Dresden, Helmholtzstrasse 20, 8027, DDR

In order to understand the structure of the amorphous state the investigation of the crystalline phases are necessary after the transformation.

The earlier investigated /1/ /Fe,Co,Ni,Cr,Mn/B,Si multi-component amorphous system has very good magnetic properties and so it is important for the industrial application. In these glassy metals the alloying elements could substitute each-other in the same crystalline structure, therefore the structure analysis by electron diffraction is not sufficient. In the present work the crystallization of some new amorphous alloys is investigated for study of the effect of the alloying elements separately and the phases were analyzed not only by electron diffraction but by their characteristic X-ray spectrum too.

The crystallization processes were followed by electrical transport properties measurements, calorimetry and electron microscopy in JEOL 100-CX and JEOL 200-CX instruments.

The ratios of the metallic components in the fcc, hcp and cementite type compounds are the same as in the amorphous matrix but the Si contents are different connected with the solubility of Si.

/1/ Á. Cziráki, et.al.: Proc. 4th Conf.on Rapidly Quenched Met.I.691 /Sendai, 1981./

PC7 THERMAL STABILITY OF AMORPHOUS METALLIZATIONS FOR SEMICONDUCTOR DEVICES

L. A. Dobisz, D. B. Aaron, K. J. Duo, J. A. Perepezko, K. L. Thomas, J. D. Wiley, University of Wisconsin, Madison, Wisconsin 53706 USA.

The thermal stability of amorphous metal films is of prime importance in high temperature semiconductor device applications. Suitable thin film (1 μ) deposits of amorphous alloys in the NiNb, NiMo, MoSi and WSi systems have been prepared by sputter deposition onto Si, GaAs and GaP substrates in an RF triode sputter system. The amorphous character and crystallization behavior of the films have been monitored by x-ray diffraction (XRD). The maximum crystallization temperatures, following one hour anneals, were found to be 600°C for Ni-43 a/o Nb, 575°C for Ni-35 a/o Mo, 600°C for Mo-40 a/o Si, 700°C for W-10 a/o Si. Polycrystalline Ni overlayers were found, by XRD, to lower the NiNb crystallization temperature by about 150°C presumably due to interdiffusion effects. Resistance change measurements are sensitive to the onset of structural relaxation and small amounts of crystal growth. For example the crystallization onset of NiNb in contact with a polycrystalline Ni overlayer was found to occur at temperatures as low as approximately 270°C. In addition Auger depth profiles were used to monitor the various interdiffusion reactions between the amorphous metal, polycrystalline metal overlayers and semiconductor substrates. The feasibility of NiNb as a diffusion barrier between Au and a semiconductor substrate was found to depend on the substrate. Following a one hour 500°C anneal, very little interdiffusion was observed in the Au/NiNb/Si system. However on a GaP substrate the Au and NiNb interdiffused extensively. These studies have demonstrated the viability of amorphous metal films as effective diffusion barriers in semiconductor contact applications.

The support of the DOE (DE-AC02-82ER12062) is gratefully acknowledged.

PC8 INVESTIGATION OF THERMAL RELAXATION IN GLASSY $Ni_{80-x}Fe_xP_{20}$

B. Fogarassy, A. Böhönyei, Á. Cziráki, I. Szabó
Institute for Solid State Physics, Eötvös University, Budapest, Muzeum krt. 6-8. 1088, Hungary
Gy. Faigel, T. Kemény, I. Vincze
Central Research Institute for Physics, Budapest
P.O.Box 49, 1525 Hungary

Thermal relaxation of metallic glasses is important both for the practical applications and for our understanding of the amorphous structure. The change in the physical properties of amorphous alloys is usually small in the relaxation process and complex methods are necessary for their detailed study.

Results will be presented here on the thermal relaxation of melt-spun amorphous $Ni_{80-x}Fe_xP_{20}$ /x = 0,1,3,5,10,20/ alloys. Measurements of dynamical Young's modulus, internal friction, electrical transport properties, Mössbauer effect, calorimetry and electron microscopy will be reported.

The aim of the investigations was to explain the unusually large thermal relaxation effects observed above 5 at% Fe content in the dynamical Young's modulus and electrical resistivity data.

Chemical ordering of the metallic components will be discussed as the possible reason of the observed large changes.

PC9 ANOMALY IN YOUNG'S MODULUS OF Fe-Zr AMORPHOUS ALLOYS
K. Fukamichi, M. Kikuchi* and T. Masumoto, The Research Institute for Iron, Steel and Other Metals, Tohoku University, 980, Sendai, Japan.

$Fe_{100-x}Zr_x$ ribbon and bulky amorphous samples have been prepared by melt-quenching and high-rate sputtering, respectively, in a wide composition range in order to investigate the temperature dependence of Young's modulus in magnetic fields. The ΔE effect decreases with increasing X. Young's modulus at the saturated field, E_s, for $Fe_{91}Zr_9$ amorphous alloy is smaller than the paramagnetic Young's modulus E_p, indicating a softening in a wide temperature range as shown in the figure. A similar behavior is often observed in Fe-based crystalline Invar alloys[1], but it is very different from the elastic property of Fe-based amorphous alloys containing metalloids, because the latter alloys exhibit a remarkable stiffening below the Curie temperature T_c[2]. It is worth noting that the value of Young's modulus at zero field, E_0, increases even above T_c with increasing temperature. Such an anomalous behavior is closely correlated with the inhomogeneous magnetic state in Fe-Zr amorphous alloy system. Other anomalous behaviors such as thermal expansion and high-field susceptibility are also explained by taking into account the magnetic inhomogeneity.

[1] G. Hausch, J. Phys. Soc. Japan, 37 (1974) 824.
[2] K. Fukamichi et al., IEEE Trans. Mag. MAG-15 (1979) 1404.

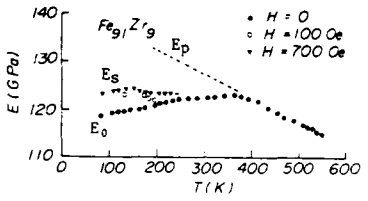

*Present address; The Research Institute of Electric and Magnetic alloys, 982, Sendai, Japan.

PC10 CRYSTALLIZATION BEHAVIOR OF BINARY METALLIC GLASSES CONTAINING PT.
Yi-Qun Gao and Sung H. Whang, Institute of Chemical Analysis, Northeastern University, Boston, MA 02115 USA

Pt containing alloys rarely form glasses for some reason. We are investigating glass forming property, crystallization behavior and mechanical properties of binary Pt glasses.

Binary M-Pt alloys, where M is an element from many different groups, were made into alloy buttons in an arc-melt furnace and rapidly quenched from the melt using hammer and anvil technique . The foil shape samples produced were checked with X-ray, Differential Scanning Calorimetry and TEM to identify amorphous structure. Binary Pt alloys with Group IVB (Ti, Zr, Hf) were found to be amorphous upon rapid quenching. A narrow glass forming compositional range was discovered near eutectics in these systems.

Crystallization kinetics of these Pt containing glasses were studied by DSC-2 calorimetry at a temperature range up to 1000K and heating rates of 5, 10, 20, 40, 80, and 160 K/min. Activation energy of crystallization for these glasses will be obtained from DSC measurement.

Mechanical properties of the glassy and devitrified states of these alloys will be studied as a function of time for a given temperature.

Activation energy obtained from different plots also is presented.

Glass forming tendency of binary Pt systems will be given and discussed with existing models.

Partially supported by Office of Naval Research

PC11 SELF-DIFFUSION IN LIQUID METALS: A GENERALIZED STOKES-EINSTEIN EQUATION.
T.Gaskell, Department of Physics, University of Sheffield Sheffield S3 7RH, UK.

Assuming that we can describe ionic dynamics in a liquid metal through an effective two-body potential, we use the concept of a configuration-dependent velocity field to derive an expression for the self-diffusion coefficient. It takes the form

$$D = \frac{nkT}{12\pi^3}\int d\underline{q}\, f(q)\frac{1}{q^2\bar{\eta}(q,\omega=0)}$$

where $f(q)$ is essentially the Fourier transform of a step function whose width is the radius of the mean ionic volume, and $\bar{\eta}(q,\omega)$ is the real part of a complex wave vector- and frequency- dependent shear viscosity coefficient. In the long-wavelength, low-frequency limit $\bar{\eta}(q,\omega)\rightarrow\eta$, the shear viscosity. The effects of the microscopic structure of the liquid are included in the diffusion mechanism, through the wave vector-dependence of $\bar{\eta}(q,\omega)$ .Although the microscopic contributions are very significant, it is shown how a Stokes-Einstein relation between D and η can still be substantially justified in the dense liquid.

In a recent molecular dynamics study of supercooled states of a liquid rubidium model, low frequency $\bar{\eta}(q,\omega)$ data has been obtained for a range of wave vectors, and at different temperatures. We discuss, through the above equation, the relevance of this data to the observed change in the diffusion mechanism as the temperature is lowered.

POSTER SESSION PD: ELECTRONIC STRUCTURE I

PD1 TEMPERATURE DEPENDENCE OF THE FREQUENCY SPECTRUM OF THE MAGNETIC PERMEABILITY AFTEREFFECT IN Co-RICH AMORPHOUS METALS. P.Allia and F.Vinai, IENGF and GNSM, I-10125 Torino, Italy

The aftereffect of the magnetic permeability of amorphous ferromagnetic alloys, $\Delta u/u$, can be interpreted in terms of the local magnetostrictive interaction between structural defects (shear stress fluctuations) and the magnetization. In Fe-based amorphous alloys the room temperature value of the aftereffect is found to scale with the square of the magnetostriction constant, λ_s [1].

In the present paper, results are reported of measurements performed on as cast, Co-rich amorphous alloys, showing that strong magnetic aftereffects are present even in glasses having compositions for which $<\lambda_s> \simeq 0$. These results can be accounted for, in terms of the proposed model, by considering that $\Delta u/u$ is actually predicted to be proportional to $<\lambda_s^2>$, i.e. to local fluctuations of the magnetostriction constant, rather than to $<\lambda_s>^2$. The frequency spectrum of $\Delta u/u$ between 10^{-1} s^{-1} and $2\cdot10^{3}$ s^{-1} was measured on various Co-rich amorphous ribbons as a function of the temperature up to the Curie point, to get information about the distribution of time constants characterizing the aftereffect at each temperature. In some of the studied alloys, a high temperature bending of the spectrum, indicating the presence of a low-frequency cutoff, has been observed. The original shape of the spectrum is totally recovered at lower temperatures. This behavior seems to indicate the presence of an upper bound to the distribution of the activation energies of the processes responsible for the magnetic aftereffect. An evaluation of this maximum activation energy in different materials is given.

[1] P.Allia and F.Vinai, Phys.Rev. B26, 6141 (1982).

PD2 ELECTRON-PHONON COUPLING AND THE TEMPERATURE COEFFICIENT OF RESISTIVITY IN Ni-Zr GLASSES. Z.Altounian, R. Harris and J.O. Strom-Olsen, McGill University, Physics Department, 3600 University Street, Montreal, Quebec, Canada, H3A 2T8

A simple relationship has been claimed (1) between the electron-phonon coupling constant, λ_{ep} and the temperature coefficient of resistivity, $\partial\rho/\partial T$. We present results on a wide range of melt-spin Ni-Zr glasses to show that this relationship is not generally valid, even when due allowance is made for the influence of spin-fluctuations. Specifically, λ_{ep} is almost constant while $\frac{\partial\rho}{\partial T}$ varies from negative at the Zr-rich end to positive at the Ni-rich end. The behavior can however be explained within the framework of the Faber-Ziman formulism, using λ_{ep} provided account is taken correctly for the partial structure factions.

(1). O. Rapp, J. Jackle and K. Frobose, J. Phys. F11, 2359, (1981).

PD3 MAGNETIC AND NMR STUDIES OF AMORPHOUS AND CRYSTALLINE Ni-B ALLOYS. I. Rakonyi[a] and P. Panissod, LMSES, Universite Louis Pasteur, 67070 Strasbourg Cedex, France; J. Durand, Universite de Nancy I, B. P. no. 239, 54506 Vandeouvre-les-Nancy Cedex, France and R. Hasegawa, Materials Laboratory, Allied Corporation, Morristown, NJ 07960 USA.

Low field (< 7 kOe) magnetization and ^{11}B NMR Knight shift were measured below room temperature for amorphous $Ni_{1-x}B_x$ (x=25, 31 33, 35 and 40) alloys and for Ni_3B, Ni_2B and Ni_4B_3 crystalline compounds to study the effect of non-crystallinity on the bulk and local magnetic and electronic properties. Separating out a small ferromagnetic term and a contribution due to giant-moment paramagnetic clusters, one finds a temperature-independent susceptibility for both types of alloys. When corrected for core diamagnetism, the observed susceptibility χ can be attributed to conduction electron Pauli paramagnetism. The value of χ decreases approximately linearly with increasing boron content following the formula $\chi = (100.5-1.87x) \cdot 10^{-6}$ emu/mol and, within experimental uncertainty, agrees with that for the crystalline alloy with the same composition. This indicates that the average electronic properties evaluated at the Fermi surface are not influenced by the lack of long-range order in the amorphous system. The ^{11}B NMR Knight shift also has similar values for the amorphous and corresponding crystalline alloys and it decreases with boron content. The decrease is small up to x=33 at which the Knight shift starts to drop faster. Since the Knight shift reflects the local chemical short-range order (CSRO), one may thus conclude that the CSRO around B atoms is not appreciably modified in the amorphous Ni-B alloys with respect to the corresponding crystalline counterparts.

a) Present and permanent address: Central Research Institute for Physics, H-1525, Budapest, P. O. B. 49, Hungary

PD4 ELECTRONIC CONDUCTION IN s-d BAND LIQUID METALS. L.E. Ballentine, S.K. Bose, J.E. Hammerberg, Simon Fraser University, Burnaby, B.C. V5A 1S6 CANADA

Computer simulation models are used to study the electronic states and conductivity of liquid transition metals, in which s and d bands are hybridized. Using generalizations of the recursion method of Haydock, Heine, and Kelly, we compute densities of states, spectral functions, and conductivities for LCAO models of a few hundred atoms. The peaks in the spectral functions indicate whether residual s or d bands exist in the liquid state. The relative magnitudes of s and d state diffusivities are also computed. In most cases the s state diffusivity exceeds that of d states, but the d states dominate the conductivity because of their much greater density.

PD5 MAGNETIC, ELECTRICAL AND THERMOELECTRIC STUDIES OF METALLIC GLASS $Fe_{39}Ni_{39}Mo_4Si_6B_{12}$, Anil K. Bhatnagar, B. Bhanu Prasad and N. Muniratnam, School of Physics, University of Hyderabad, Hyderabad - 500 134, India.

Mössbauer, electrical resistivity and thermoelectric power measurements on ferromagnetic amorphous alloy $Fe_{39}Ni_{39}Mo_4Si_6B_{12}$ (VITROVAC 4040) have been performed in the temperature range 77 - 900 K. Mössbauer measurements were done using the standard transmission geometry. The data were analyzed to obtain average values and the distribution of hyperfine magnetic fields and their temperature dependence, isomershift and its temperature dependence, spinwave coefficients $B_{3/2}$ and $C_{5/2}$, and quadrupole splitting. The hyperfine magnetic field H_{eff}(T) at room temperature is found to be approximately 217 kOe. Curie and crystallization temperatures of this alloy were found to be 575 $\pm$ 3 K and 725 $\pm$ 3 K, respectively, by thermal scan method. The resistivity was determined by four probe method. The resistivity curve showed a slight non-linear behavior below 100 K and near the crystallization temperature. The resistivity curve showed a sharp change in slope at 575 K, the Curie temperature, and a large drop at the crystallization temperature 725 K. Absolute thermoelectric power, S, was determined by the integral method and it is found to be negative throughout the temperature range 77 - 700 K. Its slope, dS/dT, has a negative slope for T < 325 K and a positive slope for T > 325 K with a rounded minimum at approximately 325 K. The value of S at this temperature is approximately - 3.0 μV/K. Data will be discussed in light of the effect of Mo on various properties of this alloy.

PD6 FIRST-PRINCIPLES CALCULATION OF ELECTRONIC STRUCTURES OF Cu_xZr_{1-x} GLASS.* W. Y. Ching and L. W. Song, University of Missouri, Kansas City, Mo. 64110, USA, and S. S. Jaswal, University of Nebraska, Lincoln, NE 68588, USA

The electronic structures of binary metallic glasses Cu_xZr_{1-x} have been studied for compositional value χ = 0.67, 0.50, 0.33 using a first-principles OLCAO method[1]. Quasi-periodic models containing 90 atoms were constructed and computer relaxed. The radial distribution function of these models are in good agreement with experiment. In addition to the density of states (DOS) and partial DOS curves, other microscopic information such as degree of localization of one-electron states, effective charges on each atom and the DOS at the Fermi level will be presented. These results will be correlated to the structural properties of the respective models and compared with available experimental data as well as other theoretical calculations.

*Supported by UMKC Research Council and DOE contract: DE-AC02-79ER10462

I. W. Y. Ching and C. C. Lin, Phys. Rev. B 12, 5536 (1975)

PD7 RELATION BETWEEN MAGNETISM AND SUPERCONDUCTIVITY IN AMORPHOUS $Zr_{1-x}Fe_x$ ALLOYS. G. Chouteau, O. Béthoux, CNRS, CRTBT and SNCI, B.P. 166 X, 38042 Grenoble Cedex, FRANCE

We have measured the high field magnetization and the susceptibility of several sputtered amorphous samples of $Zr_{1-x}Fe_x$ near the concentration at which the superconducting critical temperature T_c falls to zero : x ~ 24 %. The temperature range is 100 mK - 250 K and the field range is 0-15 T.

Two different as-prepared samples of the same nominal concentration can have different behaviors : one sample is superconducting (T_c = 2.6 K) while no superconductivity is detected in the second one down to 100 mK, by low field magnetization and resistivity measurements. For both samples the magnetization curves M(H) at 4.2 K can be expressed as $M(H) = M_O(H) + \chi_O.H$. The paramagnetic susceptibility χ_O is much higher than that of pure Zr, or ZrCu and ZrNi alloys of the same concentration. The excess susceptibility can be unambiguously attributed to spin fluctuations. The term $M_O(H)$ exhibits a strong curvature versus the field and saturates in a 1.5 T field. It originates in the magnetic, or very nearly magnetic part of the sample.

The susceptibility χ measured in a field of 1 T between 1.8 and 30 K follows approximately the law $\chi \sim C/T + \chi_O'$ where C/T is due to the localized spins and $\chi_O' \sim \chi_O$ is the paramagnetic contribution.

One remarquable feature is that the magnetic part $M_O(H)$ of the superconducting sample is hysteretic at 4.2 K. This indicates that in some cases a magnetic ordering can occur. Its nature (ferromagnetic, or anti-ferromagnetic) is not know at present. However the shape the $M_O(H)$ curve seems indicate a tendancy to the ferromagnetism.

Annealing and ageing tend to suppress the superconductivity.

These results can be interpreted in terms of coexistence of two amorphous phases. One is superconducting and the other in magnetic. Environmental effects and local concentration fluctuations are of great importance.

PD8 LINEWIDTH ASYMMETRIES IN THE MÖSSBAUER ZEEMAN SPECTRUM OF AMORPHOUS IRON-METALLOID ALLOYS
M. Eibschütz, M. E. Lines and H. S. Chen, Bell Laboratories, Murray Hill, New Jersey 07974 USA

The ^{57}Fe Mössbauer effect has been used to study the hyperfine Zeeman pattern below the Curie temperature in the amorphous metallic ferromagnet $Fe_{82}P_{18}$. Existing techniques for analyzing six-line ^{57}Fe Mössbauer spectra in iron metalloid ferromagnetic glasses concentrate on extracting the detailed shape p(H) of the hyperfine field distribution which dominates the form of the outside lines. Equations for the mean positions and root mean squares (RMS) widths of the complete six-line nuclear Zeeman pattern in an amorphous environment have been set out and used to interpret the linewidths of the Mössbauer spectrum. The spectrum exhibits a line width asymmetry which is caused by correlations between the various fluctuation variables involved. A careful analysis of the spectrum provides measures of the (RMS) fluctuations of they hyperfine field H, isomer shift δ, and quadrupole energy shift u at the iron sites, and also enables a determination of specific correlation functions. The major source of linewidths asymmetry is found to be a negative correlation between hyperfine field and isomer shift $\mu_N < \Delta H \Delta\delta > = -0.08$ (mm/s)^2 with a degree of linearity of 25%. A smaller, but still significant, additional contribution to linewidth asymmetry arises from correlations between hyperfine field, electric field gradient and their relative orientation $\mu_N < \Delta H \Delta u > = -0.02$ (mm/s)^2.

PD9 HALL-EFFECT AND THERMOPOWER OF METALLIC GLASSES. G. Fritsch, HSBw München, Neubiberg, Germany, E. Lüscher, J. Willer and A. Schulte, TU München, Garching, Germany.

At first, we report on the Hall-effect of the amorphous Alloys $Pd_{80}Si_{20}$, $Cu_{50}Ti_{50}$, $Pd_{30}Zr_{70}$ and $Ni_{24}Zr_{76}$. In addition data are given for some NiSiB-alloys. The Hall-coefficient is determined in the temperature range from 2 to 300 K. The method applied is the dc-contact method, yielding an accuracy of about 1%. The resistivity was measured simultaneously. The implications of the results on the electronic structure will be discussed.

Secondly, data on the thermopower of the alloys $Pd_{80}Si_{20}$, $Cu_{50}Ti_{50}$, $Pd_{30}Zr_{70}$ as well as $Cu_{40}Zr_{60}$ will be presented in the temperature range 80 K to 300 K. The temperature dependence of the thermopower will be analysed in terms of the well-known Ziman-formulation of the resistivity adopted to d-electrons and inserted into the Mott-expression. The results will be compared with the data obtained from the pressure dependence of the electronic resistivity. Some remarks will be added concerning the pressure dependence of the thermopower.

PD10 THE THERMOPOWERS OF AMORPHOUS TRANSITION METAL ALLOYS AND ELECTRON-PHONON ENHANCEMENT. B.L. Gallagher, A.B. Kaiser, and D. Greig, Department of Physics, University of Leeds, Leeds LS2 9JT, U.K.

We present experimental results for the thermopowers of a number of amorphous transition metal alloys in the temperature range 2 - 450 K. Analysis of the temperature dependence of the thermopower shows that it is enhanced by the electron-phonon interaction, and that the magnitude of the enhancement is close to that obtained from superconductivity data [1,2]. This provides strong support for the idea that thermopower should generally show such enhancement.

1. Gallagher, B.L. and Greig, D., (1982), J.Phys.F. 12, 1721
2. Kaiser, A.B., Phys.Rev.Lett., J.Phys.F. 12 L223 (1982)

PD11 ELECTRICAL RESISTIVITY OF BISMUTH, GERMANIUM AND BISMUTH-GERMANIUM ALLOYS IN THE LIQUID STATE.

J.G. Gasser, M. Mayoufi, G. Ginter and R. Kleim, Laboratoire de Physique des Milieux Condensés, Faculté des Sciences, Ile du Saulcy, 57045 Metz Cedex, France

The electrical resistivity of 11 bismuth-germanium alloys has been measured from the melting point to 1150°C. The temperature dependence of the pure components are discussed in the frame work of Ziman formalism with experimental interference functions and different model pseudopotentials (Heine-Abarenkov, Animalu-Heine, Shaw, Shaw-Hallers) and with the "extended Ziman formula" by using the t matrix expressed in term of phase shifts.

The composition dependence is interpreted with the same model pseudopotentials and phase shifts. But no experimental partial structure factors being available, we used Ashcroft and Langreth (1967) hard sphere partial structure factors. The experimental values are well reproduced for the alloy with the form factors giving good results for the pure metals.

PD12 FORMING ABILITY AND STABILITY OF AMORPHOUS ALLOYS $M_x Sn_{1-x}$ (M = Cr, Mn, Fe, Co, Ni, Cu) J. F. Geny, D. Malterre, M. Vergnat, M. Piecuch and G. Marchal, Laboratoire de Physique du Solide, Université de Nancy - I, B. P. 239, 54506 Vandoeuvre-les-Nancy-Cedex (France)

Amorphous films of $M_x Sn_{1-x}$ (M = Cr, Mn, Fe, Co, Ni, Cu) have been prepared by coevaporation on cooled substrates (77 K) of tin and transition metal.

Compositional ranges of forming ability, stability (as measured by crystallization temperatures) and electrical transport properties were studied.

These measurements are discussed in view of the corresponding equilibrium phase diagrams.

The crystallization and liquidus temperatures seem to be correlated.

Whenever the temperature coefficient of the resistivity is minimal, the alloys are obtained in the amorphous state.

Although Cr-Sn phase diagram is different (strong demixion tendency, non intermetallic compounds), the amorphous Cr-Sn alloys show similar properties compared to the others M-Sn amorphous systems.

PD13 TRANSPORT AND MAGNETIC PROPERTIES OF a- Ce_XAl_{100-X}

A. Guessous, K. Matho, J. Mazuer and J. Palleau
CRTBT-CNRS, BP 166 X, 38042 GRENOBLE, FRANCE

We report and discuss measurements of resistivity, thermoelectric power (TEP) and magnetic susceptibility on a- Ce_XAl_{100-X} alloys between 1.2 K and 350 K. The amorphous state could be obtained for $14 < X$ [at %] < 88, using a reactive sputtering technique.

Resistivities lie between 100 and 300 μΩcm, the highest ρ being observed for X = 57. The overall X-dependence roughly follows NORDHEIM's rule, $\rho(X) \propto X(100 - X)$. Variations ρ(T) are monotonical, with temperature coefficient (TCR) changing from positive for the lowest ρ to negative for the higher ones (TCR ≡ 0 for X = 88, $\rho \sim 135$ μΩcm), in agreement with MOOIJ's correlation. Considering the relative positions of the FERMI momentum, $k_F(X)$, and the first maximum in the total structure factor, k_p, the extended ZIMAN theory qualitatively explains the data. Strongly negative TCR's indicate the presence of KONDO scattering.

As compared to giant effects in c- $CeAl_2$ and c- $CeAl_3$, the TEP $|S(T)| < 6$ μVK^{-1} is reduced by an order of magnitude. The T-dependence is nevertheless far from linear for all X. A variety of peaks, shoulders and sign inversions are observed. Within the extended ZIMAN theory, this indicates a strongly energy dependent t-matrix, originating in the combined effect of resonant 4 f and random potential scattering.

Low T peaks in the TEP can be roughly correlated with the observation of ferromagnetic exchange enhancement in the susceptibility χ(T) below 10 K and with spin-glass freezing at temperatures $0.2 \text{ K} < Tg < 2$ K. Above 10 K, χ(T) (measured only for $x \sim 25$) obcys a CURIE like law, with evidence for a broad distribution of crystal fields acting on a $^2F_{5/2}$ state of Ce^{3+}. The effective moment, as compared to c- $CeAl_3$, is less T-dependent.

This body of data offers the possibility of comparing dense, incoherent KONDO systems with the KONDO lattices of equivalent composition.

PD14 EXPERIMENTAL EVIDENCE FOR A STRUCTURE-INDUCED MINIMUM OF THE DENSITY OF STATES AT THE FERMI ENERGY IN AMORPHOUS ALLOYS.

P. Häußler and F. Baumann, Pnysikalisches Institut der Universität Karlsruhe (TH), D-7500 Karlsruhe, FRD. and J. Krieg, G. Indlekofer, P. Oelhafen and H.-J. Güntherodt, Institut für Physik der Universität CH-4056 Basel, Switzerland.

First photoemission spectra are reported for the valence bands and core levels of quench condensed Au_xSn_{100-x} ($0 \leq x \leq 100$) films in the amorphous and the crystalline state. It is found that 1.) the valence band spectra ($20 \leq x \leq 80$) measured just after condensation exhibit a decrease in intensity towards the Fermi energy E_F which can be understood in terms of a minimum in the density of states near E_F and 2.) the valence band spectra and the core states of the amorphous and the corresponding crystalline state show distinct differences.

PD15 ATOMIC AND ELECTRONIC STRUCTURES OF THE Ca-Al METALLIC GLASS SYSTEM: AN NMR STUDY.* W.A. Hines, A. Paoluzi and J.I. Budnick, University of Connecticut, Storrs, CT 06268 USA, W.G. Clark, University of California, Los Angeles, CA 90024 USA, and C.L. Tsai, Northeastern University, Boston, MA 02115 USA

In order to investigate the atomic and electronic structures, we have carried out both steady state and pulsed NMR experiments on the melt spun metallic glass system $Ca_{100-x}Al_x$ ($15 \leq x \leq 45$ at. %). Measurements of the ^{27}Al NMR Knight shift, K, spin-lattice relaxation time, T_1, and lineshape have been obtained at 4.2 °K and room temperature, and for resonance frequencies ranging from 8 to 20 MHz. The experimental results indicate that the Knight shift ($K = +0.038\% \pm 0.010\%$ at room temperature), spin-lattice relaxation time ($T_1 = 2.0 \pm 0.2$ sec at 4.2 °K), and linewidth of the central transition remain constant throughout the entire glassy regime. Furthermore, the small value for K, and consequently the long spin-lattice relaxation time, indicates that the local density of s-electron states at the Al sites is small. This result is consistent with recent ultraviolet photoemission spectroscopy experiments and band structure calculations.[1] In addition, spin-echo NMR measurements indicate that the entire ^{27}Al spectrum is quite broad ($\approx$ 2 MHz) due to the quadrupole interaction, and also, essentially the same for all compositions. All of the NMR results indicate that certain features of the local environment remain unchanged throughout the entire glassy regime. The symmetry properties of the electric field gradient are compared with those for the related crystalline compounds which include Ca_3Al and $CaAl_2$.

*Supported in part by grants from AFOSR (80-0030), NSF (DMR 81-03085) and NSF (DMR 77-23777).

1 S.R. Nagel, et al., Phys. Rev. Letters 49, 575 (1982).

PD16 THE HALL COEFFICIENTS OF Cu_xTi_{100-x} AMORPHOUS METALLIC ALLOYS. M.A. Howson, D. Greig and B.L. Gallagher, Department of Physics, The University of Leeds, Leeds LS2 9JT, U.K.

Results are presented for the Hall coefficients of a series of Cu_xTi_{100-x} amorphous metallic alloys of varying composition. While the Hall coefficient is found to be positive and temperature independent for $x < 73\%$ it changes sign to negative at $x = 73\%$. It is argued that the positive Hall coefficients can be understood as a consequence of negative group velocities at the Fermi surface due to s-d hybridisation. This leads to a qualitative description of the compositional dependence of R_H in these alloys.

PD17 ELECTRICAL RESISTIVITY, MAGNETIC SUSCEPTIBILITY AND THERMOELECTRIC POWER OF AMORPHOUS NIOBIUM-NICKEL ALLOYS SYNTHETIZED BY VAPOUR QUENCHING GH. ILONCA, Faculty of Physics, Babeş-Bolyai University, 3400 Cluj-Napoca, Romania

Thin film samples (10-20μ thick) of niobium-nickel alloys in the composition range Nb-5 to 95% Ni were vapour quenched by R.F. sputtering onto fused quartz substrates held at a temperature of 450 K. It was found that fully glassy alloys were synthetized in the composition range Nb-30 to 85 at % Ni, 2.5 times larger than reported for splat-quenched alloys. At room temperature, the electrical resistivity ρ of these alloys lies between 176-210$\mu\Omega$cm, and the absolute thermoelectric power S between 2.20-2.52μV/K. On increasing the temperature from 4.2 to 775 K, up to which the amorphous alloys are stable, the resistivity of the alloy with x=0.50 decreases by about 1.5 %; the value of $d\rho/dT$ progressively increases with increasing Ni content, becoming positive at $0.50 < x < 0.75$.

Magnetic susceptibility was performed in the temperature range 77-1100 K on the crystalline alloys in the composition range 0-12.25 Nb at % and it obeying the Curie-Weiss law. Magnetic susceptibility for $Ni_{0.5}Nb_{0.5}$ and $Ni_{0.4}Nb_{0.6}$ amorphous alloys show a Pauli magnetic behaviour with the χ about 1.5×10^{-4} g^{-1} and 1.8×10^{-4} g^{-1} respectively.

The electrical and magnetic behaviour of these alloys may be treated in terms of electron scattering in disordered structures assuming the nearly free-electron model, in a manner analogous to Ziman's theory of electron transport in liquid metals.

PD18 A REPLY TO FABER'S QUESTION ABOUT THE MINIMUM IN THE THERMOELECTRIC POWER OF LIQUID MERCURY ALLOYS. T. Itami, N. Takahashi and M. Shimoji. Department of Chemistry, Faculty of Science, Hokkaido University, Sapporo 060, JAPAN

As is well known, mercury alloys containing alkali elements and trivalent B sub-group elements show a minimum at a few at% solute concentration in the isothermal curve of the thermoelectric power Q plotted against the composition C. This phenomenon ("the minimum in Q") has been a curious unresolved problem. For example, in his book(An introduction to the Theory of Liquid Metals, Cambridge 1972), Faber presented the question why the addition of small quantities of In increases $|Q|$ while adding small quantities of Sn decrease it though their effect on the resistivity ρ is the same.

Recently authors revealed the close relationship between the origin of the minimum in Q and the higher order atom-atom correlation function effects; that is the physical quantities containing the temperature derivative of the radial distribution functions or the partial structure factors show anomaly at the concentration where the minimum in Q occurs.

Here the experimental results of ρ of liquid Hg-In and Hg-Sn alloys are reported. The ρ of both systems decreases smoothly with the addition of In or Sn, as pointed out by Faber. But the temperature dependence of ρ, $\partial\rho/\partial T$, of liquid Hg-In alloys shows hump at 5 at% In where the minimum in Q occurs; on the other hand the $\partial\rho/\partial T$ of liquid Hg-Sn alloys (with no minimum in Q) shows no such behaviour. Thus the reply to Faber's question is as follows; there exists a difference of ρ between liquid Hg-In and Hg-Sn alloys in its temperature dependence, arising from the higher order correlation function effects. The origin of the minimum in Q and the picture of the higher order correlation function effects are also discussed in some detail.

POSTER SESSION PE: METAL-NONMETAL TRANSITIONS

PE1 AN NMR COMPARISON OF SOME ALKALI-ANTIMONY ALLOYS AROUND THE METAL NON-METAL TRANSITION. R. Dupree and L. Bottyan, University of Warwick, Coventry, UK, and W. Freyland, Universität Marburg, D-3550 Marburg F.R. Germany.

A few alloys of elemental liquid metals exhibit nonmetallic properties around particular stoichiometric compositions. Alkali metal-antimony systems belong to this group near the X_3Sb composition. Theoretical models of these alloys suggest that they should be regarded as charge transfer compounds with a bond ionicity ranging from 0.60 for Cs_3Sb to 0.05 for Li_3Sb (Robertson (1983)). We have measured the NMR Knight shift and relaxation time of the alkali metal in Cs-Sb and Na-Sb in order to obtain some experimental information about the relative ionicity of these systems. For Cs-Sb the ^{133}Cs shift and relaxation rate drop rapidly as antimony is added to caesium whereas the ^{23}Na shift and relaxation rate change move slowly with addition of antimony. In Cs-Sb the large charge transfer gives rise to virtual bound states in the dilute alloy. For Na-Sb the situation is less clear although the shift drops more rapidly than in the truly ionic alloy Cs-Au where it follows free electron like behaviour until near the metal-nonmetal transition. For the composition Na_3Sb the shift and relaxation rate drop to non-metallic values as they do for Cs_3Sb. However in Cs_3Sb the relaxation rate is more sensitive to excess alkali than for Na_3Sb and the NMR behaviour is consistent with non-degenerate states localized within a mobility gap in contrast to CsAu where we found F centres.

PE2 **PROPERTIES OF HOT EXPANDED LIQUID ALUMINUM. G. Roger Gathers and Marvin Ross, Lawrence Livermore National Laboratory, Livermore, CA 94550 USA**

Measurements of temperature, volume, enthalpy and electrical resistivity have been made on aluminum expanded isobarically by 50% in volume to temperatures of about 4000 K. These measurements are compared with the predictions of liquid metal pseudopotential theory.

***Work performed under the auspices of the U.S. Department of Energy by Lawrence Livermore National Laboratory under contract #W-7405-Eng-48.**

PE3 THEORY OF STRONG SCATTERING IN LIQUID COMPOUND-FORMING ALLOYS, W. Geertsma and A.B. van Oosten, Solid State Physics Laboratory, Materials Science Center, University of Groningen, 1 Melkweg, 9718 EP Groningen, The Netherlands.

Liquid alloys of alkali metals with post-transition metals exhibit peculiar behaviour in their physical properties around one or more compositions. This behaviour is interpreted as being due to either charge transfer or charge transfer accompanied by strong covalent bonding between the non-alkali metal ions. In this contribution we will focus attention on effects due to intermediate p-type scattering of electrons. Obviously, the simple Ziman-formalism for calculating the resistivity is no longer valid in these systems; accordingly, we have used the extended Ziman equation for the resistivity as given by Greenwood, Lloyd and Evans. We have calculated the resistivity over the whole concentration range of Li-In and Li-Pb. A problem is the consistent choice of k_F, E_F and the electron concentration.

To determine these quantities unambiguously we have set up a calculation starting with the Kubo-Greenwood equation. We approximated the kernel of the Bethe-Salpeter equation in second order in such a way as to be consistent with the approximation used for the electron self-energy. This set of equations determined the electronic density of states and the resistivity. Results of calculations for Li-Pb using this formalism will be presented.

PE4 SELF-CONSISTENT STUDY OF CHEMICAL SHORT-RANGE ORDER AND CHARGE TRANSFER IN LIQUID ALLOYS. Ch. Holzhey*, J. Franz**, F. Brouers*** and W. Schirmacher*

Based on a self-consistent theory of electronic and atomic structure of liquid alloys developed recently by the authors we study the relationship between chemical short-range order and charge transfer as a function of temperature in alloys that have strong deviations from metallic behaviour. The pair correlation functions are calculated in the mean spherical approximation from exponentially screened Coulomb potentials with effective charges subject to charge neutrality. Self-consistency is established by relating the effective charges to the electronic charge transfer and the screening parameter to the electronic density of states at the Fermi level $N(E_F)$. We find a decrease of charge transfer with increasing temperature which also leads to a higher value of $N(E_F)$ in agreement with experimental findings. This change from ionic to metallic character is also reflected in the atomic structure.

*Physik-Department, Technische Universität München, 8046 Garching, W.Germany
**Department of Physics, Indiana University, Bloomington, Indiana 47405, USA
***Fachbereich Physik, Freie Universität Berlin, 1000 Berlin 33, W.Germany

PE5 SEMICONDUCTOR-METAL TRANSITION IN LIQUID SELENIUM-TELLURIUM MIXTURES AT HIGH TEMPERATURES AND PRESSURES, H.Hoshino, Hirosaki University, Hirosaki, 036, Japan, and K.Tamura and H.Endo, Kyoto University, Kyoto, 606, Japan.

It is observed for liquid Se[1] that the isochore curves on the P-T plane tend to bend by raising the temperature and the pressure. In the vicinity of the inflection in the isochore curves a transition from semiconductor to metal occurs. The measurement of the density for the liquid Se-Te mixtures was made up to 1300°C and 300 bar by using the Archimedean method with alumina balls as sinker. The isochore curves for various mixtures determined on the P-T plane show similar temperature variations to those for liquid Se at higher pressures. This suggests that there is a qualitative equivalence of the effects of increased Te content and increased pressure. Near the semiconductor-metal transition region the fluctuations of the dihedral angle are large and various types of connectivities of covalent bonds (chain-like, ring-like and zigzag connectivities) appear, which causes dangling bonds and various conformational defects. The number of the dangling bond state C_1^o increases by bond breaking and unstable zigzag chains create a weakly localised three-fold state C_3^o in the process $C_1^o + C_2^o \rightarrow C_3^o$. As a consequence of the collapse of chain structure, there appears a kind of lamellar structure similar to the crystalline As.

The speculation mentioned above will be discussed in connection with the results of the electrical conductivity, sound velocity and optical reflectance at high temperatures and pressures.

1) R.Fischer, R.W.Schmutzler and F.Hensel, J.Non-cryst.Solids, 35-36, 1295 (1980).

PE6 NONMETAL-METAL TRANSITION IN LIQUID Bi-$BiBr_3$ MIXTURES UNDER PRESSURE, S.Hosokawa and H.Endo, Kyoto University, Kyoto, 606, Japan, and H.Hoshino, Hirosaki University, Hirosaki, 036, Japan.

The measurements of the electrical conductivity σ and the sound velocity v_s were made up to 600°C and 20 kbar by using the piston-cylinder apparatus.

The values of σ increase with increasing Bi concentration, showing the nonmetal-metal transition. Taking x the mole fraction of Bi in the mixture, the concentration derivative of σ at constant pressure, $(\partial \ln\sigma/\partial x)_P$ increases sharply by adding Bi to liquid $BiBr_3$, reaches a maximum and then decreases rapidly by further increase of x. This means a transition from nonmetal to metal. The concentration at which the maximum appears shifts to lower x with increasing pressure. It is also found that the pressure derivative of σ at constant temperature, $(\partial \ln\sigma/\partial P)_T$ shows similar concentration variations to those of $(\partial \ln\sigma/\partial x)_P$.

The sound velocity v_s is nearly constant in the salt-rich region up to about x=0.3 and then increases gradually with increasing x. The excess molar volume of mixing estimated by the results of v_s is negative and becomes zero with increasing pressure.

When Bi is added to liquid $BiBr_3$, it may occupy the empty holes in $BiBr_3$ structure and cause a destruction of strong correlation between bismuth and bromide ions. Such a structural change due to destruction of the strong correlation may be accelerated by application of pressure.

PE7 THE SPECIFIC HEAT OF MERCURY AT SUB- AND SUPERCRITICAL TEMPERATURES AND PRESSURES.

M. Levin and R.W. Schmutzler, Physikalische Chemie Ia, Universität Dortmund, Postf. 500 500, 46 Dortmund 50, FRG

The paper reports on measurements of the molar heat capacity at constant pressure, Cp, of mercury up to 1800 K and 2400 bar, i.e. up to supercritical temperatures and pressures. For this purpose a mercury sample of known geometry, maintained at the required temperatures and pressures in an internally heated autoclave, is slightly heated by a short, calibrated current pulse (duration ~ 30 µsec, repetition rate 50 sec^{-1}) by about 0.1 to 5 K. This temperature increase is determined by the change of the electrical resistance of the sample. Knowing the energy per pulse, the increase of temperature due to the pulse and the mass of mercury within the sample volume taking pVT-data from the literature (1), the molar heat capacity Cp can be evaluated.

The results show nearly no pressure dependence and only a slight temperature dependence for T < 1400 K. So Cp changes from 27.6 J/mol K to 33.5 J/mol K if the temperature is increased from 800 K to 1400 K irrespective of pressure for 1000 bar < p < 2400 bar. A further increase of T up to 1800 K at 2400 bar causes an increase of Cp by more than a factor of two to 80.4 J/mol K. In addition the pressure dependence of Cp becomes strong at these temperatures.

With the help of density data from literature (1) the molar heat capacity at constant volume, Cv is evaluated. The results are discussed in connection with the metal-nonmetal transition observed in liquid mercury at these temperatures and pressures.

(1) G. Schönherr, R.W. Schmutzler and F. Hensel, Philos. Mag. B 40, 411 (1979)

PE8 LOW ANGLE STRUCTURE FACTORS OF EXPANDED LIQUID RUBIDIUM. I.L. McLaughlin, La Trobe University, Bundoora, Victoria 3083, Australia, and W.H. Young, University of East Anglia, Norwich NR4 7TJ, U.K.

The low angle structure factors of expanded liquid rubidium are calculated by first finding interatomic potentials using pseudopotential theory and then applying the random phase and mean density approximations of liquid structure theory. Good agreement with experiment is obtained in the mean density approximation for $k \leq 0.5$ $Å^{-1}$; at higher k a hard sphere description is appropriate.

PE9 ELECTRICAL CONDUCTIVITY OF LIQUID Cs-CsI MIXTURES.
S.Sotier,H.Ehm,F.Maidl,Fachhochschule München and Physik Department E 13 T.U. München,W.Germany.

The electrical conductivity of liquid $Cs_x(CsI)_{1-x}$ has been measured over the whole range of concentrations from pure Cs to pure CsI.In the metallic range and down to conductivities of about $\sigma = 500\Omega^{-1}cm^{-1}$ we used thin walled metallic containers as sample cells.Several potential electrodes made it possible to study the homogeneity of the mixtures.The measurements of low conductivities were performed in Al_2O_3-ceramic cells with Nb electrodes using a AC-bridge with frequencies up to 10 KHz.

The concentration dependence of the electrical conductivity of $Cs_x(CsI)_{1-x}$ is similar to the one found in $Cs_x(CsCl)_{1-x}$ but differs considerably from σ in $Cs_x(CsAu)_{1-x}$.The Metal-Nonmetal Transition can be further discussed using NMR-shift and relaxation data in the same systems.

PE10 NEW RESULTS IN LIQUID ALKALI-GROUP IV-A ALLOYS,
W. van der Lugt, C. van der Marel, W. Geertsma, J.A. Meijer, A.B. van Oosten, J. Dijkstra, P.C. Stein and B.P. Alblas, Solid State Physics Laboratory, Materials Science Center, University of Groningen, 1 Melkweg, 9718 EP Groningen, The Netherlands.

Measurements of the neutron diffraction pattern, the resistivity and the Knight shift have been performed on a number of alkali-group IV-A alloys. The behaviour of the Li-Sn system is rather similar to that of the Li-Pb system, although the effects of compound formation are significantly stronger in Li-Sn. They culminate at the composition Li_4Sn. In Na-Sn, Li-Ge and Rb-Pb a second distinct composition of compound formation has been found, corresponding to 43% alkali metal. Neutron diffraction measurements and comparison with the solid state structure provide strong evidence for the existence, at this composition, of negatively charged tin-tetrahedra, internally covalently bonded, forming an ionic mixture with the alkali ions.

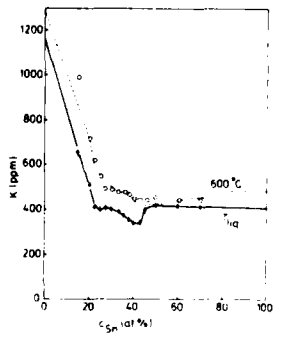

The ^{23}Na Knight shift in liquid Na-Sn.
full curve : experiment, liquidus
dashed curve : experiment, 600 °C
ooooooo : calculated

PE11 THERMODYNAMIC PROPERTIES OF LIQUID Na-IVb ALLOYS.
S. Tamaki, S. Matsunaga, T. Ishiguro and S. Takeda, Niigata University, Niigata, 950-21, JAPAN

The previous descriptions(Tamaki et al, 1982 and Matsunaga et al, 1983) of the thermodynamic properties of liquid Na-IVb alloys are referred to and extended, in order to explore the mechanism of compound formation in them.

The presence of compound or chemical complex in liquid alloys is usually confirmed by the electrical resistivity, the concentration-concentration fluctuation in the long wavelength limit, $S_{cc}(0)$, the Stillinger-Lovett condition and the additional specific heat, ΔC_p. In particular, the temperature dependence of ΔC_p is a direct measure of the dissociation of the compound.

All these quantities of liquid Na-IVb alloys are consistently combined and it is concluded that the compound formation in liquid Na-Sn alloys occurrs near the composition of Na_4Sn_3 and Na_3Sn, respectively, and that in liquid Na-Pb alloys is near the compositions of NaPb and Na_4Pb.

Tamaki S, Ishiguro T and Takeda S, 1982, J. Phys. F: Metal Phys., 12, 1613
Matsunaga S, Ishiguro T and Tamaki S, 1983, J. Phys. F: Metal Phys., 13, 587

POSTER SESSION PF: STRUCTURE II

PF1 STRUCTURAL RELAXATION OF Fe-B ALLOY BY X-RAY DIFFRACTION

M. Laridjani**, J.F. Sadoc* and R. Krishnan**
** C.N.R.S. I place A. Briand 92195 Meudon
* Laboratoire de Physique des Solides 91405 Orsay.

The structural relaxation of different $Fe_{1-x}B_x$ alloys (x = 16, 17, 18.5, 20, 21.5) prepared by melt-spining technique, have been studied by X-ray diffraction. The interference functions for the different compositions are obtained by two techniques : the classical θ-2θ diffraction using monochromatic radiation (AgKα) and the energy dispersive methods (variable λ).

The interference and high resolution radial distribution functions show a composition dependence. W(r) main peaks intensities depend on the B content, however the position of peaks remains unchanged. The second peak shoulder in I(K) is very sensitive to the B content. The I(K) and W(r) for $Fe_{84}B_{16}$ are explained using a model for pure metal (from curved space model). The interference and the radial distribution functions evolve with an increase of the temperature (20°C-340°C). If the isothermal annealing time at high temperature is short ($\sim$ hour) there is a quasi-reversible behaviour. This structural reversibility can explain the reversible changes in Curie temperature observed on alternate annealing at 250°C and 300°C. If the annealing time is long (300°C during 24 hours) the interference function obtained after returning at room temperature is modified relative to the initial function.

By modeling, we attemp to describe the effect of temperature on the structure.

PF2 VIBRATIONAL DYNAMICS OF LIQUID TELLURIUM. R.J. Magaña and J.S. Lannin, The Pennsylvania State University, University Park, PA 16802 USA.*

First order Raman scattering measurements are reported in liquid Te between the melting point and 600C. Both polarized, HH, and depolarized, VH, Raman spectral components have been studied using a pseudo-backscattering geometry. Three distinct vibrational bands are observed in the VH spectra which yield the form of the spectrally weighted phonon density of states. The phonon spectum thus differs significantly from that of amorphous or liquid Se in form. A comparison with the form of the phonon spectrum of amorphous Te also differs significantly from the observed spectra. In addition, the ℓ-Te VH spectra for the higher optic-like modes is shifted significantly to lower frequencies. This is interpreted as an increase in metallic interactions in ℓ-Te relative to greater covalency in crystalline and amorphous Te. The HH Raman scattering spectra further indicate one strongly polarized peak centered at ~112cm^{-1}. Both the polarization behavior of the ℓ-Te spectra as well as the form of the VH and HH components differs substantially from that of 2-fold coordinated, chain dominated ℓ-Se as well as from that of 3-fold coordinated amorphous As. The results will be discussed in terms of various structural models proposed for ℓ-Te, including 2-site models.

*Supported by NSF Grant DMR 8109033

PF3 STRUCTURE OF $Be_{43}Hf_xZr_{57-x}$ METALLIC GLASSES

M. Maret, Institut Laue-Langevin, 156X, 38042 Grenoble, France,
A. Soper, University of Guelph, Ontario NIG 2W1, Canada,
G. Etherington and C.N.J. Wagner, University of California, Los Angeles, CA 90024 USA.

The $Be_{43}Hf_xZr_{57-x}$ metallic glasses were prepared by the melt-spinning technique in Livermore Laboratory by L.E. Tanner. The structure of these glasses was investigated by X-ray diffraction for x = 5, 25, 54 at.% with the variable-2θ method using the Ag-K_α radiation, and by neutron diffraction for x = 25 at.%. Neutron diffraction measurements were carried out at the pulsed spallation source in Los Alamos using the high epithermal flux, and also on the D1B (with λ = 2.52 Å) and D2 (λ = 0.94 Å) instruments in ILL Grenoble.

The isomorphous substitution allowed us to determine accurately the partial structure factor I_{MT-MT} (MT = Hf or Zr) from the two interference functions $I^x(k)$ corresponding to x = 5 and 54 at.%, since the contribution of the I_{Be-Be} function is negligible in $I^x(k)$. The two other partial functions I_{Be-Be} and I_{Be-TM} were evaluated from the two total functions $I^x(k)$ and $I^n(k)$ measured for x = 25 at.%, and assuming I_{MT-MT} known. The r_{ij} nearest neighbour distances, obtained from the $g_{Zr-Zr}(r)$ and $g^n(r)$ pair correlation functions, are very close to those existing in the Be_2MT crystalline compound. From the z_{ij} partial coordination numbers, we calculated a negative value of the generalized Warren CSRO parameter $\alpha \simeq -0.2$, indicating a chemical ordering of the same magnitude order than that found in the Ni_{40}-Ti_{60} glass.

PF4 X-RAY DIFFRACTION STUDIES WITH LIQUID NI-B AND MN-Si ALLOYS. E. Nassif, P. Lamparter and S. Steeb, Max-Planck-Institut für Metallforschung, Seestraße 92, 7000 Stuttgart-1, Germany

The structure factors as well as the pair correlation functions of molten Ni-B and Mn-Si alloys have been determined by X-ray diffraction.
The structural results for molten $Ni_{81}B_{19}$ and $Mn_{74}Si_{26}$ are compared with the structure of the corresponding metallic glasses which can be obtained by rapid quenching of the melt. While the normalized atomic distances of the amorphous alloys can be well described by tetrahedral packing models, those obtained with the molten alloys show marked deviations from the models. On the other hand structural similarities between the glass forming molten alloys and the amorphous alloys have been observed. The shoulder on the second maximum of the structure factors, characteristic for metallic glasses, is still present in the molten state. This structural feature cannot be observed with molten $Ni_{53}B_{47}$ and $Mn_{33.5}Si_{66.5}$ which do not fall in the glass forming composition ranges of these systems. Significant changes of the structure of the molten alloys with increasing metalloid content are discussed.
The results for the liquid Ni-B alloys are compared with previous results for liquid Fe-B alloys.

PF5 **STRUCTURE AND CRYSTALLIZATION OF THE AMORPHOUS $Co_{76}Mo_{16}B_8$ ALLOY.**

Shen Ning-Fu*, I.P. Jones**, and J.N. Pratt**. *Department of Mechanical Engineering Zhenzhou Institute of Technology, Zhengzhou, Henan, China. **Department of Metallurgy and Materials, University of Birmingham, Birmingham, U.K.

The ribbon of the amorphous $Co_{76}Mo_{16}B_8$ alloy was obtained by melt spinning. X-ray diffraction, electron diffraction and computer simulating were carried out to establish the structure model in the amorphous alloy. In-situ heating experiments at a 1000 kv high voltage transmission electron microscope, X-ray microanalysis at EM400 (STEM) and DSC analysis were used to investigate the crystallization sequence and mechanism is this amorphous alloy.

The main results are following:

1. Phase separation exits in the as-quenched amorphous $CO_{76}Mo_{16}B_8$ Alloy.

2. The Co-riched amorphous phase has the glass transition temperature of 520 °K, the second amorphous phase has the glass transition temperature of 900 °K.

3. The crystallization sequence consists of: AmorphousI+AmorphousII⟶Co(h.c.p. metastable)+amorphous ⟶Co(f.c.c.)+Co_3Mo(metastable)h.c.p.+AmorphousII' ⟶Co(f.c.c.)+Co_3Mo+CoMoB(orthorhombic).

4. The precipitation of Co (h.c.p.) is controlled by long distance diffusion of solute atoms. The combined growth of Co_3Mo and CoMoB is controlled by the interfacial diffusion.

PF6 **EXAFS STUDY OF ELECTRODEPOSITED Ni-P BINARY ALLOYS**

Tokuhiko Okamoto and Yoshiaki Fukushima
Toyota Central Research and Development Labs., Inc.
Nagakute-cho, Aichi, Japan

EXAFS measurement was made for the region above the nickel K-absorption edge of Ni-P binary amorphous alloys, prepared by electrodeposition and rapid quenched techniques. Experimental data were Fourier transformed to $|\phi_3(r)|$.

Figure 1 illustrates typical $|\phi_3(r)|$ patterns of the alloys, with different phosphorous contents. Comparison of the spectra in Figure 1 reveals that the peak positions of electrodeposited alloys and fcc nickel are similar to each other, while their EXAFS patterns are quite different from that of rapid quenched Ni-P amorphous alloys. Increased phosphorous content in electrodeposited Ni-P alloys was found to shift the 1st peak to the lower side and increase the intensity of the 2nd peak.

These results suggest that the atomic arrangements in the alloys are varied by method of preparation and the contents of additives.

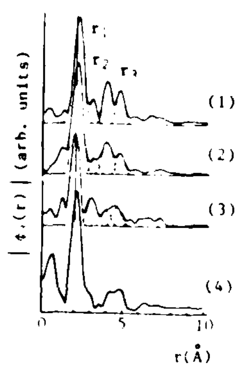

Figure 1 $|\phi_3(r)|$ patterns. (1): fcc Ni, (2): electrodeposited Ni-(8.5 at.%)P alloy, (3): electrodeposited Ni-(23.9 at.%)P alloy and (4): rapid quenched Ni-(18.3 at.%)P alloy.

PF7 **CRYSTAL-FIELD EFFECTS IN AMORPHOUS ALLOYS CONTAINING PRASEODYMIUM.**

[illegible], [illegible], [illegible]*, [illegible].Bertrand and A. R. Fert, Université Paul Sabatier, [illegible] Toulouse (France), and *Université de Nancy - I, [illegible] Vandoeuvre-les-Nancy (France).

In order to obtain some information about the nature and the fluctuations of the local symmetry around rare-earth ions in amorphous alloys, we studied the "crystal-field" effects on Pr substituted for La in amorphous and crystalline La_3Al and La_3Ga compounds. Crystalline La_3Al and La_3Ga compounds were obtained in hexagonal and cubic phases, respectively. Corresponding amorphous alloys were produced by liquid quenching. Pr, being a non-Kramers ion with relatively low J value, is known to provide a sensitive probe to crystal-field effects. The Pr content (about [illegible] at. %) was determined as high enough to avoid superconducting phenomena and low enough to neglect the exchange interactions. "Crystal-field" effects were experimentally evidenced by means of low-temperature magnetization and magnetoresistivity measurements along with the temperature dependence of the initial susceptibility. From analysis of the data, the following conclusions can be drawn. First, the crystal-field effects are not the same in amorphous alloys with Al and in those with Ga, which implies that the average local symmetry about Pr ions is different in nature in these two amorphous systems. Second, the average symmetry in these amorphous alloys is somewhat reminiscent of that prevailing in the crystalline (cubic, hexagonal) counterparts. Third, the distribution of the local symmetry around Pr is broader in amorphous La_3Ga than in La_3Al alloys. This is in good agreement with conclusions obtained from analysis of NMR quadrupolar spectra on the glass-former nuclei (Ga and Al) in the same alloys.

PF8 *STRUCTURAL AND ELECTROCHEMICAL EFFECTS INDUCED IN METALLIC GLASSES BY MECHANICAL DEFORMATION*

M.Popescu and O.Mihăilă, Institute of Physics and Technology of Materials, Bucharest, P.O.Box MG-7, ROMANIA

Methods were devised for studying the effects of the deformation forces in metallic glasses. X-ray diffraction was performed on in-situ deformed samples. Electrochemical measurements were performed in a special cell where one of the metallic glass electrodes is subjected to uniaxial mechanical stress.

The mechanical forces applied to metal-metalloid glassy ribbons, beyond the elasticity limit, induce specific modifications in the atomic short-range order. The main structural transformation consists in the partial destruction of the short-range compositional order of the material. In amorphous $Fe_{80}B_{20}$ the uniaxial stress leads to a compositional splitting. In the deformed sample there was evidenced a b.c.c. α-Fe short-range order accompanied by a short-range order characteristic to tetragonal Fe_3B.

The electrochemical potential measured between two electrodes made from metallic glass ribbons (one free ribbon and other ribbon subjected to uniaxial extension) is strongly dependent on the deformation of the material. The stressed and deformed electrode becomes negative as compared to the unstressed one. The electrochemical potential shows a non-linear dependence on mechanical deformation as opposite to the linear behaviour in the case of a micro-crystalline iron wire.

The observed effects can be correlated with aging in the metallic glasses and allow to explain the decrease of corrosion resistance of the glassy metals when subjected to deformation forces.

PF9 MÖSSBAUER AND X-RAY STUDIES OF AMORPHOUS $Fe_{67}Co_{18}B_{14}Si_{1}$

B. Bhanu Prasad, A.K. Bhatnagar, D. Ganesan and R. Jagannathan, University of Hyderabad, Hyderabad-500134, India and T.R. Anantharaman, Banaras Hindu University, Varanasi-221005, India.

Amorphous alloy $Fe_{67}Co_{18}B_{14}Si_{1}$ (METGLAS 2605CO) has been investigated by Mössbauer spectroscopy in the temperature range ? - 900 K. The spectra have been analyzed to obtain the temperature dependence of average hyperfine magnetic field, $H_{eff}(T)$, the probability distribution of internal magnetic field and other hyperfine parameters. The crystallization of the amorphous alloy takes place at approximately 650 K, before the sample becomes paramagnetic. The Curie temperature was estimated to be 830 ± ? K by extrapolation of $H_{eff}(T)$ vs T data to $H_{eff}(T) = 0$. The inclusion of Co in iron metal-metalloid system always seems to increase the Curie temperature. As observed for other metallic glasses the data, $H_{eff}(T)/H_{eff}(0)$ vs T/T_c, lies below the Brillouin curve for S = 1/2 or 1. Data can be fitted to the empirically modified Handrich's model by Prasad et al /1/. The temperature dependence of $H_{eff}(T) = H_{eff}(0)\left[1-B_{3/2}(T/T_c)^{3/2}-C_{5/2}(T/T_c)^{5/2}-..\right]$ over a large temperature interval. Detailed crystallization studies by Mössbauer spectroscopy and X-ray diffraction will also be reported.

1. B. Bhanu Prasad, Anil K. Bhatnagar and R. Jagannathan, Solid State Commun. 36, 661 (1980).

PF10 STRUCTURAL HOMOGENEITY AND CRYSTALLIZATION OF AMORPHOUS $Fe_{81}B_{13.5}Si_{3.5}C_{2}$.

Angela Leimkuhler Frasasco, Robert B. Pond, Sr., and Robert E. Green, Jr., The Johns Hopkins University, Department of Materials Science and Engineering, Maryland Hall Room 102, Baltimore, MD 21218

Structural homogeneity and crystallization of 50 mm wide Metglas 2605SC ribbon ($Fe_{81}B_{13.5}Si_{3.5}C_{2}$) were investigated using angular dispersive diffractometry, energy dispersive diffractometry, and scanning electron microscopy. Inspection of numerous areas of a 1.2 meter length of the Metglas to determine the degree of crystallinity indicated a lack of homogeneity. Transition temperatures were determined by annealing an array of specimens for 3 to 7 hours at temperatures ranging from 400°C to 480°C as well as by heating from 24°C to 400°C during which time diffraction data were recorded. Transformation to a semi-crystalline state was [illegible] at temperatures well below the accepted transition temperature for this alloy. Crystallization temperatures and products witnessed were compared [illegible] previously reported.

PF11 XPS and Mössbauer Study on Amorphous FeBSi Alloys

M.Taniwaki, K.Makiuchi, M.Sugiyama and M.Maeda, Dept. of Electronic Engineering, Faculty of Engineering, Hokkaido University, Sapporo 060, Japan

The electronic structure of amorphous FeBSi alloys was studied by Xray Photoelectron Spectroscopy (MgKα) and Mössbauer Spectroscopy (^{57}Fe). $Fe_{80}B_{20}$-xSix and $Fe_{75}B_{25}$-xSix specimens were prepared by single-roll-technique in argon atmosphere. The isomer shifts and the internal magnetic fields of specimens were analyzed by MS and the binding energies of core electrons of Fe, B and Si and their peak intensities were analyzed by XPS.

The dependence of the internal magnetic field on Si concentration was almost same as the report by Gonser et al (ref). The internal magnetic field of $Fe_{80}B_{20}$-xSix increased slightly with the increase of Si, while it of $Fe_{75}B_{25}$-xSix decreased abruptly with the increase of Si. Two kinds of B2P peak were observed in XPS spectra. Their binding energies were 188.5eV (B(I)) and 203eV(B(II)). And at higher binding energy(210eV) another weak peak was recognized. The high binding energy indicates that electrons are taken off from the atom. In the case of $Fe_{80}B_{20}$-xSix, B(I) decreased with the increasing Si and the decrease of B(II) was slight. That is to say, in the alloys, increasing Si atoms replaced B(I) having little effect on the electronic structure of Fe. So the internal magnetic field of $Fe_{80}B_{20}$-xSix didn't change remarkably. While in $Fe_{75}B_{25}$-xSix the decrease of B(II) was remarkable with increasing Si comparing the decrease of B(I) indicating that Si atoms replaced Boron atoms which had considerable effect on the change of Fe electronic structure. Si with four valence electrons may transfer more electrons to d shell of Fe than B with three valence electrons. As the result the internal magnetic field might have decreased abruptly.

REFERENCE

Gonser, M.Ghafari, M.Ackermann, H.P.Klein, J.Bauer and H.-G. Wagner, Proc. 4th Int. Conf. on Rapidly Quenched Metals, vol.1 (1981) 639

PF12 THE ACCURACY OF EXPERIMENTAL RADIAL DISTRIBUTION FUNCTIONS.

B.J. Thijsse, Laboratory of Metallurgy, Delft University of Technology, Rotterdamseweg 137, 2628 AL Delft, The Netherlands, and J. Sietsma, Netherlands Energy Research Foundation (ECN), Petten, The Netherlands

Both statistical and systematic errors have a considerable impact on the results derived from diffraction experiments. On-line minicomputers permit the use of an optimum strategy.

Statistical arguments show that by sampling an X-ray diffraction pattern at points that are equidistant in $Q = 4\pi\lambda^{-1}\sin\theta$, and using a variable counting time per point of the form [illegible] is the intensity and [illegible] a certain analytical function [illegible], one obtains a reduced radial distribution function [illegible] with the very attractive property that its standard error is predictable and constant over r.

A necessary additional requirement is that systematic errors are held at a minimum level. This [illegible] conveniently checked by comparing diffraction data measured in reflection geometry with those obtained in transmission [illegible] experiments are necessary.

[illegible]

PF13 MÖSSBAUER INVESTIGATIONS OF AMORPHOUS METAL-METAL ALLOYS. H.-G. Wagner, M. Ghafari, H.-P. Klein, U. Gonser, Angewandte Physik, Universität des Saarlandes, D-6600 Saarbrücken, Federal Republic of Germany

Mössbauer measurements of amorphous ZrFe and NiZr(Fe) alloys are presented. It is found that the spectra of both materials are very similar. Fitting a distribution of quadrupole splittings to the experimental data one observes that the distributions are also almost identical for both alloys. This suggests that the Fe environment is the same in both cases. A comparison with spectra of crystalline phases allows a tentative identification of the local units around Fe.

PF14 THE EFFECT OF QUENCHING TEMPERATURE ON THE STRUCTURE AND CRYSTALLIZATION OF GLASSY $NiZr_2$. J.L. Walter, General Electric Research and Development Center, Schenectady, N.Y. and Z. Altounian and J.O. Strom-Olsen, McGill University, Department of Physics, 3600 University Street, Montreal, Quebec, Canada H3A 2T8

Melt-spun $NiZr_2$ glasses quenched from different temperatures show markedly different crystallization characteristics. Glasses quenched from higher temperatures exhibit a double DSC crystallization peak, those from the lowest temperatures a single peak, though the crystallization products in both cases are the same. The superconducting transition temperature for glassy $NiZr_2$ also decreased with increasing quench temperature. Electron microprobe and TEM analyses showed all glassy samples to be homogeneous with identical structures. Electron diffraction photographs gave no evidence for phase separation in any sample. Crystallization kinetics studies indicate that the differences in crystallization characteristics are due to differences in the number of quenched-in nuclei and in growth and nucleation rates. The decrease in superconducting transition temperature is explained by changes in electron density of states, which are in turn consistent with electron diffraction data.

PF15 AN X-RAY DIFFRACTION STUDY OF LIQUID ZINC. G. Etherington and C.N.J. Wagner, Materials Science and Engineering Department, University of California, Los Angeles, California 90024.

The structure factor I(K) for liquid zinc has been evaluated at five temperatures in the range of 446°C to 750°C. The maximum temperature was limited by the high vapor pressure and the chemical reactivity of liquid zinc, but is higher than that obtained in previous X-ray and neutron diffraction studies. Measurements were made in transmission geometry using Ag-Kα radiation, and covered a K-range of 0.4 to 10 $Å^{-1}$. The data were corrected for sample and cell absorption, incoherent and multiple scattering, and the resulting I(K) were subsequently transformed to yield the total correlation functions T(R). In contrast to previous X-ray studies, the structure factors were found to agree well with those obtained by neutron diffraction. The structure factor data were used to determine the temperature dependence of the electrical resistivity using the Ziman theory, while the correlation function data provided information on the short-range order in the liquid.

This research was supported by grant DMR80-07939 from the National Science Foundation.

POSTER SESSION PG: ATOMIC TRANSPORT AND STRUCTURAL RELAXATION II

PG1 Re-Amorphisation of Crystallized $Fe_{40}Ni_{40}{}^{10}B_{20}$ by Neutron Irradiation

R. Gerling, R. Wagner and F.P. Schimansky, GKSS-Forschungszentrum, Institut für Physik, D 2054 Geesthacht, Box 1160, FR Germany

After thermal crystallization $Fe_{40}Ni_{40}{}^{10}B_{20}$ ribbons have been exposed to incore reactor irradiation. By the nuclear reaction: $^{10}B(n,\alpha)^{7}Li$ + 2.71 MeV damage levels up to 30 dpa were reached. The irradiated specimens were investigated by means of thermal analyses (DSC) and transmission-electron-microscopy. Both methods yielded the irradiation to induce a re-amorphisation. Thermal analyses of the irradiated specimens exhibited exothermal reactions, single peaked at lower damage levels and double peaked above ~ 20 dpa. The onset-temperature T_x of the crystallization increases continuously with increasing damage level. At 30 dpa T_x is about 680 K (for as-qu. $Fe_{40}Ni_{40}{}^{10}B_{20}$ T_x = 690 K, ΔH = 24 cal/g). Simultaneously the heat of crystallization also increases, reaching ΔH = 12 cal/g at 30 dpa. The radiation induced re-amorphisation can also be inferred from the development of broad halos in the electron diffraction patterns. In bright field TEM images the presence of irradiation-induced bubbles can be observed. They presumably contain the He-atoms resulting from the nuclear reactions. After 2.6 dpa, small bubbles (diameter about 10 Å) appear mainly along the grain boundaries of the micro-crystalline material. Around 8 dpa the bubbles have reached their maximum size and concentration (diameter about 50 Å). At this stage, specimens contain already some extended amorphous regions. The presence of bubbles, however, is confined to crystalline regions. After 20 dpa, bubbles can no longer be observed, although the material has not yet transformed completely to the amorphous state but rather contains still some crystallites. The amorphous structure seems to be able either to absorb the bubbles, or they migrate during the re-amorphisation process. Nevertheless, amorphous regions appear bubble-free. At 20 dpa the remaining crystallites are chiefly γ(Fe-Ni)-type. Their re-amorphisation commences beyond 20 dpa as can be observed by TEM.

PG2 LOG TIME RELAXATION KINETICS AND THE ACTIVATION ENERGY SPECTRUM MODEL. M.R.J. Gibbs, D.W. Stephens and J.E. Evetts, Department of Metallurgy and Materials Science, University of Cambridge, Cambridge, England.

When the measured value of a physical property varies linearly with the logarithm of the isothermal annealing time, log time kinetics are said to be obeyed. Such kinetics have been observed for a wide range of properties in metallic glasses. In a previous paper (1) we reported stress relaxation in cold rolled $Fe_{40}Ni_{40}B_{20}$ using measurements of magnetic coercive field, finding log time kinetics in all cases except for specimens that had been pre-annealed. We have recently proposed a model, based on a spectrum of available activation energies, which can account for the appearance or non-appearance of log time kinetics (2). In order to test the validity of this model in detail, the experiments of (1) have been extended over a wider time-temperature regime. Data have also been generated by computer simulation using a box distribution for the initial state of the spectrum of available activation energies. Using such a simulation it has been possible to calculate accurately the expected shape of relaxation curves, even after complex thermal treatments. Account has been taken of the effects of repeatedly removing the specimens from the furnace for measurement, and the agreement between calculation and experiment is excellent.

Thus, the activation energy spectrum model is shown to be of considerable value in understanding relaxation kinetics in metallic glasses.

(1) M.R.J. Gibbs and J.E. Evetts: Proc. 4th Int. Conf. Rapidly Quenched Metals (Sendai, 1981), Vol. I, p. 479.
(2) M.R.J. Gibbs, J.E. Evetts and J.A. Leake: J. Mat. Sci. 18 (1983) 278.

a) Dr. M.R.J. Gibbs, Department of Metallurgy and Materials Science, University of Cambridge, Pembroke Street, Cambridge, CB2 3QZ Tel. (0223) 65151.
b) Log time relaxation kinetics and the activation energy spectrum model.
c) Subject class 5.

PG3 THE DILATOMETRIC ESTIMATION OF FREE VOLUME IN THERMALLY TREATED $Ni_{38}Zr_{62}$ SAMPLES

E.Girt, K.Novalija, Ž.Majstorović and T.Mihać, Institute of Physics, University of Sarajevo, 71000 Sarajevo, Yugoslavia

The amount of the excess free volume in amorphous $Ni_{38}Zr_{62}$ samples was controlled by an own method of dilatometric measurements during the iso - thermal treatment. The idea was to show that the free volume is generated by the thermal motion. The specific thermal treatment was as follows: the samples were heated to 350°C and than annealed by lowering the temperature i.e. on 350°C, 250°C and 200°C. The analysis of the sample contraction, which enabled us to estimate the excess free volume showed that the thermal vibration of the atoms increases the free volume.

The measurements were compared with the measurements of viscosity on Ni-Zr and Cu-Zr systems.

Also, the measurements showed that the increased tensile stress begins to generate the free volume.

PG4 CALORIMETRIC EVIDENCE OF STRUCTURAL CHANGES IN THERMAL AGED CuZr, NiZr, FeBSi(C) AND FeCoBSi AMORPHOUS ALLOYS. M. Harmelin*, Y. Calvayrac*, A. Quivy*, J. Bigot*, P. Burnier**, M. Fayard* (*) Centre d'Etudes de Chimie Métallurgique, CNRS 94400 Vitry-sur-Seine. (**) Compagnie Electro Mécanique 93350 Le Bourget, France

Differential scanning calorimetry was applied for detecting structural changes due to thermal aging in different metal-metal and metal-metalloid amorphous systems : $Cu_xZr_{(1-x)}$ (x=.33, .46 and .60), $Ni_xZr_{(1-x)}$ (x=.635 and .65) melt spun ribbons and 2605 S2, 2605 SC and 2605 CO Metglas. Isothermal heat treatments were applied near Tg for CuZr and NiZr systems and in a wide range of temperature (from 130 up to 300°C) and of time (a few minutes to several months) for Metglas ribbons. Mechanical and electrical resistances of the Metglas ribbons were also followed as a function of thermal aging.

Two main kinetically different structural relaxation processes were detected : one occurs rapidly in a large range of temperature and is irreversible on cooling, the other one occurs with a slow rate and is a reversible one. Differences are observed between the systems with or without glass transition.

Results agree with the model based on a spectrum of available processes distributed in activation energy proposed by M.R.G. Gibbs et al.(1) and by H.S. Chen(2). The existence of localized clusters(3) which would undergo structural relaxation cooperatively therein may explained the calorimetric behaviour of the annealed amorphous Metglas.

(1) M.R.G. Gibbs, J.E. Evetts, J.A. Leake, Journ. Mater. Sci. 18 (1983) 278
(2) H.S. Chen, Journ. Non-Cryst. Solids 46 (1981) 289
(3) H.S. Chen, Proc. 4th Int. Conf. Rapidly Quenched Metals, Sendai, 1981, p. 555

PG5 EFFECTS OF QUENCH RATE AND COLD DRAWING ON THE STRUCTURAL RELAXATION AND YOUNG'S MODULUS OF AN AMORPHOUS $Pd_{77.5}Cu_6Si_{16.5}$ WIRE. A. Inoue, H.S. Chen*, J.T. Krause* and T. Masumoto, The Research Institute for Iron, Steel and Other Metals, Tohoku University, Sendai 980, Japan, *Bell Laboratories, Murray Hill, New Jersey 07974, USA.

The effects of wire diameter(e.g. quench rate) and cold drawing on the structural relaxation and Young's modulus of an amorphous $Pd_{77.5}Cu_6Si_{16.5}$ wire were examined with a differential scanning calorimeter and the pulse-echo technique. The results obtained are summarized as follows: (1)With decreasing wire diameter(e.g. with increasing quench rate) and increasing cold-drawn reduction in area, the temperature at which the structural relaxation starts upon heating lowers and the heat of structural relaxation(ΔH) increases, indicating that the faster the quench rate or the larger the reduction in area the higher is the degree of structural disorder in the amorphous phase. (2)The Young's modulus(E) decreases with decreasing wire diameter and with increasing reduction in area and there is a tendency that the less relaxed alloy exhibits a lower E value. (3)There exists a strong correlation between ΔH and E; the larger the ΔH the smaller is the E. One plausible explanation for such a strong correlation is that in the relaxed amorphous alloy having a high degree of short-range ordering between metal and metalloid atoms the internal displacement of constituent atoms becomes difficult, resulting in a larger E value. (4)In the order of wire(160 μm diameter)>ribbon(35 μm thickness)>cylinder(1 mm diameter), the difference in the specific heat between the as-quenched and the annealed state(ΔC_p) and ΔH increase and E decreases. This indicates that the amorphous phase in the wire possesses a more random structure as compared with the ribbon and the cylinder, despite that the diameter of the wire is larger by about 4-5 times than the thickness of the ribbon. From these results, it may be said that the in-rotating-water spinning method, by which an amorphous wire is manufactured, is a more useful technique for producing an unrelaxed amorphous phase having a high degree of structural disorder as compared with the conventional roller-type quenching method.

PG6 YOUNG'S MODULUS OF Fe BASED AMORPHOUS INVAR ALLOYS. S. Ishio, Y. Sato, T. Ikeda and M. Takahashi, Dept. Appl. Phys., Tohoku University, Sendai, 980 JAPAN

Young's modulus in rapidly quenched amorphous Invar alloys exhibits a stiffening below a Curie temperature and a relaxation in consequence of annealing: these phenomena would give an important information to make clear not only the magnetism in a random structure but also the origin of the Invar effect in transition metal alloys. However, to study an elastic property in ferromagnetic alloys, a temperature dependence of elastic constant must be measured up to a paramagnetic state in fields enough for saturation of magnetization, and only a few works have been performed up to now. This paper describes experimental results of the systematic study about the Young's modulus in Fe based amorphous Invar alloys.

Amorphous $Fe_{100-x}B_x$ ($12 \leq x \leq 25$), $Fe_{100-x}P_x$ ($15 \leq x \leq 21$), $Co_{100-x}B_x$ ($17 \leq x \leq 33$) and $(Fe,Co,Ni)_{77}Si_{10}B_{13}$ alloys were fabricated using a disk method. The Young's modulus was measured using an ultrasonic pulse echo method (pulse width: 1 μsec, duty cycle: 100 kHz) in fields up to 4 kOe.

The composition dependence of E in the Fe-B alloy is shown in Fig.1. Note here that the value of E at 4 kOe increases considerably with B concentration. This tendency is contrary to the composition dependence of the Debye temperature in this alloy but very close to that of E for the f.c.c. Fe-Ni alloy.

The mechanism of the Invar effect and the magnetic property in amorphous alloys will be discussed in the Conference.

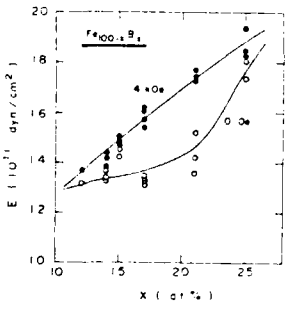

Fig.1. Composition dependence of Young's modulus in the Fe-B alloy.

PG7 SHOCK WAVE CONSOLIDATION OF AN AMORPHOUS ALLOY. P. Kasiraj, D. Kostka, T. Vreeland, Jr. and T. J. Ahrens, California Institute of Technology, Pasadena, CA 91125 USA

Irregular and refractory flakes prepared from ~ 50 μm thick melt spun ribbons of an amorphous MARKO 1064 alloy (51.5% Ni, 39% Mo, 8% Cr, 1.5% B by weight) were consolidated by shock waves resulting from high velocity projectile impact. Recovered samples were observed to have achieved full densification. Metallographic observations and x-ray diffractometer scans indicate that the degree of interparticle bonding and the amount of crystallization increase with shock energy input. Substantial crystallization is observed in our highest pressure consolidations while at lower pressures compacts have little or no crystallization.

PG8 DIFFUSION OF GOLD AND NICKEL IN METALLIC GLASSES. M. Kijek and D.W. Palmer, School of Mathematical Sciences, University of Sussex, Brighton BN1 9QH, U.K.

The Rutherford backscattering technique has been utilized to determine the diffusion coefficients D of gold solute atoms in as-quenched and relaxed $Ni_{67.5}Nb_{32.5}$ and $Ti_{70}Ni_{25}Si_5$ metallic glass ribbons. The samples were sputter-coated with gold and then were each diffusion annealed at four different temperatures and times chosen so that crystallization did not occur. The temperatures used were in the range 335-380°C and 400-600°C for $Ti_{70}Ni_{25}Si_5$ and $Ni_{67.5}Nb_{32.5}$ glasses, respectively.

The concentration-depth profiles of gold were determined from the backscattered-ion energy spectra obtained with an incident 2.0 MeV $^4He^+$ ion beam. The combined effects of energy straggling of helium ions in the medium and of the system energy resolution were included in the analysis.

The D values were evaluated from thick-source solutions to the diffusion equation. The results indicated that for gold contents greater than 20 at % in the Ni-Nb glass the diffusion coefficient was dependent on the gold concentration. For gold contration smaller than 20 at % the values of the pre-exponential factor D_0 and activation energy Q, determined from an Arrhenius plot, were 1.3×10^{-7} m^2/s and 1.6 eV. The diffusion coefficient of gold in $Ti_{70}Ni_{25}Si_5$ was, however, found to be independent of gold concentration; in this case the values of D_0 and Q were 2.5×10^{-4} m^2/s and 2.1 eV, repectively. The same RBS method was used for the determination of the nickel self diffusion coefficient in the $Ni_{67.5}Nb_{32.5}$ glass.

PG9 THERMAL STABILITY AND CREEP BEHAVIOUR OF Fe-Ni METALLIC GLASSES. A. Kursumovic, School of Engineering and Applied Sciences, University of Sussex, Falmer, Sussex, BN1 9QT, U.K. and B. Tolouí, Oxford Research Unit, The Open University, Foxcombe Hall, Oxford, OX1 5HR, U.K..

Thermal stability of $(Fe,Ni)_{80}B_{18}Si_2$ glassy ribbons was studied by dilatometry and differential scanning calorimetry techniques. The results showed that length and energy changes during crystallization corresponded to each other, having identical kinetics of crystallization in both cases. Similar dilation techniques were utilized for creep measurements. It was found that crystallization temperatures increased by increasing the Fe content at 10 k min^{-1} heating rate. Creep onset temperatures behaved in the same manner, indicating that viscous flow plays an important role in these fairly stable metallic glasses.

PG10 THERMAL STABILITY, MAGNETIC AND MECHANICAL PROPERTIES OF AMORPHOUS $Fe_{80-x}M_xB_{14}Si_6$ WITH M = Mn, Cr, V, Mo, W. S. T. Lin, H. B. Wu and W. T. Ku. Department of Physics, National Cheng Kung University, Tainan, Taiwan, Republic of China.

Effects of Mn, Cr, V, Mo, W on the density, magnetization, Curie temperature, crystallization temperature, hardness and embrittlement temperature of amorphous $Fe_{80-x}M_xB_{14}Si_6$ alloys have been studied in detail. It has been found that most of the values of the packing fraction calculated from the measured densities are at 0.69 ± 5%, indicating the structure similarities among these series of alloy compositions; substitution of Mn, Cr, V, Mo, W for Fe in amorphous $Fe_{80-x}M_xB_{14}Si_6$ decreases the magnetization, Curie temperature and embrittlement temperature, but increases both the crystallization temperature and hardness.

The composition dependence of Curie temperature can be explained by CPA calculation, assuming that J_{Fe-Fe} is positive and J_{Fe-M} is negative. This suggests that Mn, Cr, V, Mo, W atoms interact antiferromagnetically with Fe atoms in these amorphous alloys. Hardness like Young's modulus could be related to the average spin value by the relation $H_v = a + b \langle s \rangle^2$, where b was determined to be negative in these alloys studied.

A possible correlation between embrittlement temperature and hardness will also be discussed.

PG11 CRYSTALLIZATION BEHAVIOR IN AMORPHOUS INTER-TRANSITION METAL ALLOYS, A.F. Marshall, R.G. Walmsley, Y.S. Lee and D.A. Stevenson, Stanford University, Stanford, CA 94305

The crystallization behavior of several amorphous Cu-Zr and Cu-Ti alloys was studied using differential scanning calorimetry (DSC), X-ray diffraction and transmission electron microscopy. The crystallization paths and the crystallization kinetics of these alloys were characterized to obtain insight into the structure and relative stability of the amorphous state. The compositions $Cu_{80}Zr_{20}$, $Cu_{60}Zr_{40}$ and $Cu_{60}Ti_{40}$ were prepared by the vapor-quench (VQ) technique of planar magnetron sputter deposition; $Cu_{60}Ti_{40}$ was also prepared using a liquid quench (LQ) meltspinning technique.

$Cu_{60}Zr_{40}$ crystallizes by direct nucleation and growth of the equilibrium phase. The isocompositional $Cu_{60}Ti_{40}$ forms a metastable microcrystalline phase as an intermediate step prior to nucleation and growth of the equilibrium phase; the DSC scan showed two corresponding exotherms. $Cu_{80}Zr_{20}$ also forms an intermediate microcrystalline phase during crystallization. Although these intermediate phases for $Cu_{80}Zr_{20}$ and $Cu_{60}Ti_{40}$ are based on small simple unit cells, they are easily bypassed upon quenching. This may be related to changes in chemical short range order upon crystallization.The kinetics of crystallization during isothermal annealing of $Cu_{60}Zr_{40}$ appear slow relative to results reported by others for LQ $Cu_{60}Zr_{40}$; such a result may be interpreted in terms of the mode of nucleation at that temperature and differences in the quenched-in structures. Comparison of VQ and LQ $Cu_{60}Ti_{40}$ also show different kinetic and morphological changes upon isothermal annealing. In the temperature range for homogeneous nucleation, the incubation time for the LQ alloy is longer than for the VQ alloy. Crystal shape and orientation are also different for the two alloys. These results are again attributed to differences in the as-synthesized structures.

POSTER SESSION PH: ELECTRONIC PROPERTIES II

PH1 THEORY OF ELECTRONIC TRANSPORT IN LIQUID NON-SIMPLE METALS. M. Itoh, University of East Anglia, Norwich, NR4 7TJ, UK, K. Niizeki, Tohoku University, Sendai 980, Japan, and M. Watabe, Hiroshima University, Hiroshima 730, Japan.

A theory of electronic transport is further developed based on the effective medium approximation and the tight-binding model. The basic formulation for the dc conductivity σ_{xx} presented at the last Conference (Itoh et. al., Roth and Singh) is extended to the Hall conductivity σ_H. We present the results of the numerical application of our theory to a model liquid metal. Detailed analysis is made for σ_{xx}, and the discussion will also be given for σ_H.

For ordinary liquid-like atomic structure, we found very large positive vertex corrections for σ_{xx} when the Fermi energy is in the lower energy part of the band. As a function of the filling fraction of the tight-binding band, σ_{xx} has accordingly a sharp maximum at low filling fraction, and this suggests the relative importance of d-electrons as carriers in the conduction process in some earlier elements of the transition metal series.

PH2 ELECTRONIC STRUCTURE OF TRANSITION METAL GLASSES: Zr_xT_{1-x}. S.S. Jaswal, University of Nebraska, Lincoln, NE 68588 USA, and W.Y. Ching, University of Missouri, Kansas City MO 64115 USA

Our recent electronic structure calculations on Zr_xCu_{1-x} glasses have shown that the position of a local d-band below the Fermi level due to a given Cu atom is very sensitive to its surroundings.[1] Therefore the calculated electronic structure when compared with the photoemission data is a very sensitive tool to study the chemical short-range order in transition metal glasses. We are extending our calculations to Zr_xT_{1-x} glasses with T = Ni, Co and Fe. The glass is simulated by a large cluster (40-50 atoms) with periodic boundary conditions. The atoms are randomly packed and then relaxed with Lennard-Jones potentials. The calculated radial distribution functions will be compared with the available experimental data. The orthogonalized linear combination of atomic orbitals method is used to calculate the electronic structure. The calculated electronic structure will be compared with the photoemission data[2] to study the chemical short-range order. Finally, the calculated density of states at the Fermi level will be compared with the experimental results.[3]

[1] S.S. Jaswal, W.Y. Ching, D.J. Sellmyer and P. Edwardson, Solid State Commun. 42, 247 (1982); S.S. Jaswal and W.Y. Ching, Phys. Rev. B 26, 1064 (1982).
[2] P. Oelhafen, "Glassy Metals II", Ed. H.-J Guntherodt and H. Beck (Springer-Verlag, New York)(in press).
[3] Z. Altonnian and J.O. Strom-Olsen, Phys. Rev. B (in press).

PH3 ELECTRICAL RESISTIVITIES OF LIQUID Ag, In, Sn and Sb SOLVENTS WITH LIGHT RARE EARTH SOLUTES. H.Kakinuma, M.Haruta and S.Ohno, Niigata College of Pharmacy, 5829 Kamishin'ei-cho, Niigata, JAPAN

We report measurements of the electrical resistivity of liquid Ag and Sb solvents with light rare earth (RE) solutes and discuss the behaviour of light RE solutes in liquid Ag, In, Sn and Sb solvents. The electrical resistivities of liquid Ag solvent with light RE solutes were measured with a four probe method from the melting point to about 1200 °C. The additional resistivities in liquid Ag solvent are 6.20, 7.35, 7.70 and 7.90 μΩ·cm for La, Ce, Pr and Nd solutes, respectively. The additional resistivities in liquid Sb solvent are 4.85, 1.20, 1.70 and 1.95 μΩ·cm for La, Ce, Pr and Nd solutes, respectively. The value of La solute is considerably larger than those of Ce, Pr and Nd solutes. The additional resistivities in liquid In and Sn solvents increase gradually from La to Nd, peak at Nd and decrease gradually from Nd to Yb.

We discuss the additional resistivities of La solute in liquid metal solvents from the effect due to the 5d-resonance scattering as follows,

$$\Delta\rho = \frac{20\pi\hbar c}{ne^2k_F}\sin^2\frac{\pi}{10}N_d \qquad (1)$$

where n is the number of conduction electrons per solvent atom, k_F is the wave number at the Fermi level and N_d is the number of the localized 5d-electrons. Assuming that $N_d = 2.5$ for La solute, the additional resistivities are calculated from eq.(1). The calculated values of La solute in liquid Ag, In and Sn solvents agree with the experimental values. However, the experimental values of La solute in liquid Sb solvent can not be explained from the resonant scattering effect.

The additional resistivities of Ce, Pr and Nd solutes in liquid metal solvents increase with increasing the number of 4f-electrons. This trend is less marked in liquid Ag solvent and is noticeable in liquid In solvent. The systematic variation of the additional resistivities due to Ce, Pr and Nd solutes in liquid metal solvents may be attributed to s,d-f mixing.

PH4 ANOMALOUS TEMPERATURE DEPENDENCE OF RESISTIVITY FOR AMORPHOUS $(Fe_{1-x}Ni_x)_{77}Si_{10}B_{13}$ ALLOYS. T.K.Kim and Y.F Ihm, Chungnam University, Daejon 300-31, Korea, B.W.Lau, Korea University, Seoul 132, Korea.

It was reported that the temperature dependence of electrical resistivity in amorphous $(Fe_{1-x}Ni_x)_{77}Si_{10}B_{13}$ alloys has anomalous characteristics when x=0.8 and 0.9: the electrical resistivity at the crystallized state is larger than that at the amorphous state. In order to investigate this anomalous characteristics, this work presents the experimental results of the electrical resistivity, the Hall resistivity, the saturation magnetization and the structure analysis in $(Fe_{1-x}Ni_x)_{77}Si_{10}B_{13}$ alloys.

The amorphous $(Fe_{1-x}Ni_x)_{77}Si_{10}B_{13}$ alloys were fabricated into a ribbon form by a rapid quenching technique. The resistivity of samples was measured by a four probe technique in the temperature range from 77 to 1200 K. The Hall resistivity of samples was measured up to 17 KOe of magnetic field in the same temperature range for electrical resistivity, and the saturation magnetization was measured with a vibrating sample magnetometer at 77 K.

The effective numbers of the conduction electron and the 3d electrons of the transition elements are calculated from the Hall coefficient and the magnetic moment, and are compared with theoretical predictions.

The structure of samples around the crystallization temperature was examined by a X-ray diffractometer. It is found that β-Ni_2Si is formed at the first step of the crystallization when x=0.8 and 0.9 so that the resistivity is increased at crystallization temperature.

1) T.K.Kim, C.G.Kim, Y.F.Ihm and B.W.Lau, JMMM to be published.(at ICM, Kyoto in Japan)

PH5 HIGH FREQUENCY PROPERTIES IN A PARTICLE-DISPERSED AMORPHOUS $Co_{70.5}Fe_{4.5}Si_{10}B_{15}$ COMPOSITE WITH ZERO MAGNETOSTRICTION K.Kimura, T.Masumoto, A.Makino* and T.Sasaki*, The Research Institute for Iron, Steel and Other Metals, Tohoku University, Sendai 980, Japan.

We employ the new technique to prepare two-phase amorphous materials(amorphous composites) in an attempt to improve the soft magnetic properties at high frequency.

Amorphous $Co_{70.5}Fe_{4.5}Si_{10}B_{15}$ composites were produced by the single-roller method, and shown to be consisted of an alloy matrix with a three dimensional dispersion of the second phase particles of WC, using a compositional backscattering mode in a scanning electron microscope. The volume fraction (V_f) of these composites were varied, with V_f ranging from 1-5 %. Ring samples with the outer diameter of 10 mm and the inner diameter of 6 mm were used to determine the effective permeability(μeff) over a range of the frequency from 1 kHz to 10 MHz, and the ac core loss ranging from 30 to 200 kHz.

The saturation magnetic induction of an amorphous $Co_{70.5}Fe_{4.5}Si_{10}B_{15}$ composite(B_{sc}) do not undergo a rapid decrease from the level of B_s for a non-dispersed alloy; i.e., within the accuracy of this study's measurement, a simple relation of $B_{sc}=B_s(1-V_f/100)$ is confirmed, indicating that second phase particles in a magnetic matrix act as equivalent holes. The curve of effective permeability for an amorphous $Co_{70.5}Fe_{4.5}Si_{10}B_{15}$ composite, annealed above a Curie temperature, versus frequency is normal and appears to be dependent on WC-volume fraction, extending a plateau to a higher regime of the frequency beyond 20 kHz as the V_f increases. However, the scatter in the effective permeability data(arising mostly from thickness variation) is such that more accurate measurements are needed to establish unambigously particle-dispersion effects on high frequecny properties. The ac core loss for particle-dispersed amorphous $Co_{70.5}Fe_{4.5}Si_{10}B_{15}$ is defintely improved relative to the non-dispersed alloy beyond the frequency of 50 kHz; the difference tends to increase with frequency.

A systematic study on the relationship between μeff and core loss at high frequency and the particle-volume fraction and size is now being carried out.

* On leave from the Alps Electric Co., Ltd., Niigata 946, Japan

PH6 THERMOELECTRIC POWER OF THE Sn-Se LIQUID ALLOY, D. H. Kurlat, Universidad de Buenos Aires, Facultad de Ingeniería, Buenos Aires, Argentina.

The Seebeck coefficient (S) of Sn_x-Se_{1-x} (x: atomic fraction) was measured as a function of concentration temperature. The samples were synthesized by fusing the components in quartz ampoules, which were evacuated to 10^{-6} mm Hg and then were filled with Ar up to pressure of 200 mmHg. Each sample was kept at 150°C higher than the liquidus temperature for 60 hours. To obtain the S values a quartz container of 80 mm long was filled with the substance being investigated. At each end of the container a hole was made, through which a graphite electrodes. The voltage drop between either the Al leads or the Mo leads was measured either by a potentiometric method or using a digital microvoltimeter. Knowing the absolute thermoelectric power of the wires, the Seebeck coefficient of each liquid alloy can be found. The temperature gradient was always less than 12° C and all the experiment were performed under Ar overpressure (7-8 kg cm^{-2}) after previous de-gassing under vacuum. In the concentration range $1 \leqslant x \leqslant 0.91$ the alloy is metallic. For $x=0.95$ we have measured S in the temperature interval $873\,K \leqslant T \leqslant 1273\,K$. The liquid alloy is p-type and presents a maximum ($S=6.2\,\mu V/K$) at 1176 K. In pure liquid Se, Mahdjuri has observed S positive value for $T>990$ K and a maximum ($S \cong 300\,\mu V/K$) about $T \cong 1100\,K$.
Because the Seebeck coefficient of Sn is very little, we can explain S values, by supposing a simple additional linear law of the type $S = \Sigma x_i S_i$.
For $x=0.35$ ($Sn-Se_2$) a transition semiconductor → semimetal was observed. For $930\,K \leqslant T \leqslant 1015\,K$, S is positive and follows a $f(T^{-1})$ law, with $E_F - E_v \approx 0.73$ eV and $\beta/k_B = 5.54$. In the temperature interval $1055\,K \leqslant T \leqslant 1176\,K$, S is p-type but it remains nearly constant ($55\,\mu V/K \leqslant S \leqslant 65\,\mu V/K$). This behavior may be explained because when temperature rises, chemical bonds are broken, electrons pass to the conduction band, and so the relative number of holes is lowered.

PH7 EFFECT OF STRUCTURAL RELAXATION ON CRITICAL FIELDS H_c AND H_{c2} AND RESISTIVITY IN SPUTTERED AMORPHOUS ALLOYS $Zr_{76}Cu_{24}$ AND $Zr_{76}Ni_{24}$. O. Laborde, O. Béthoux, J.C. Lasjaunias and A. Ravex, CNRS, CRTBT, B.P. 166 X, 38042 Grenoble Cédex, FRANCE

We report critical field and resistivity results on sputtered amorphous $Zr_{76}Cu_{24}$ and $Zr_{76}Ni_{24}$ alloys. Measurements were done on the same samples, firstly in their as-prepared state and after an annealing well below the crystallization temperature.

The superconducting thermodynamic critical field $H_c(T)$ is obtained from calorimetric measurements at very low temperature. The absolute value and the thermal variation of this property are well described by assuming that both alloys are weak-coupling superconductors and using for the electronic density of states N(0) the value deduced from the γ coefficient measured above T_c.

A similar good agreement is not found for the upper critical field $H_{c2}(T)$ measured by a resistive method ; the values of H'_{c2}, slope of $H_{c2}(T)$ near T_c, are different for both systems but do not vary significantly on annealing or on conditions of preparation. While the product $\gamma\rho$ which would be proportional to H'_{c2} varies by more than 20 % on annealing, an experimentaly detectable effect. Tentative explanations of this unexpected result is suggested.

We also report resistivity measurements between room temperature and T_c for $Zr_{76}Ni_{24}$ alloy. Results are well-interpreted in the framework of the Faber-Ziman diffraction model without adjustable parameters. The structure factor $S(2k_F)$ is obtained from literature and θ_D, the Debye temperature, from specific heat measurement. The observed variation of these parameters takes correctly in account the results. Alternative explanations such as Kondo-like model for two-level systems are also discussed.

PH8 MAGNETIC PROPERTIES OF AMORPHOUS METAL-METALLOID ALLOYS. B.W.Lau, Korea University, Seoul 132, Korea, T.K.Kim and Y.E.Ihm, Chungnam University, Daejon 300-31, Korea.

In order to investigate the effects of alloying elements and their concentrations on the magnetic properties in amorphous alloys, the systematic measurements of the saturation magnetization, coercive force and Curie point in amorphous $Fe_{80}(Si_{1-x}B_x)_{20}$, $(Fe_{1-x}Co_x)_{80}B_{20}$ and $(Fe_{1-x}Ni_x)_{80}B_{20}$ alloys in the temperature range of 77 and 1200 K have been carried out and discussed.

The amorphous alloys used in this study were fabricated into a ribbon form by a rapid quenching technique. The composition ranges of these alloys are $0.1 \leqslant x \leqslant 0.8$, where x is the atomic concentration. The structures of samples were carefully checked by a X-ray diffractometer. The saturation magnetization and Curie point were measured by a vibrating sample magnetometer and a magnetic balance. The coercive force was measured by a hysteresis loop tracer.

The saturation magnetization in $Fe_{80}(Si_{1-x}B_x)_{20}$ and $(Fe_{1-x}Ni_x)_{80}B_{20}$ at room temperature decreases linearly with increasing Si and Ni contents, respectively, but that in $(Fe_{1-x}Co_x)_{80}B_{20}$ rises with increasing Co content and passes through a maximum value at about x=0.5, and then decreases again. The crystallization temperature in $Fe_{80}(Si_{1-x}B_x)_{20}$ increases linearly with increasing B content, but those in $(Fe_{1-x}Co_x)_{80}B_{20}$ and $(Fe_{1-x}Ni_x)_{80}B_{20}$ are almost independent on the concentrations of alloying elements, and are 690 K and 660 K, respectively. The magnetic moments of alloying elements are calculated from the saturation magnetizations measured at 77 K.

The results are compared with theoretical predictions and those for the other simillar amorphous alloys.

PH9 OPTICAL PROPERTIES OF AMORPHOUS $Fe_{1-x}B_x$ALLOYS. N. Lustig, L.J. Pilione, K.C. Woo and J.S. Lannin.* The Pennsylvania State University, University Park, PA 16802 U.S.A.

Thin films of amorphous $Fe_{1-x}B_x$ alloys have been prepared by sputtering over an extensive composition range from x = 0.15 to x = 1.0. Both dc sputtering of arc melted alloys as well as composite targets prepared by rf diode sputtering have been employed. Reflectivity measurements have been performed on thick films from the infrared to ultraviolet, while transmission measurements employed thin films. With increasing B concentrations the reflectivity at 0.5eV is found to decrease rapidly from that at x ≈ 0.2. In addition, the weak shoulder at ~1.7eV becomes more distinct as B concentration is increased, suggesting a peak in the joint electronic density of states at this energy. The optical spectra further indicate the transition from amorphous metal to amorphous semiconductor.

*Supported by DOE Contract DE-AC02-82ER12083

PH10 DRUDE OPTICAL PROPERTIES OF AMORPHOUS NICKEL-PHOSPHORUS ALLOYS.* S. W. McKnight and A. Ibrahim, Northeastern University, Boston, MA 02115 USA

The free electron theory would seem to be a good approximation for the infrared properties of amorphous metals because the effects of band structure are greatly reduced. We have measured the reflectivity in the spectral range 0.02 - 2.5 eV of electro-deposited Ni-P amorphous alloys containing 15 - 26 at. % phosphorus. The data are well fit in the low frequency region by the Drude model and the optical conductivities determined from the fit are in agreement with the published DC conductivities for these materials. Alloys with greater than 20 at. % P appear Drude-like to frequencies as high a 1.5 eV while those alloys with less than 20 at. % P begin to deviate from free electron behavior at frequencies around 1.0 eV. Crystalline samples examined for comparison show structure at even lower frequencies. These changes are correlated with an abrupt increase in the peak height of the first x-ray diffraction maximum in amorphous alloys under 20 at. % P.

Values of the plasma frequency ω_p and the inverse scattering time $1/\tau$ have been extracted for the amorphous alloys and both are found to decrease with increasing phosphorus content. Such a result can be consistent with a nickel rigid-band model since a transfer of carriers from P to Ni will raise the fermi level out of the d-band and decrease the density of states. This reduces the plasma frequency and, through the effect on the density of final states, also decreases the scattering. The model would imply, however, that the d- and s-electron density of states enter additively into a single Drude term--possibly as a result of strong s-d scattering. In addition, to be consistent with the magnetization results, each P atom must be considered to contribute 3 rather than 5 electrons to the Ni bands.

*Work supported by AFOSR, the Research Corporation, and the Northeastern U. Research and Scholarship Development Fund.

PH11 TEST OF DIFFRACTION MODEL PREDICTIONS FOR LOW RESISTIVITY AMORPHOUS METALS. L. V. Meisel and P. J. Cote, US Army Armament Research & Development Command, Large Caliber Weapon Systems Laboratory, Benet Weapons Laboratory, Watervliet, NY, 12189

The Faber-Ziman theory of electrical transport (the diffraction model) is expected to be valid if the electron mean free path Λ is not too small. Most metallic glasses have electrical resistivities ρ in excess of 100 $\mu\Omega$cm corresponding to Λ of the order of ionic spacings where application of the diffraction model is questionable. Nevertheless the Faber-Ziman theory apparently describes the concentration dependence in these alloys reasonably well and discrepancies become apparent only under examination of the temperature T dependence of ρ. If phonon ineffectiveness effects (saturation effects) are incorporated in the electron-phonon matrix element in the diffraction model improved agreement with the observed $\rho(T)/\rho(\Theta_o)$ is obtained in high resistivity glasses.

At present data are available for a number of low resistivity alloys (ρ < 100 $\mu\Omega$cm) over extensive ranges of temperature. We have applied the diffraction model to these alloys incorporating appropriate potentials, structure factors, etc. The following general results were obtained: 1. Born approximation pseudopotentials yield reasonable values for the magnitude of ρ but poor results for the T dependence of ρ. 2. Phase shift expanded scattering matrix elements can be adjusted to give the magnitude of ρ and qualitative agreement with $\rho(T)$ in the Faber-Ziman theory. 3. The magnitude of ρ is quite sensitive to the phase shifts; however, $\rho(T)/\rho(\Theta_o)$ is essentially insensitive to the phase shift values within appropriate ranges. 4. When phonon ineffectiveness effects are included (as in the high ρ glasses) greatly improved agreement with the data is obtained. In particular: (i) The range of $2k_F/k_p$, for which computations yield negative TCR, is broadened and shifted with respect to that given in the "backscattering dominant" approximation and is in accord with the data. (ii) The observed positions and sizes of the small maxima in ρ for negative TCR cases are given by the theory. (iii) The quadratic behavior of $\rho(T)$, observed below about 30K, is also described.

PH12 EFFECT OF $2k_F/K_p$ ON ELECTRON TRANSPORT AND DENSITY OF STATES IN HUME-ROTHERY TYPE METALLIC GLASSES. U.Mizutani and K.Yoshino, Nagoya University, Nagoya 464 Japan.

The ratio of the Fermi momentum $2k_F$ to the wave number K_p, corresponding to the first peak of the structure factor, plays an important role in the discussion of the electronic structure of a disordered alloy system. The reliable determination of $2k_F$ is made possible in an alloy, which is composed only of simple elements having definite valencies. Here, we employed liquid quenched metallic glasses in the alloy system obtained by adding the third element X (=Mg, Si, Ge, Sn and Sb) to the eutectic Ag-Cu binary. The $2k_F$ value is determined from the Hall effect and positron annihilation and is in excellent agreement with the free electron value.

The electrical resistivity ρ_{300K} of the Ag-Cu-X (X=Mg and Sn) metallic glasses is fairly small and is in the neighborhood of 50 $\mu\Omega$-cm. This, together with the well-defined $2k_F$, assures the application of the extended Ziman theory to the electron transport properties of these metallic glasses. Indeed, we can show that the behavior of ρ_{300K} and TCR can be well described in terms of $2k_F/K_p$; the TCR changes its sign at $2k_F/K_p$=1.0. In contrast, the ρ_{300K} value for Ag-Cu-metalloid glasses (X=Si, Ge and Sb) generally exceeds 100 $\mu\Omega$-cm. The saturation effect comes into play and causes the resistivity to level off at low temperatures in the form of $(1-AT^2)/(A>0)$. This greatly differs from the low temperature resistivity behavior in the low resistivity metallic glasses such as those with X=Mg and Sn.

In both liquid and amorphous metals, there have been a number of arguments concerning whether $2k_F/K_p$ value exerts a discernible effect on the density of states at the Fermi level. The Ag-Cu-Mg metallic glass is considered to be best suited to the performance of this test, since $2k_F/K_p$ covers the range 0.96-1.1. The electronic specific heat measurements clearly showed the absence of the appreciable effect of $2k_F/K_p$ on the density of states near

PH13 CALCULATION OF THE FULL SPECTRAL FUNCTION FOR AN AMORPHOUS TRANSITION METAL. G.J. Morgan and G.F. Weir, Department of Physics, University of Leeds, Leeds LS2 9JT, UK

We have applied the equation of motion method to calculate the total spectral function for s and d electrons in a model amorphous transition metal containing 797 'hard sphere' atoms. Details of the effects of hybridisation on the 'free electron like' band are presented for a range of band parameters. Finally a simple model of photoemission is used to predict the photo-electric current for two excitation energies and these are compared with the predictions of the Random Phase Model (RPM). It is found that, as in the case of electronic conduction, the RPM for the d electrons gives quite good agreement with the more exact calculation.

PH14 IN SITU INVESTIGATIONS OF THE ELECTRONIC PROPERTIES OF CO-EVAPORATED AMORPHOUS MgZn ALLOY FILMS. *V. Nguyen Van, S. Fesson and M-L. Thèye*, Laboratoire d'Optique des Solides, ERA CNRS 462, Université P. et M. Curie, 4 Place Jussieu, 75230 Paris Cedex 05, France.

Amorphous $Mg_{1-x}Zn_x$ alloy films have been obtained by controlled co-evaporation onto sapphire substrates maintained at low temperature ($\sim$10 K) under ultra-high vacuum ($\sim 10^{-9}$ Torr), for Zn concentrations around 30 at.%. Due to the rapid oxidation of these films under ambient atmosphere, all optical (transmittance and reflectance at near-normal incidence from 0.6 to 4 eV) and transport (electrical resistivity) measurements have been performed in situ, first just after deposition, then at different annealing steps up to room temperature. The complex dielectric constant $\hat{\varepsilon}$ deduced from the optical measurements has been analyzed in terms of the Drude free-electron model. $\hat{\varepsilon}$ is found to closely follow a free electron behaviour over a large spectral range allowing the determination of the characteristic parameters of the alloy conduction electrons : average effective number per atom n_{eff} and optical relaxation time τ_0. The n_{eff} value is shown to be smaller than the value predicted by a simple rigid band model and confirmed by various experiments on rapidly-quenched samples. The variation with temperature T of the electrical resistivity ρ of alloy films still amorphous at room temperature has been studied in detail over a large temperature range (from 10 to 300 K) and the existence of a broad maximum in ρ (T) is clearly shown. The results are compared to existing theories.

PH15 ON THE NATURE OF BONDING IN LIQUID SEMICONDUCTOR Cs_3Sb AND SOME OTHER ALKALI ANTIMONIDES. K. Niizeki and H. Tanaka, Tohoku University, Sendai 980 Japan and K. Shindo, Iwate University Morioka 020 Japan

Cs_3Sb and some other alkali antimonides are semiconductors in both the solid and liquid states and there are several evidences indicating that the mechanism of bonding in these compounds remains unchanged on melting. However, there has been a controversy about the nature of the bonding. It is concluded from a measurement of the XPS spectra of Cs_3Sb in solid state that the bonding is predominantly ionic, while an N.M.R. study and a magnetic susceptibility study emphasised covalency.

In order to resolve the apparent conflict, we have undertaken a band structure calculation of the compounds in solid states by means of the self-consistent pseudopotential calculation. The calculated charge densities of the valence electrons are found to be distributed almost spherically arround Sb atoms, indicating that the bonding is predominantly ionic, but it is observed also that the charge penetrates weakly in anionic sphere being centred on an alkali site. However, no pile up of the charge is found between neighbouring Sb and alkali atoms. Thus, we can conclude that the bonding is principally ionic but a 'non-directional covalent bonding' admixtures slightly in it. Our calculation clearly excludes the possibility of a directional covalent bonding which has been advocated by several authors.

PH16 THE RELATIVISTIC KKR-EMA DENSITIES OF STATES OF LIQUID HEAVY POLYVALENT METALS.
A.Nishikawa and K.Niizeki
Department of Physics, Tohoku University, Sendai 980, Japan

The resistivities and some other electronic properties of the liquid states of heavy polyvalent metals (Tl, Pb, Bi) have been analyzed by means of the nearly free electron model, probably because their conduction electrons are originated from atomic s and p electrons. Several authors calculated their electronic densities of states by means of the second order perturbation theory and obtained results which are not so different from those in the free electron model. However, the Hall coefficients of these liquid metals have been known to be appreciably different from the free-electron values. Moreover, it was shown recently by the measurement of the UPS that their band structures are very different from those in the free electron model. The deviation may be ascribed to the strong attractive force on s electrons (6s-like) due to the relativistic mass enhancement in the neighbourhood of nuclei. In order to confirm it, we have undertaken the calculation of the densities of states by means of the relativistic version of the KKR-EMA. The result of a preliminary calculation based on the phase shift of an attractive short-range model potential is shown in the figure. We are now carring out a more realistic calculation.

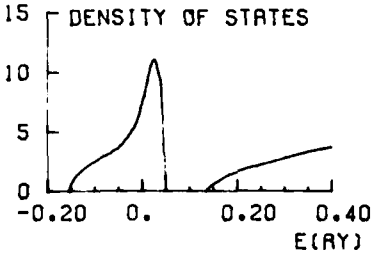

PH17 ON THE STABILITY OF AN AMORPHOUS HUME-ROTHARY-PHASE.

H.-J. Nowak, Physikalisches Institut der Universität Karlsruhe, D-7500 Karlsruhe, FRG.

The stability of amorphous metallic glasses of the type noble metal-polyvalent element seems to be governed by the valence electrons of the system and not by chemical bonding effects /1/. Following ideas used for crystalline Hume-Rothary-Phases, we calculate with pseudopotential formalism effective pairpotentials of the type Au_xSn_{1-x}, assuming a statistical distribution of the constituents.
Comparison with measured pair-distribution functions /2/ show a remarcable close matching between the minima in the pairpotential and the maxima in the pair-distribution function at an electron concentration of $Z \approx 1.8$ electron/atom.

1. P. Häußler and F. Baumann: Physica 108 B (1981) 909-910.
2. H. Leitz: Z. Phys. B 40 (1980) 65-70.

PH18 MAGNETIC PROPERTY OF TRANSITION METAL SOLUTES IN LIQUID In, Sn, Sb, Te and Se-Te ALLOY SOLVENTS. S. Ohno Niigata College of Pharmacy, 5829 Kamishin'ei-cho, Niigata, JAPAN.

We have made careful measurements of the susceptibilities of V, Cr, Mn, Fe, Co and Ni solutes in liquid In, Sn, Sb, Te and Se-Te alloy solvents. The additional susceptibilities of these transition metal (TM) solutes decrease with increasing the valence electron number of solvent metals. Those of Mn, Fe, Co and Ni exhibit each minimum at liquid Sb solvent and rapid increase in going from liquid Sb to liquid Te and Se-Te alloy solvents, while those of Cr and V exhibit slight decrease in going from liquid Sb to liquid Te. That is, $\Delta\chi_d(Cr) > \Delta\chi_d(Fe)$ and $\Delta\chi_d(V) > \Delta\chi_d(Co)$ in liquid In, Sn and Sb metal solvents and the experimental results in liquid Te and Se-Te alloy solvents are contrary to these relationship in liquid metal solvents.

We discuss the additional susceptibilities with the change of solvents. On the basis of Anderson model, the additional susceptibility of non-magnetic state is given by,

$$\chi_d = \frac{\mu_B^2 \rho_d(E_F)}{1 - (U + 4J)\,\rho_d(E_F)/10} \qquad (1)$$

where $U + 4J$ is the effective intra-atomic Coulomb interaction and $\rho_d(E_F)$ is the density of states of TM solutes at the Fermi level as follows,

$$\rho_d(E_F) = \frac{10}{\pi} \frac{\Delta}{(E_F - E_d)^2 + \Delta^2} = \frac{10}{\pi\Delta} \sin^2\left(\frac{\pi N_d}{10}\right) \qquad (2)$$

where N_d is the number of localized 3d-electrons. These parameters N_d, Δ and $U + 4J$ are estimated using eq.(1) from the experimental values of V, Co and Ni solutes. According to this approach, the additional susceptibilities for liquid metal solvents mainly depend on the change of Δ which relates to the density of states of solvent metals. Moreover, the changing trend of additional susceptibilities in going from liquid Sb to liquid Te solvent is explained from the decreasing of N_d and the increasing of $(U + 4J)/\Delta$. The additional susceptibilities of Cr, Mn and Fe solutes are expressed by Curie-Weiss low and can be fitted by choosing the suitable parameters.

PH19 D-C ELECTRICAL RESISTIVITY IN THE AMORPHOUS-CRYSTALLINE TRANSITION OF Cu_{60}-Zr_{40} ALLOY SYSTEM. M. A. Otooni, Metallic Materials Branch, Materials and Manufacturing Technology Division, Fire Control and Small Caliber Weapon Systems Laboratory, US Army Armament Research and Development Command, Dover, NJ 07801.

Rapidly solidified copper - 40 at % zirconium, prepared by melt-quenching techniques, have been examined through D-C electrical resistivity response analysis, as a function of isothermal annealing. Associative techniques of differential scanning calorimetry, high resolution transmission microscopy, and high energy electron diffraction microscopy are employed to assess the onset of crystallization and attendant microstructural evolution. Low temperature resistivity measurements of isothermally annealed specimens reveal an abrupt increase in the D-C resistivity values followed by more moderate increase in the resistivity with increasing annealing times and temperatures. The resistivity record is void of any discontinuity suggesting absence of plausible stages in the crystallization procedures. The electron microscopic examinations of the amorphous specimens, however, indicate that crystallization event progresses through several stages. This lack of correlation is interpretable when viewed from point of the insensitivity of the electrical response of the localized perturbations of near atomic size dimensions occuring at the onset of each stage of the crystallization.

POSTER SESSION PI: SURFACES AND HYDRIDES

PI1 THERMODYNAMICS OF HYDROGEN ABSORPTION IN AMORPHOUS Zr Ni ALLOYS

K Aoki, M.Kamachi and T Masumoto, The Research Institute for Iron, Steel and Other Metals, Tohoku University, Sendai 980, Japan

The pressure-composition-temperature(PCT) relationships are presented for amorphous and crystalline Zr-Ni alloys in the range of 373 to 573K. The hydrogen absorbed in the amorphous alloys forms solid solution. The hydrogen absorption in the amorphous alloys obeys Sieverts' law in the range of low hydrogen concentration and deviates positively from the law with increasing hydrogen content. The hydrogen absorbed in the crystalline alloys forms the metal hydrides.

Partial molar thermodynamic parameters, $\Delta\bar{H}$ and $\Delta\bar{S}$, obtained from PCT, for the absorption of hydrogen in the amorphous alloys take minimum values. For instance, for the $Zr_{50}Ni_{50}$, $\Delta\bar{H}$ and $\Delta\bar{S}$ decrease to minima at 0.4 H/M, and their values are 36(KJ/mol H) and 57(J/K·mol H), respectively as seen in Fig. 1. For the crystalline $Zr_{50}Ni_{50}$, both $\Delta\bar{H}$ and $\Delta\bar{S}$ decrease monotonously with hydrogen content and get to a constant level. The characteristic variation of $\Delta\bar{H}$ and $\Delta\bar{S}$ with hydrogen content in the amorphous alloys correspond to the change in the local environment around hydrogen atoms.

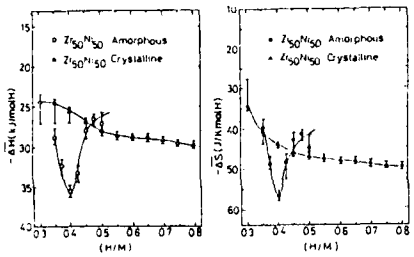

Fig.1 Variations in the relative partial molar enthalpy and entropy for the Zr-Ni-H.

PI3 HYDROGEN IN AMORPHOROUS MAGNETIC RE-TM ALLOYS: A NEW APPROACH

D.W. Forester, P. Lubitz, J.H. Schelleng, and C. Vittoria, Naval Research Laboratory, Washington, DC 20375

We have developed a synthesis procedure which allows rapid rate absorption and subsequent storage of hydrogen in amorphous rare earth-transition metal (RE-TM) alloys. The procedure employs electron beam thin film deposition of the RE-TM alloy films with appropriate overcoating. Surface activation energy is virtually eliminated and hydrogen readily enters the composite at ambient temperature and at pressures < 1 micro-meter Hg. Measured H/RE atomic ratios vary from 2 to 6 depending on composition. The magnetic properties are altered dramatically especially with respect to the Curie and compensation temperatures. Data will be presented for representative alloy systems including Gd_xFe_{1-x}. Potential applications will also be discussed.

PI2 EXPERIMENTAL STUDY OF DENSITY PROFILE IN THE LIQUID-VAPOR INTERFACE OF MERCURY AND GALLIUM

L. Bosio, R. Cortès, A. Defrain and M. Oumezine, G.R.4 du CNRS, Tour 22, 4 Place Jussieu, 752[illegible] IS CEDEX 05, France.

While the bulk isotropic fluids have been intensively studied, i.e. the structure of most of the liquid metals is now relatively well-known, the interfacial region between liquid and vapor (or gas) still remains an open subject both for theoretical approaches and for experimental determinations [1]. Except the results from computer simulation, little is known about the density profile in the surface zone and there is scarcely any experimental information on the structure of the interface [2].

Taking advantage of the fact that at X-ray frequencies the refractive index of condensed matter is less than unity, it is possible to obtain reflection from surface if the grazing angles do not exceed one order of magnitude of some critical angle, typically equal to 10 mrad. By comparing the X-ray reflectivity as a function of angle to the one calculated using various density profile models it is possible to conclude about the validity of the models. Since the pioneer-work of Steps [3] the method has been improved and successfully developped by S. Rice and his group [4]. Using a similar technique we have determined within 0-80 mrad the angular dependence of the Cr-K_α-radiation reflection of liquid mercury in the temperature range 270 to 310 K. Experiments have also been performed on liquid gallium at 323 K. Subdividing the transition region into a subset of elemental strata, the thickness of the interphase zone has been calculated.

[1] C.A. Croxton, "Statistical Mechanics of Liquid Surface", Wiley, Chichester (1980)

[2] J.S. Rowlinson and B. Widom, "Molecular Theory of Capillarity", Clarendon Press, Oxford (1982).

[3] H. Steps, Ann. der Phys. (1933), 16, 949.

[4] D. Sluis et al., J. Chem. Phys. (1983), 78, 1611.

PI4 MONTE CARLO SIMULATIONS OF THE LIQUID-VAPOR INTERFACE OF SODIUM-CESIUM ALLOYS.

J.Gryko and S.A.Rice, Department of Chemistry and The James Franck Institute, The University of Chicago, Chicago, Ill 60637 USA

Using an effective hamiltonian derived from a pseudopotential theory we have carried out Monte Carlo simulation of the liquid- vapor interface of sodium-cesium alloys. In the framework of this effective hamiltonian the total energy of the metal is the sum of a so called structure independent energy and an ion-ion interaction. The ion-ion interaction potential and structure independent energy are calculated using an energy independent pseudopotential. This pseudopotential gives satisfactory results for the total energy of sodium and cesium and also for the pair correlation function of sodium-cesium alloys. In our calculations ions in the surface layer where the average electron density is less than the density of the critical point are considered "vaporized". The interaction of such vaporized atoms with the metal surface is described by a modified van der Waals potential.

The results of our simulations show that ion density oscillations extend from the surface into bulk of the alloy for several atomic layers. The oscillations of the total ion density, in the case of sodium-cesium alloys, are similar to those observed in pure metals. However, the atomic composition of the surface layer of the alloy is different from the composition of the bulk metal. We have found that the concentration of cesium in the surface layer is significantly higher than in the bulk. This surface segregation is ascribed to the large difference between the ionic radii of sodium and cesium.

PI5 THEORY OF SURFACE PROPERTIES OF LIQUID METALS.
M. Hasegawa and M. Watabe, Faculty of Integrated Arts and Sciences, Hiroshima University, Hiroshima 730 Japan

A new formulation for the liquid metal surface is presented. Liquid metals may be considered as a collection of coduction electrons and classical ions, and the total Hamiltonian can be rearranged into a form which consists of the electron gas (or jellium) term, one component classical plasma (OCP) term, and the interaction between them. Inhomogeneous electron gas with a planer surface is taken as the unperturbed system and the electronic state is calculated up to second order in the electron ion pseudopotential. By this procedure screening effect is included, which plays an important role in determining surface properties. The problem then reduces to that of a classical system interacting via position-dependent two-body potential. To solve the energetics of this system we employ the variational method using an inhomogeneous OCP as the reference system. The gradient expansion is used to treat both the electron gas and OCP.

We find that the surface tension of liquid alkali metals can be reproduced by this method with the use of the local density approximation for the screening function and the bulk structure factor in the surface region. But the surface profile is too steep and unrealistic. Consistent treatments of the gradient expansion of the OCP and its structure factor in the surface region are found to be essential in determining the surface profile in the present approach. This problem will be examined extensively. Comparisons also will be made with the previous calculations in which the hard-sphere reference system was used instead of the OCP.

References

R. Evans and M. Hasegawa, J. Phys. C : Solid St. Phys. 14 5225 (1981)

M. Hasegawa and M. Watabe, J. Phys. C : Solid St. Phys. 15 353 (1982)

PI6 DISTRIBUTION OF ACTIVATION ENERGIES IN Zr_2PdH_x. L. E. Hazelton, California Institute of Technology, Pasadena, CA 91125 USA

Internal friction measurements using the vibrating-reed method have been made on melt-spun ribbons of Zr_2Pd, annealed or hydrogenated in the gas at 200 C As hydrogen was added a peak grew and shifted to lower temperatures with increasing X The peak is broader than a single Debye peak, particularly on the low-temperature side where there is a long tail. Evidence will be presented that this is due to a distribution of activation energies for hopping, lying below about 0.5 eV The relaxation spectrum calculated by deconvoluting the internal friction data at different values of X will be presented, with comments on the shape of the spectrum.

PI7 HYDROGEN IN Ni-Zr-B METALLIC GLASSES

U. Köster and H.-W. Schroeder, Dept. Chem. Eng., University Dortmund, D-4600 Dortmund, F.R.Germany

With increasing boron content Ni-Zr-B metallic glasses may exhibit a phase transformation (1) or a more continuous transition from the structure of an intertransition metal glass to that of a metal-metalloid-glass. Ni-Zr glasses are know for a large solubility of hydrogen, whereas most metal-metalloid glasses have been found to solve only minor amounts (2). Such structural changes should influence hydrogen solubility significantly.

Ni-Zr-B glasses were prepared by melt spinning under a helium atmosphere of 200 mbar He. Cathodic hydrogen charging was done in 1 N H_2SO_4-solution with addition of Na_2HAsO_4 (4mg/l) at a current density i=500 A/m². Hydrogen concentrations have been estimated using a microbalance with an accuracy of 1ug or an electrochemical permeation technique.

With increasing boron content a significant decrease in hydrogen solubility have been observed for a number of Ni-Zr glasses. Hydrogen solubility depends strongly on the amount of relaxation of the metallic glass. Therefore, the influence of relaxation was studied systematically to ensure, that not only differences in quenched-in excess free volume are responsible for the observed differences in hydrogen solubility.

Our results will be discussed in comparison with structural models and electronic structure data of other authors. Such a decrease in hydrogen solubility with increasing boron content may be considered to be due to a phase separation into the two different glass structures or due to an increasing electron transfer from the boron atoms. Additional investigations on ductility versus hydrogen content by bending tests and fractography indicate that hydrogen as well as boron reduces the cohesion between interatomic bonds, thus giving more evidence for a model assuming an increasing electron transfer.

(1) W.L. Johnson, A.Y.L. Mak, private communication

(2) A.J. Maeland, "Hydrogen Absorption in Metallic Glasses", in: Metal Hydrides, Plenum Press 1981, p.177ff.

PI8 EFFECTS OF ELEMENTAL ADDITIONS AND SUPERHEAT ON MELT SURFACE TENSION AND METALLIC GLASS EMBRITTLEMENT. H.H. Liebermann, Metglas Products - An Allied Company, 6 Eastmans Rd., Parsippany, NJ 07054 USA

Alloys such as $Fe_{81.5}B_{14.5}Si_4$, $Fe_{40}Ni_{40}B_{20}$, and $Ni_{81.5}B_{14.5}Si_4$ are known to form metallic glasses on rapid quenching from the melt. The elements Sb, Se and Te are strongly surface active in molten iron. Additions of these and some other elements to the base alloys cited have been investigated with regard to effects on melt surface tension and resultant metallic glass formation and characteristics. Surface tension of the molten alloys has been measured as a function of composition and temperature using a variation of the maximum bubble pressure method. The density of molten $Fe_{40}Ni_{20}B_{20}$ alloy has been measured as a function of temperature. Attempts to chill block melt-spin the alloys of the present investigation into metallic glass ribbons were largely successful. A few compositions were partially crystalline in the as-cast state and even fewer were not at all castable. The amorphous structure of ribbons made was assessed by transmission Laue X-ray diffraction. Differential scanning calorimetry and embrittlement temperatures for one hour anneals have been used to provide additional characterization. A correlation has been established between changes in melt surface tension and metallic glass embrittlement temperature with the addition of surface active elements.

PI9 SURFACE MODES IN SPIN WAVE RESONANCE IN THIN AMORPHOUS FILMS

L. J. Maksymowicz, D. Sendorek
Academy of Mining and Metallurgy, Department of Solid State Physics, 30-059 Kraków, al. Mickiewicza 30

Surface modes in spin wave resonance in thin amorphous films of GdCoMo alloys were studied. The samples were obtained with RF sputtering technique and a bias voltage was applied. Technical conditions were carefully predetermined for which surface modes were excited in the resonance experiment. One surface mode was present for samples just after deposition and two modes could be observed in some cases for the same samples kept at room temperature for two or three months.

The observed surface modes were described within the Surface Inhomogeneity (SI) model with symmetrical or non - symmetrical boundary conditions for one or two surface modes, respectively. The experimental data on the position of the surface modes and the first volume mode against the orientation of the external field determine surface anisotropy constant K_s. The fitted values K_s agree with theoretically predicted ones and they are also compatible with numbers found by experimentalists for monocrystalline, polycrystalline or amorphous films. Temperature dependence of K_s was also studied.

For all samples we determined the critical angles Θ_c's between the external magnetic field and the normal to the film plane for which the position of the surface mode coincides with the position of the first volume mode. The corresponding critical angles Ψ_c's for the magnetization differ from $\pi/4$ which suggest the presence of surface inhomogeneities of the magnetization distribution.

PI10 DIFFUSION OF HYDROGEN IN SOME AMORPHOUS ALLOYS

Y. Sakamoto and K. Baba, Department of Materials Science and Engineering, Nagasaki University, Nagasaki 852, Japan

The hydrogen diffusivities in Pd-Si base amorphous alloys of $(Pd_{0.9}X_{0.1})_{82}Si_{18}$ (X = Ag, Cu, Ni, Fe, Cr) and Fe base amorphous alloys of $Fe_{81}B_{13.5}Si_{3.5}C_2$ and $Fe_{78}B_{13}Si_9$ were measured in the vicinity of room temperature by an electrochemical permeation method.

The specimens were 30 ~ 35 μm thick and they were electrolytically charged with hydrogen in 160 mol m^{-3} H_2SO_4 + 2.5×10^{-3} kg m^{-3} H_2SeO_3 solution, and for permeation measurement through Fe base alloys in 30 mol m^{-3} H_2SO_4 + 2.0×10^{-2} kg m^{-3} H_2SeO_3 solution at various current densities of i_c = 5 ~ 250 A m^{-2} and a 0.1 kmol m^{-3} NaOH solution on the diffusion side was used. The diffusivity (D) and concentration of hydrogen beneath the cathodic surface were determined from the build-up transient by the relation of $\log(t^{1/2} J_t)$ vs. $1/t$, which is the first term approximation of diffusion equation derived under the boundary condition of constant hydrogen concentration beneath the cathodic surface.

The diffusivity in all the specimens increased more or less with increasing cathodic current density, i.e., with hydrogen concentration. The hydrogen concentration dependence of diffusivity was qualitatively explained by the thermodynamic factor based on the chemical potential gradient of hydrogen for the driving force of diffusion. The diffusivity values at 301 K in Pd-Si base alloys were $D = 8.5 \times 10^{-13} \sim 1.4 \times 10^{-12}$ $m^2 s^{-1}$ at i_c = 100 A m^{-2}, nearly not depending on the alloying composition. These values exhibited a decrease of about 1 ~ 2 orders of magnitude, compared with that in crystalline pure Pd. The activation energies for diffusion in Pd-Si base alloys were about ΔH_D = 16 ~ 21 kJ mol^{-1}. The diffusivity value in $Fe_{81}B_{13.5}Si_{3.5}C_2$ alloy at 301 K was $D = 1.2 \times 10^{-14}$ $m^2 s^{-1}$ and the value in $Fe_{78}B_{13}Si_9$ alloy was $D = 2.5 \times 10^{-15}$ $m^2 s^{-1}$ at i_c = 100 A m^{-2} and these values were smaller about 5 orders of magnitude than that in annealed crystalline iron. The activation energies for diffusion in both Fe base alloys were ΔH_D = 32 ~ 38 kJ mol^{-1}.

PI11 ELECTROCHEMICAL CHARACTERIZATION OF AMORPHOUS AND MICROCRYSTALLINE METALS

R.G. Walmsley, Y.S. Lee, A.F. Marshall and D.A. Stevenson, Stanford University, Stanford, CA 94305 USA

A study of the relation between the preparation, the microstructure and the corrosion behavior of Cu-Zr and Cu-Ti amorphous and microcrystalline alloys is reported, with particular reference to differences between the amorphous and the stable crystalline forms of these alloys. The passive current density upon potentiodynamic anodic polarization was used as a criterion for corrosion tendency.

Samples were prepared by planar magnetron sputter deposition using a phase spread and a rotating substrate method and were characterized using x-ray diffraction (XRD) electron microprobe analysis, differential scanning calorimetry (DSC), transmission electron microscopy (TEM) and a small area potentiodynamic anodic polarization cell.

Significantly lower passive current densities were observed for the amorphous or microcrystalline state (compared with the crystallized alloys) in both alloy systems for compositions < 20 at% Zr or Ti in Cu. For higher concentrations, however, there is little difference between the crystallized and the amorphous state, for the amorphous samples prepared by the rotating substrate deposition mode. This behavior was explained by the presence of an active Cu rich phase at the lower concentrations for the crystallized alloys, as predicted from the equilibrium phase diagram and confirmed by TEM. For Cu-Zr samples, in the range of 30-65 at% Zr in Cu prepared by the phase spread technique, however, significantly higher passive current densities were observed. A proposed explanation for this unexpected behavior is the development of amorphous-amorphous phase separation for the phase spread samples. Confirming evidence for this proposal is provided by XRD, DSC and TEM.

PI12 THE SURFACE COMPOSITION OF LIQUID Fe-Mn AND Fe-S SYSTEMS. Jingtang Wang, Maoshu Bian, Luming Ma, Institute of Metal Research Academic Sinica.

The effect of sulfur and manganese on the surface tension of liquid iron was measured by the sessile drop method, and further their adsorption values at iron surface were calculated by Gibbs equation. In order to compare the calculated adsorption values with certain directly measured values and to further investigate the distribution f surfaceactive elements in different depth from the surface, the surface composition of binary systems (Fe-S and Fe-Mn) was analyzed layer by layer by Auger Electron Spectroscopy (AES) and/or glowing analysis technique. The experimental samples were prepared in high purity Ar atmosphere and maintained a bit above melting point for a period of time, in order to approach thermodynamic balance, and then rapidly solidified. After that, the samples were analyzed layer by layer. A low manganese concentration range is observed on the curve of manganese distribution, and a low sulfur concentration range on the curve of sulfur distribution.

In is observed that the segregation coefficient of high surface- active element sulfur is larger than that of the element Mn about two orders of magnitude. These results show some analogy to that obtained from the study of surface tension for the binary systems (Fe-S and Fe-Mn).

POSTER SESSION PJ: MODELING

PJ1 ISOTROPIC VARIATION IN $s^{-\alpha}$ OF THE SMALL ANGLE SCATTERING OBTAINED FROM A DENSITY MODEL BASED ON A RANDOM SPACE FUNCTION (POINT GEOMETRY). APPLICATION TO $\alpha = 3$.
B. Boucher, P. Chieux*, P. Convert*, M. Tournarie ; DPh.G-SRM CEN-Saclay, 91191 Gif-sur-Yvette Cedex, France ; *ILL, 156X 38042 Grenoble, France.

We calculate the scattering from a system of parallel planes with random separations. The density h(x) (electronic, nuclear or magnetic) is taken to vary as a function of x the distance from the planes. The particular variation would depend on the sample and is taken to be the same for all the planes. We assume that there are N families of planes (N is large) whose directions are randomly oriented. We show that the scattering along a direction in reciprocal space is : $I(s) = N \beta v V |H(s)|^2/(2\pi s^2)$ where β is the probability of crossing 1 plane per unit length, Nv is the exposed volume of the sample, V is the reciprocal space volume examined by the spectrometer, H(s) is the linear Fourier transform of the density h(x). If $|h(x)|$ varies as $1/\sqrt{|x|}$, then $|H(s)|$ varies as $1/\sqrt{|s|}$ and I(s) varies as s^{-3}. This relation is isotropic and holds for all (except very large values) of s. In this model no limiting hypothesis is made a) concerning the distribution of orientations of the planes and it remains valid if the family of planes are either superimposed or juxtaposed ; b) concerning the nature of the sample (crystalline/amorphous) although a random distribution of separation between planes is more relevant to amorphous systems.

We discuss the limits and applicability of the model which accounts for the experimentally observed variation in s^{-3}(1,2). This result complements those of a previous model (3) where h(x) was related to a spherical shell. This suggests that the same result could be obtained if the surface was not taken to be a regular plane or sphere.

(1) B. BOUCHER, J. de Phys. C8 (1980) 135
(2) E. NOLD, S. STEEB, P. LAMPARTER, G. RAINER-HARBACH de Phys. C8 (1980) 186.
(3) B. BOUCHER, P. CHIEUX, P. CONVERT, M. TOURNARIE, J. of Physics F. (in press).

PJ2 SPECTRUM OF ELECTRIC FIELD-GRADIENT FLUCTUATIONS IN LIQUID RUBIDIUM. J. Bosse and C. Wetzel, Freie Universität Berlin, Berlin (West), Germany

Mode-coupling theory results of the spectral function of electric field-gradient (Efg) correlations in the liquid metal rubidium are presented. The small-frequency behavior of the calculated quantity determines the quadrupolar contributions to NMR-linewidths. We used the Price,Singwi,Tosi pair-potential and an Efg-potential which takes account of r-dependent Sternheimer antishielding effects.

The theoretical results are compared with computer simulation results using the same potential functions. The comparison shows that our mode-coupling approximation presents a reliable tool for the calculation of Efg-correlation times, the knowledge of which is essential for the interpretation of NMR-relaxation data in liquid metals.

PJ3 DISORDER STRUCTURE OF MOLTEN MONATOMIC METALS, SEMIMETALS AND SEMICONDUCTORS
M.Davidović, M.Stojić and Dj.Jović, Boris Kidrič Institute of Nuclear Sciences, Vinča, Belgrade, Yugoslavia

In the last twenty years the static properties of liquid metals, semimetals and semiconductors in molten state are mainly studied experimentally and numerically without extensive modelling of the structure. From numerous neutron or X-ray data it is obvious that the liquid phase shows much more structure irregularity than the solid state. Recently we proposed the model[1,2] of disordered structure of liquid through a certain atomic state degeneracy which apears around single vacancies in order to explain the experimentally observed double structure of S(q). A quantitative proof of the existence of irregular structure located in the vicinity of a single vacancy is a main goal of this work. Namely, around the vacancy an additional structure exists in which the mean interatomic distance $\langle r' \rangle$ is smaller compared to the distance r in the regular liquid structure. From neutron diffraction data the irregularity of S(q) is more pronounced in semiconductors and semimetals than in simple monatomic liquid metals. Such a real liquid structure consisting of two substructures, characterised by interatomic distances r and r', is expected to manifest physical properties such as electrical conductivity, visocosity, selfdiffusion etc. The inclusion of mean values $\langle r \rangle$ and $\langle r' \rangle$ in the existing models defining the above quantities should give better agreement between theoretical and experimental results.

References

1. M.Davidović, M.Stojić and Dj.Jović, J.Phys.C. 000,000(1983).
2. M.Davidović, M.Stojić and Dj.Jović, to be published.

PJ4 COLLECTIVE EXCITATIONS IN METALLIC GLASSES
J.Hafner, Institut für Theoretische Physik, Technische Universität, A 1040 Wien, Austria and Laboratoire de Thermodynamique et Physico-Chimie Métallurgiques, E.N.S.E.E.G., F 38402 Saint Martin d'Hères, France

The results of ab-initio calculations of the normal modes of vibration of amorphous alloys of normal metals are presented. The computations are based on pseudopotential-derived interatomic forces, a novel variant of the cluster-relaxation technique for the determination of the static equilibrium density and structure, and on the recursion technique for the calculation of the vibrational spectra. For both longitudinal and transverse vibrations the dispersion relations of two distinct modes - corresponding to the acoustic and optic modes of a two-component crystal - could be determined. At very long wavelength these modes correspond to collective density and concentration fluctuations, at shorter wavelength they can be identified with the incoherent vibrations of the two atomic species. For longitudinal excitations the result can be compared with recent neutron inelastic scattering experiments and good agreement is found.

The influence of variations of the local structural parameters and of the external pressure on the vibrational spectrum has been investigated.

PJ5 STRUCTURE OF MULTI-COMPONENT HARD-SPHERE MIXTURES --- APPLICATION TO THE LIQUID Li-Pb ALLOY

Kozo Hoshino, Faculty of Engineering, Niigata University, Niigata 950-21, Japan

A general formula for the partial structure factors of an m-component mixture is derived. The compressibility of the mixture obtained by Kirkwood and Buff(1) can be written in terms of the partial structure factors in the long-wavelength limit.

For the m-component hard-sphere system, the explicit expressions for the partial structure factors are obtained based on the exact solution of the Ornstein-Zernike equation due to Hiroike(2). The total structure factor, which can be obtained experimentally by the neutrons, the X-rays and the electrons diffraction, can be expressed by the partial structure factors.

The formulae are applied to the liquid Li-Pb alloy. Following Hoshino and Young(3) we consider the liquid Li-Pb alloy as a ternary mixture of Li, Pb and Li_4Pb and approximate these by the hard spheres with different diameters. The total structure factor is calculated for the ternary hard-sphere mixture based on the coherent neutron scattering intensity formulated by Bhatia and Ratti(4). It is shown that the theoretical total structure factor can reproduce the characteristic features of the recent neutron diffraction data due to Ruppersberg and Reiter(5).

(1) Kirkwood J G and Buff F P 1951 J.Chem.Phys. 19 774
(2) Hiroike K 1969 J.Phys.Soc.Jpn. 27 1415
(3) Hoshino K and Young W H 1980 J.Phys.F 10 1365
(4) Bhatia A B and Ratti V K 1976 J.Phys. F 6 927
(5) Ruppersberg H and Reiter H 1982 J.Phys.F 12 1311

PJ6 THE DISCLINATION MODEL OF NON-HOMOGENEOUS DEFORMATION IN AMORPHOUS ALLOYS. Gui Jianin and Wang Zixiao, Department of Physics, Wuhan University, Wuhan, China.

A disclination model, containing partial disclination rings, which is based on the amorphous alloy structure of close-packed polyhedral microclusters proposed by Hoare, is proposed to explain the non- homogeneous deformation and localized strain harding observed on amorphous alloys.

The approximate strain energy density of the model is estimated. As the shear modulus of amorphous alloy is lower, and the characteristic vector ω and radius R for partial disclination rings may be very small, the energetic feasibility of the model is demonstrated.

The function of disclination as sources and sinks for dislocations during deformation is discussed. Under the action of applied stress, the plastic flow initiates at stress concentration by the displacement of disclinations and the emission and absorption of dislocation by them.

It is suggested that in amorphous alloys, in a sense, dislocation may be a kind of instantaneous structure defect, which exists only in the period of motion, as suggested by Pampillo.

The multiplication of disclinations and the interaction between the disclinations, and disclinations and dislocations may be the causes of the localized strain harding.

PJ7 NATURE OF AMORPHOUS AND LIQUID STRUCTURES — COMPUTER SIMULATIONS AND STATISTICAL GEOMETRY

M.Kimura, Tokyo Institute of Technology, Tokyo 152 Japan and F.Yonezawa, Keio University, Yokohama 223 Japan

A purpose of our work is to study the nature of liquid and amorphous structures by making the best use of computer simulations.

Generally, materials in liquid and amorphous states are known to contain topological disorder in atomic distributions. However, the characterization of topologically-disordered structure, important though it is, remains under-developed because of its extreme difficulty. The experimentally measurable structural properties are the structure factor S(q) and its Fourier transform g(r). They are described in linearlized forms where the detailed three-dimensional information is lost as a result of statistical averages. In particular, S(q) and g(r) tell nothing about the intermediate-range structures which are believed to distinguish different kinds of topological disorder. Therefore, it is highly significant to exploit some methods of three-dimensional characterization of these structures.

With this situation in mind, we have carried out:
1) Synthesis of various liquid and amorphous structures by computer simulations. The advantage of computer-produced model systems consists in that all molecular-level outputs are available.
2) Characterization of topologically-disordered structures in these model systems by means of the Voronoi-Delaunay analyses and other methods of statistical geometry. We have introduced several new ways of structure characterization.
3) Measurements of various physical properties of the model systems and the identification of the relationships between the atomic-level structures and the macroscopically observable physical properties.

We put emphasis on the discussions of; how glasses and liquids are characterized by the intermediate-range structures (IRS), in what way the IRS is influenced by the interatomic potentials and how far the IRS is reflected to the macroscopic physical quantities.

PJ8 TOPOLOGICAL AND CHEMICAL ORDERING IN A TWO-ATOMS SIMULATED AMORPHOUS STRUCTURE.

F. Lançon, L. Billard, A. Chamberod, Centre d'Etudes Nucléaires de Grenoble, Département de Recherche Fondamentale Section de Physique du Solide, 85 X, 38041, Grenoble Cedex, France.

As there is still some controversy about the nature of topological and chemical ordering in soft sphere packings, we have tried to analyze some aspects of this problem with an application to $Pd_{80}Si_{20}$.

We have constructed a sample of prismatic units.We have relaxed it ,using three pair potentials associated with the three types of pairs. We have been able to follow the progressive destruction of prisms along the numerical relaxation process.

On the other hand, we have also relaxed another packing with topological and chemical initial randomness. It appears that the resulting relaxed sample has the same characteristics as that starting with prismatic units, and we have thus no evidence of local well defined geometric units in a relaxed sample.

Furthermore we propose an analysis of the local structure ; we first define the so-called Voronoï pairs of nearst neighbours. This gives a full decomposition of the random network into tetrahedral units. Then, we distinguish between short and long pairs, so that we can obtain polyhedral units made of tetrahedra sharing long pairs. We give a description of the variety of entities thus obtained.

Finally, in a relaxed sample of one-type atoms, we introduce metalloïds in the interstices of convenient size. Then relaxing this binary packing, we show that metalloïds keep this metallic environment. However, this simple scheme breaks down for a metalloïd concentration above about six per cent : in this case, a full reorganization occurs during relaxation.

AD-A134 441 INTERNATIONEL CONFERENCE ON LIQUID AND AMORPHOUS MET2L 1/2
(5TH) HELD AT LOS..(U) CALIFORNIA UNIV LOS ANGELES DEPT
OF MATERIALS SCIENCE AND ENG.. 19 AUG 83

UNCLASSIFIED F/G 11/6 NL

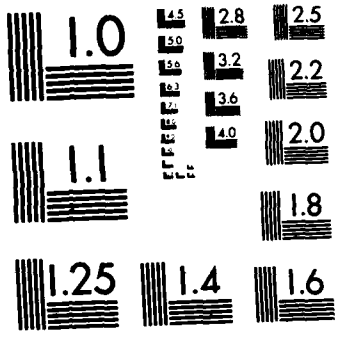

MICROCOPY RESOLUTION TEST CHART
NATIONAL BUREAU OF STANDARDS-1963-A

PJ9 A COMPUTER-SIMULATED STRUCTURAL MODEL FOR $Fe_{80}B_{20}$. L.J. Lewis and R. Harris, Department of Physics, McGill University, Montreal, Quebec, Canada H3A 2T8.

A computer-simulated model for the structure of the $Fe_{80}B_{20}$ metallic glass is presented and discussed. As in our previous calculations (1), this model is based on the analogy between local environments in crystalline and amorphous phases. The structure is generated using a generalization of Bennett's DRPHS algorithm and further relaxed by a conjugate-gradient steepest-descent search. In addition, a rigorous control of composition has now been implemented in the algorithm, which results in a precise description of the structure.

Structural information from our model is compared with recent measurements by Nold et al (2) of the partial structure factors for this material. In particular, our model gives a good account of the pair and number-concentration structure factors and radial distribution functions. Further, analysis of the model in terms of coordination numbers and Warren parameters shows the material to possess strong short-range order, in accord with experimental data. Finally, comparison of the concentration correlation structure factor with that of crystalline Fe_3B could provide some insight into the behavior of thermopower in Fe-B glasses.

(1) R. Harris and L.J. Lewis, Phys. Rev. B25, 4997 (1982).
(2) E. Nold, P. Lamparter, H. Olbrich, G. Rainer-Harbach and S. Steeb, Z. Naturforsch, 36a, 1032 (1981).

PJ10 A MODEL FOR THE KINETICS OF TSRO AND CSRO STRUCTURAL RELAXATION IN METALLIC GLASSES: COMPARISON WITH EXPERIMENTAL RESULTS. I. Majewska-Glabus, B.J. Thijsse and S. Radelaar, Laboratory of Metallurgy, Delft University of Technology, Rotterdamseweg 137, 2628 AL Delft, The Netherlands

Recently a model was developed for the simultaneous description of topological and chemical structural relaxation in metallic glasses (1). We have extended this model by introducing a spectrum of activation energies for the reversible chemical part of the relaxation processes. Also the influence of a free volume dependent activation energy for topological relaxation was studied.

It will be demonstrated that the results of the present model

a) agree well with experimentally observed DSC results, both for as-quenched and for preannealed glasses,
b) permit a study of the influence of the quenching rate on subsequent structural relaxation.
c) provide guidelines for the experimental separation of CSRO and TSRO contributions to DSC behaviour.

Moreover, it will be shown that the effect of relaxation on the electrical resistance, as measured for $Fe_{40}Ni_{40}P_{14}B_6$ (2), is also closely predicted by the model.

1) A. van den Beukel and S. Radelaar, Acta Met. 31 (1983) 419.
2) M.E. Sonius, B.J. Thijsse and A. van den Beukel. To appear in Scripta Met. (1983).

PJ11 GEOMETRICAL FEATURES OF DENSE RANDOM PACKED STRUCTURE OF SPHERES. T. Ninomiya, Department of Physics, University of Tokyo, Bunkyo-ku, Tokyo 113, JAPAN

Geometrical features of the structure of amorphous metals are investigated by regarding the structure as random packing of tetrahedra (T) and octahedra (O) which have spheres at the vertices. Sequential connection of T's and O's with a common axis forms a planar ring cluster by allowing small elastic distortion. The network showing connectivity of tetrahedra and octahedra consists of the ring clusters. It is found from examination of cells in the network that the existence of noncrystalline rings introduces curvature of local space and that one can draw lines threading through the noncrystalline rings in the same sense as that considered by Rivier for the continuous random network model. In the TO network there are two kinds of lines associated with different local curvatures. The volume of the cell has negative correlation with the coordination number, but has positive correlation with the number of the faces of Voronoi polyhedra.

The lengths of the lines are determined by the deviation of the ratio of the numbers of tetrahedra and octahedra from the crystalline case and by the averaged curvature. It is shown that the structure containing two sizes of atoms such as metal-metalloid systems can be regarded as the structure containing one size of atoms with non-zero averaged curvature.

PJ12 THERMAL PRESSURE COEFFICIENTS OF LIQUID ALKALI METALS. S. Ono, Department of Applied Physics, National Defense Academy, Yokosuka 239, Japan (Tel: 0468-41-3810 ext 2209), I. Yokoyama+, School of Mathematics and Physics, University of East Anglia, Norwich, NR4 7TJ, UK, and T. Satoh, Department of Mathematics and Physics, National Defense Academy, Yokosuka 239, Japan.

The Percus-Yevick[1] phonon method is applied to liquid alkali metals for predicting thermal pressure coefficients using the analytic expression of the classical one-component plasma structure factor $a_{ocp}(k)$ developed by Chaturvedi and coworkers[2-4]. Satisfactory agreement with experimental results is obtained, though this could be somewhat fortuitous in the light of the inadequate description of $a_{ocp}(k)$ in the low k-region.

REFERENCES

1) J.K. Percus and G.J. Yevick, Phys. Rev., 110, 1 (1958)
2) D.K. Chaturvedi, G. Senatore and M.P. Tosi, Lett. N. Cimento, 30, 47 (1981)
3) D.K. Chaturvedi, M. Rovere, G. Senatore and M.P. Tosi, Physica 111B, 11 (1981)
4) D.K. Chaturvedi, G. Senatore and M.P. Tosi, N. Cimento, 62B, 375 (1981)

PJ13 COUPLING OF TWO-LEVEL SYSTEMS WITH ^{91}Zr NUCLEI IN ZIRCONIUM-BASED AMORPHOUS ALLOYS, A. Ravex and J.C. Lasjaunias, CNRS-CRTBT, BP 166 X,38042 Grenoble Cédex, France

We analyse the very low-temperature specific heat, in the superconducting state, of a series of Zr-based amorphous alloys with two distinct contributions : (i) the low-energy excitations (TLS) characteristic of the amorphous state, with a contribution $C_{TLS} = aT^n$, (ii) a quadrupolar nuclear contribution $C_N T^{-2}$ due to ^{91}Zr nuclei.

The experimental results point out a systematic correlation between the amplitude of the TLS specific heat anomaly and of the nuclear contribution ; this correlation is independant either of the thermal history of samples (temperatures of the sputtering deposition, thermal annealing below the crystallization temperature) or of the nuclear spin of the additional element (Cu, Ni, Ag, Pt). This suggests that the relaxation of the nuclei, which can no longer be ensured in the superconducting state by means of electrons, is restored by a new process via the TLS.

A simple description arguing that relaxation is induced through the modulation of the electric field gradient at a nuclear site by its nearest neighbour TLS, and thereafter achieved by nuclear spin diffusion among Zr nuclei, takes well in account the experimental data.

These results strongly support the existence of TLS at the origin of the low-temperature specific heat excess.

PJ14 RADIATION-INDUCED GROWTH IN AMORPHOUS $Pd_{80}Si_{20}$ AND $Cu_{50}Zr_{50}$ G. Schumacher, S. Klaumünzer, S. Rentzsch, and G. Vogl, Hahn-Meitner-Institut für Kernforschung and Freie Universität Berlin, D-1000 Berlin, Germany

About 30 samples of glassy $Pd_{80}Si_{20}$ and $Cu_{50}Zr_{50}$ were irradiated at temperatures between 50 K and 500 K with high energy (up to 285 MeV) heavy ions (Ar, Kr). Special care was taken to avoid implantation and to achieve a homogeneous distribution of radiation damage. Before and after the bombardments the dimensions of the specimens were measured at room temperature. For some selected samples the mass density was determined by using a modified flotation method. Additionally, the structure factor S(Q) was calculated from measured X-ray data.

No clear changes in S(Q) appeared in the irradiated samples. While changes in mass density are smaller than the measurement error of about 0.2 % drastic growth of the sample dimensions was observed during the irradiations. At a fluence of $5.3 \cdot 10^{14}$ Kr/cm^2, corresponding to about $3 \cdot 10^{-2}$ displacements per sample atom, increases in the sample dimensions perpendicular to the beam direction as large as 16 % were found at irradiation temperatures below 100 K. No tendency to saturation was seen at these high growth levels. This growth is linear in fluence, highly anisotropic and depends strongly on projectile mass and irradiation temperature. There is clear evidence that its anisotropy is determined by the paths of the primary recoil atoms only and not by the structure of the alloy. This is very different from what is known about radiation-induced growth in crystalline metals.

Presumably growth in metallic glasses is a collective atomic phenomenon and common to all amorphous metals. This would imply that under certain (anisotropic) irradiation conditions metallic glasses are very sensitive to radiation damage and not as stable as commonly believed.

PJ15
DISORDERED SYSTEMS: DETERMINATION OF EFFECTIVE PAIR POTENTIALS FROM EXPERIMENTAL STRUCTURE DATA
Wolfram Schommers, Kernforschungszentrum Karlsruhe, Institut für Angewandte Kernphysik I, P.O.B. 3640, D-7500 Karlsruhe, Federal Republic of Germany

In this paper we have compared several methods which connect the effective pair potential to the pair correlation function. These methods are: a self-consistent method using molecular dynamics, the so-called modified STLS theory, the Weeks-Chandler-Andersen approach, the Percus-Yevick theory, the hypernetted chain approximation and the Born-Green equation. Since the pair potential is in general very sensitive to small variations in the pair correlation functions, we had to use structure data with sufficient accuracy in the determination of the pair potentials from the pair correlation function. Narten performed measurements on liquid gallium with high precision, and, therefore, all calculations given in this paper have been performed on the basis on Narten's structure data.

The test of the methods could be done in a rigorous way for the following reason:(i) there is no free parameter in the relations between the pair potential and the pair correlation function, and (ii) we used molecular dynamics in our analysis. It turned out that the self-consistent method and the Weeks-Chandler-Andersen approach lead to reasonable results. The results for the pair potential obtained from the other methods are unsatisfactory and cannot be used in the determination of liquid gallium properties.

PJ16 MOLECULAR DYNAMICS STUDY OF ATOMIC-LEVEL STRUCTURAL PARAMETERS *IN LIQUID AND AMORPHOUS METALS*. V. Vitek, S. P. Chen and T. Egami, Department of Materials Science and Engineering, University of Pennsylvania, Philadelphia, PA. 19104, USA

Atomic level parameters characterizing the local structural fluctuations in amorphous metals, the hydrostatic stress, p, and the von Mises shear stress, τ, have been introduced previously. The structural relaxation was quantitatively explained by considering annihilation of structural fluctuations corresponding to large positive and negative p, and the microscopic events involved in the plastic deformation were correlated with regions of large τ. Furthermore, it has been suggested that the glass transition may be related to freezing of these structural fluctuations.

To investigate the local structural developments at finite temperatures a molecular dynamics study has been carried out for the block containing 867 identical particles interacting via a modified Johnson's potential. The calculation started by first generating a liquid at a high temperature and then gradually cooling the sample while keeping the total volume fixed. The cooling process consisted of gradually decreasing the average velocity of the particles and equilibrating the sample at every step, until the desired lower temperature has been achieved. The local structure and its changes have been analyzed in terms of atomic level stresses throughout this process. When the sample was cooled to the room temperature the average second moments, $\langle p^2 \rangle$ and $\langle \tau^2 \rangle$, reached constant values which were close to those found in the previous static simulations. The dependences of $\langle p^2 \rangle$ and $\langle \tau^2 \rangle$ on temperature show sharp changes of slope at two different temperatures (1900K and 800K, respectively). This supports the recent suggestion of two transition temperatures, the lower being identified with the conventional glass-transition and the upper with the shear glass-transition. The bond orientation order, recently observed by Steinhardt et al., has also been found and its relationship to the above transition temperature phenomena investigated together with the corresponding topological changes.

PJ17 FLUX-PINNING, DEFECTS, AND STRUCTURAL RELAXATION IN AMORPHOUS SUPERCONDUCTING Mo_5Ge_3 FILMS. S. Yoshizumi, W. L. Carter, and T. H. Geballe, Stanford University, Stanford, CA 94305 USA

An investigation to relate flux-pinning behavior in amorphous thin films of Mo_5Ge_3 to their defects or inhomogeneities will be reported. The films were synthesized at room temperature by magnetron sputtering; their amorphous structure has been confirmed by X-ray diffraction and TEM studies. Two types of pinning mechanisms have been observed for amorphous Mo_5Ge_3 films; one dominates at low magnetic field ($h<0.1$) and the other at high magnetic field ($h>0.1$). Films were annealed under purified Ar atmosphere at different temperatures for different periods of time to study structural relaxation. It has been observed that the pinning force at high field is reduced by nucleating Mo_5Ge_3 crystallites in the amorphous matrix, which is contrary to the enhancement of the pinning force observed in other amorphous systems when crystallites are introduced. Flux-pinning behavior for films with different thermal treatments will be presented. Studies are being continued with films synthesized at liquid nitrogen temperatures.

This work is supported by the Air Force Office of Scientific Research Contract No. F49620-82-C0014.

PJ18 PHONON THEORY OF LIQUIDS AND AMORPHOUS METALS:EXTENSION TO UNIVERSAL GENERALIZED-DISORDER VIA STATIC SYNERGETICS. Edward Siegel,415 Seventh Avenue,San Francisco,CA.94118 USA

Static Synergetics[1], the time independent limit of Haken's[2] dynamic synergetics, is used to extend the phonon theory of liquids[3] and frozen liquid phonon theory of glasses[4] dicnotomously to universal generalized-disorder:powders,ferrofluids[5], slushes,suspensions,gels,sols,mixtures,blends,thixotropic liquids...;and to universal function properties:Anderson localization,relaxation response,dielectric function and all dielectric properties,A.C. and D.C.electrical conductivity, 1/f flicker noise(voltage and current)power spectrum,low temperature(homologuous)"two"-level system anomalous thermal, acoustic,...properties....This confluence of the Brillouin-Landau-Feynman-Morrison-Hubbard-Beeby-Omini-Young-Okashima-Matsubara-Nakanishi-Harch-Tosi-Siegel[7] generalized-disorder collective-boson mode-softening universality-principle(G..[6]F) (a collective effort over some fifty years)with Jonscher's[6] universal (dielectric,mechanical,magnetic...)relaxation response with Ngai's[7] universal 1/f flicker noise power spectrum via universal Wigner-Dyson-Ngai infra-red divergence,provides a powerful,flexible tool.Static synergetics is a universal, scalable,reversible mathematical algorithm/experimental model. It requires as input the external radiation inelastic differential scattering cross-section(frequency averaged,integrated or unresolved) $S(k)$,the familiar static structure factor. Applicationis indicated to the liquid metal based ferrofluids ($Hg...Fe_2O_3$)of Poppelwell[8] and the Guntherodt liquid spin glass, liquid metal based ferromagnet (AuCo)...

1.E.Siegel,Electrochemical Soc.Meeting,San Francisco(1983)
2.H.Haken,Series in Synergetics,Springer-Verlag(1970's-1980's)
3.E.Siegel,J.Phys.Chem.Liquids,4,4(1975);5,1(1976)
4.E.Siegel,Int'l.Conf.Latt.Dynam.,Paris(1977);Statphys,Haifa(77)
5.E.Siegel,J.Magnetic Fluids-to be published.;J.Noncryst.Sol. 40,453(1980);S.Takeno & M.Goda,Prog.Theo.Phys.48,5,1468(1972)
6.A.K.Jonscher,Physics of Dielectrics,I.O.P.58,22(1980)
7.K.L.Ngai,Comm.Sol.State Physics,4,127(1979);9,5,141(1980)
8.A.Poppelwell;H.Guntherodt & H.Kunzi,-private communication.

POSTER SESSION PK: ELECTRONIC PROPERTIES III

PK1 FERROMAGNETIC RESONANCE STUDY OF THERMAL STABILITY IN $Fe_{40}Ni_{40}B_{20}$ AMORPHOUS ALLOY, R.S. Parashar, C.S. Sunandana and Anil K. Bhatnagar, School of Physics, University of Hyderabad, Hyderabad 500 134, INDIA

We report here the Ferromagnetic Resonance observations on mechanically polished and isothermally annealed $Fe_{40}Ni_{40}B_{20}$ (VITROVAC 0040) amorphous alloy ribbons in the temperature range 100 - 300°C. Measurements were made on JEOL X Band ESR spectrometer suitably modified for FMR measurements. Observations were made in parallel-vertical (PV) and parallel-Horizontal configurations. The FMR spectra of the as received polished samples exhibit a single resonance curve having a line width of approximately 235 Gauss in the PV configuration. Significant changes are observed in the line widths and the resonance magnetic field depending upon the temperature and annealing time used. Specimens annealed for longer periods show two peaks, each about 150 Gauss wide but differing considerably in intensity and exhibiting distinct saturation behavior. FMR line widths exhibit two maxima when plotted against isothermal annealing time. The first peak is weak in nature and occurs for short annealing times, while the second peak is more intense and occurs for prolonged anneals. This behavior is suggestive of a thermally-induced structural relaxation leading to a two-step crystallization process. There seems to be two magnetic sub-systems each with its own relaxation behavior, precipitating out of the parent amorphous alloy. Additional studies are being carried out to understand these observations.

PK2 ON THE MAGNITUDE OF ELECTRICAL RESISTIVITY OF AMORPHOUS, LIQUID AND CONCENTRATED CRYSTALLINE ALLOYS
D. Pavuna, Department of Physics, University of Leeds, Leeds LS2 9JT, U.K.

The magnitude of electrical resistivity, $\rho_{4.2}$, of glassy alloys varies from ~ 60μΩcm in MgZn up to ~ 300μΩcm in Ti Be Zr. The magnitude of the corresponding liquid phases at the melting point is typically ~ 10-15% lower; a fact closely associated with the temperature coefficient of resistivity at room temperature which is often found to be negative in glassy alloys.

We present the results of detailed measurements of the variation of magnitude of the electrical resistivity across the compositional range in CuTi, CuZr and CuHf glassy alloys and compare them with those obtained for liquid and polycrystalline counterparts. We discuss the role of various conduction mechanisms including the quantum diffusion with interference effects, tunnelling, and d-conduction. We argue that our results can be qualitatively understood in terms of a simple phenomenological two-band model; the nearly free electron models, like the Ziman model, are applicable only at the copper rich end of the alloying range.

We introduce the concept of a reduced phase diagram for resistivity (and possibly other properties) of glassy alloys and show that the change in the magnitude of resistivity within the diagram follows the Nordheim rule similarly to liquid or concentrated crystalline alloys. We correlate this behaviour with the changes in the chemical and/or topological short range order and discuss it by refering to the metallurgical phase diagrams of the alloy-systems studied.

On the basis of the model we suggest several experiments including further resistivity studies and neutron scattering measurements that should strengthen or disprove the validity of the present physical picture.

PK3 ON THE LOCAL DENSITY OF UNOCCUPIED D STATES IN TRANSITION METAL-METALLOID METALLIC GLASSES. Douglas M. Pease, Guy Hayes, M. C. Choi, J. I. Budnick, W. A. Hines, University of Connecticut, Storrs, CT 06268 and R. Hasegawa, Allied Corporation, Morristown, N.J. 07960

New data on the x-ray absorption edge near-in structure of the $(Ni_yPt_{1-y})_{75}P_{25}$ system is compared with previous results on random solid solution alloys and other M-TM metallic glasses. Whereas experimental probes of the density of d states at the Fermi energy, $\rho_d(E_f)$, often indicate a sharp reduction in $\rho_d(E_f)$ due to the presence of metalloids or nontransition metals, absorption edge results usually indicate a negligible decrease in the total number of d holes per transition metal atom in these alloy systems. Results of a recent calculation for a random solid solution alloy suggest a possible means of resolving the apparent discrepancy between measured changes in $\rho_d(E_f)$ and absorption edge results.

PK4 *RESISTOMETRIC STUDY OF SHORT RANGE ORDERING IN METALLIC GLASSES HAVING DIFFERENT FREE VOLUME CONTENT.*
G.Riontino, Chemistry Dept., Fac.Pharmacy, University, I-10125 Torino, Italy
P.Allia and F.Vinai, IENGF and GNSM, I-10125 Torino, Italy

The behavior of the electrical resistivity of metallic glasses, ρ, can be analyzed to investigate compositional and topological short range ordering processes occurring in these alloys during structural relaxation in the glassy state[1].

In the present paper, new results are reported of isothermal resistance measurements at various temperatures T on amorphous ribbons of composition (Fe,Ni)-(Cr,Mo)-P-B prepared by melt spinning at different quenching rates. In these glasses, two temperature regions can be distinguished on the basis of the behavior of the isothermal resistivity as a function of the annealing time t. In the lower temperature region, compositional ordering processes associated with an increase of $\rho_T(t)$ are observed, while in a higher temperature range large variations of the topological short range order occur, resulting in a decrease of $\rho_T(t)$. A coherent shift of all observed resistivity changes towards higher temperature values is observed in alloys prepared with higher quenching rates, suggesting a close relationship between the height of local potential barriers for atomic diffusion processes, and the local excess atomic volume. The rearrangement processes involved in compositional and in topological short range ordering are equally affected by the variation of the free volume, indicating that during structural relaxation either uncorrelated, and more collective atomic motions are regulated in a similar way by the local excess atomic volume.

[1] P.Allia et al., J.Appl.Phys., 53, 8798 (1982)

PK5 THERMAL STABILITY AND MAGNETIC AND ELECTRICAL PROPERTIES IN AMORPHOUS RE-Al ALLOYS

K. Shirakawa, The Research Institute of Electric and Magnetic Alloys, 982, Sendai, Japan, and K. Aoki and T. Masumoto, The Research Institute for Iron, Steel and Other Metals, Tohoku University, 980, Sendai, Japan.

Recently, rare earth (RE) based amorphous alloys have been investigated intensively. In the present study, thermal stability and magnetic and electrical properties have been investigated the various amorphous RE-Al alloys. The ribbon samples of $RE_{1-x}Al_x$ ($0.2 < x < 0.8$) have been prepared by melt-quenching in an argon atomosphere. The thermal stability was studied by means of a differential scanning calorimeter (DSC) with a heating of 10 °C/min. The crystallization temperature increases with increasing the melting point of RE metals. The feature of thermomagnetization curve for amorphous $Gd_{70}Al_{30}$ alloy is remarkably affected by the strength of external magnetic field. The electrical resistivity does not show a monotonic decrease around 60 K as shown in the figure. Magnetic phase diagrom of amorphous Gd-Al alloy system has been established by McGuire et al. [1], and in low Gd contents, amorphous Gd-Al alloys show spin-glass behaviors and transform from an intermediate state to a ferromagnetic one in high Gd contents. Therefore, these anomalous behaviors may be correlated to the intermediate magnetic state pointed out by them.

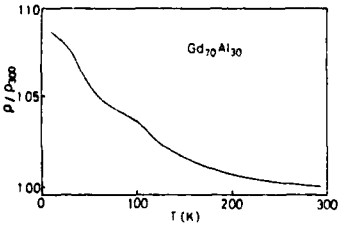

[1] T. R. McGuire, T. Mizoguchi, R. J. Gambino and S. Kirkpatrick, J. Appl. Phys. 49(3) (1978) 1689.

PK6 ELECTRICAL AND MAGNETIC PROPERTIES OF AMORPHOUS FeZr and FeGd FILMS

T. Stobiecki, J. Sokulski, K. Kowalski
Solid State Physics Department Academy of Mining and Metallurgy, 30-059 Kraków, P o l a n d
F. Stobiecki,
Institute of Molecular Physics of the Polish Academy of Science, 60-179 Poznań, P o l a n d

$Fe_{1-x}Zr_x$ ($0 \leqslant x < 0.50$) and $Fe_{1-x}Gd_x$ ($0 \leqslant x < 0.30$) amorphous films were prepared by RF sputtering. The electrical resistivity and the Hall effect as a function of concentration and of temperature were investigated. From this measurements the anomalous Hall constant R_s, ordinary Hall constant R_o, the Hall angle ρ_H/ρ resistivity ρ and temperature coefficient of resistivity at room temperature TCR as a function of Zr and Gd concentration was determined. Fukamichi et al [1] reported a minimum of resistivity against temperature at the Curie temperature T_c for low Zr concentration ($x < 0.15$). From our measurements it is seen that the minimum differs from the T_c for higher Zr concentration. The Curie temperature T_c and the extrapolated para - magnetic Curie temperature θ were determined versus Zr and Gd concentration (for different samples) from temperature measurements of the magnetization M_s and the Hall resistivity ρ_H.

[1] K. Fukamichi, R. J. Gambino and T.R. Mc Guire J. Appl. Phys., 53 (1982), 2310

PK7 RESISTIVITY AND HALL EFFECT OF AMORPHOUS GdCo, GdCoMo AND CoMo FILMS

T. Stobiecki, K. Kowalski, and J. Sokulski,
Solid State Physics Department, Academy of Mining and Metallurgy, 30-059 Kraków, P o l a n d

Amorphous $Co_{1-y}Mo_y$ ($0 \leqslant y < 0.30$), $Gd_{1-x}Co_x$ ($0.65 < x \leqslant 1$) and $(Gd_{1-x}Co_x)_{1-y}Mo_y$ ($0.70 < x \leqslant 1$ and $y=0.04$, 0.06, 0.13, 0.17) films were prepared by RF sputtering. The electrical resistivity and the Hall effect as function of concentration and of temperature were investigated. Influence of Mo concentration on resistivity ρ, temperature coefficient of resistivity at room temperature TCR, Hall angle ρ_H/ρ and magnetization M_s was also studied for these films. Samples of $Co_{1-y}Mo_y$ proved to be amorphous for $0.12 \leqslant y \leqslant 0.24$ and show negative TCR in this range of y. Hall angle linearly decreases with increasing concentration of Mo. Anomalous Hall constant R_s depends only very weakly on the concentration for $0.12 \leqslant y \leqslant 0.26$.

Films of GdCoMo and GdCo with $\rho \gg 160\ \mu\Omega$cm have negative TCR. With increasing content of Mo we observe a shift of the point at which TCR=0 towards smaller Gd concentration as it is predicted by the free electron model with $2k_F \cong k_p$. We obtained different Hall angle (ρ_H/ρ) alloy dependence for GdCo and GdCoMo alloys than cited by Mc Guire et al [1]. From our measurements and calculations we deduce that the change in Hall angle $(\rho_H/\rho)_{Co}$ is due to the charge transfer from Gd and Mo while the Hall angle $(\rho_H/\rho)_{Gd}$ of Gd is nearly constant. The value of Hall angle $(\rho_H/\rho)_{Co} \cong 0.027$ for pure amorphous Co taken from [1] seems too large, our measurements yield $(\rho_H/\rho)_{Co} \cong 0.015$.

The dependence of the Hall constant R_s against resistivity ρ for the films studied is also discussed.

[1] T. R. Mc Guire, R. J. Gambino and R. C. Taylor, J. Appl. Phys., 48 (1977), 2965.

PK8 MUFFIN-TIN MODEL CALCULATION OF THE DENSITY OF STATES OF LIQUID COPPER

Margaret St.Peters
California Polytechnic State University

A comparison is made of various single-site theories for the density of states (DOS) of disordered, strongly scattering systems. Lloyd's formula, derived from a multiple-scattering series expansion for the Green's function, is employed. An expression for the integrated density of states, following Niizeki[1], is formulated for the energy-shell Ishida-Yonezawa (ES-IY) approximation[2] as well as for the effective medium approximation (EMA) of Roth[3], for which a Kirkwood type ionic correlation is included. An explicit calculation of the DOS for liquid copper is made using the multi-phase-shift muffin-tin ES-IY approximation. We conclude that the self-consistent ES-IY is the simplest viable theory for liquid metals. Both the bandwidth and shape of the DOS in the d-resonance region compare well with experimental liquid copper optical density of states measurements and with the general shape of fcc copper calculations. A comparison by Aloisio, Singh and Roth[4] of a tight-binding model ES-IY and EMA with computer simulations of Fujiwara and Tanabe[5] suggests that the more complex EMA gives a better band shape than the ES-IY. We propose that the ES-IY model calculation developed here could provide a useful basis for an EMA calculation for a liquid metal. The simplicity of the ES-IY itself might be very useful in investigating liquid and amorphous transition metal alloys and in including vertex corrections in electrical conductivity calculations.

[1] Niizeki, K. (1979) J. Phys. F: Met. Phys. 9, L185.
[2] Yonezawa, F., Y. Ishida and F. Martino (1976) J. Phys. F: Met. Phys. 6, 1041.
[3] Roth, L.M. (1974) Phys. Rev. B 9, 2476.
[4] Aloisio, M.A., V.A. Singh and L.M. Roth (1981) J. Phys. F: Met. Phys. 11, 1823.
[5] Fujiwara, T. and Y. Tanabe (1979) J. Phys. F: Met. Phys. 9, 1085.

PK9 THE THERMOPOWER OF Fe-B METALLIC GLASSES. J.O. Strom-Olsen, M. Olivier, Physics Department, McGill University, 3600 University Street, Montreal, Quebec, Canada, H3A 2T8 and R.W. Cochrane, Universite de Montreal, Physics Department, P.O. Box 6128, Station A, Montreal, Quebec, Canada H3C 3J7.

The thermopower of melt spun Fe-B glasses for boron concentrations in the range 13 at % to 22 at % has been measured from 4.2K to 500K. In contrast to the magnetic properties and electrical resistivity, the thermopower shows a very strong dependence on boron concentration, especially in the range 13 to 18 at %. Further, for the more boron rich alloys, the thermopower develops a pronounced maximum as a function of temperature at about room temperature. The absence of any correlation between the magnetisation and the thermopower precludes any explanation based on magnetic scattering and attempts to explain the behavior on the basis of chemical short range order have been equally unsuccessful. Instead the general features of data may be explained using the Faber-Ziman model taking account of the temperature dependence of the 'r' term which itself reflects the energy derivatives of the electron scattering at $K = 2K_F$.

PK10 MODIFIED C.P.A. THEORY FOR AMORPHOUS AND CRYSTALLINE ALLOYS FOR CONSTITUENTS OF DIFFERENT BAND STRUCTURE

B. Szpunar*, P. Dawber+,
Department of Physics, University of Durham, South Road, Durham DH1 3LE, U.K.
+School of Mathematical and Physical Sciences, University of Sussex, Falmer Brighton, Sussex, BN1 9QH, U.K.

The method of modifying the usual C.P.A. theory of alloys is suggested to cover the physically important situation where the two components of a binary alloy have different densities of states. By using energy dependent single site potentials it is possible to refer back to a reference constituent with a simple analytic density of states. The C.P.A. condition becomes a cubic equation for the propagator, which can be solved analytically at any energy. The method can also be viewed as a modification of the C.P.P.A. theory of Bolton and Dawber (1975) and overcomes some of the difficulties encountered in that approach.

The authors have carried out calculations for examplary model systems where the bands have densities of states with elliptic or rectangular form and different band widths.

The results of calculations of the specific heat for silver gold alloys as a function of concentration is presented. The good agreement with the experimental data justified the method.

References
1) Bolton J.P.R. and Dawber P.G. (1975) J. Phys. F: Metal Phys. 5 2079-88.

PK11 THE MAGNETIC PROPERTIES OF LIQUID Cd-Sb ALLOYS

P. Terzieff and K.L. Komarek, Institute of Inorganic Chemistry, University of Vienna, Austria; E. Wachtel and B. Predel, Max-Planck-Institut für Metallforschung, Stuttgart, Federal Republic of Germany

The magnetic properties of Cd-Sb alloys in the liquid state were investigated by measuring the magnetic susceptibility up to about 1100 K. Special attention was paid to alloys with compositions in the range of the metastable phases Cd_3Sb_2 and Cd_4Sb_3, where anomalous thermodynamic properties had been observed. The susceptibility curves obtained on heating and cooling coincided only far above the liquidus temperature. On approaching the liquidus temperature the curves diverged, which was most pronounced in the range of the metastable phases. The variation of the magnetic susceptibility with concentration could not be explained in terms of a simple mixture of the components. The deviations from such a simple behaviour is presumably due to chemical short range order in the liquid state. A quantitative description has been attempted by using thermodynamic data.

PK12 ELECTRICAL TRANSPORT PROPERTIES OF METALLIC GLASSES*

C.L. Tsai and F.C. Lu, Materials Science Division, Institute of Chemical Analysis, Northeastern University, Boston, MA 02115 USA

Electrical transport properties such as electrical resistivity, ρ, magnetoresistivity, $\Delta\rho/\rho$, and Hall Coefficient, R_H, have been measured for Ca-Al and La-Al metallic glasses over a wide temperature range and in magnetic field up to 15 T. The value of ρ for Ca-Al metallic glasses varies from ~ 100 μΩcm to ~ 400 μΩcm while ρ for La-Al metallic glasses changes from 180 μΩcm to 310 μΩcm. The values of R_H and $\Delta\rho/\rho$ for Ca-Al system are negative at low temperatures; in contrast, they are positive for La-Al metallic glasses. The negative $\Delta\rho/\rho$ of Ca-Al metallic glasses can be attributed largely to the incipient localization effect, while the positive $\Delta\rho/\rho$ of La-Al metallic glasses is due to the electron-electron interaction. Consequently, the electrical conductivity of La-Al metallic glasses displays a $\sqrt{T}$ dependence at low temperatures, while that of Ca-Al metallic glasses show a rather strong temperature dependence. The details of the experimental results and the analysis of the electrical transport properties of these metallic glasses in terms of the incipient localization effect and electron-electron interaction will be presented.

*Supported by AFOSR (F49620-82-C-0076); part of this work was performed at Francis Bitter National Lab at MIT supported by NSF.

PK13 COMPOSITION DEPENDENCE OF THE EFFECTIVE HYPERFINE FIELD IN AMORPHOUS Fe-EARLY TRANSITION METAL ALLOYS* K. M. Unruh and C. L. Chien, The Johns Hopkins University, Baltimore, MD 21218 USA

We have prepared a number of amorphous Fe-early transition metal (Fe-EM; EM = Y, Ti, Zr, Hf, V, Nb, Ta, Mo, W) alloys in order to systematically study the effects of composition and alloying element on the magnetic properties. All the samples were prepared under similar conditions by a high rate sputtering technique and were studied by Mossbauer spectroscopy.

For all the magnetic samples, the effective hyperfine field (H_{eff}) varies in an essentially linear way through the relation

$$H_{eff}(x) = m\,x + b$$

where x is the Fe concentration, m is nearly independent of the EM alloying element, and b is characteristics of a particular alloy. We have also observed that the size of the EM element plays an important role in determining the magnitude of H_{eff}. Specifically, the magnitude of H_{eff}, at a given composition, is found to scale with the size of the EM element such that larger sizes are associated with larger values of H_{eff}. In addition, it is found that at a given composition there is a minimum EM element size required for an alloy to be magnetic. As a consequence $Fe_{70}V_{30}$, $Fe_{70}Mo_{30}$ and $Fe_{70}W_{30}$ are not magnetic. Such an analysis makes it possible, based on a simple empirical formula, to predict the effective hyperfine field in a number of as yet unstudied alloys of Fe with a transition metal.

Our empirical observations can be put on a more fundamental basis by comparison with recent band structure calculations of Malozemoff et al[1] These calculations provide a qualitative basis for understanding the important role played by the size of the alloying element and also the apparently anomalous behavior of the Fe-Ti alloys.

[1]A.P. Malozemoff, A. R. Williams, K. Terakura, V. L. Moruzzi and K. Fukamichi, ICM, Kyoto (1982).

*Work supported by the NSF Grant No. DMR82-05135.

PK14 NEW CONSTRUCTION OF FIRST-PRINCIPLES PSEUDOPOTENTIALS AND THEIR APPLICATIONS TO LIQUID METALS. M. Watabe and M. Hasegawa, Faculty of Integrated Arts and Sciences, Hiroshima University, Hiroshima 730, Japan

In spite of extensive theoretical studies for liquid as well as crystalline metals some important problems of electronic and thermodynamic properties still remains unsolved from first principles even for simple metals. One of reasons for this is that the pseudo- or model potentials used in these studies are not sufficiently reliable. We propose here a metod of costructing a new type of first-principles pseodopotentials which have several advantages over the previous ones and are expected to be reliable enough to apply to some subtle problems. Our method is a modification of the "norm-conserving" pseudopotentials due to Hamann, Schlüter and Chiang (Phys. Rev. Lett. 43 1494 (1979)). Our pseudopotentials are constructed by using the valence states of a free atom or the APW-like states in the atomic sphere as the reference state. Generated pseudopotentials are energy-independent as a consequence of the norm-conserving nature and are expressed in terms of simple analytic functions.

The pseudopotentials are free from the complications and uncertainties in treating the depletion hole, effective mass corrections, etc., which are inevitable for the usual pseudo- or model potentials. Hence they are quite useful for studying various properties of metals and alloys. To illustrate the usefulness of the pseudopotentials, we have applied them to the calculations of some properties of Zn and Cd. We have found that the pseudopotentials predict quite successfully the unusual features of the equilibrium crystalline and liquid structures of these metals (e.g. large deviations of the c/a ratios from the ideal value and the skewness of the first peaks of the liquid structure factors). Applications to the electronic transport properties in liquid phase are also quite successful

PK15 STUDY OF MAGNETIC REGIMES IN a-Fe_xB_{100-x} BY DC MAGNETIZATION MEASUREMENTS. D. J. Webb and S. M. Bhagat, University of Maryland, College Park, MD 20742, K. Moorjani, F. G. Satkiewicz and T. O. Poehler, Johns Hopkins University, Appl. Phys. Lab., Laurel, MD 20810, and M. A. Manheimer, Lab. for Phys. Sci., College Park, MD 20740.

Magnetic resonance[1] data on a-Fe_xB_{100-x} sputtered films have delineated various magnetic regimes in these rather simple glassy alloys. For $26 < x < 32$ they show spin glass behavior at low temperatures (T) while for $40 < x < 49$ they exhibit reentrant magnetism. Considering the sensitivity[2] of such behavior to external magnetic fields (B_a), it is desirable to explore these magnetic states in low fields. We have made low field ($10 < B_a < 1000$ Oe) dc magnetization (M) measurements between 4 and 360 K using the Faraday balance technique. The field and field gradient were applied parallel to the plane of the thin film samples. In addition to confirming the existence of the magnetic regimes revealed by the resonance data, the present results give us further insight into the nature of the "ferromagnetism" in these alloys in the reentrant regime and also help determine the phase diagram in the vicinity of the multi-critical point.

For $40 < x < 49$ we observe a discontinuous drop in (dM/dT) on lowering T and use this to define T_c. Below T_c, with $B_a < 30$ Oe, M remains relatively independent of T down to $\sim 0.5\ T_c$. This constant value of M is well below that consistent with demagnetization limiting. On further reduction of T, M drops slowly indicating reentrant magnetism. Also M becomes time dependent and sensitive to field cooling.

For $x \leq 40$, we find Curie Weiss behavior at high T. However, as also found for other spin glass alloys, the paramagnetic θ decreases progressively with reducing T. At ≈ 10 K the low field susceptibility has a peak characteristic of a spin glass transition. For T below the peak temperature the other properties of spin glasses, time dependence and sensitivity to field cooling, reveal themselves.

1. Webb et al., Sol. St. Comm. 43 239 (1982), Bull. APS 28, 414 (1983).
2. Manheimer et al., Jour. Appl. Phys. 53, 7737 (1982).

POSTER SESSION PL: ATOMIC TRANSPORT AND STRUCTURAL RELAXATION III

PL1 ACTIVATION ENERGIES FOR CRYSTALLIZATION OF AMORPHOUS Fe-Ni-P-B ALLOYS. H. Miura and S. Isa, Iron and Steel Technical College, Nishikoya, Amagasaki 661, Japan

A method of estimating the solid-liquid surface energy of an alloy was proposed to obtain the thermal activation energy for crystallization ΔG^* of the amorphous alloy based on the classic theory of nucleation. In this method, the data of the solid-vapor surface energy, the liquid-vapor surface energy, and the heat of fusion of the alloy were employed. An example of its application was given of the amorphous $Fe_{64}Ni_{16}P_{14}B_6$, $Fe_{40}Ni_{40}P_{14}B_6$, and $Fe_{16}Ni_{64}P_{14}B_6$ alloys. Calculation of the value of ΔG^* resulted in 148 kJ/mol for $Fe_{64}Ni_{16}P_{14}B_6$, 173 kJ/mol for $Fe_{40}Ni_{40}P_{14}B_6$, and 179 kJ/mol for $Fe_{16}Ni_{64}P_{14}B_6$ alloys. Here the free energies of crystallization used in these calculations were determined with the aid of the method to be reported by the present authors in this conference.

From the above values of ΔG^* and those of the apparent activation energy for crystallization determined by the Kissinger method, the diffusion activation energies for crystallization ΔG_D of the present alloys were also calculated. The values of ΔG_D decreased with nickel content of the alloys. The fluidities of the binary $Fe_{64}Ni_{16}$, $Fe_{40}Ni_{40}$, and $Fe_{16}Ni_{64}$ alloys were approximately determined by using the reciprocal of viscosity of the constituent elements of each alloy. The fluidities thus obtained increased with nickel content of these binaries. This seems to support the tendency of composition dependence of ΔG_D as mentioned above.

PL2 CORRELATION OF THE SHEAR MODULUS AND INTERNAL FRICTION IN THE REVERSIBLE STRUCTURAL RELAXATION OF A GLASSY METAL. N. Morito* and T. Egami, University of Pennsylvania, Philadelphia, PA 19104, USA, and *Research Laboratories, Kawasaki Steel Corporation, Chiba, JAPAN

The reversible structural relaxation due to annealing in glassy metals is known to influence magnetic properties such as Curie temperature T_c, field-induced magnetic anisotropy K_u and disaccommodation, and mechanical properties such as Young's modulus and internal friction Q^{-1}. Very recently changes in T_c, K_u and Q^{-1} due to annealing have been shown by the present authors to share the same microscopic mechanism, which we believe to be the anelastic structural defects such as local shear stress fluctuations. In this paper we show that the anelastic relaxation effect is also reflected in the change of shear modulus G.

The measurements of Q^{-1} and G (square of osciallation frequency) were carried out simultaneously, using an inverted torsion pendulum apparatus. Above 300°C, the glassy metal $Fe_{32}Ni_{36}Cr_{14}P_{12}B_6$ can attain a pseudo-equilibrium amorphous state as reflected in the saturated values of T_c and Q^{-1} just prior to crystallization at each temperature. The magnitude of Q^{-1} in the pseudo-equilibrium state for each annealing temperature, was found to be linearly correlated with the pseudo-equilibrium value of G at the same temperature. Transition from a higher temperature to a lower temperature pseudo-equilibrium structure resulted in a lower value of Q^{-1} and an increased value of G. The kinetics of the changes in these two properties are similar. The strong correspondence between G and Q^{-1} in the pseudo-equilibrium state and in their kinetics indicates that they represent the same anelastic relaxation effect. Furthermore, the extrapolation of the pseudo-equilibrium values of G above 300°C to G = 0 gives 1500 - 2000°C as the freezing temperature of the shearable components in the glassy metal, which is very close to the value, ~ 1800°C, expected for T_g' the upper glass transition temperature of τ defects or local shear stress fluctuations[1].

1. T. Egami and D. Srolovitz, J. Phys. F 12, 2141 (1982).

PL3 ON THE KINETICS OF STRUCTURAL RELAXATION IN AMORPHOUS $Fe_{40}Ni_{40}B_{20}$. A.L. Mulder, S. van der Zwaag and A. van den Beukel, Delft University of Technology, Laboratory of Metallurgy, Rotterdamseweg 137, 2628 AL Delft, The Netherlands.

Structural relaxation consists of an irreversible annealing out of free volume and reversible order-disorder processes.

Recently a model has been developed which describes quantitatively the kinetics of the annealing of free volume and which predicts that the kinetics of the ordering processes depends on the amount of free volume present [1]. In this paper we present experimental results confirming the validity of the model.

A high resolution pulse-echo technique for R.T.-measurements of small changes in Young's modulus of $Fe_{40}Ni_{40}B_{20}$ was used to follow structural relaxation during isothermal annealing. It is demonstrated that Young's modulus depends on both the amount of free volume and the degree of order. Due to the reversibility of the ordering process the contribution of the two processes to Young's modulus can be separated by means of suitable heat treatments.

The changes in Young's modulus during annealing, which are due to changes in the amount of free volume are very well described by the model. Using a single activation energy of 170 kJ/mol the annealing out of free volume could be described over a wide range of annealing temperatures and times.

The predicted dependence of the kinetics of the ordering process on the amount of free volume present has been observed giving additional support for the model.

[1] A. van den Beukel and S. Radelaar, Acta Met. 31(1983) 419.

PL4 KINETICS OF CRYSTALLIZATION IN THE Cu_{60}-Zr_{40} ALLOY SYSTEM. M. A. Otooni, Metallic Materials Branch, Materials and Manufacturing Technology Division, Fire Control and Small Caliber Weapon Systems Laboratory, US Army Armament Research and Development Command, Dover, NJ 07801

Amorphous alloy of copper - 40 at % Zr has been allowed to undergo crystallization during a series of isothermal annealing of samples at temperature intervals of 651, 673, 703, and 720°K respectively. Differential Scanning Calorimetry (DSC), X-Ray Diffraction (XRD), High Resolution Transmission Electron Microscopy (HREM), Reflection High Energy Electron Diffraction (RHEED), Microhardness (MH), and Electrical Resistivity (ER) techniques have been employed to assess the onset of crystallization processes. Results from MH and ER measurements indicate an abrupt increase of these parameters during the first hour of annealing of the sample. A more subtle and continuous trend in increasing MH and ER data develops during subsequent annealing times. High Resolution Transmission Electron Micrograph of samples annealed at 651°K for 60-70 minutes reveal the appearance of cluster-like regions of approximately 15-20 A° in size and randomly distributed throughout the sample. Reflection High Energy Electron Diffraction Micrographs from unannealed samples indicate highly diffused diffraction patterns. Insitu annealing of these samples results in further sharpening of the RHEED pattern with increasing time and temperature. This latter analysis clearly indicates that the amorphous surface layers undergo transformation similar to that of the matrix.

PL5 SYNTHESIS AND THERMAL RELAXATION OF METALLIC GLASSES QUENCHED AT AMBIENT AND ELEVATED SUBSTRATE TEMPERATURES.
S.J. Poon and S.E. Anderson, University of Virginia, Charlottesville, VA 22901 USA

Amorphous metallic foils and ribbons are obtained at variable substrate temperatures. The synthesis techniques (piston-anvil, melt spinning) are described and discussed. Superconductivity is used as a probe to study the thermal states of the samples. Homogeneity of the samples are emphasized. The thermal relaxation of samples quenched at elevated temperature is compared with that obtained at room temperature. For the room temperature quenched samples, 'equilibrium' amorphous phases are only observed in systems which undergo polymorphous crystallization (e.g. Zr_2Ni, Zr_2Pd, Zr_3Rh). Long term annealing in alloys undergoing eutectic crystallization (e.g. Zr_3Ni, Zr_3Pd) leads initially to microscopic composition modulation (phase separation) and eventually to crystallization. The stability of the equilibrium structures are discussed.

PL6 ATOMIC DIFFUSION AND STRUCTURAL RELAXATION IN AMORPHOUS CuAg FILMS
I.M.Reda, A.Wagendristel and H.Bangert, Institute of Applied and Technical Physics, Technical University of Vienna, A-1040, Karlsplatz 13, Austria

Ag-Cu films prepared by vapour quenching onto liquid nitrogen cooled substrates are amorphous and stable above room temperature in the concentration range 35:63 at%Cu. Such films exhibit a strong dependence of crystallization temperature on the concentration and a pronounced parabolic dependence of electrical resistivity on concentration. These two properties allow to monitor the diffusion mixing process in thin film couples. For this purpose three substrates were mounted and with a special masking system, concentration modulated films were deposited on one of them whereas the two others were exposed to a constant concentration vapour beam. A typical modulation wavelength was 4 nm with concentration amplitude of 10 at% around the mean concentration. These films were annealed at temperatures between 295 K and 323 K. Their electrical resistivities were measured "in situ". The rise of resistivity due to the diffusional mixing process made the assessment of an average diffusion coefficient possible:

$$D = 3.7 \times 10^{-5} \exp(-0.85\ eV/kT) \quad cm^2/s$$

The structural relaxation effect has been studied as well. The activation energy of the isoconfigurational diffusivity is 1.2 eV and the frequency factor is $7.3 \times 10^{-3} cm^2/s$.

PL7 SUPERCONDUCTIVITY AND THERMAL RELAXATION OF AMORPHOUS Be-Nb-Zr ALLOYS. H. Riesemeier, K. Lüders, Fachbereich Physik der Freien Universität Berlin, H.C. Freyhardt, J. Reichelt, Institut für Metallphysik der Universität Göttingen and SFB 126

The superconducting behavior of rapidly quenched $Be_{32.5}Nb_xZr_{67.5-x}$ (x=0, 2.5, 4 and 5 at.%) alloys was investigated. Measurements were made in the as-quenched state as well as after several annealing procedures. The samples were prepared by a melt-spinning technique. The amorphous structure was confirmed by X-ray investigations using Cr-K_α radiation. DSC measurements revealed a glass temperature of about 350°C and, generally, a two-step crystallization with an activation energy of ≈1eV for the first step.

The superconducting transition curves were determined resistively and inductively. Furthermore the upper critical field $B_{c2}(T)$ was measured by means of a superconducting magnet.

Isochronous annealing in an argon atmosphere was performed successively from room temperature to the beginning of crystallization.

With increasing annealing temperature, the superconducting transition temperature T_c is shifted to lower values. As an example values for $Be_{32.5}Nb_5Zr_{62.5}$ are given: As quenched, T_c = 3.39 K; 200°C, T_c = 3.21 K; 300°C, T_c = 2.84 K; 350°C, T_c = 2.77 K; and 375°C, T_c = 2.29 K. At the same time the critical field curves are also shifted to lower temperatures without a remarkable change of the slope $(dB_{c2}/dT)_{T_c}$. The residual resistivity ϱ is not influenced up to about 200°C and then increases slightly up to 300 - 350°C, indicating a topological relaxation only. Between 350°C and 375°C ϱ decreases strongly.

From an evaluation of $(dB_{c2}/dT)_{T_c}$ and ϱ the influence of $N(E_F)$ on T_c is discussed in comparison with possible changes of the electron-phonon interaction.

PL8 EVOLUTION OF PHASE SEPARATION IN $Cu_{0.5}Zr_{0.5}$ METALLIC GLASSES. R. Schulz, K. Samwer* and W. L. Johnson, California Institute of Technology, Pasadena, CA 91125 USA

A resistivity anomaly is seen in $Cu_{0.5}Zr_{0.5}$ upon annealing between 300 C and 360 C which is similar to that observed in the electrical resistivity of alloys during the phase separation which occurs following a quench into a two phase region. Together with radial distribution function (RDF) and electronic microscopy measurements (TEM), these data suggest that phase separation into a Cu rich and a Cu poor amorphous phase is taking place. In the early stages of phase separation, the excess resistivity change above that expected due to the usual free volume relaxation is consistent with the linear theory of spinodal decomposition. Samples previously annealed in this temperature range and subsequently reheated at a rate of 20C/min show a well defined two step crystallization.

X-ray results show that during phase separation the main peak of the interference function shifts, gets wider and becomes asymmetric. This contrasts with the usual relaxtion behavior described by Egami et al. The change in the RDF can be explained if we assume that the following transformation occurs in the glass.

$$CuZr \rightarrow a \times (Cu_{10}Zr_7) + b \times (CuZr_2)$$

The coefficients a and b can be used to follow the progress of the reaction with annealing time. There is no evidence of crystalline precipitation from high angle X-ray and TEM during this process.

*Permanent Address: I. Physikalisches Institut, Bunsen str. 9, D-3400 Göttingen, West Germany

PL9 ENTHALPY RELAXATION OF SOME METALLIC GLASSES NEAR T_g

R.O.Suzuki and P.H.Shingu, Dept. of Metal Science and Technology, Kyoto Univ., Sakyo-Ku, Kyoto 606 Japan

Quantitative measurements of the enthalpy of relaxation in Pd-Cu-Si, Pd-Au-Si, Cu-Zr and Te-Ge glassy alloys, prepared by rapid quenching, were performed. As shown in the figure, the heat absorption observed on heating up to T_g, of samples annealed at a fixed temperature below T_g, is interpreted as being due to structural relaxation. The amount of absorbed heat (enthalpy of relaxation) increased with the increase in the annealing time up to a saturation value. The kinetics of this relaxation analyzed in terms of Johnson-Mehl-Avrami equation produced $(\text{time})^{1/2}$ dependence of log (relaxed fraction).

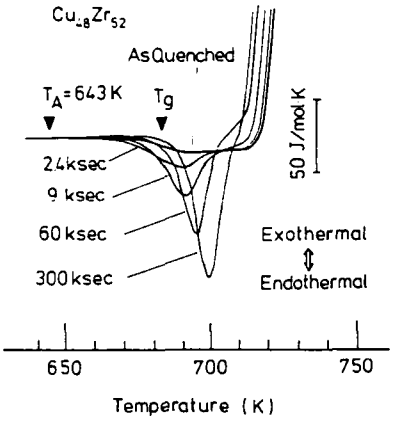

PL10 ANNEALING EFFECTS ON ELECTRICAL RESISTIVITY, THERMOELECTRIC POWER AND CRYSTALLIZATION OF IRON-RICH METALLIC GLASSES CONTAINING MOLYBDENUM,

S. Venkataraman, K.V. Reddy, Uno N. Virata Swaroop, G. Venugopal Rao and A.K. Bhatnagar, School of Physics, University of Hyderabad, Hyderabad 500134, India

Thermal Stability of metallic glasses is an important criterion for their applications. It is, therefore, important to study the effect of annealing at low temperatures but for long durations. We have investigated annealing effects on electrical resistivity, thermoelectric power and crystallization of metallic glasses $Fe_{40}Ni_{38}Mo_4B_{18}$, $Fe_{78}Mo_2B_{20}$ and $Fe_{39}Ni_{39}Mo_4Si_6B_{12}$. For example, we have found that the sample $Fe_{78}Mo_2B_{20}$, when annealed at 50 C for 20 hrs, shows approximately 10% decrease in the resistivity. The resistivity ratio, $\rho(T)/\rho(300)$, of the annealed and unannealed samples almost coincided with each other upto 450 K beyond which this ratio increased much faster for the annealed sample. The resistivity did not seem to be proportional to T over the full range of temperature studied. The Crystallization temperature was found to change from 773 K for the as received sample to 733 K for the annealed sample. Thermoelectric power of the 'as received' samples showed some minor structures which seem to disappear on annealing. Detailed data on all three metallic glasses will be presented and discussed.

PL11 FORMATION AND STABILITY OF AMORPHOUS AND PART-CRYSTALLINE $Zr_{76}Ni_{24}$ ALLOYS.

B. Tolour, Oxford Research Unit, The Open University, Foxcombe Hall, Oxford, OX1 4HR, U.K. G. Gregan, Department of Metallurgy, University of Sheffield, Sheffield, S1 3JD, U.K. and M.G. Scott, Standard Telecommunication Laboratories Ltd., Harlow, Essex, CM17 9NA, U.K.

By varying the quenching rate during melt-spinning it is possible to produce either amorphous or partially crystalline $Zr_{76}Ni_{24}$ alloy. The quenched-in crystals are α-Zr whereas those produced by thermal decomposition of the glassy phase have an off-stoichiometric C16 (Zr_2Ni) structure. The part crystalline material is more stable against further crystallisation than is the fully amorphous material. Possible explanations for this behaviour are presented. The pre-existing crystals do not act as heterogenous nucleation sites for further crystallisation.

PL12 Ductility and Swelling of Neutron-Irradiated Amorphous $Fe_{40}Ni_{40}B_{20}$

R. Wagner, R. Gerling and F.P. Schimansky, GKSS-Forschungszentrum, Institut für Physik, D 2054 Geesthacht, Box 1160, FR Germany

Amorphous ribbons of $Fe_{40}Ni_{40}B_{20}$ in the as-quenched state and in different states of relaxation were exposed to incore reactor irradiation at ~ 70°C. The inelastic transmutations of the ^{10}B-isotope by the capture of thermal neutrons resulted in high energy α- and Li-projectiles (2.7 MeV) causing damage levels up to 5 dpa. With increasing damage level the density of both the as-quenched and the thermally relaxed specimen decreased continuously; however, beyond 0.65 dpa the swelling of the glassy alloy reached a saturation level of ~ 0.8 % with respect to the density of the unirradiated specimens. This swelling behaviour points clearly towards the existence of radiation-induced defects which contain a fair amount of excess free volume. In an analogous manner to crystalline alloys the generation of such a 'vacancy-type' defect within the amorphous structure requires the simultaneous generation of a corresponding anti-defect, i.e. an'interstitial-type' defect with a locally higher than average density. The observed swelling effect, however, suggests a higher mobility of the 'interstitial-type' defects.

Beyond 0.16 dpa the as-quenched material starts to embrittle; ductility is completely lost at damage levels > 0.65 dpa. The relaxed specimen, the density of which has increased by 0.07 % during thermal relaxation, was brittle at the beginning of irradiation. After irradiation to only 0.016 dpa the ductility was completely restored stressing the important role of excess free volume with respect to mechanical properties of metallic glasses.

Beyond 0.16 dpa the ductility again starts to decrease in an identical manner to that of the as-quenched specimen. This loss of ductility during irradiation is attributed to the radiation-enhanced formation of embrittling amorphous $(Fe,Ni)_3B$-clusters which compensates the positive effect of the radiation-induced excess free volume upon the ductility of $Fe_{40}Ni_{40}B_{20}$.

PL13 THE CRYSTALLIZATION KINETICS OF AMORPHOUS SELENIUM. J.T. Wang, X.L. Wei, B.Z. Din, S.L. Li, Institute of Metal Research Academia Sinica, Wenhua Road, Shenyang, China.

The crystallization process of evaporated high purity amorphous selenium at a constant heating rate (40, 20, 10, 5, 2.5 1.25 K/min) and at constant temperature near the glass transformation temperature Tg (319, 318, 317, 316, 315, 314 K) were studied by means of differential scanning calorimeter DSC II, and the incubation periods at different temperatures were measured. In order to determine accurately the fraction transformed X(t) at any time, a formula of correcting the baseline of DSC-curve was deducted. The experimental data were calculated by a compiled computer general program. The result shows that when the ends of incubation periods were taken s the starting pints of transformation, and the fraction transformed (X) as a function of time (t), the exponent n found by Johnsen-Mehl-Avrami equation [$X = 1-\exp(-bt^n)$], which generally increases with rising the fraction transformed, only when $0.15 < X < 0.95$, the value *n keeps approximately* constant, being between 3.29 ± 0.04 - 3.69 ± 0.04.

The crystallization activation energies (E) were calculated based on the experimental results by Arrhenius equation. It is found, that apparent activation energies are not completely the same value in different transformation stage. In the initial stage E increases with increasing fraction transformed, and when $0.5 < X < 0.95$E is nearly a constant, being 66 $\pm$ 1 kcal/mol. In the later stage, nowever, E decreases with X(t). These results reflect the objective law of nucleation and growth in the transformation process.

PL14 LOW-FREQUENCY INTERNAL FRICTION OF METALLIC GLASSES DURING STRUCTURE RELAXATION AND CRYSTALLIZATION. Xia Wurong, Gui Jianian, Wang Zixiao and Zhou Rusong, Department of Physics, Wuhan University, Wuhan, China.

The temperature dependence of internal friction and elastic modulus (f^{-1}) associated with the structure relaxation and crystallization process in metallic glasses $Pd_{82}Si_{18}$ and $(Fe_{0.6}Ni_{0.4})_{82}Si_8B_{10}$ are measured by torsion pendulum (0.2~1.0 HZ). An internal friction peak at 379°C for $Pd_{82}Si_{18}$ and two peaks at 435°C and 490°C for $(Fe_{0.6}Ni_{0.4})_{82}Si_8B_{10}$, each having a corresponding frequency minimum, are observed. They are assigned to a diffusion controlled irreversible transition to crystalline phases, which may be achieved through cooperative atomic displacement, a phonon mode softening accompanies the occurrence of each of the peaks. An isothermal internal friction peak is also observed during the isothermal crystallization transition.

A stable internal friction peak, like that in the martensitic phase transition of crystalline NiTi alloy observed by Mercier, has been found for first time reported in metallic glasses. It can be seen that both in the structure relaxation process and in the crystallization process, the internal friction may be divided to two parts, one is the stable internal friction, independent of heating rate, an he other, associated with temperature changes, dependen eating rate. The different mechanisms of these two parts internal friction are discussed.

It is of interest to note that e metallic glass $(Fe_{0.6}Ni_{0.4})_{82}Si_8B_{10}$ exhibits Invar b r at as-quenched state and Elinvar behavior in a wider te re range after a proper pre-annealing treatment.

PL14 **CRYSTALLIZATION OF AMORPHOUS ALLOYS - DETERMINATION OF ACTIVATION ENERGIES FROM ELECTRICAL RESISTIVITY MEASUREMENTS.** J. Wolny and J. Sołtys+, L. Smardz, J.M. Dubois++, A. Całka++, Inst. Phys. and Nuclear Techniques, Academy of Mining and Metallurgy, 30-059 Cracow, Poland; + Jagiellonian Univ., Inst. of Phys., Cracow; ++ Lab. Metallurgie, Ecole des Mines, Nancy, France; ++ Technical University, Warsaw

The paper presents a review of various methods currently used to determine the activation energy for crystallization of amorphous alloys from their electrical resistivity data. Both isothermal and isochronous approaches are discussed. Most attention has been payed to the former one, which means that the following methods have been compared: 1/ that of the relaxation time; 2/ estimation of time needed by the sample to reach certain crystallization degree; 3/ determining of maximum of the time derivative of electrical resistivity. The latter one has been presented in a somewhat more detailed way. The idea is to estimate the activation energy from the dependence of $\ln(|dR/dt|)$ upon $1/T$, where R is the relative electrical resistivity, t is time, and T stands for temperature. The results were subjected to careful numerical stability tests, both with respect to the influence of initial parameter values and with respect to the particular method of numerical differentation used. The possibility of generalization of the concept, towards employing higher order derivatives, has been suggested. For illustration, results from the second time derivative of electrical resistivity have been presented and compared with those obtained by other methods.

PL16 RELAXATION AND EMBRITTLEMENT OF $Fe_{40}Ni_{40}Si_8B_{12}$ GLASS. P.G. Zielinski & D.G. Ast, Cornell Univ., Ithaca, NY 14853, USA.

The structural relaxation of Fe[40]Ni[40]Si[8]B[12] was investigated by differential scanning calorimetry of isochronically (15 min.) pre-annealed samples subjected to temperatures up to 680 K; i.e. to within 50 K of the crystallization temperature Tx.

The enthalpy relaxation spectrum consisted of two exothermic peaks, centered approximately at 550 and 650 K. The activation energies, derived from an analysis of the decrease of peak area with pre-annealing temperature, were 0.42 and 0.89 eV, respectively. A broad reversible peak, endothermic upon heating and exothermic upon cooling, developed when the specimen was temperature cycled repeatedly between 500 and 665 K; i.e. roughly in the temperature region separating the two peaks.

The two exothermic peaks I and II decreased smoothly with increasing pre-annealing temperature. The magnetic Curie temperature stayed constant up to pre-annealing temperatures corresponding to the onset of peak II and underwent reversible shifts when the specimen was cycled between 500 and 650 K.

Bending tests were carried out by compressing hairpin configurated specimens in an Instron testing machine and recording displacement vs force. In un-annealed specimens, the deformation consisted of three stages: (i) homogenous (ii) shear band formation (iii) plastic hinge formation and cracking. Pre-annealing shifted the onset of deformation mechanisms (i) smoothly to higher strain values but left the onset of stage (ii) unchanged. The fracture strain (termination of stage (iii)) decreased sharply when annealing was carried out in the temperature range of peak II.

These results are consistent with a model which assigns annihilation of volume defects to peak I and cluster formation on the nm scale to stage II. Once formed, the clusters undergo reversible degrees of association in temperature cycling experiments. A quantitative theory will be presented which shows that the temperature dependence of the apparent specific is functionally similar to a glass transition. Causes for the similarity will be discussed in context with related theories.

PL17 **GLASSY Pd-RE-Si ALLOYS: FORMATION, PROPERTIES AND DEVITRIFICATION**, Y.Q. Gao and B.C. Giessen, Materials Science Division, Institute of Chemical Analysis, Northeastern University, Boston, MA 02115

It is well known that Pd-Si alloys with between 14 and 20% Si readily form metallic glasses upon solidification at relatively moderate cooling rates; at lower Si contents, glass formation requires increasingly higher cooling rates and techniques other than melt spinning must be used for preparation. On the other hand, if it is desired to form ductile bulk alloys containing hardening precipitates by devitrification of Pd glasses, the concentration of Si in the glass must be lowered while retaining glass formation. This dual goal is accomplished by adding two synergistic constituents such as an early transition metal (e.g., a rare earth metal, RE, or Y) and a metalloid (e.g., Si) in approximately equal proportions. The resulting glass can be devitrified to form a hardened alloy of moderate ductility. The composition ranges of ready glass formation and the mechanical properties of the glasses and devitrified alloys will be presented.

PL18 **APPLICATION OF PATTERN RECOGNITION TECHNIQUES TO THE PREDICTION OF READY GLASS FORMATION**, B.C. Giessen and Y.Q. Gao, Materials Science Division, Institute of Chemical Analysis, and Department of Chemistry, Northeastern University, Boston, MA 02115

In the recent past, a substantial amount of effort has been devoted to forecasting the occurrence of ready glass formation (RGF) in alloys upon rapid quenching. For binary systems, prediction has been relatively successful generally using two criteria that can be depicted in a map (examples are heat of mixing and size ratio or eutectic temperature and composition); in certain cases, single criteria such as VEC or alloy crystal structure have been used. However, for ternary and higher systems (where RGF is relatively more common) single or dual criteria have not yet been successfully applied. In a new approach to this problem we have adapted methods of pattern recognition taken primarily from applications in analytical chemistry to the present concerns. These methods allow the treatment of representations involving more than two independent factors spanning spaces of order higher than two, using hyperplane separations, dendrograms and other statistical procedures accordingly, more than two factors each of which is individually weakly correlated to RGF can be jointly evaluated.

Brentwood Motor Inn
600 Beverly Park Dr.
Brentwood

Bel Air
Sands Hotel
11461 Sunset Bl.
Brentwood

Holiday Inn
170 North Church Lane
Brentwood

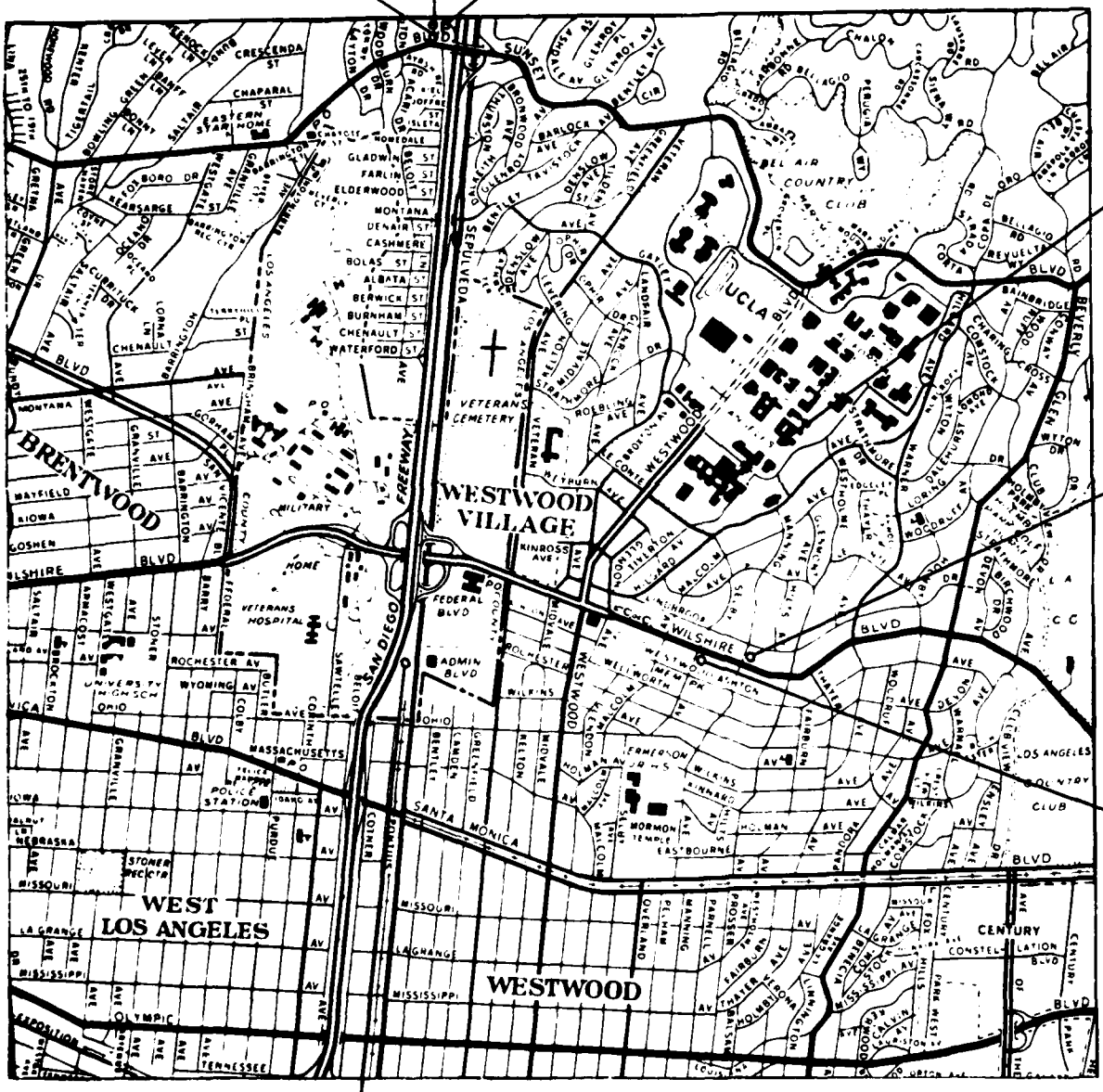

YOUNG HALL: LAMS
Conference
Center

Del Capri Hotel
10587 Wilshire Bl.
Westwood

Holiday Inn
10740 Wilshire Bl.
Westwood

West Los Angeles (WLA) Terminal
(Fly-Away Service Express Bus)

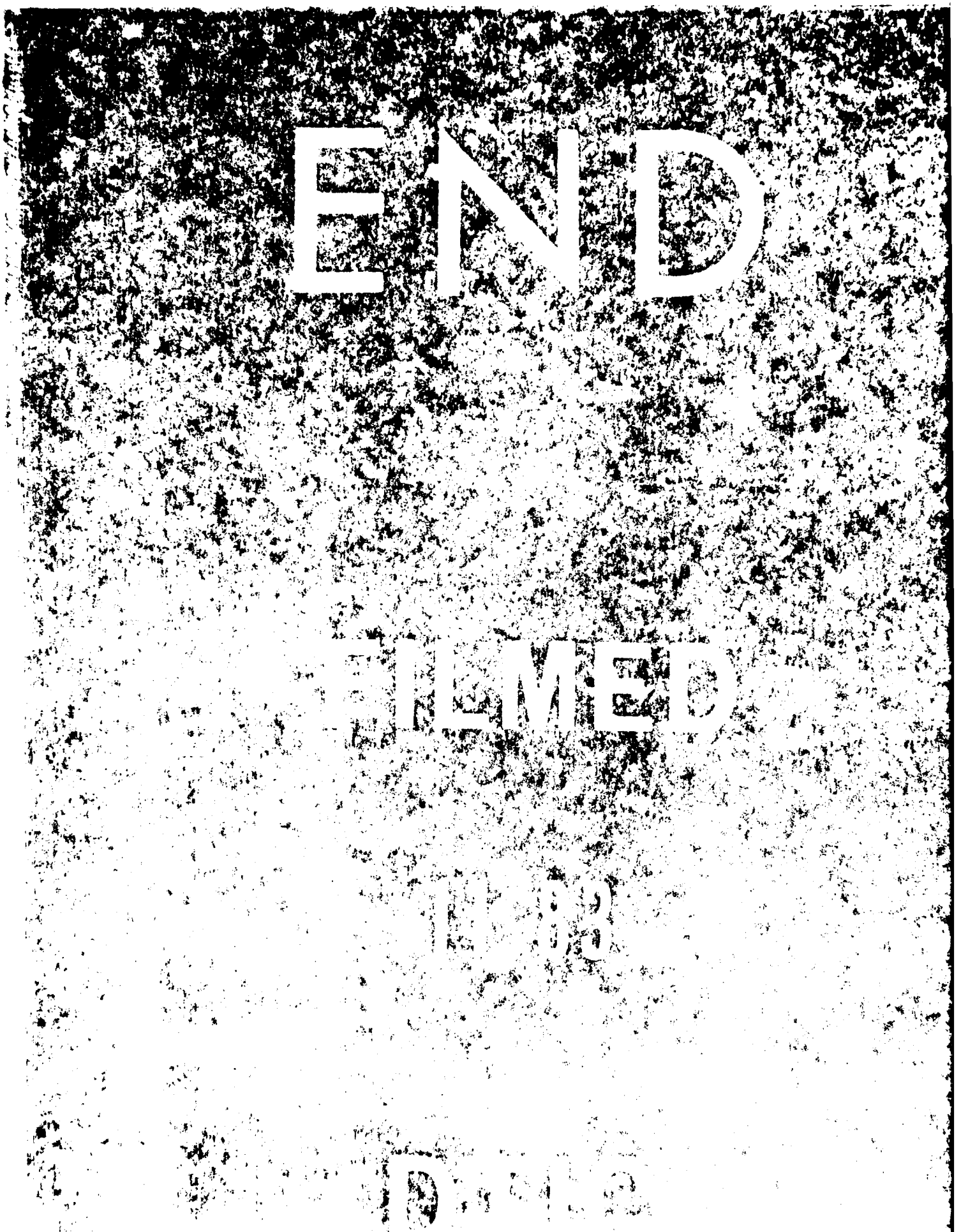
END
FILMED